TUMOUR MOTILITY:
Cell migration analysis and
effects of EMAP-II on TNF antitumour activities

TUMOREN IN BEWEGING:
Analyse van celmigratie en
EMAP-II effecten op antitumour activiteiten van TNF

Remco van Horssen

Tumour motility: cell migration analysis and effects of EMAP-II on TNF antitumour activities

Thesis, Erasmus University Rotterdam, The Netherlands

Electronically published by Medical Library, Erasmus MC, Rotterdam, The Netherlands.

ISBN-10	90-9020874-7
ISBN-13	978-90-9020874-9
Cover	Endothelial cell (stained for actin and VASP) migrating towards a tumour (crab). Movie-strip shows migrating breast tumour cells.
Design	Remco van Horssen
Printing	Febodruk B.V., The Netherlands
Correspondence	remcovanhorssen@hotmail.com

Tumour motility:
Cell migration analysis and
effects of EMAP-II on TNF antitumour activities

Tumoren in beweging:
Analyse van celmigratie en
EMAP-II effecten op antitumour activiteit van TNF

PROEFSCHRIFT

ter verkrijging van de graad van doctor aan de
Erasmus Universiteit Rotterdam
op gezag van de rector magnificus
Prof.dr. S.W.J. Lamberts
en volgens besluit van het College voor Promoties.

De openbare verdediging zal plaatsvinden op
woensdag 6 september 2006 om 13:45 uur

door

Remco van Horssen

geboren te Dordrecht

Promotiecommissie

Promotor:	Prof.dr. A.M.M. Eggermont
Overige leden:	Prof.dr. W. Buurman Prof.dr. R. Fodde Dr.ir. N. Galjart
Copromotor:	Dr. T.L.M. ten Hagen

The work described in this thesis was performed in the Laboratory of Experimental Surgical Oncology of the Department of Surgical Oncology at Erasmus MC – Daniel den Hoed Cancer Centre in Rotterdam, The Netherlands and was funded by grants from Mrace Translational Research Fund (Erasmus MC), Foundation 'Vanderes' and Foundation 'Erasmus Heelkundig Kankeronderzoek' (SEHK).

Printing of this thesis was financially supported by:

Boehringer Ingelheim Pharma GmbH
J.E. Jurriaanse Stichting
Oko-Lab (www.microscopeincubator.com)
Tebu-Bio
BioSource

Science without religion is lame
Religion without science is blind

Wetenschap zonder religie is lam
Religie zonder wetenschap is blind

Albert Einstein

voor mijn
schoonmoeder

CONTENTS

ABBREVIATIONS

aa	amino acid
Ab	Antibody
AcTub	Acetylated Tubulin
ATP	Adenosine Triphosphate
APC	Adenomatous Polyposis Coli
bFGF	basic Fibroblast Growth Factor
bp	basepair
BN	Brown Norway
BSA	Bovine Serum Albumin
CLASP	CLIP-Associated Protein
CLIP	Cytoplasmic Linker Protein
Col-I	Collagen-I
CR	Complete Response
DNA	Deoxyribonucleic Acid
EC	Endothelial Cell
ECM	Extra Cellular Matrix
Ena/VASP	Enabled / Vasodilator Activated Protein
EMAP-II	Endothelial Monocyte-Activating Polypeptide-II
EMT	Epithelial-Mesenchymal Transition
FADD	Fas-Associated Death Domain
FCS	Fetal Calf Serum
FN	Fibronectin
GAPs	GTPase Activating Proteins
GEFs	Guanine nucleotide Exchange Factors
GFP	Green Fluorescent Protein
HMVEC	Human Micro Vascular Endothelial Cells
HUVEC	Human Umbilical Vein Endothelial Cells
IFN	Interferon
ILP	Isolated Limb Pefusion
kb	kilo basepairs

kDa	kilo Dalton
LPA	Lysophosphatidic Acid
LR	Local Recurrence
MAP	Microtubule-Associated Proteins
MEF	Mouse Embryonic Fibroblast
MMP	Matrix Metalloproteinase
MTs	Microtubules
MTOC	Microtubule Organizing Centre
NC	No Change
NF- B	Nuclear Factor-kappa B transcription factor
NO	Nitric Oxide
NOS	Nitric Oxide Synthase
PBS	Phosphate Buffered Saline
PD	Progressive Disease
PIP2	phosphatidylinositol bisphosphate
PR	Partial Response
PT	Primary Tumour
RIP-1	Receptor Interacting Protein 1
RNA	Ribonucleic Acid
RNAi	RNA Interference
ROS	Reactive Oxygen Species
SD	Stable Disease
SEM	Standard Error of the Mean
STS	Soft-tissue Sarcoma
TACE	TNF-converting enzyme
TNF	Tumour Necrosis Factor-α
TNF-R1	TNF-Receptor 1
TNF-R2	TNF-Receptor 2
TRADD	TNF-Associated Death Domain
TRAF-2	TNF-Associated Factor 2
VEGF	Vascular Endothelial Growth Factor
VEGF-R2	VEGF-Receptor 2

WASP	Wiskott-Aldrich Syndrome Protein
+EBP	Plus-end Binding Proteins
+TIPs	Plus-end Binding Proteins

SCOPE OF THIS THESIS

Solid tumours are built up of many more cells than solely tumour cells. Besides tumour cells, solid tumours consist of immune cells, endothelial cells, fibroblasts and extra cellular matrix. Solid tumours can develop into well structured - but due to high growth rates often badly organised - dynamic organs with their own vasculature. Tumours develop an own network of vessels to supply themselves with nutrients and oxygen and connect to the circulation to enable growth and metastasis formation. This process is called angiogenesis and is an important focus of cancer research. Despite a lot of knowledge, the possibilities to treat cancer patients by reducing angiogenesis are still limited. Tumour formation and angiogenesis are very dynamic. In addition, dynamic processes within the different cell types determine the future (direction) of the cells. Tumour treatment should therefore rather be defined as manipulation of tumour dynamics rather than killing tumour cells. Understanding the molecular players during these processes is crucial to enlarge the possibilities of anti-angiogenic, anti-metastatic and anti-tumour therapies.

The aim of this thesis is to study several steps during tumour genesis, to obtain more insight into these steps and to understand and improve current treatment modalities. Motility in tumours is studied on several levels: migration of cells, mobilisation of signalling proteins in endothelial cells and redistribution of cells within tumours after Tumour Necrosis Factor-alpha (TNF)-treatment. The first part of this thesis will focus on cell migration. This essential step during tumour- and angiogenesis is not fully understood; cell migration was studied of different cell types along different matrix components. For this purpose a novel cell migration assay is developed to analyse intrinsic migratory capacities and response to external factors of endothelial and tumour cells.

The second part of this thesis focuses on treatment of solid tumours and induction of apoptosis in endothelial cells. As treatment modality TNF-based Isolated Limb Perfusion (ILP) is taken as basis. Studies are set up, from molecule to patient, to unravel the underlying mechanisms of this successful treatment and to search for explanations for non-responding tumours. Central role in this part of the thesis is played by the novel cytokine Endothelial Monocyte-Activating Polypeptide-II (EMAP-II).

In **Chapter 1** the cell migration is introduced. Besides the process and its molecular regulation, cell polarization and external factors influencing cell migration are mentioned. Experiments on cell migration are described in Chapter 2-4. **Chapter 2** describes a novel cell migration assay to study the role of extra cellular matrix (ECM) components in combination with growth factors in cell migration. This chapter describes the testing and validation of this novel assay by comparing it with the well-

known and broadly-used 'scratch' assay. One major and novel finding is that, solely by using the novel assay, Fibronectin (FN) was found to inhibit endothelial migration while fibroblast migration was induced. In **Chapter 3** the migration response and patterns of EC are studied upon treatment with basic Fibroblast Growth Factor (bFGF) and Vascular Endothelial Growth Factor (VEGF) using the novel assay. These two major angiogenic factors induce very different migration profiles that are accompanied by differences in cytoskeleton organisation and regulation. Focus will be on the microtubules and microtubule-associated proteins. The first part of this thesis ends with **Chapter 4**, which shows another example of an application of the novel cell migration assay. In this chapter tumour cell migration is studied using different breast cancer cell lines.

The second part of this thesis starts with the broad introduction of the two cytokines in focus: TNF (**Chapter 5**) and EMAP-II (**Chapter 6**). For TNF the focus is on its background, molecular signalling and use in cancer treatment. The review of EMAP-II covers all the available literature nowadays of this novel cytokine. In **Chapter 7** the protease responsible for cleavage of proEMAP into EMAP-II by tumour cells is presented. We demonstrate evidence that Matrix Metalloproteinase-7 (MMP-7) is responsible for this cleavage. **Chapter 8** describes the role of EMAP-II on the apoptotic signalling of TNF-R1 in EC upon TNF treatment. The presented data show that EMAP-II is capable of sensitizing EC towards TNF-induced apoptosis and that the mechanism involves mobilisation of the adaptor protein TNF-Receptor-Associated Death Domain (TRADD). In **Chapter 9** we evaluate the response of rats with soft-tissue sarcomas with different EMAP-II levels in the limb to TNF-based ILP. We show that tumours transfected with EMAP-II show a better response compared to the wild-type. Finally, studies on patient material are described in **Chapter 10**. Experiments are shown where expression and distribution of EMAP-II and TNF-R1 are evaluated before and after ILP treatment of patients with metastatic melanoma or sarcoma. A positive correlation was found between an upregulation of EMAP-II after ILP and a complete response of melanoma patients to TNF-based ILP. These data justify analysis of EMAP-II expression in biopsies of ILP-patients to predict the final outcome and eventually adapt (further) treatment. The major results and conclusions are summarised at the end of this thesis.

PART 1

Cell migration analysis

Chapter 1

Cell migration under physiologic and pathologic conditions

Remco van Horssen

Note: This chapter contains figures that are also available in full colour (labeled with 'CLR'). These colour figures can be found in the Appendix of this book (page 209) and in the online version (via Medical Library, Erasmus MC).

INTRODUCTION

Cell migration is the movement of a cell from one place to another and can be divided in directed and random motility. Cells migration already starts shortly after conception [1] and is involved during the development of an embryo. Migrating cells play an essential role throughout our life and is frequently – at least in part – associated with our death. Besides morphogenesis, cell migration contributes to tissue-turnover (in the skin and intestine renewal), tissue-repair and –regeneration (for example wound healing), immunologic responses, and is an important factor during disease progression including vascular diseases like atherosclerosis, osteoporosis, rheumatoid arthritis, multiple sclerosis, cancer progression (tumour growth, -metastasis and -angiogenesis), and mental retardation [2]. The process of cell migration however is also essential in other organisms like single cell organisms and plants [3]. Because of this great importance, cell migration is a broadly studied. Detailed understanding of the fundamental mechanisms underlying cell migration might be very useful for the therapeutic approaches of a whole set of diseases. In this short introductory chapter cell polarity and cell migration are summarized and differences between cell types and environments are discussed. For a complete overview of the process of cell migration, see for example references 2, 4, 28 and 35.

CELL POLARIZATION

Cell polarity is a hallmark of cell migration; a cell must be highly polarized in order to migrate. In a polarized cell, cytoskeletal components, molecular processes like transport, membrane compartmentalization and organelle distribution are different in distinct regions of the cell. Based on this definition all cells are polarized to certain content because cells are not symmetric. For a cell to migrate this polarization needs to be further extended. Two major features of cell polarity during migration are the formation of protrusions in the direction of migration and asymmetric positioning of intracellular structures [4].

Membrane protrusions, consisting of lamellipodia and filopodia, are very actin-rich and coupled to actin polymerisation as discussed above. The small Rho GTPases are key regulators of cell polarity. In slow-moving cells, the microtubule organizing centre (MTOC) and the Golgi apparatus often are positioned in front of the nucleus and MTs are selectively stabilized in the migration direction resulting in highly polarized cells [5-8]. The repositioning of the MTOC is regulated by Cdc42 [9] and recently movement of the nucleus has been observed resulting in MTOC orientation towards the migration direction [10]. For fast-moving cells however, these processes are differently regulated because in migrating T cells and neutrophils the MTOC is located behind the nucleus [11]. Cdc42

activity is one of the temporal localised molecular processes in cell polarity [12]. Also localised activity of PI3K at leading edges and the phosphatase PTEN at the rear and side of the cell is present in a chemotaxis induced moving cell [13,14]. For Rac, also a localized activation is observed which is linked to directionality of cell movements [15,16]. Downstream proteins activated by GTPases include actin binding proteins and microtubule-associated proteins [17]. Next to the proteins mentioned there are many other proteins involved in cell polarization. Migration of polarized cells is a well-coordinated cooperation between the actin and microtubule cytoskeleton and their binding proteins [18].

SEQUENTIAL STEPS DURING CELL MIGRATION

To study the process of cell migration cultured cells like mouse fibroblasts and fish keratinocytes and the amoeba *Dictyostelium* are often used as model systems. These easy-to-use and manipulative model systems have provided valuable molecular and cellular knowledge on cell migration. Different studies with these (and other) different cell types and environments have resulted in a general concept of cell migration. The process of cell migration is a cyclic event [4]. The sequential steps are schematically depicted in Figure 1. A resting non-migrating cell is tightly attached to the substratum and lacks sufficient polarity to move (there is no front or back). When a cell is exposed to a migration-promoting factor, the first response is a further polarization of the cell to enable cell movements. This includes intracellular reorganization, directed transport and membrane compartmentalization assures that the cell acquires a front and a backside.

This process is regulated by the actin and microtubule cytoskeleton [18]. After and along with cell polarization the cell forms protrusions in the direction of migration. These protrusions consist of membrane ruffles, large lamellipodia and tiny, spike-like filopodia [19]. Formation of these cellular structures is regulated by the recruitment of specific molecular scaffolds into these protrusions and is driven by actin polymerisation [20]. Actin filaments are polarized structures with slow and fast growing ends that are the driving force of membrane protrusion. The kinetics of actin polymerisation is affected by adenosine triphosphate (ATP) hydrolysis [21]. This ATP hydrolysis takes place within the actin filaments. ATP-bound actin monomers bind to the plus end while ADP-bound actin monomers dissociate from the minus end. At specific sites in the cytoplasm, ADP-actin is recharged with ATP to facilitate plus end binding. This intriguing process is called ‘tread-milling’ [22]. At the leading edge of the cell, in the protruding lammelipodia a so-called actin cortex is built up. This dense actin network consists of many branched filaments. Out of a single actin filament, daughter filaments are formed, a process mediated by the Arp2/3 complex [23,24]. WASP (Wiskott-Aldrich syndrome protein) protein

family members activate this Arp2/3 complex and these WASP proteins in turn are activated at the cell membrane by Rho GTPases and PIP2 (phosphatidylinositol bisphosphate) [25,26]. Formation and growth of new filaments at the leading edge of migrating cells is initiated by extracellular stimuli and has been named dendritic nucleation of actin assembly (reviewed in [27]). The rate of actin polymerisation is regulated by the small protein profilin, which catalyses the exchange of ADP for ATP and binds to ATP-actin monomers that serve to elongate filaments [25]. At the depolymerising end of the filaments ADP-actin monomers are disassembled, a process promoted by proteins of the ADF/cofilin family [28].

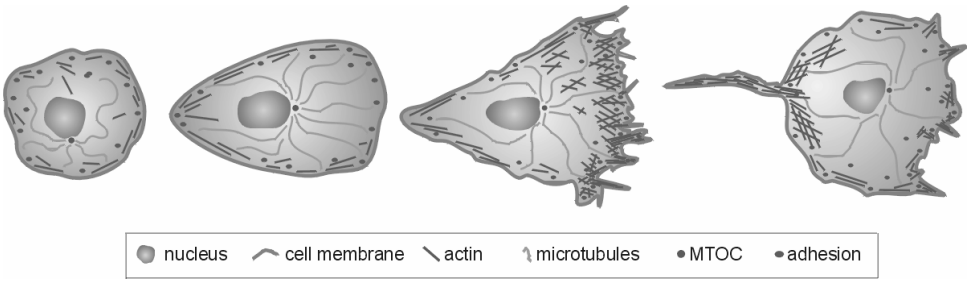

FIGURE 1. Sequential steps during cell migration **(CLR)**.
Schematic representation of a cell migrating to the right and of the processes occurring during this movement. Upon a migratory stimulus the cell polarizes and intra cellular structures like MTs and the MTOC are redistributed. Then cellular protrusions are formed by actin polymerisation at the leading edge. New adhesions are formed in the regions of protrusion. MTs target adhesions behind the cell front and at the rear of the cell to support adhesion turnover. Adhesions at the rear of the cell are disassembled and the – often very tiny – tail is retracted by actin-Myosin II interactions. As a result there is a net movement of the cell body.

Growing and branching filaments are terminated in their elongation by capping protein, which specifically binds to barbed ends of the filaments [29]. Anti-capping proteins like Ena/VASP regulate this activity [30,31]. The local activation of Arp2/3 complex and (anti)- capping proteins induces the growth of the lammelipodium in a particular direction and thus these proteins are involved in directed cell migration. The smaller filopodial extension is regulated differently although some proteins are shared. Filopodia have actin organized as parallel bundles and by forming long tiny spikes they serve to explore the matrix and microenvironment. These filopodia are involved in chemotactic cell movements, for example guidance of endothelial sprouts during angiogenesis and migration towards vessels of metastasising tumour cells [32,33].

The Rho GTPases are key regulators of both actin organization and adhesion formation [26,34]. Rho GTPases are members of the large GTP-binding proteins family consisting of proteins with a GTP-binding globular domain. GTP can be hydrolyzed to GDP thereby inducing a conformational change and inactivation of the protein. Rho GTPases are Ras-related small GTPases and activated

and inactivated by guanine nucleotide exchange factors (GEFs) and GTPase activating proteins (GAPs) respectively. These factors regulate the binding of GTP (active) and GDP (inactive) [35]. Important members of the Rho GTPases family are Rac, Cdc42 and RhoA. For Rac functions have been described in lammellipodial extension, formation of small focal adhesion complexes in the leading edge and, recently, a role in directionality of cell movements [16,36,37]. Cdc42 is a master regulator of cell polarity [38,39]. From the cell body towards the leading edge of migrating cells Cdc42 is activated and Cdc42 has a inhibiting role at sites where lammellipodia are formed [40,41]. For RhoA roles in adhesion maturation at sites behind the leading edge and MTs stabilisation have been described [35,42].

Within newly formed protrusions novel cell adhesions have to be established to attach the cell to the underlying extra cellular matrix (ECM). These adhesions are transient and depending on the cell type, substratum and migration profile, their turnover can be very high [43]. Adhesions initiate as small so-called focal complexes, which are mainly localised at the cell leading edge. These newly formed adhesions stabilize the lammelipodium and attach the protrusion to the ECM. In tightly adhering and non-motile or slowly migrating cells these focal complexes mature into focal adhesions. As mentioned earlier small Rho GTPases exhibit a regulating role in formation and maturation of adhesions. Among many other receptors involved in attachment to the matrix, the integrin receptors are major adhesion and migration inducing factors [44]. Integrins support adhesion to the ECM (or other cells) by linking matrix components outside the cell to actin filaments inside the cell [45]. Next to this adhering function, integrins are known for their 'inside-out signalling' via activation by cytoplasmic signals [46]. Binding of matrix components results in clustering of integrins, which triggers intracellular signals that regulate formation and strengthening of adhesions. The exact composition of the complex of proteins can be seen as a kind of measure for the lifetime of the adhesions [43]. During the turnover and maturation of new adhesions at the front of migrating cells MTs are reported to serve as transport route for adhesion components as growing MTs target adhesions at leading edges of migrating cells [47,48]. In addition, these adhesions are the sites that generate propulsive force, serving as tracking sites of migration as the cell moves forward [49]. This force is generated by the interactions of actin filaments with Myosin II. Myosin Light Chain Kinase (MLCK) and Rho kinase (ROCK) regulate activation of Myosin II in the new membrane protrusion and sites where new adhesions are formed [50]. Activation of Myosin II results in an increased contractility which in turn may consequence in a propulsive force.

Finally, for a cell to move from one place to another, adhesions in the rear of the cell are disassembled, allowing detachment and movement of the cell body. Due to the adhesions in the rear of migrating cells that are not completely disassembled cells often show a long tail. The generated force needs to release integrins from the actin cytoskeleton. When a cell has retracted its tail, the net movement of the cell has completed and the cell initiates the next movement. Movement of a cell in a particular direction for a certain period of time is defined as directed migration. High directional cell migration is observed during chemotaxis.

INTRINSIC AND EXTERNAL FACTORS INFLUENCING CELL MIGRATION

Although fundamental cell migration mechanisms are shared between different migrating cells, the cell type and its environment are crucial for the migration response. As mentioned above some cells, like fibroblasts and astrocytes, are known as slow-moving, while other cell types, like T-cells and tumour cells, are fast-moving. In addition, different tumour cells can differ strongly in their intrinsic migratory capacity.

Next to cell type, the nature of the surrounding matrix determines to great extent the migration response of cells. From studies applying different *in vitro* experimental set ups attribution of different matrix components has been studied. However, the methods used did influence the effects found [51,52] (see also Chapter 2 of this thesis). An additional complication of *in vitro* methods is the translation to the *in vivo* situation. The composition of the ECM, availability of growth factors and cytokines, physiological circumstances like pH and pO2 and, of course, intracellular constituents, all together regulate cell polarity and migration. Recently, novel data on *in vivo* tumour cell migration during metastasis formation has revealed that the same tumour cells *in vivo* can migrate up to 10 times faster as compared to *in vitro* cell migration assays [33,53]. This strongly confirms the dependency on environmental settings of the migration response of cells. An additional example of different settings and their effects on migration is the motility of EC during angiogenesis in wounds versus tumours. EC have to migrate in order to form or repair blood vessels but the triggers and environmental settings strongly differ and will influence the migratory response. The process of tumour angiogenisis is described in Chapter 5 of this thesis. These differences and the need for an assay to study contribution of specific matrix components to cell migration led us to develop a novel migration approach. The validation and application of this assay is the theme of the first part of this thesis.

REFERENCES

1. Gilbert S.F.ed (2003). "Developmental Biology," Sinauer, Sunderland, MA.
2. Ridley, A. J., Schwartz, M. A., Burridge, K., Firtel, R. A., Ginsberg, M. H., Borisy, G., Parsons, J. T., and Horwitz, A. R. (2003). Cell migration: integrating signals from front to back. *Science.* 302, 1704-1709.
3. Cotran, R. S., Kumar, V., Collins, T., Robbins, S. L., and Schmitt, B. (1999). "Robbins Pathological Basis of Disease," Saunders, Philadelphia, PA.
4. Lauffenburger, D. A. and Horwitz, A. F. (1996). Cell migration: a physically integrated molecular process. *Cell* 84, 359-369.
5. Nabi, I. R. (1999). The polarization of the motile cell. *J Cell Sci* 112 (Pt 12), 1803-1811.
6. Gundersen, G. G. and Bulinski, J. C. (1988). Selective stabilization of microtubules oriented toward the direction of cell migration. *Proc.Natl.Acad.Sci.U.S.A* 85, 5946-5950.
7. Gotlieb, A. I., Subrahmanyan, L., and Kalnins, V. I. (1983). Microtubule-organizing centers and cell migration: effect of inhibition of migration and microtubule disruption in endothelial cells. *J Cell Biol* 96, 1266-1272.
8. Gotlieb, A. I., May, L. M., Subrahmanyan, L., and Kalnins, V. I. (1981). Distribution of microtubule organizing centers in migrating sheets of endothelial cells. *J Cell Biol* 91, 589-594.
9. Palazzo, A. F., Joseph, H. L., Chen, Y. J., Dujardin, D. L., Alberts, A. S., Pfister, K. K., Vallee, R. B., and Gundersen, G. G. (2001). Cdc42, dynein, and dynactin regulate MTOC reorientation independent of Rho-regulated microtubule stabilization. *Curr Biol* 11, 1536-1541.
10. Gomes, E. R., Jani, S., and Gundersen, G. G. (2005). Nuclear movement regulated by Cdc42, MRCK, myosin, and actin flow establishes MTOC polarization in migrating cells. *Cell* 121, 451-463.
11. Serrador, J. M., Nieto, M., and Sanchez-Madrid, F. (1999). Cytoskeletal rearrangement during migration and activation of T lymphocytes. *Trends Cell Biol* 9, 228-233.
12. Etienne-Manneville, S. (2004). Cdc42--the centre of polarity. *J Cell Sci* 117, 1291-1300.
13. Raftopoulou, M., Etienne-Manneville, S., Self, A., Nicholls, S., and Hall, A. (2004). Regulation of cell migration by the C2 domain of the tumour suppressor PTEN. *Science.* 303, 1179-1181.
14. Merlot, S. and Firtel, R. A. (2003). Leading the way: Directional sensing through phosphatidylinositol 3-kinase and other signaling pathways. *J Cell Sci* 116, 3471-3478.
15. Rodriguez, O. C., Schaefer, A. W., Mandato, C. A., Forscher, P., Bement, W. M., and Waterman-Storer, C. M. (2003). Conserved microtubule-actin interactions in cell movement and morphogenesis. *Nat.Cell Biol.* 5, 599-609.
16. Pankov, R., Endo, Y., Even-Ram, S., Araki, M., Clark, K., Cukierman, E., Matsumoto, K., and Yamada, K. M. (2005). A Rac switch regulates random versus directionally persistent cell migration. *J.Cell Biol.* 170, 793-802.
17. Wen, Y., Eng, C. H., Schmoranzer, J., Cabrera-Poch, N., Morris, E. J., Chen, M., Wallar, B. J., Alberts, A. S., and Gundersen, G. G. (2004). EB1 and APC bind to mDia to stabilize microtubules downstream of Rho and promote cell migration. *Nat.Cell Biol.* 6, 820-830.
18. Goode, B. L., Drubin, D. G., and Barnes, G. (2000). Functional cooperation between the microtubule and actin cytoskeletons. *Curr Opin Cell Biol* 12, 63-71.
19. Small, J. V., Stradal, T., Vignal, E., and Rottner, K. (2002). The lamellipodium: where motility begins. *Trends Cell Biol* 12, 112-120.
20. Mitchison, T. J. and Cramer, L. P. (1996). Actin-based cell motility and cell locomotion. *Cell* 84, 371-379.
21. De La Cruz, E. M., Mandinova, A., Steinmetz, M. O., Stoffler, D., Aebi, U., and Pollard, T. D. (2000). Polymerization and structure of nucleotide-free actin filaments. *J.Mol.Biol* 295, 517-526.
22. Kirschner, M. W. (1980). Implications of treadmilling for the stability and polarity of actin and tubulin polymers in vivo. *J.Cell Biol* 86, 330-334.
23. Machesky, L. M., Atkinson, S. J., Ampe, C., Vandekerckhove, J., and Pollard, T. D. (1994). Purification of a cortical complex containing two unconventional actins from Acanthamoeba by affinity chromatography on profilin-agarose. *J.Cell Biol* 127, 107-115.
24. Welch, M. D. and Mullins, R. D. (2002). Cellular control of actin nucleation. *Annu.Rev.Cell Dev.Biol* 18, 247-288.
25. Pollard, T. D., Blanchoin, L., and Mullins, R. D. (2000). Molecular mechanisms controlling actin filament dynamics in nonmuscle cells. *Annu.Rev.Biophys.Biomol.Struct.* 29, 545-576.
26. Nobes, C. D. and Hall, A. (1999). Rho GTPases control polarity, protrusion, and adhesion during cell movement. *J Cell Biol* 144, 1235-1244.
27. Pollard, T. D. and Borisy, G. G. (2003). Cellular motility driven by assembly and disassembly of actin filaments. *Cell* 112, 453-465.
28. Bamburg, J. R., McGough, A., and Ono, S. (1999). Putting a new twist on actin: ADF/cofilins modulate actin dynamics. *Trends Cell Biol.* 9, 364-370.
29. Cooper, J. A. and Schafer, D. A. (2000). Control of actin assembly and disassembly at filament ends. *Curr.Opin.Cell Biol.* 12, 97-103.

30. Bear, J. E., Loureiro, J. J., Libova, I., Fassler, R., Wehland, J., and Gertler, F. B. (2000). Negative regulation of fibroblast motility by Ena/VASP proteins. *Cell* 101, 717-728.
31. Bear, J. E., Svitkina, T. M., Krause, M., Schafer, D. A., Loureiro, J. J., Strasser, G. A., Maly, I. V., Chaga, O. Y., Cooper, J. A., Borisy, G. G., and Gertler, F. B. (2002). Antagonism between Ena/VASP proteins and actin filament capping regulates fibroblast motility. *Cell* 109, 509-521.
32. Gerhardt, H., Golding, M., Fruttiger, M., Ruhrberg, C., Lundkvist, A., Abramsson, A., Jeltsch, M., Mitchell, C., Alitalo, K., Shima, D., and Betsholtz, C. (2003). VEGF guides angiogenic sprouting utilizing endothelial tip cell filopodia. *J.Cell Biol.* 161, 1163-1177.
33. Condeelis, J. and Segall, J. E. (2003). Intravital imaging of cell movement in tumours. *Nat.Rev.Cancer* 3, 921-930.
34. Nobes, C. D. and Hall, A. (1995). Rho, rac, and cdc42 GTPases regulate the assembly of multimolecular focal complexes associated with actin stress fibers, lamellipodia, and filopodia. *Cell* 81, 53-62.
35. Wittmann, T. and Waterman-Storer, C. M. (2001). Cell motility: can Rho GTPases and microtubules point the way? *J Cell Sci* 114, 3795-3803.
36. Cory, G. O. and Ridley, A. J. (2002). Cell motility: braking WAVEs. *Nature* 418, 732-733.
37. Rottner, K., Hall, A., and Small, J. V. (1999). Interplay between Rac and Rho in the control of substrate contact dynamics. *Curr Biol* 9, 640-648.
38. Etienne-Manneville, S. and Hall, A. (2001). Integrin-mediated activation of Cdc42 controls cell polarity in migrating astrocytes through PKCzeta. *Cell* 106, 489-498.
39. Etienne-Manneville, S. and Hall, A. (2003). Cdc42 regulates GSK-3beta and adenomatous polyposis coli to control cell polarity. *Nature* 421, 753-756.
40. Itoh, R. E., Kurokawa, K., Ohba, Y., Yoshizaki, H., Mochizuki, N., and Matsuda, M. (2002). Activation of rac and cdc42 video imaged by fluorescent resonance energy transfer-based single-molecule probes in the membrane of living cells. *Mol.Cell Biol* 22, 6582-6591.
41. Srinivasan, S., Wang, F., Glavas, S., Ott, A., Hofmann, F., Aktories, K., Kalman, D., and Bourne, H. R. (2003). Rac and Cdc42 play distinct roles in regulating PI(3,4,5)P3 and polarity during neutrophil chemotaxis. *J Cell Biol* 160, 375-385.
42. Ridley, A. J. (2001). Rho GTPases and cell migration. *J Cell Sci* 114, 2713-2722.
43. Webb, D. J., Parsons, J. T., and Horwitz, A. F. (2002). Adhesion assembly, disassembly and turnover in migrating cells -- over and over and over again. *Nat Cell Biol* 4, E97-100.
44. Mostafavi-Pour, Z., Askari, J. A., Parkinson, S. J., Parker, P. J., Ng, T. T., and Humphries, M. J. (2003). Integrin-specific signaling pathways controlling focal adhesion formation and cell migration. *J Cell Biol* 161, 155-167.
45. Hood, J. D. and Cheresh, D. A. (2002). Role of integrins in cell invasion and migration. *Nat Rev Cancer* 2, 91-100.
46. Geiger, B., Bershadsky, A., Pankov, R., and Yamada, K. M. (2001). Transmembrane crosstalk between the extracellular matrix--cytoskeleton crosstalk. *Nat.Rev.Mol.Cell Biol.* 2, 793-805.
47. Small, J. V., Geiger, B., Kaverina, I., and Bershadsky, A. (2002). How do microtubules guide migrating cells? *Nat Rev Mol Cell Biol* 3, 957-964.
48. Small, J. V. and Kaverina, I. (2003). Microtubules meet substrate adhesions to arrange cell polarity. *Curr Opin Cell Biol* 15, 40-47.
49. Beningo, K. A., Dembo, M., Kaverina, I., Small, J. V., and Wang, Y. L. (2001). Nascent focal adhesions are responsible for the generation of strong propulsive forces in migrating fibroblasts. *J Cell Biol* 153, 881-888.
50. Totsukawa, G., Wu, Y., Sasaki, Y., Hartshorne, D. J., Yamakita, Y., Yamashiro, S., and Matsumura, F. (2004). Distinct roles of MLCK and ROCK in the regulation of membrane protrusions and focal adhesion dynamics during cell migration of fibroblasts. *J.Cell Biol.* 164, 427-439.
51. Herbst, T. J., McCarthy, J. B., Tsilibary, E. C., and Furcht, L. T. (1988). Differential effects of laminin, intact type IV collagen, and specific domains of type IV collagen on endothelial cell adhesion and migration. *J.Cell Biol.* 106, 1365-1373.
52. Pratt, B. M., Harris, A. S., Morrow, J. S., and Madri, J. A. (1984). Mechanisms of cytoskeletal regulation. Modulation of aortic endothelial cell spectrin by the extracellular matrix. *Am.J.Pathol.* 117, 349-354.
53. Wang, W., Goswami, S., Sahai, E., Wyckoff, J. B., Segall, J. E., and Condeelis, J. S. (2005). Tumour cells caught in the act of invading: their strategy for enhanced cell motility. *Trends Cell Biol.* 15, 138-145.

Chapter 2

Differential Effects of Matrix and Growth Factors on Endothelial and Fibroblast Motility: Application of a Modified Cell Migration Assay

Remco van Horssen[1]
Niels Galjart[2]
Joost A. P. Rens[1]
Alexander M. M. Eggermont[1]
Timo L. M. ten Hagen[1]

[1]Laboratory of Experimental Surgical Oncology, Department of Surgical Oncology, Erasmus MC – Daniel den Hoed Cancer Centre and [2]Department of Cell Biology and Genetics, Erasmus MC, Rotterdam, The Netherlands

J Cell Biochem (2006) 30 Jun Epub

Note: This chapter contains figures that are also available in full colour (labeled with 'CLR'). These colour figures can be found in the Appendix of this book (page 209) and in the online version (via Medical Library, Erasmus MC). The supplementary movies are available online via *Journal of Cellular Biochemistry*.

ABSTRACT

Cell migration is crucial in virtually every biological process and strongly depends on the nature of the surrounding matrix. An assay, which enables real-time studies on the effects of defined matrix components and growth factors on cell migration, is not available. We have set up a novel, quantitative migration assay, which enables unharmed cells to migrate along a defined matrix. Here, we used this "barrier-based" assay to define the contribution of fibronectin (FN) and Collagen-I (Col-I) to Vascular Endothelial Growth Factor (VEGF), basic Fibroblast Growth Factor (bFGF) and Lysophosphatidic acid (LPA)-induced cell migration of endothelial cells (EC) and fibroblasts. In EC, both FN and Col-I stimulated migration, but FN-induced motility was random, while net movement was inhibited. Addition of bFGF and VEGF overcame the effect of FN, with VEGF causing directional movement. In contrast, in 3T3 fibroblasts, FN stimulated motility and this effect was enhanced by bFGF. This motility was more efficient and morphologically completely different compared to LPA stimulation. Strikingly, directional migration of EC was not paralleled by higher amounts of stable microtubules or an increased reorientation of the microtubule-organizing centre. For EC the FN-effect appeared concentration dependent, high FN was able to induce migration, while for fibroblasts both low and high concentrations of FN induced motility. Besides showing distinct responses of the different cells to the same factors, these results address contradictive reports on FN and show that the interplay between matrix components and growth factors determines both pattern and regulation of cell migration.

INTRODUCTION

Cell migration is essential in virtually all processes during life. Migration of cells is fundamental in both physiological and pathological processes, like embryonic development, wound healing, cancer metastasis and angiogenesis. Migration of a cell starts with the formation of membrane protrusions in the direction of migration, resulting from actin polymerisation [1,2]. In order for a cell to migrate, it also needs to polarize itself, which may lead to the formation of triangular cell morphology, with a broad leading edge at the front of the cell and a thinning trailing edge at the back. During polarized migration, the Golgi apparatus and microtubule-organizing centre (MTOC) often are positioned in front of the nucleus. In a number of cells types microtubules (MTs) selectively stabilize in the migration direction during polarization of the cell [3]. To sustain polarity and migration, new adhesions between the cell and the extracellular matrix (ECM), called focal complexes, are established at the leading edge [4], some of which develop into focal adhesions, while focal adhesions at the trailing

edge of the cell are broken down. Cell migration can be subdivided into random motility and directed migration, the latter indicating whether a cell is able to maintain a single direction of migration for prolonged periods of time. The composition of the ECM, availability of growth factors and cytokines, physiological circumstances like pH and pO2 and, of course, intracellular constituents, all together regulate cell polarity and migration.

The nature of the surrounding matrix determines to great extent the migration response of cells. For example during angiogenesis, migration of endothelial cells (EC) is crucial [5,6]. However, the setting in which EC migration takes place strongly differs. During tumour angiogenesis activated EC migrate along a newly formed matrix, of which the components are synthesized by EC, tumour cells, and stromal cells [7]. During wound angiogenesis, in contrast, migration is stimulated by factors triggered by damage to EC and ECM. These differences affect migratory response of the EC. However, currently no assay is available to address these differences.

Among angiogenic factors, vascular endothelial growth factor (VEGF) and basic fibroblast growth factor (bFGF) are well known for their regulation of proliferation, migration and differentiation of EC [8], but how these two factors relate to each other and to ECM-components, when inducing EC migration during tumour angiogenesis, remains to be elucidated. It would be of great benefit if an assay existed in which these distinct signalling cascades leading to EC migration could be dissected [9].

Measurement of freely moving and spreading cells ('single cell movements') has provided valuable knowledge on cell migration, including that of EC [10], but these studies do not address properties of a layer of cells in which cells are migrating into a defined cell-free area. Moreover the matrix-composition is not completely defined. Several migration assays have been developed to deal with this, such as the "Agarose droplet" [11], the "Teflon ring" [12] and the "Flexi perm disc" [13] assays. The two latter are used rarely and are not always applicable for living cell imaging. The agarose droplet assay has practical disadvantages regarding reproducibility and standardisation. Using the "Teflon Ring" it has been reported that fibronectin (FN) has an inhibitory effect while Collagen-I (Col-I) has a stimulatory effect on EC migration. However only a fixed time-point of 6 days was taken [12]. To address some of these disadvantages the "Boyden Chamber" assay and the "scratch" or "wound healing" assay are often used [14]. In the first, cells are scored for their ability to pass a filter, but cellular behaviour during migration cannot be monitored. To study the role of ECM-components in this assay either migration towards (factors in lower chamber) or into (pre-coated filters) migration mediators can be evaluated. A migration-promoting role for ECM-components like

FN, Col-I and laminin has been reported for several cell types like fibroblasts, tumour cells and EC. For EC, Col-I and FN have been suggested to be more effective than laminin [15-17]. For FN the results seem dependent on the assay used, suggesting that either other factors are involved or that the assay does not properly address the effect of FN.

In the "scratch" assay, cells are grown until they reach confluence and a mechanical wound (the "scratch") is made, for example with a tip or needle, after which cells can migrate into the novel cell-free area (the "wound"). For EC it has been reported that no differences exist between FN and Col-I in their effect on migration [18]. For fibroblasts and other stromal cells FN is reported to provide a trail for the cells during migration into the wound [19]. Strikingly in 3-D assays the migration of fibroblasts is not induced by FN [20]. Using the 'scratch' assay, the behaviour of cells can be monitored accurately, however, cells have to be removed in order to generate a cell-free area. The remaining cells first have to recover from wounding, and the composition of ECM in the newly generated, cell-free region, cannot be controlled. The "scratch" assay is therefore a suitable *in vitro* model for wound healing and tissue repair, but whether it represents an authentic migration model has not yet been addressed.

We developed a novel migration assay that overcomes most of the restrictions of the other methods and enabled us to study the distinct contributions of ECM-components and growth factors. Using this novel "barrier" migration assay we studied migration of EC and 3T3 fibroblasts, to enable comparison of well-established cell culture systems for motility. For EC we document a migration promoting effect of Col-I and FN, yet a strong inhibitory effect of FN on directional movement. The addition of Vascular Endothelial Growth Factor (VEGF) or basic Fibroblast Growth Factor (bFGF) mitigated the effect of FN, with VEGF being a stimulator of effective migration and bFGF a stimulator of general motility. In contrast, in 3T3 fibroblasts, FN stimulated migration in the absence of growth factors. Addition of bFGF augmented migration distance induced with FN. Lysophosphatidic acid (LPA), a known regulator of fibroblast polarity in the "scratch" assay [21-23], induced comparable migration in the presence or absence of FN, while migration was less directional and morphologically different compared to bFGF. For EC we observed a FN dose dependent migration, while for fibroblasts FN appeared capable of inducing motility in all concentrations tested. Firstly, together these data reveal novel interplay between growth factors and the ECM in cell motility. Secondly, we expect wide spread application of the "barrier" assay because of its ease of use. This will lead to a more detailed dissection of the molecular mechanisms and signalling pathways underlying cell

migration and the specific functions of ECM-components and growth factors in this fundamental process.

MATERIALS AND METHODS

Cell culture and reagents

Human Umbilical Vein Endothelial Cells (HUVEC) were isolated as described [24]. Human Micro Vascular Endothelial Cells (HMVEC) and Swiss 3T3 fibroblasts were obtained commercially (Biowhittaker). EC were used between passage 3 and 7 and cultured in Human Endothelial-SFM (Invitrogen) supplemented with 10% New Born Calf Serum, 5% Human Serum, 20 ng/ml bFGF and 100 ng/ml EGF, in gelatine-coated flasks. Swiss 3T3 fibroblasts were cultured in DMEM/Ham's F10, 1:1 (Biowhittaker) supplemented with 10% Fetal Calf Serum. VEGF-165 and bFGF were from PeproTech. Gelatine, Thalidomide and LPA were from Sigma-Aldrich. Collagen-I was from Biowhittaker, Fibronectin from Roche Diagnostics and SU-5416 was a gift of dr. W. Leenders, department of Pathology, University Medical Centre St Radboud, Nijmegen, The Netherlands.

Migration Assays

For the novel "barrier-based" migration assay, a cover slip was placed in an Attofluor incubation chamber (Molecular Probes), which was subsequently sterilized. In this set up a removable, sterile circular migration barrier was placed (see Fig. 1D), which fits tightly in the chamber and prevents cell growth in the middle of the coated cover slip. Cells were seeded around this barrier and grown until confluence. Subsequently, the migration barrier was removed; cells were washed twice and then incubated with the appropriate medium. The incubation chamber was placed on an inverted microscope and migration of cells was measured for 24 h. The "scratch" or "wound healing" assay was essentially performed as described by many others [22], using the same Attofluor incubation chamber, but instead of the barrier a scratch was made to generate a cell-free area.

Time-lapse imaging of both types of cell migration assays was done on Axiovert 100 M microscopes, equipped with either an AxioCam HRC digital camera or an AxioCam MRC digital camera (Carl Zeiss). Microscopes were controlled by AxioVision software, version 3.1 and 4.0 respectively. Cells in the incubation chamber were maintained at 37 ^{o}C in a constantly humidified atmosphere, with controlled and heated CO_2-flow. Cells were imaged every 12 min with a 10X/0.30 PLAN-NEOFLUAR objective lens or every 2 min with a 20X/0.40 LD ACHROPLAN objective lens (Carl Zeiss).

During migration of HUVEC, Human Endothelial-SFM without standard growth factors was added to the cells, supplemented with bFGF (200 ng/ml), or VEGF-165 (10 ng/ml). In specific experiments the inhibitors Thalidomide (40 μg/ml) or SU-5416 (30 μM) were also added. Preceding 3T3 fibroblast migration, cells were starved in serum-free culture medium (supplemented with 5 mg/ml fatty-acid free BSA) for 24-48 h [23] before the barrier was removed, or the scratch was induced. During migration the same medium was added, supplemented with LPA (5 μM) or bFGF (200 ng/ml). Coated cover slips were made by adding FN (1, 10 or 100 μg/ml) or Col-I (1 or 60 μg/ml) in serum-free medium to the cover slips and incubated for at least 1 h at 37 ^{o}C.

Analysis of cell migration

Parameters of cell migration, including the total and average migrated distance, migration velocity, effective migration distance, number of cell divisions and cell polarity, were obtained from time-lapse movies, taking the nucleus as a reference. For each treatment at least 10 migrating cells per experiment and at least 3 independent migration assays were performed. After cell division one of the daughter cells was followed. Migration velocity was calculated after 2 and 24 h, by dividing migration distance by time. Both the total distance (reflecting random motility) and effective distance (reflecting directed migration) were calculated, the latter being the distance that cells travelled towards the centre of the cover slip (see Fig. 1E). We also calculated effective migration, being the percentage of movement towards the centre of the cover slip reflecting directionality during migration with the lesser changes in direction being defined as more effective migration. We determined the cell elongation in the migration direction as extend of cell polarity (expressed as the ratio of the length of the major to the length of the minor cell axis) as described [25], from at least 8 migrating cells per time point and at least 3 independent assays. All measurements were done using AxioVision 3.0 software. Images from the time-lapse analysis were processed in Adobe Premiere to generate movies for publication.

Immunofluorescence Staining

After time-lapse microscopy, cells were washed twice with PBS and fixed in 4% paraformaldehyde at room temperature for 15 min or in ice-cold methanol at –20 ^{o}C. After washing in PBS, cells were permeabilized using 0,15% Triton-X-100 for 10 min and blocked in blocking solution (1% BSA / 0,05% Tween-20 / PBS) for 45 min. Incubations with first (1/200) and secondary (1/500) antibody-mixtures were done for 1 h at room temperature in blocking solution. In between incubations cells were washed 3 times with PBS / 0,05% Tween-20. Thereafter cells were briefly washed in 70% and

100% ethanol respectively, air dried and mounted onto microscope slides using 10 µl of a 1:1 solution of VectaShield (Vector Laboratories) and DAPI-DABCO (Molecular Probes). Primary antibodies used: β-tubulin, acetylated microtubules, vinculin (Sigma-Aldrich) and f-actin (Molecular Probes). Secondary antibodies used: Alexa Fluor 594 (Molecular Probes) and FITC (Nordic) conjugated antibodies. Immunofluorescent images were taken using an Axiovert 100 M microscope with 40X/1.30 Oil-FLUAR objective lens (Carl Zeiss) and an ORCA II ER camera (C4742-98, Hamamatsu Photonics Systems). Image analysis, including MTs stabilization, MTOC reorientation and f-actin staining pattern analysis was performed using Openlab 3.1.5 software (Improvision). Cells were scored as positive for acetylated tubulin if the cell contained 10 or more brightly stained MTs [26], MTOC were considered reoriented using the 'triangle-method' as described [27], f-actin staining pattern was analysed by counting the stress fibre and dense peripheral bands containing cells and vinculin-positive adhesions were counted per cell. For all measurements a total of 50-150 cells in 3 different experiments were counted. Images were processed using Adobe Photoshop.

Statistics

Groups were compared with the Kruskal-Wallis H test and considered significant different when $p<0.05$. Different groups were compared using the Mann-Whitney U test (Bonferroni correction for multiple testing).

Supplemental online material

All movies, except 1-3, are phase-contrast or DIC movies of HUVEC and 3T3 cells migrating for 24 h. Movies contain 121 frames and were accelerated resulting in a 12 s movie. Movies 1-3 are phase-contrast movies of HUVEC migrating for 8 h and contain 960 frames. QuickTime movies correspond with still images in the figures: movie 1-3 (Fig. 1A-C), movie 4-6 (Fig. 2A), movie 7-11 (Fig. 4B), movie 12-23 (Fig. 6B), movie 24-27 (Fig. 8B) and movie 27-30 (Fig. 8D). Movie legends can be found at the end of this chapter and movies are available online via the *Journal of Cellular Biochemistry*.

RESULTS

Novel cell migration assay

To study cell migration into a defined cell-free area often the 'scratch' assay is used. However, by introducing the 'scratch', damage is inflicted to the cells (Fig. 1A, Movie 1). Damaged cells leak cytoplasm and secrete growth factors and cytokines. Most importantly, the matrix is not defined. It is

made up of cell-secreted ECM-components, growth factors and contaminated with cell-remnants. A defined matrix is also absent when single cell motility is studied. Spreading and migrating cells modify matrix composition and cells will follow patterns of other cells (Fig 1B, Movie 2). Within the novel cell migration assay both the cells and the matrix are intact and the matrix can be strictly controlled (Fig. 1C, Movie 3). A round, removable barrier, which prevents cell growth in the middle of the cover slip, is placed in a culture device (Fig. 1D, top view). After removal of the barrier, cells can migrate into the cell-free area, which has a matrix composition that has been defined a priori. In this "barrier-based" or "barrier" assay, cells and matrix are untouched.

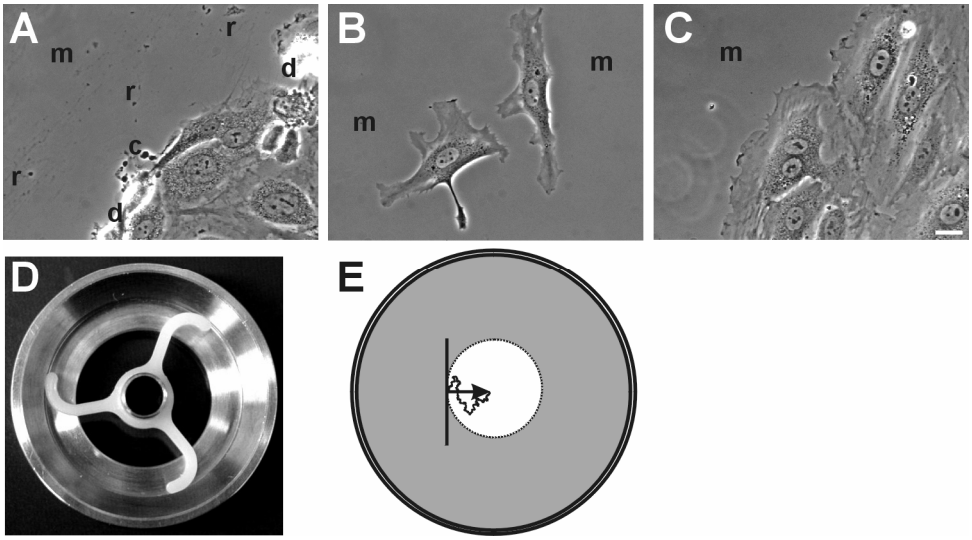

FIGURE 1. Set up and rationale of the "barrier-based" migration assay.
A. High magnification of HUVEC at migration front in the "scratch" assay. The cells are damaged (d) and leak cytoplasm (c). The matrix (m) in the cell-free area is contaminated with cell secreted ECM-components, growth factors and cell remnants (r). See also Movie 1.
B. High magnification of HUVEC migrating in a 'single cell motility assay'. During attachment, spreading and prior to the assay the cells have manipulated the matrix (m). Migrating cells follow paths of other cells where the matrix is optimal. See also Movie 2.
C. High magnification of HUVEC at migration front in the novel assay. Cells and matrix (m) are left unharmed. The matrix can be defined and manipulated. Bar, 10 μm, See also Movie 3.
D. Top-view photograph of the Attofluor incubation chamber with the migration barrier in place. The barrier-insert fits tightly but can be removed easily. Cells are seeded on the cover slip outside the insert and are grown until confluence, after which the barrier is removed.
E. Schematic representation of the "barrier-based" migration assay as *in vitro* model for cell migration. After removal of the barrier a cell-free area (white) is present next to a cell-dense region (grey). Cells are able to migrate into an area whose matrix composition is defined. The freehand line indicates the hypothetical path of a single cell (not in scale). The total migrated distance of this cell is tracked over time. Migration towards the centre of the cover slip (arrow) is defined as effective distance reflecting the directionality of cell movements. Other parameters like velocity, cell divisions and cell morphology changes were obtained from migration movies.

Cell movement and morphology are tracked over time and several parameters can be determined, including (effective) migration distance (Fig. 1E), velocity, cell polarity and number of cell divisions.

Response of EC to growth factors and inhibitors using the novel migration assay

The "barrier" migration assay was tested by studying the response of EC to VEGF and bFGF, and inhibitors of these growth factors to verify the assay (Fig. 2). In basal medium (containing serum, without additional growth factors) HUVEC showed little motility and cells started to die at later time points, due to the lack of growth factors [8] (Fig. 2A, left panel, Movie 4). When bFGF or VEGF was added, EC started to migrate into the gelatin-coated cell-free area. Under these conditions, remarkable differences were observed between the two growth factors (Fig. 2A, see also Movie 5, 6). bFGF triggered EC to migrate long distances and induced frequent cell divisions over 24 h. VEGF also induced migration but, cells migrated over less distance and sporadically divided during migration. However, the effective distance migrated (migration towards the middle of the cover slip, Fig. 2C) was the same for both growth factors, so the migration efficiency (effective migration divided by total migration) is higher under a VEGF regime (Fig. 2E). In accordance with these results, cell elongation measurements revealed that bFGF treatment increased the ratio of major to minor axis length approximately 1.5 fold, while treatment with VEGF caused a steeper increase of approximately 2.5-3 fold (Fig. 2D). Interestingly this steeper increase became visible only after 12 h and later.

Next to migration-induction in this novel assay we studied inhibition of migration as well using two well-defined inhibitors. Thalidomide, known to affect bFGF [28] and SU-5416 (a Flk-1/KDR receptor-kinase inhibitor), known to inhibit VEGF [29]-induced cell activity. Thalidomide blocked the migration distance and efficiency induced by bFGF, albeit incompletely. Addition of SU-5416 only slightly affected migrated distance induced by VEGF, but migration efficiency was completely inhibited (Fig. 2B, C). These results indicate that VEGF-signalling through Flk-1 is essential for directed EC migration. Flk-1 is known to effect VEGF-induced EC migration [30], but the effect on directionality is novel. Experiments done with HMVEC showed similar results (data not shown). We confirmed specificity of these two inhibitors by combining them with the non-matching growth factors. No inhibitory effects were seen when SU-5416 was used in combination with bFGF or Thalidomide with VEGF (Fig. 2 F, G).

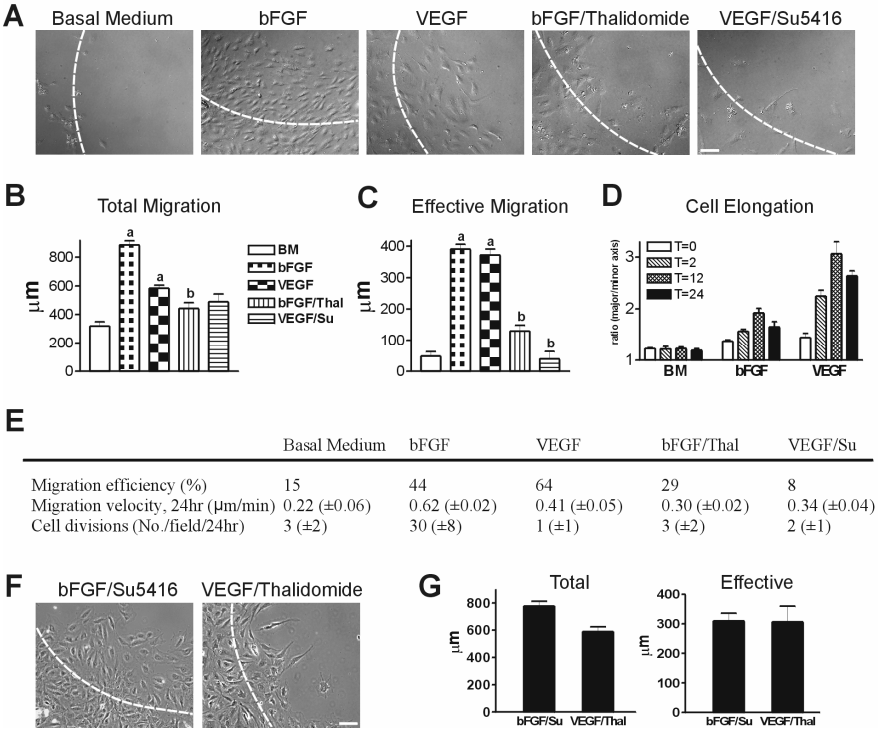

E

	Basal Medium	bFGF	VEGF	bFGF/Thal	VEGF/Su
Migration efficiency (%)	15	44	64	29	8
Migration velocity, 24hr (μm/min)	0.22 (±0.06)	0.62 (±0.02)	0.41 (±0.05)	0.30 (±0.02)	0.34 (±0.04)
Cell divisions (No./field/24hr)	3 (±2)	30 (±8)	1 (±1)	3 (±2)	2 (±1)

FIGURE 2. bFGF and VEGF induced HUVEC migration in "barrier" assay.
Confluent HUVEC grown on gelatin were allowed to migrate for 24 h using the "barrier" migration assay.
A. HUVEC migration under different treatments (basal medium (with serum, without additional growth factors), bFGF (200 ng/ml), VEGF (10 ng/ml), bFGF/Thalidomide (200 ng/ml, 40 μg/ml), VEGF/SU5416 (10 ng/ml, 30 μM)) respectively. The white dashed line indicates the migration front at T=0 h. Pictures are at T=24 h and obtained from migration movies available in supplemental movies 4-6, Bar, 100 μm
B. Total migrated distance (μm) per cell. At least 30 cells in at least 3 separate experiments were measured.
C. Effective migrated distance (μm) per cell. Effective migration is the distance towards the centre of the cover slip (straight line from starting-point to end-point, perpendicular to the migration front, reflecting directionality of the movement). At least 30 cells in at least 3 separate experiments were measured. Data in B and C represent mean ± SEM of at least three independent experiments; [a] P<0.05 compared to basal medium; [b] P<0.05 compared to non-inhibited control.
D. Cell elongation measurements as indication for cell polarity for bFGF and VEGF compared to basal medium (BM). Ratios of major and minor axis were measured in 24 cells in three separate experiments.
E. Migration efficiency and velocity were calculated from the measurements shown in B and C. Cell divisions were counted over the time course of the experiment. Numbers represent the average ± SD of three independent experiments.
F. Specificity of bFGF and VEGF inhibitors. SU5416 and Thalidomide were used in combination with their unmatched growth factors. No inhibition was observed. Bar, 100 μm
G: Total and effective distance (μm) per cell after 24 h of growth factors with their unmatched inhibitors. Data represent mean ± SEM of three independent experiments.

bFGF and VEGF induce differential effects on cytoskeleton and adhesions

To examine the effect of bFGF and VEGF on cytoskeleton and adhesions, we stained fixed cells for actin, MTs and vinculin after 24 h of migration (Fig. 3). In non-stimulated cells f-actin appeared mostly as dense peripheral bands, no stress-fibres were seen and the MT network was poorly developed. In

bFGF-induced cells, we observed stress-fibres, f-actin accumulation at the edge of cells, and a well-developed MT network. Interestingly, in most of the VEGF-induced cells f-actin is predominantly organized into stress-fibres and hardly as dense peripheral bands (Fig. 3A, C). In these cells the MT network is well organized, with network endings in what could be focal adhesions. To test the effect on adhesions we stained for vinculin. In addition to the cytoskeleton, adhesions are also distinct between the growth factors. We observed many vinculin-positive adhesions in VEGF-treated cells (Fig. 3B, C). When exposed to bFGF, cells displayed a rather heterogeneous expression of vinculin-positive adhesions, and were lacking in some cells. Interestingly, bFGF treated cells displayed longer and stretched adhesions compared to VEGF. These results suggest differential organization of the EC cytoskeleton and adhesions upon stimulation with bFGF of VEGF.

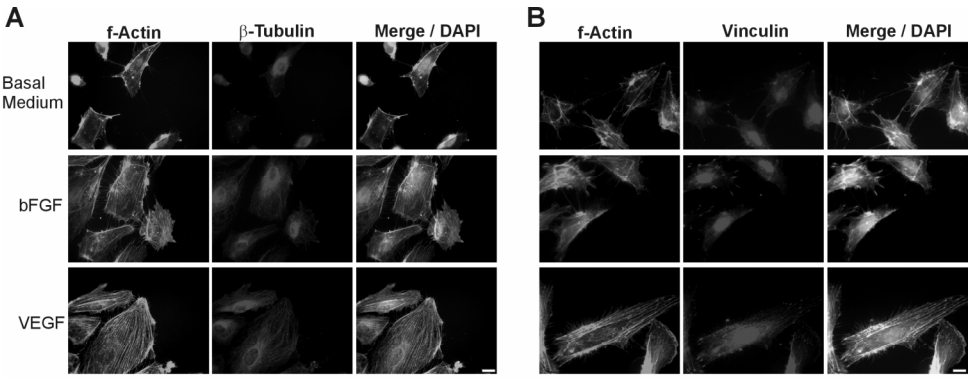

C

f-Actin	BM	bFGF	VEGF
Stress Fibers (%)	13,33	44,83	92,31
Dense Peripheral Bands (%)	100	65,52	15,38
No. FA/cell (±SD)	3 (±1)	6 (±7)	14 (±7)

FIGURE 3. Visualization of cytoskeleton and adhesions of HUVEC in "barrier-based" assay **(CLR)**.
HUVEC were induced to migrate for 24 h, fixed and stained for f-actin, β-tubulin and nuclei (A) or f-actin, vinculin and nuclei (B).
A. Cytoskeleton differences in cells at migration front in a negative control with basal medium, treated with bFGF (200 ng/ml) or treated with VEGF (10 ng/ml), Bar, 10 μm.
B. Differences in adhesions number and structure in cells migrating in a negative control with basal medium, treated with bFGF (200 ng/ml) or treated with VEGF (10 ng/ml), bar, 10 μm
C. Quantification of stress fibres, dense peripheral bands and vinculin-positive focal adhesions (FA). For actin some cells contain both types of staining resulting in more than 100 % total.

Contribution of ECM components to EC migration studied in "barrier" and "scratch" assays

Our findings with the "barrier" assay are in accordance with previous reports on EC migration [28,29], indicating the validity of this assay. Next we used this setup to examine contribution of growth factors and ECM components to EC migration and compared these results with the "scratch" assay (Fig. 4).

FN coating induced migration of EC, but inhibited effective migration (Fig. 4A, B). After several hours the cells started to die (Movie 7). FN was reported to inhibit EC migration using the Teflon ring assay [12], while on freely moving EC it induced migration [31]. Here we show that FN indeed can induce migration of a layer of EC, but that individual cell movement is random resulting in an inhibition of net movement. Col-I, a known inducer of EC migration [12], induced total and effective migration (Fig. 4A, B, Movie 8). These data indicate that Col-I is able to promote EC migration in basal medium. Strikingly, neither the effect of FN, nor that of Col-I, as compared to gelatine-controls, was observed in the "scratch" assay after 2 h (Fig. 4A). After 24 h effective migration distances showed the same trend in the "scratch" assay as in the "barrier" assay after 2 h, but the differences were much less pronounced (Fig. 4A, B and Movies 9-11). These results are not unexpected since during the days prior to wounding EC have been able to deposit their own ECM, thereby obscuring effects of the defined coating. Interestingly, in the "scratch" assay less EC died after 24 h than in the "barrier" assay (Fig. 4B).

When bFGF was added in the two assays, EC migration was stimulated and only little variation was seen between the coatings (Fig. 4A, B). bFGF is a potent stimulator of EC migration, which is able to supersede the inhibitory effects of FN on directionality even after 2 h, as shown in the novel assay.

Addition of VEGF to EC in the "barrier" assay induced migration along gelatin and FN (Fig. 4A, B). Compared to bFGF, VEGF induced similar effective migration distances after 2 and 24 h, but the total migration distance was lower, resulting in higher migration efficiency (see also Fig. 2). VEGF had no additive effect on cell migrating along Col-I. Addition of VEGF in the "scratch" assay had similar but smaller effects on the effective distance because this distance was already high without addition of growth factors in this assay.

Taken together, using the "scratch" assay, only mild differences between coatings and growth factors became apparent after 24 h. We hypothesize that, molecules secreted by EC cells prior to the assay, obscure migration responses. Due to the nature of the "scratch" assay, in particular the wounding and the presence of cell secreted material, one can not distinguish between the contribution of ECM components and growth factors to cell migration. Hence, crucial effects are overlooked.

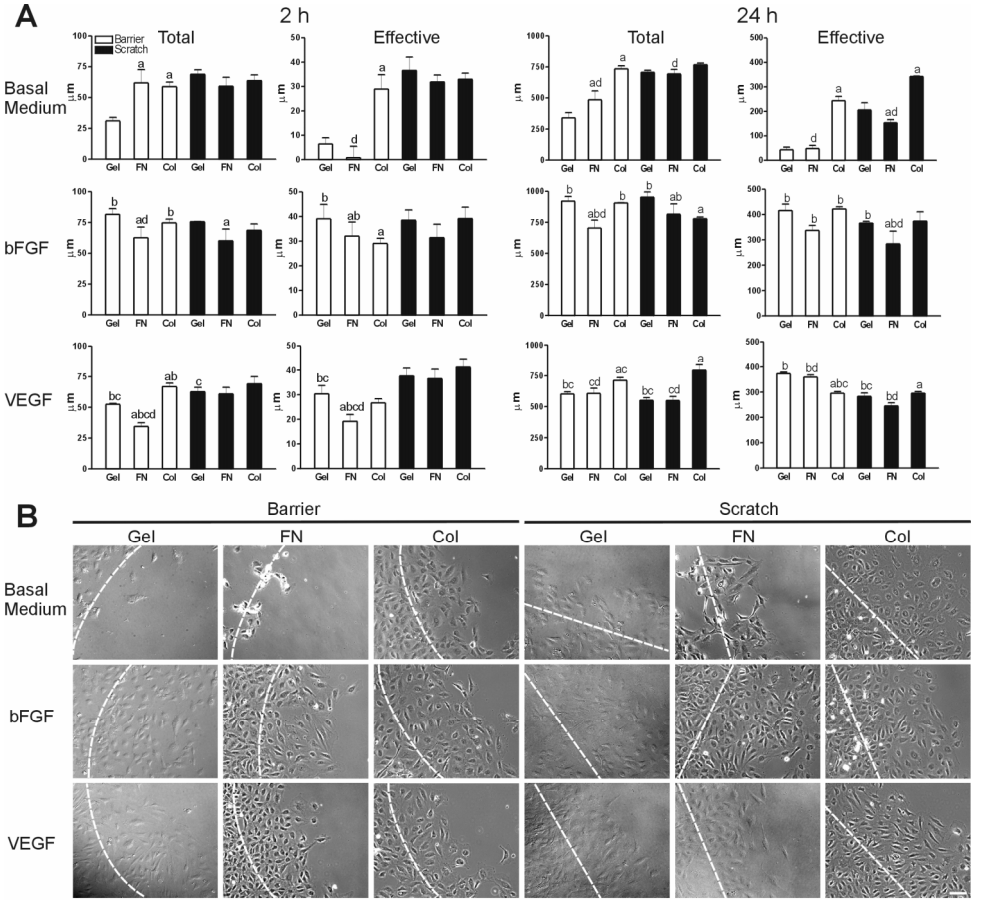

FIGURE 4. Effect of ECM-components on HUVEC migration in "barrier" and "scratch" assays.
HUVEC were grown on different coatings until confluence and followed for 24 h after removal of the barrier or introduction of a scratch.
A. Total and effective migration distances (µm) after 2 and 24 h of HUVEC treated with basal medium (control), bFGF (200 ng/ml) or VEGF (10 ng/ml) compared between "scratch" and "barrier" assay when coated with gelatine, FN or Col-I. At least 30 cells in at least 3 separate experiments were measured. Especially after 2 h (before cell division takes place) almost all differences found in the "barrier" assay are overlooked when using the "scratch" assay. All data represent mean ± SEM of at least three independent experiments; [a] P<0.05 FN and Col-I compared to gelatine; [b] P<0.05 bFGF and VEGF compared to basal medium (BM); [c] P<0.05 bFGF compared to VEGF on same coating; [d] P<0.05 FN compared to Col-I in same treatment.
B. Pictures of migrating HUVEC in both assays, after 24 h obtained from migration movies (Movies 7-11 for basal medium experiments). White dashed lines indicate the migration front at T=0 h, bar, 100 µm.

MT stabilization and MTOC reorientation during EC migration in "barrier" and "scratch" assays

In a number of cell types stable MTs are selectively formed after wounding and subsequent addition of serum [3,26]. Because stabilization of MTs and MTOC reorientation are involved in migration and directionality [23,32,33] we studied these phenomena in EC using the "barrier" and the "scratch"

assay. Before induction of migration we did not observe differences in stable MTs staining in either assay and between coatings (Fig. 5A, C, T=0). In the "scratch" assay VEGF treatment caused a mild increase in the number of cells with stable MTs, on gelatine and Col-I. Using the "barrier" assay this increase was much more pronounced (Fig. 5C).

The organization of the stable MT network was different between bFGF and VEGF. VEGF induced more stable MTs, presumably because EC were quite elongated and flattened (Fig. 5B). The MTs staining pattern was used to estimate the orientation of the MTOC with respect to the migration direction. At T=0 the percentage of MTOC oriented towards the cell-free area was approximately 33%, as expected (Fig. 5D). In the "barrier" assay MTOC reorientation towards the cell-free area increased, irrespective of coating used or factor added. In the "scratch" assay we found more cells with reoriented MTOC after bFGF and VEGF treatment, an effect that was dependent on the coating used (Fig. 5D). These results indicate that orientation of the MTOC was influence by the assay used: a purely defined matrix and removal of contact inhibition reoriented the MTOC irrespective of treatment. Importantly, our results on MT stabilization and MTOC reorientation do not correlate with cell migration. For example, addition of bFGF has little effect on stable MTs, while migration is strongly stimulated.

Contribution of ECM components to fibroblast migration studied in "barrier" and "scratch" assays

To further study the contribution of ECM and growth factors to migration we tested the widely used 3T3 fibroblast cells. Without growth factors or FN-coating, 3T3 cells migrated similarly in "barrier" and "scratch" assays with respect to total and effective distances, both after 2 and 24 h (Fig. 6A). However, on FN-coated glass total and effective migration was strongly stimulated in the "barrier" assay (Fig. 6A, B, Movies 12-15). Thus, using the "barrier" assay we identified FN as a stimulant of fibroblast migration which is in accordance with previous literature [19]. Lysophosphatidic acid (LPA) is a known regulator of 3T3 fibroblast polarity and migration in the "scratch" assay [21,22]. We recapitulated these results in our "scratch" setup (Fig. 6). In the "barrier" assay without coating, LPA had a stimulatory effect on total and effective 3T3 migration (Fig. 6A). Strikingly, coating with FN did not alter migration induction by LPA (Fig. 6A, B, Movies 16-19). Thus, the "barrier" assay revealed that FN does not influence the migration pattern stimulated by LPA or vice versa.

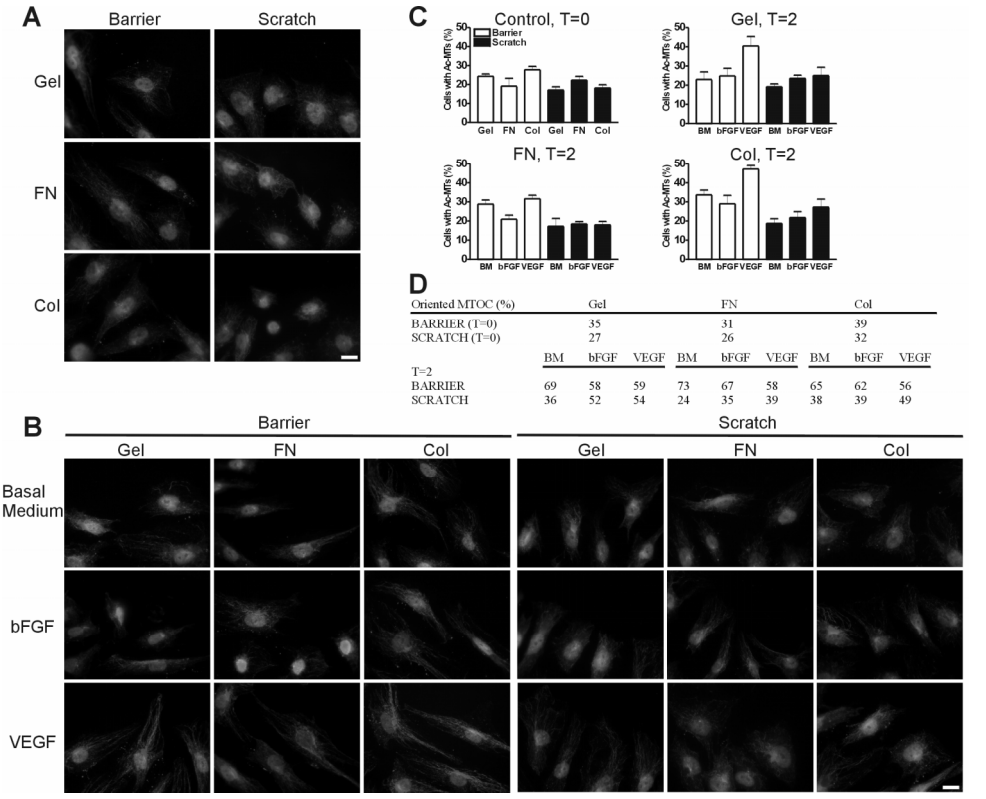

FIGURE 5. MT stabilization and MTOC reorientation during HUVEC migration **(CLR)**.
HUVEC were grown on different coatings until confluence and allowed to migrate for 2 h after removal of the barrier, or introduction of a scratch. After 0 h (control) or 2 h the cells were fixed and stained for acetylated MTs (red) and nuclei (blue). Cell-free area is at upper/upper-right for all pictures.
A. Control cells at T=0 h. HUVEC were grown until confluence and immediately after removing the barrier or introducing the scratch, cells were fixed and stained. Bar, 100 μm
B. Migrating HUVEC in both assays, fixed at T=2 h. Except for VEGF-treated cells in the "barrier" assay no differences were seen. The elongated cells bundle their stable MTs. Bar, 100 μm
C. Quantification of acetylated MTs. Cells with stable MTs are depicted as percentage of total counted cells. Data represent mean ± SEM of 3 independent experiments.
D. Table represents percentage of cells with MTOC oriented towards the cell-free area after 0 and 2 h for the different treatments in the two assays.

Without coating, bFGF treatment resulted in similar induction of migration in both assays (Fig. 6). Noticeably, bFGF combined with FN increased total and effective migration considerably in the "barrier" assay. In contrast, using the "scratch" assay, this stimulatory effect of bFGF on FN action was not perceptible (Fig. 6A). The morphology of 3T3 cells after treatment with bFGF and FN was remarkably different, as compared to LPA-treated fibroblasts. LPA-induced cells demonstrate a triangle-like morphology, while cells exposed to bFGF are very elongated and forming long thin extensions that seem to probe the environment (Fig. 6B, Movies 20-23). Thus, for fibroblasts we

showed an enhancing effect of bFGF on the FN-induced cell migration when we used the assay with defined matrix composition.

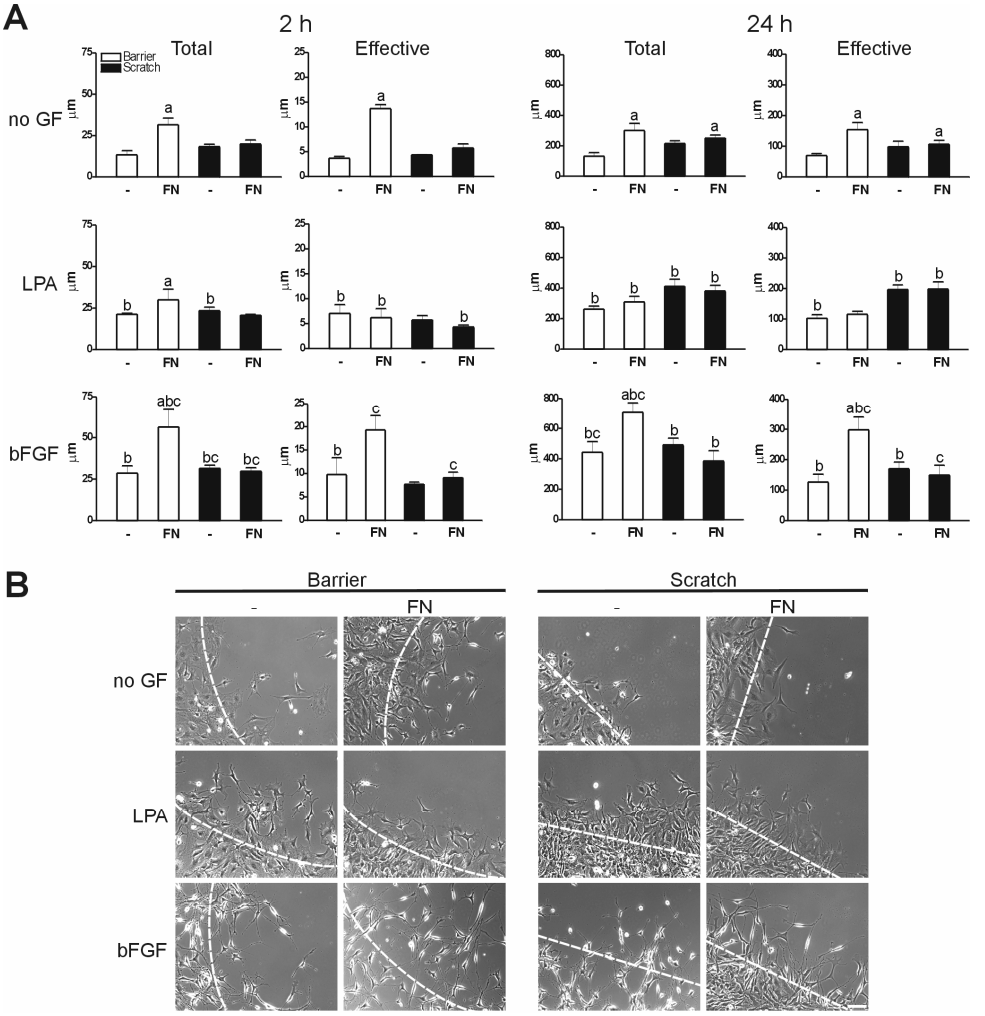

FIGURE 6. Effect of FN on 3T3 migration in "barrier" and "scratch" assays

3T3 fibroblasts were grown with and without FN coating until confluence, starved for 24-48 h and followed for 24 h after removal of the barrier, or introduction of a scratch.

A. Total and effective migration distances (μm) after 2 and 24 h of 3T3 cells treated with serum-free medium (no GF, control), LPA (5 μM) or bFGF (200 ng/ml) compared between "scratch" and "barrier" assay with and without FN-coating. At least 30 cells in at least 3 separate experiments were measured. In the "barrier" assay FN induces migration that was strongly augmented by bFGF, a feature not observed when the "scratch" assay was used. All data represent mean ± SEM of at least three independent experiments; [a] $P<0.05$ FN compared to non-coated controls; [b] $P<0.05$ LPA and bFGF compared to no GF; [c] $P<0.05$ bFGF compared to LPA on same coating.

B. Pictures of migrating 3T3 cells in both assays, after 24 h obtained from migration movies (Movies 12-23). The white dashed line indicates the migration front at T=0 h. Movies clearly show major differences in migration profile and cell morphology, Bar, 100 μm.

MT stabilization and MTOC reorientation during fibroblast migration in "barrier" and "scratch" assays

LPA is reported to induce stable MTs during fibroblast migration [23,34]. We investigated whether this also holds true for bFGF in the presence or absence of FN. Before induction of migration, similar numbers of fibroblasts were expressing stable MTs, irrespective of coating (Fig. 7A, C).

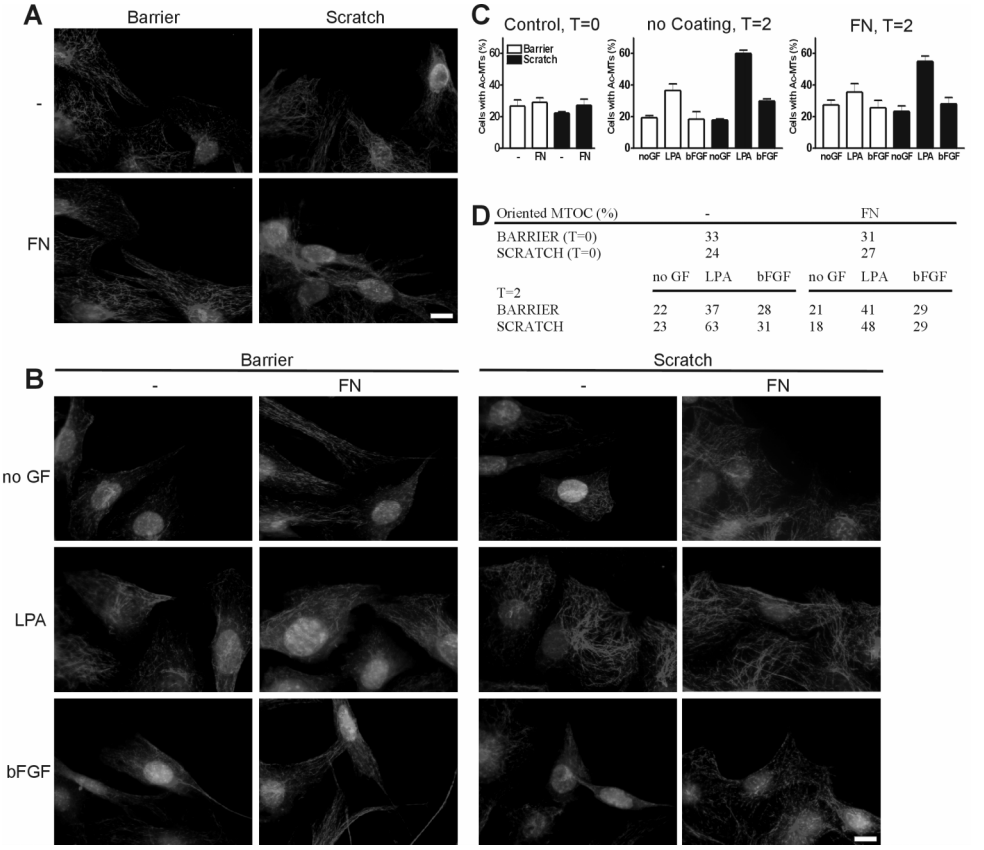

FIGURE 7. MT stabilization and MTOC reorientation during 3T3 migration **(CLR)**.
3T3 fibroblasts were grown with and without FN-coating until confluence and allowed to migrate for 2 h after removal of the barrier or introduction of a scratch. After 0 h (control) or 2 h the cells were fixed and stained for acetylated MTs (red) and nuclei (blue). Cell-free area is at upper/upper-right for all pictures.
A. Control cells at T=0 h. 3T3 cells were grown until confluence and immediately after removing the barrier or introducing the scratch, cells were fixed and stained. Bar, 100 μm.
B. Migrating 3T3 cells in both assays, fixed at T=2 h. Especially in the "scratch" assay LPA induced MT stabilization irrespective of coating. Bar, 100 μm.
C. Quantification of acetylated MTs. Cells with stable MTs are depicted as percentage of total counted cells. Data represent mean ± SEM of 3 independent experiments.
D. Table represents percentage of cells with MTOC oriented towards the cell-free area. LPA induces MTOC reorientation in "scratch" assay both with and without FN. In spite of a lack in MTOC reorientation a strong migration profile with accompanied cell morphology was seen when the cells were exposed to bFGF and FN (Fig. 6)

In both assays LPA treatment increased the number of cells with stable MTs. However, the increase in stable MTs was much higher in the "scratch" assay (Fig. 7B, C). The findings with LPA are consistent with other reports on LPA [3,21]. In addition, we showed that the 'scratch' attributed strongly to the LPA-induced MT stabilization. Exposure of the cells to bFGF however only slightly increased the number of cells with stable MTs (Fig. 7B, C). When we used the stable MTs staining pattern to estimate the reorientation of the MTOC we found that LPA is most effective in both assays, irrespective of coating. MTOC reorientation after bFGF treatment is hardly influenced (Fig. 7D). These results again indicate that increased MT stabilization and MTOC reorientation do not correlate with enhanced migration capacity, as the migration induced by bFGF and FN is higher and more effective than LPA. The pattern of migration, rather than the induction of migration itself, seems to correlate with MT stabilization.

Effect of matrix-concentration on EC and fibroblast migration

Because it is known that the concentration of matrix components can influence migration properties [31,35] we tested whether our FN results were concentration dependent. To validate the effect on EC we performed migration assays with 1, 10 and 100 μg/ml FN-coating. With low FN (1 μg/ml) we found the same inhibitory effect compared to 10 μg/ml (Fig. 4A), however high FN (100 μg/ml) induced EC migration (Fig. 8A). In addition, we used low Col-I (1 μg/ml) and migration was still strongly induced. For both the high FN and low Col-I the cells lost contact during migration (Fig. 8B, Movies 24-26). Interestingly, when we lowered or increased FN concentration in fibroblast migration assays we did not observed any differences. For both the low, intermediate (Fig. 6), and high FN concentration migration was stimulated and enhanced when combined with bFGF (Fig. 8C). Morphological changes during migration were also comparable between the different FN concentrations. Without GF cells migrated into the FN-coated cell-free area and long and tiny extensions were formed that was increased when bFGF was added (Fig. 8 D, Movies 27-30). These results show that along a defined FN-coating EC migration is dependent on the concentration (low inhibitory and high stimulatory), while for fibroblasts induction of migration seems independent on FN concentration and seems a capacity of FN itself.

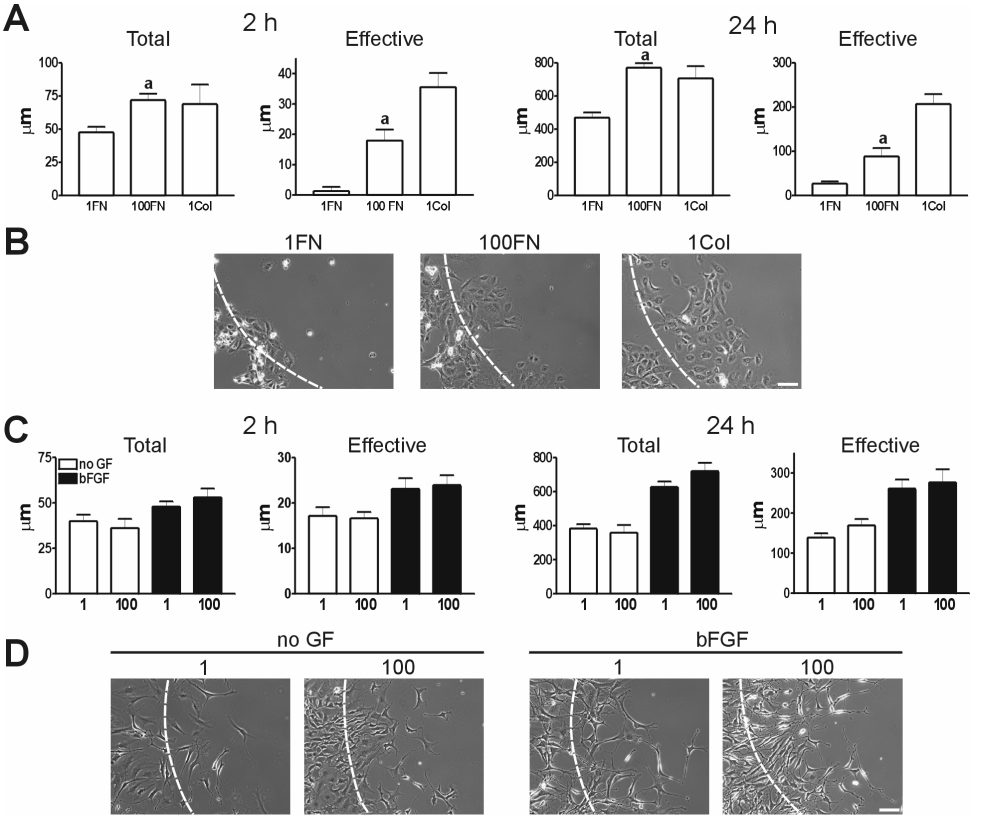

FIGURE 8. Effect of matrix concentration on migration response in "barrier" assay.

A. Total and effective migration distances (μm) after 2 and 24 h of HUVEC migration along high (100 μg/ml) and low (1 μg/ml) FN and low (1 μg/ml) Col-I concentration. Data represent mean ± SEM of at least three independent experiments. [a] $P<0.05$ 1FN compared to 100FN.

B. Pictures of migrating HUVEC in basal medium after 24 h obtained from migration movies (Movies 24-26). White dashed lines indicate the migration front at T=0 h, Bar, 100 μm.

C. Total and effective migration distances (μm) after 2 and 24 h of 3T3 migration along high (100 μg/ml) and low (1 μg/ml) FN concentration treated with serum-free medium (no GF) of bFGF (200 ng/ml). Data represent mean ± SEM of at least three independent experiments. No statistical differences were found between low and high FN.

D. Pictures of migrating 3T3 cells after 24 h obtained from migration movies (Movies 27-30) revealing no obvious differences when FN concentration is altered. The white dashed line indicates the migration front at T=0 h, Bar, 100 μm.

DISCUSSION

During the process of tumourangiogenesis EC are activated and migrate along a tightly controlled (provisional) matrix. During wound healing, in contrast, the EC and matrix are damaged before migration starts. An assay to overcome these differences is currently not available. In this chapter we present a novel approach to study cell migration to address these differences. Using this novel "barrier-based migration" assay, we showed that both FN and Col-I stimulate EC migration. Col-I thereby induced directionality as well, while FN-induced migration was completely random resulting in

an inhibition of the net cell movement. In earlier reports using the "Teflon ring" assay FN inhibited and Col-I stimulated EC migration [12]. However, these results were obtained after 6 days. With the "Boyden Chamber" assay both FN and Col-I were reported to stimulate EC migration [15]. Our finding, that FN can induce migration but not directionality, could explain the previous opposing data. Using the previous assays no continuous monitoring of the cells was possible so no distinction could be made between distance and directionality, overlooking the actual effect of FN. FN is known to be an essential substrate for EC adhesion and growth [36]. Possibly, turnover of adhesion sites in EC cultured on FN is too slow to facilitate net movement of the cells. Our results with the novel "barrier-based" migration assay indicate that questions in cell migration research can be addressed which are overlooked by the 'scratch' assay. Cells can be stimulated with (secreted) factors of choice and migrate along a predetermined and controlled matrix and are not harmed at the onset of the experiment. The interplay between matrix and growth factors strongly determines migration response and pattern.

EC migration appeared dependent on the FN concentration. Compared to low concentrations, high FN levels induced migration. In contrast to Col-I, cells do not migrate in sheets, but gaps appear. These gaps are absent when FN is combined with growth factors. Addition of bFGF or VEGF overcame the matrix effects, which was not seen when the "scratch" assay was used. These data indicate that in the latter set-up EC have secreted ECM-components prior to the assay, which strongly interfere with the migratory response. The inhibitory effect of FN, as observed in the "barrier" assay, was overlooked in the "scratch assay".

Recently it was shown that cells can migrate without the formation of lamellipodia [37]. Our results with EC show that a far-reaching cell body is not necessary for migration, although this increases directionality as shown by the differences in migration pattern between bFGF and VEGF. The formation of a tightly organized cell body, as induced by VEGF results in directionality, pointing at lamellipodium-forming factors as likely candidates in sustaining cell-polarity [38,39]. The cytoskeletal distinction we found between the two growth factors are in agreement with endothelial wound healing [40]. How these and the effects on adhesions relate to migration pattern and matrix compositions have to be studied in further experiments.

In EC a mild MT stabilization was found for VEGF-treatment in the "barrier" assay with gelatine and Col-I coating. In all other treatments no change in stable MTs expressing cells was found. This may imply that MT stabilization in EC is not necessary for (directional) cell movement along defined matrix components. However, MT stabilization might be involved in determining migration pattern and

morphology. Simultaneously, MTOC reorientation was not linked to migration or treatment of EC. These differences indicate that reorientation of the MTOC might be regulated by particular ECM-components but also occurs when contact inhibition is obviated. The contact inhibition feature of EC might interfere with studying the role of matrix proteins on MTOC reorientation in this novel system. Other cell types will be used in future experiments to elucidate this phenomenon. Moreover other factors are likely involved in regulation of directionality of EC migration, as is shown for other cell types as well [33]. MT stabilization and MTOC reorientation may be involved in other steps during EC migration, like the formation and stabilization of a widely spread cell body (strongly induced by VEGF). MTs and MTOC are essential for EC migration and angiogenesis, but their functions and regulation may be more complex than assumed until now [41,42].

3T3 fibroblasts, which are slow-moving cells, have been very well-documented in terms of migration in the “scratch” assay and the cytoskeletal rearrangements that accompany this process [43,44]. In this setup, LPA was shown to be a unique regulator of 3T3 cell polarity [22,23]. We therefore used 3T3 cells to compare “barrier” and “scratch” assays and examined the effect of LPA in relation to bFGF and FN. Surprisingly, when FN was used as coating, a strong induction of migration was observed with the “barrier” assay in the absence of LPA. With the “scratch” assay we did not observe this effect. These data indicate that the “scratch” assay is not suited to study the role of defined ECM-components in migration. FN, reported to be an inhibitor of EC migration [45], is an inducer of fibroblast migration. Different cell types respond dissimilar to the same matrix-component, which shows that the composition of the matrix is essential for cell motility.

In the “barrier” assay the action of bFGF is more pronounced on 3T3 cell migration compared to LPA. In addition, bFGF enhances FN-induced migration, whereas LPA does not. Besides the matrix itself, the interplay with growth factors is crucial for both migration response and morphology. The strong synergistic bFGF-FN effect was not observed using the “scratch” assay. The marked differences in morphology between the bFGF and LPA-induced migrating cells may imply that migration signalling is distinct as well. Additionally, bFGF and FN-induced migration was not accompanied by increased stabilization of MTs or MTOC reorientation, whereas LPA in the “scratch” assay induced stable MTs very efficiently, as reported previously [22,46]. The treatments however, resulted in strongly different migration profiles and morphologies of the 3T3 cells during migration. Whereas MT stabilization and MTOC reorientation is induced in fibroblasts stimulated with LPA in the “scratch” assay, this does not imply that efficient migration of 3T3 cells always requires such drastic intracellular rearrangements. Recently it has been reported that FN induces the stabilization of MTs

in cells that have started to adhere to glass [26]. We hypothesize that the FN-induced stabilization is important for cell adherence and spreading, and might occur when cells prepare to migrate and polarize. During actual movement of a cell the regulation of MT stabilization likely is altered. MTs will be stabilized but for a smaller time frame when the cell is quickly moving as seen when stimulated with bFGF. In addition, the stable MTs show a complete distinct distribution in bFGF vs LPA treated cells. This may be related to the strongly different morphology of the cells and complicates the comparison and measurements made in this study.

Taken together, the introduction of the novel migration assay strongly expands the possibilities for cell migration research and reveals that the interplay between matrix and growth factors determines migration response and morphology. Our results show that FN differentially affects cell migration between cell types and growth factors. The assay is easy to imply, overcomes restrictions of other assays and reveals differences overlooked by other assays. Contribution of the cytoskeleton, cell-matrix interactions, matrix-growth factor interactions and signalling during migration of unharmed cells are open avenues for future research. Wider application of this novel “barrier-based” migration assay has the potential to answer important questions related to cell migration in many physiological and pathological processes.

ACKNOWLEDGEMENTS

We thank the Erasmus Medical Instrumentation Service (EMI) for technical assistance with development of materials and the people of the Oncology and Cell Biology departments for discussions and comments on the manuscript.

REFERENCES

1. Horwitz, A. R. and Parsons, J. T. (1999). Cell migration--movin' on. *Science* 286, 1102-1103.
2. Lauffenburger, D. A. and Horwitz, A. F. (1996). Cell migration: a physically integrated molecular process. *Cell* 84, 359-369.
3. Gundersen, G. G. and Bulinski, J. C. (1988). Selective stabilization of microtubules oriented toward the direction of cell migration. *Proc.Natl.Acad.Sci.U.S.A* 85, 5946-5950.
4. Nobes, C. D. and Hall, A. (1995). Rho, rac, and cdc42 GTPases regulate the assembly of multimolecular focal complexes associated with actin stress fibers, lamellipodia, and filopodia. *Cell* 81, 53-62.
5. Carmeliet, P. (2003). Angiogenesis in health and disease. *Nat.Med.* 9, 653-660.
6. Bergers, G. and Benjamin, L. E. (2003). Tumourigenesis and the angiogenic switch. *Nat.Rev.Cancer* 3, 401-410.
7. Bussolino, F., Mantovani, A., and Persico, G. (1997). Molecular mechanisms of blood vessel formation. *Trends Biochem Sci* 22, 251-256.
8. Cross, M. J. and Claesson-Welsh, L. (2001). FGF and VEGF function in angiogenesis: signalling pathways, biological responses and therapeutic inhibition. *Trends Pharmacol Sci* 22, 201-207.
9. McDonald, D. M., Teicher, B. A., Stetler-Stevenson, W., Ng, S. S., Figg, W. D., Folkman, J., Hanahan, D., Auerbach, R., O'Reilly, M., Herbst, R., Cheresh, D., Gordon, M., Eggermont, A., and Libutti, S. K. (2004). Report from the

society for biological therapy and vascular biology faculty of the NCI workshop on angiogenesis monitoring. *J.Immunother.* 27, 161-175.

10. Fischer, R. S., Fritz-Six, K. L., and Fowler, V. M. (2003). Pointed-end capping by tropomodulin3 negatively regulates endothelial cell motility. *J Cell Biol* 161, 371-380.
11. Varani, J., Orr, W., and Ward, P. A. (1978). A comparison of the migration patterns of normal and malignant cells in two assay systems. *Am.J.Pathol.* 90, 159-171.
12. Pratt, B. M., Harris, A. S., Morrow, J. S., and Madri, J. A. (1984). Mechanisms of cytoskeletal regulation. Modulation of aortic endothelial cell spectrin by the extracellular matrix. *Am.J.Pathol.* 117, 349-354.
13. Ohtaka, K., Watanabe, S., Iwazaki, R., Hirose, M., and Sato, N. (1996). Role of extracellular matrix on colonic cancer cell migration and proliferation. *Biochem.Biophys.Res.Commun.* 220, 346-352.
14. Auerbach, R., Auerbach, W., and Polakowski, I. (1991). Assays for angiogenesis: a review. *Pharmacol Ther* 51, 1-11.
15. Herbst, T. J., McCarthy, J. B., Tsilibary, E. C., and Furcht, L. T. (1988). Differential effects of laminin, intact type IV collagen, and specific domains of type IV collagen on endothelial cell adhesion and migration. *J.Cell Biol.* 106, 1365-1373.
16. McCarthy, J. B. and Furcht, L. T. (1984). Laminin and fibronectin promote the haptotactic migration of B16 mouse melanoma cells in vitro. *J.Cell Biol.* 98, 1474-1480.
17. Postlethwaite, A. E., Keski-Oja, J., Balian, G., and Kang, A. H. (1981). Induction of fibroblast chemotaxis by fibronectin. Localization of the chemotactic region to a 140,000-molecular weight non-gelatin-binding fragment. *J.Exp.Med.* 153, 494-499.
18. Young, W. C. and Herman, I. M. (1985). Extracellular matrix modulation of endothelial cell shape and motility following injury in vitro. *J.Cell Sci.* 73, 19-32.
19. Clark, R. A., An, J. Q., Greiling, D., Khan, A., and Schwarzbauer, J. E. (2003). Fibroblast migration on fibronectin requires three distinct functional domains. *J.Invest Dermatol.* 121, 695-705.
20. Schor, S. L., Ellis, I., Dolman, C., Banyard, J., Humphries, M. J., Mosher, D. F., Grey, A. M., Mould, A. P., Sottile, J., and Schor, A. M. (1996). Substratum-dependent stimulation of fibroblast migration by the gelatin-binding domain of fibronectin. *J.Cell Sci.* 109 (Pt 10), 2581-2590.
21. Cook, T. A., Nagasaki, T., and Gundersen, G. G. (1998). Rho guanosine triphosphatase mediates the selective stabilization of microtubules induced by lysophosphatidic acid. *J.Cell Biol.* 141, 175-185.
22. Nagasaki, T. and Gundersen, G. G. (1996). Depletion of lysophosphatidic acid triggers a loss of oriented detyrosinated microtubules in motile fibroblasts. *J.Cell Sci.* 109 (Pt 10), 2461-2469.
23. Wen, Y., Eng, C. H., Schmoranzer, J., Cabrera-Poch, N., Morris, E. J., Chen, M., Wallar, B. J., Alberts, A. S., and Gundersen, G. G. (2004). EB1 and APC bind to mDia to stabilize microtubules downstream of Rho and promote cell migration. *Nat.Cell Biol.* 6, 820-830.
24. Jaffe, E. A., Nachman, R. L., Becker, C. G., and Minick, C. R. (1973). Culture of human endothelial cells derived from umbilical veins. Identification by morphologic and immunologic criteria. *J Clin Invest* 52, 2745-2756.
25. Totsukawa, G., Wu, Y., Sasaki, Y., Hartshorne, D. J., Yamakita, Y., Yamashiro, S., and Matsumura, F. (2004). Distinct roles of MLCK and ROCK in the regulation of membrane protrusions and focal adhesion dynamics during cell migration of fibroblasts. *J.Cell Biol.* 164, 427-439.
26. Palazzo, A. F., Eng, C. H., Schlaepfer, D. D., Marcantonio, E. E., and Gundersen, G. G. (2004). Localized stabilization of microtubules by integrin- and FAK-facilitated Rho signaling. *Science.* 303, 836-839.
27. Palazzo, A. F., Joseph, H. L., Chen, Y. J., Dujardin, D. L., Alberts, A. S., Pfister, K. K., Vallee, R. B., and Gundersen, G. G. (2001). Cdc42, dynein, and dynactin regulate MTOC reorientation independent of Rho-regulated microtubule stabilization. *Curr Biol* 11, 1536-1541.
28. D'Amato, R. J., Loughnan, M. S., Flynn, E., and Folkman, J. (1994). Thalidomide is an inhibitor of angiogenesis. *Proc.Natl.Acad.Sci.U.S.A* 91, 4082-4085.
29. Fong, T. A., Shawver, L. K., Sun, L., Tang, C., App, H., Powell, T. J., Kim, Y. H., Schreck, R., Wang, X., Risau, W., Ullrich, A., Hirth, K. P., and McMahon, G. (1999). SU5416 is a potent and selective inhibitor of the vascular endothelial growth factor receptor (Flk-1/KDR) that inhibits tyrosine kinase catalysis, tumour vascularization, and growth of multiple tumour types. *Cancer Res* 59, 99-106.
30. Bernatchez, P. N., Soker, S., and Sirois, M. G. (1999). Vascular endothelial growth factor effect on endothelial cell proliferation, migration, and platelet-activating factor synthesis is Flk-1-dependent. *J.Biol.Chem.* 274, 31047-31054.
31. Chon, J. H., Netzel, R., Rock, B. M., and Chaikof, E. L. (1998). Alpha4beta1 and alpha5beta1 control cell migration on fibronectin by differentially regulating cell speed and motile cell phenotype. *Ann.Biomed.Eng* 26, 1091-1101.
32. Gotlieb, A. I., Subrahmanyan, L., and Kalnins, V. I. (1983). Microtubule-organizing centers and cell migration: effect of inhibition of migration and microtubule disruption in endothelial cells. *J Cell Biol* 96, 1266-1272.
33. Ueda, M., Graf, R., MacWilliams, H. K., Schliwa, M., and Euteneuer, U. (1997). Centrosome positioning and directionality of cell movements. *Proc Natl Acad Sci U S A* 94, 9674-9678.
34. Gundersen, G. G., Kim, I., and Chapin, C. J. (1994). Induction of stable microtubules in 3T3 fibroblasts by TGF-beta and serum. *J.Cell Sci.* 107 (Pt 3), 645-659.

35. DiMilla, P. A., Stone, J. A., Quinn, J. A., Albelda, S. M., and Lauffenburger, D. A. (1993). Maximal migration of human smooth muscle cells on fibronectin and type IV collagen occurs at an intermediate attachment strength. *J.Cell Biol.* 122, 729-737.
36. Danen, E. H. and Yamada, K. M. (2001). Fibronectin, integrins, and growth control. *J.Cell Physiol* 189, 1-13.
37. Gupton, S. L., Anderson, K. L., Kole, T. P., Fischer, R. S., Ponti, A., Hitchcock-Degregori, S. E., Danuser, G., Fowler, V. M., Wirtz, D., Hanein, D., and Waterman-Storer, C. M. (2005). Cell migration without a lamellipodium: translation of actin dynamics into cell movement mediated by tropomyosin. *J.Cell Biol.* 168, 619-631.
38. Small, J. V., Stradal, T., Vignal, E., and Rottner, K. (2002). The lamellipodium: where motility begins. *Trends Cell Biol* 12, 112-120.
39. Waterman-Storer, C. M., Worthylake, R. A., Liu, B. P., Burridge, K., and Salmon, E. D. (1999). Microtubule growth activates Rac1 to promote lamellipodial protrusion in fibroblasts. *Nat Cell Biol* 1, 45-50.
40. Lee, T. Y. and Gotlieb, A. I. (1999). Early stages of endothelial wound repair: conversion of quiescent to migrating endothelial cells involves tyrosine phosphorylation and actin microfilament reorganization. *Cell Tissue Res.* 297, 435-450.
41. Hotchkiss, K. A., Ashton, A. W., Mahmood, R., Russell, R. G., Sparano, J. A., and Schwartz, E. L. (2002). Inhibition of endothelial cell function in vitro and angiogenesis in vivo by docetaxel (Taxotere): association with impaired repositioning of the microtubule organizing center. *Mol Cancer Ther* 1, 1191-1200.
42. Small, J. V., Geiger, B., Kaverina, I., and Bershadsky, A. (2002). How do microtubules guide migrating cells? *Nat Rev Mol Cell Biol* 3, 957-964.
43. Conrad, P. A., Nederlof, M. A., Herman, I. M., and Taylor, D. L. (1989). Correlated distribution of actin, myosin, and microtubules at the leading edge of migrating Swiss 3T3 fibroblasts. *Cell Motil.Cytoskeleton* 14, 527-543.
44. Berven, L. A., Willard, F. S., and Crouch, M. F. (2004). Role of the p70(S6K) pathway in regulating the actin cytoskeleton and cell migration. *Exp.Cell Res.* 296, 183-195.
45. Madri, J. A., Bell, L., Marx, M., Merwin, J. R., Basson, C., and Prinz, C. (1991). Effects of soluble factors and extracellular matrix components on vascular cell behavior in vitro and in vivo: models of de-endothelialization and repair. *J.Cell Biochem.* 45, 123-130.
46. Palazzo, A. F., Cook, T. A., Alberts, A. S., and Gundersen, G. G. (2001). mDia mediates Rho-regulated formation and orientation of stable microtubules. *Nat.Cell Biol.* 3, 723-729.

MOVIE LEGENDS (movies available online via *Journal of Cellular Biochemistry*)

Movie 1 - High magnification of HUVEC at migration front in the "scratch" assay. The cells are damaged and leak cytoplasm. The matrix in the cell-free area is contaminated with cell secreted ECM-components, growth factors and cell remnants. FN was used as coating, cells were treated with bFGF (200 ng/ml). Cell migration was recorded by time-lapse phase-contrast microscopy collecting an image very 30 sec for 8 h. Movie takes 12 s and display rate is 10 frames/s.

Movie 2 - High magnification of HUVEC migrating in a 'single cell motility assay'. During attachment, spreading and prior to the assay the cells have manipulated the matrix. Migrating cells follow paths of other cells where the matrix is optimal but not defined. FN was used as coating, cells were treated with bFGF (200 ng/ml). Cell migration was recorded by time-lapse phase-contrast microscopy collecting an image very 30 sec for 8 h. Movie takes 12 s and display rate is 10 frames/s.

Movie 3 - High magnification of HUVEC at migration front in the novel assay. Cells and matrix are left unharmed. The matrix can be defined and manipulated. FN was used as coating, cells were treated with bFGF (200 ng/ml). Cell migration was recorded by time-lapse phase-contrast microscopy collecting an image very 30 sec for 8 h. Movie takes 12 s and display rate is 10 frames/s.

Movie 4 - HUVEC migration in the "barrier" assay in basal medium. When no GF are added to the basal medium and Gel is used as coating the EC hardly migrate and die at later time points. Cell migration was recorded by time-lapse DIC microscopy collecting an image very 12 min for 24 h. Movie takes 12 s and display rate is 10 frames/s

Movie 5 - bFGF-induced HUVEC migration in the "barrier" assay. Migration is induced by adding bFGF (200 ng/ml) and Gel was used as coating. EC migrate very fast while cell morphology changes are moderate. Cell migration was recorded by time-lapse DIC microscopy collecting an image very 12 min for 24 h. Movie takes 12 s and display rate is 10 frames/s.

Movie 6 - VEGF-induced HUVEC migration in the "barrier" assay. Treatment of HUVEC with VEGF (10 ng/ml) along Gel-coating resulted in a strong migration induction and the cells show an elongated morphology. In addition the migration patterns of the cells have less directional changes as compared to bFGF. Cell migration was recorded by time-lapse DIC microscopy collecting an image very 12 min for 24 h. Movie takes 12 s and display rate is 10 frames/s.

Movie 7 - HUVEC migration along FN-matrix with basal medium in the "barrier" assay. When no GF were added to HUVEC migrating along FN the cell migration is without a persistent direction in rather random patterns. At later time points the cells start do die. Cell migration was recorded by time-lapse Phase-Contrast microscopy collecting an image very 12 min for 24 h. Movie takes 12 s and display rate is 10 frames/s.

Movie 8 - HUVEC migration along Col-I-matrix with basal medium in the "barrier" assay. Col-I induces EC to migration and directionality even without addition of GF to the basal medium. Cell migration was recorded by time-lapse Phase-Contrast microscopy collecting an image very 12 min for 24 h. Movie takes 12 s and display rate is 10 frames/s.

Movie 9 - HUVEC migration along Gel-coating with basal medium in the "scratch" assay. Introduction of the "scratch" induced EC to migrate along the control-matrix Gel. Compared to the same treatment in the "barrier" assay (Movie 4) migration is increased. Cell migration was recorded by time-lapse DIC microscopy collecting an image very 12 min for 24 h. Movie takes 12 s and display rate is 10 frames/s.

Movie 10 - HUVEC migration along FN-matrix with basal medium in the "scratch" assay. Using the "scratch" assay the inhibitory effect of FN on directionality of the EC migration is absent. At later time points the migration decreases but the cells do not die (compared to Movie 7). Cell migration was recorded by time-lapse Phase-Contrast microscopy collecting an image very 12 min for 24 h. Movie takes 12 s and display rate is 10 frames/s.

Movie 11 - HUVEC migration along Col-I-matrix with basal medium in the "scratch" assay. Col-I-matrix in the "scratch" assay induces massive EC migration and directionality as well. Cell migration was recorded by time-lapse Phase-Contrast microscopy collecting an image very 12 min for 24 h. Movie takes 12 s and display rate is 10 frames/s.

Movie 12 - 3T3 fibroblast migration without GF and coating in the "barrier" assay. 3T3 cells hardly migrate without GF and coating in the "barrier" assay. Cell migration was recorded by time-lapse Phase-Contrast microscopy collecting an image very 12 min for 24 h. Movie takes 12 s and display rate is 10 frames/s.

Movie 13 - 3T3 fibroblast migration without GF along FN-matrix in the "barrier" assay. FN induces 3T3 cells to migrate and the migration patterns show some directionality as well. Cell migration was recorded by time-lapse Phase-Contrast microscopy collecting an image very 12 min for 24 h. Movie takes 12 s and display rate is 10 frames/s.

Movie 14 - 3T3 fibroblast migration without GF and coating in the "scratch" assay. The 3T3 cells hardly migrate without GF and coating in the "scratch" assay. Cell migration was recorded by time-lapse Phase-Contrast microscopy collecting an image very 12 min for 24 h. Movie takes 12 s and display rate is 10 frames/s.

Movie 15 - 3T3 fibroblast migration without GF along FN-matrix in the "scratch" assay. FN-induced 3T3 migration is very mild, only small differences are observed compared to the same treatments in the "barrier" assay (Video 12, 13). Cell migration was recorded by time-lapse Phase-Contrast microscopy collecting an image very 12 min for 24 h. Movie takes 12 s and display rate is 10 frames/s.

Movie 16 - LPA-induced 3T3 fibroblast migration without coating in the "barrier" assay. LPA (5 μM) induces 3T3 cells to migrate without coating. Cell migration was recorded by time-lapse Phase-Contrast microscopy collecting an image very 12 min for 24 h. Movie takes 12 s and display rate is 10 frames/s.

Movie 17 - LPA-induced 3T3 fibroblast migration along FN-matrix in the "barrier" assay. LPA-induced 3T3 migration is comparable with and without FN-coating. Cell migration was recorded by time-lapse Phase-Contrast microscopy collecting an image very 12 min for 24 h. Movie takes 12 s and display rate is 10 frames/s.

Movie 18 - LPA-induced 3T3 fibroblast migration without coating in the "scratch" assay. LPA (5 μM) induces 3T3 cells to migrate into the "scratch" without coating. Cell migration was recorded by time-lapse Phase-Contrast microscopy collecting an image very 12 min for 24 h. Movie takes 12 s and display rate is 10 frames/s.

Movie 19 - LPA-induced 3T3 fibroblast migration along FN-matrix in the "scratch" assay. LPA-induced 3T3 migration is comparable with and without FN-coating and somewhat higher in the "scratch" assay compared to the "barrier" assay. Cell migration was recorded by time-lapse Phase-Contrast microscopy collecting an image very 12 min for 24 h. Movie takes 12 s and display rate is 10 frames/s.

Movie 20 - bFGF-induced 3T3 fibroblast migration without coating in the "barrier" assay. bFGF (200 ng/ml) induces 3T3 cells to migrate and the cells have an elongated morphology with long extensions during migration. Cell migration was recorded by

time-lapse Phase-Contrast microscopy collecting an image very 12 min for 24 h. Movie takes 12 s and display rate is 10 frames/s.

Movie 21 - bFGF-induced 3T3 fibroblast migration along FN-matrix in the "barrier" assay. bFGF (200 ng/ml) combined with FN-matrix in the "barrier" assay results in a very strong and enhanced induction of 3T3 migration. The cells are very elongated and form long extensions during migration. Cell migration was recorded by time-lapse Phase-Contrast microscopy collecting an image very 12 min for 24 h. Movie takes 12 s and display rate is 10 frames/s.

Movie 22 - bFGF-induced 3T3 fibroblast migration without coating in the "scratch" assay. bFGF-induced 3T3 migration into the "scratch" is comparable to the same treatment in the "barrier" assay (Video 20). The cells have an elongated morphology and long extensions during migration. Cell migration was recorded by time-lapse Phase-Contrast microscopy collecting an image very 12 min for 24 h. Movie takes 12 s and display rate is 10 frames/s.

Movie 23 - bFGF-induced 3T3 fibroblast migration along FN-matrix in the "scratch" assay. The FN-effect on the bFGF-induced 3T3 migration is absent in the "scratch" assay. Morphology and migration is comparable with and without FN-coating. The cells are elongated and form long extensions during migration. Cell migration was recorded by time-lapse Phase-Contrast microscopy collecting an image very 12 min for 24 h. Movie takes 12 s and display rate is 10 frames/s.

Movie 24 - HUVEC migration along low FN (1 μg/ml) in the "barrier" assay. Net cell movement is inhibited. Cell migration was recorded by time-lapse Phase-Contrast microscopy collecting an image very 12 min for 24 h. Movie takes 12 s and display rate is 10 frames/s.

Movie 25 - HUVEC migration along high FN (100 μg/ml) in the "barrier" assay. In contrast to low and intermediate FN concentration EC migration is induced, cells do not migrate in sheets. Cell migration was recorded by time-lapse Phase-Contrast microscopy collecting an image very 12 min for 24 h. Movie takes 12 s and display rate is 10 frames/s.

Movie 26 - HUVEC migration along low Col-I (1 μg/ml) in the "barrier" assay. Low Col-I still induces EC migration but cells do not migrate in sheets as compared to high Col-I (Fig. 4). Cell migration was recorded by time-lapse Phase-Contrast microscopy collecting an image very 12 min for 24 h. Movie takes 12 s and display rate is 10 frames/s.

Movie 27 – 3T3 migration without GF along low FN (1 μg/ml) in the "barrier" assay. Low FN still induces 3T3 cells to migrate. Cell migration was recorded by time-lapse Phase-Contrast microscopy collecting an image very 12 min for 24 h. Movie takes 12 s and display rate is 10 frames/s.

Movie 28 – 3T3 migration without GF along high FN (100 μg/ml) in the "barrier" assay. High FN induces 3T3 cells to migrate. Cell migration was recorded by time-lapse Phase-Contrast microscopy collecting an image very 12 min for 24 h. Movie takes 12 s and display rate is 10 frames/s.

Movie 29 – 3T3 migration upon bFGF (200 ng/ml) treatment along low FN (1 μg/ml) in the "barrier" assay. The FGF-FN effect is still observed along low FN concentrations. Cell migration was recorded by time-lapse Phase-Contrast microscopy collecting an image very 12 min for 24 h. Movie takes 12 s and display rate is 10 frames/s.

Movie 30 – 3T3 migration upon bFGF (200 ng/ml) treatment along high FN (100 μg/ml) in the "barrier" assay. High FN results in comparable responses as low and intermediate concentrations Cell migration was recorded by time-lapse Phase-Contrast microscopy collecting an image very 12 min for 24 h. Movie takes 12 s and display rate is 10 frames/s.

Chapter 3

Microtubules and microtubule-associated proteins in endothelial cell migration induced by VEGF and bFGF

Remco van Horssen[1]
Joost A.P. Rens[1]
Ksenija Drabek[2]
Alexander M. M. Eggermont[1]
Niels Galjart[2]
Timo L.M. ten Hagen[1]

[1]Laboratory of Experimental Surgical Oncology, Department of Surgical Oncology, Erasmus MC – Daniel den Hoed Cancer Centre and [2]Department of Cell Biology and Genetics, Erasmus MC, Rotterdam, The Netherlands

In Preparation

Note: This chapter contains figures that are also available in full colour (labeled with 'CLR'). These colour figures can be found in the Appendix of this book (page 209) and in the online version (via Medical Library, Erasmus MC).

ABSTRACT

Directed cell migration (cell movement in one direction) occurs both during chemotaxis and during intrinsically determined cell motility and depends on the capacity to maintain cell polarity in one direction for a certain period of time. For endothelial cells (EC) directed migration is very important during the formation of new vessels. Although the effects of major endothelial stimuli, bFGF and VEGF, are widely studied, mechanistic data still are hardly available. Here we report that bFGF and VEGF induce distinct migration patterns of EC, with VEGF causing more directed motility. These differences were accompanied by actin-cytoskeleton and adhesion differences. Immunofluorescence analysis of specific microtubule-associated proteins (MAP) in HUVEC revealed distinct cellular distribution. We observed a higher microtubule growth rate in VEGF-induced migrating EC. Finally, we studied distribution of CLASPs after migration induction. For CLASP1, in contrast to CLASP2, we observed some accumulation at the leading edge after VEGF stimulation. We suggest that CLASP1 might be one of the signalling molecules involved in the directional migration of EC induced by VEGF.

INTRODUCTION

Cell migration plays a crucial role in normal processes like embryogenesis, renewal of the skin and intestine and tissue repair but also in pathological settings like inflammation-related diseases and tumour development [1,2]. During tumour development, tumour cell migration is essential during invasion and metastasis, during angiogenesis endothelial cell migration is crucial [3-5]. Cell migration is initiated by formation of actin-rich membrane protrusions in the direction of migration regulated by small Rho GTPases, like Cdc42 and Rac [6-8]. Recently, for Rac an important regulatory role in migration directionality has been reported [9]. Directionality of cell migration is strongly dependent on persistence of cell polarity. Cell polarity is initiated and sustained by protrusion formation and asymmetric positioning of intracellular structures, like the microtubule-organizing centre (MTOC) and Golgi apparatus [10].

Microtubules (MTs) are involved in various processes of cell migration and therefore essential for cell guidance during motility [11]. Both repositioning of the MTOC [12,13] and formation of cellular protrusions [14] are dependent on MTs. MTs are hollow cylindrical tubes consisting of tubulin polymers. These polymers in turn are built up by heterodimers of α and β-tubulin subunits and organized in a polarized fashion with a fast growing plus end and slow growing minus end. An important feature of MTs is their so-called dynamic instability, being the intrinsic capacity to continuously switch between growth and shrinkage [15,16].

Another important function of MTs is contribution to focal adhesion turnover during migration [17]. These focal adhesions, linking intracellular structures, like actin, to matrix components, like fibronectin, are key regulators of force generation needed for movement of the cell body [18]. Growing MTs have been shown to target focal adhesions to deliver certain components of the focal adhesion complexes [19]. Additionally, MTs have been reported to selectively stabilize in the direction of migration when cells are triggered to migrate into *in vitro* generated wounds [20]. Stabilization of MTs is an important component of cell polarity, however, it seems to differ strongly between cell types and treatment [21]. Many findings about MTs and their role in migration and polarity have been achieved in fibroblasts and astrocytes, known to be slow moving cells [14,22]. For fast moving cells like endothelial and tumour cells, MTs will also be involved, but details in the regulatory mechanisms may differ. Recently, we reported that migrating EC, in contrast to fibroblast, actually have lower amounts of stable MTs during migration [21]., Moreover, the distribution of stable MTs was strongly dependent of the treatment (see Chapter 2 of this thesis).

MT dynamics is regulated by a broad set of microtubule-associated proteins (MAP). The group of proteins specifically binding to MT plus ends (called Plus-end binding proteins (+EBP) or +TIPs) has been studied widely as these proteins regulate both MT dynamics and interactions of MTs with other proteins [23,24]. Examples of +TIPs are EBs (end binding proteins), APC (adenomatous polyposis coli), LIS-1 (Lissencephaly-1), CLIPs (cytoplasmic linker proteins) and CLASPs (CLIP associated proteins). These proteins can interact with MT plus ends and/or with each other [25-28]. In mammals two CLASPs have been identified, CLASP1 and CLASP2, that shares 77% sequence homology. Both CLASPs bind to MTs and to CLIP-115 and CLIP-170 through their C-terminal domain. At leading edges of motile fibroblasts CLASPs are involved in local stabilization of MTs [25]. When CLASP-levels are reduced MTs display an abnormal distribution and the plus ends loose their ability to localize near the cell cortex [27].

EC migrate in a directed fashion during angiogenesis, a process called angiogenic sprouting [29]. Migrating EC are suggested to be guided by factors stored in the extracellular matrix, like VEGF. In addition, angiogenic growth factors bFGF and VEGF are reported to induce chemokinetic and chemotactic migration respectively [30]. These features implicate differences in intracellular response to these two angiogenic stimuli. Next to chemotactic migration induction, cells have an intrinsic migration capacity and we hypothesize that various triggers induce different signals resulting in distinct migration pattern. In this study, we analysed the migration patterns of human EC upon bFGF and VEGF treatment. We observed a higher directional motility after VEGF treatment as compared to

bFGF. In consecutive experiments we linked these differences to changes in actin and MT cytoskeleton, MT dynamics and identified CLASP1 as a possible target for VEGF induced directionality in EC migration.

MATERIALS AND METHODS

Cell culture and reagents

Human Umbilical Vein Endothelial Cells (HUVEC) were isolated as described [31] and purchased from Biowhittaker. EC were used between passage 3 and 7 and cultured in Human Endothelial-SFM (Invitrogen) supplemented with 10% New Born Calf Serum, 5% Human Serum, 20 ng/ml bFGF and 100 ng/ml EGF, in gelatine-coated flasks. Serum was purchased from Invitrogen. VEGF-165, bFGF and EGF were from PeproTech.

Migration Assay

Migration assays were done using the barrier-migration assay as described [21]. Briefly, a cover slip was placed in an Attofluor incubation chamber (Molecular Probes), which was subsequently sterilized and coated with fibronectin (10 μg/ml). In this chamber a removable circular migration barrier was placed which prevents cell growth in the middle of the cover slip. HUVEC were seeded around this barrier and grown until confluence. Subsequently, the migration barrier was removed, cells were washed twice and then incubated with Human Endothelial-SFM without standard growth factors (basal medium control), supplemented with bFGF (200 ng/ml), or VEGF-165 (10 ng/ml). Cell chambers were placed on an inverted microscope and migration of cells was measured for 24 h. Each experiment was repeated at least 3 times. Time-lapse imaging of cell migration was done on Axiovert 100 M microscopes, equipped with either an AxioCam HRC digital camera or an AxioCam MRC digital camera (Carl Zeiss). Microscopes were controlled by AxioVision software, version 4.5. Cells in the incubation chamber were maintained at 37 ^{o}C in a constantly humidified atmosphere, with controlled and heated CO_2-flow. Cells were imaged every 12 min with a 10X/0.30 PLAN-NEOFLUAR objective lens or every 2 min with a 20X/0.40 LD ACHROPLAN objective lens (Carl Zeiss).

For analysis of mouse-embryonic fibroblasts (MEF), single cell motility assays after adhesion were performed. Briefly, Cells (1.10E5) were diluted in Serum-free medium and bFGF (400 ng/ml) was added to induce migration. Cell suspensions were plated in incubation chambers coated with 10 μg/ml fibronectin. After 10 min. adhesion and single cell motility was monitored under the

microscope. Cells were analysed for 6 hr and images were collected every 2 min. and AxioVision software (Carl Zeiss) was used to analyse cell movements.

Cell migration analysis

Cell migration response and profile were quantified by measuring migrated distance and migratory directionality. Using time-lapse movies cells were tracked taking the nuclei as reference. For each treatment at least 10 migrating cells of 3 or 4 independent migration assays were analysed. After cell division one of the daughter cells was followed. The total track distance (T) and the direct distance from start to end point (D) were used to calculate D/T ratios reflecting the directionality of cell movements [9]. Measurements were done using AxioVision measurement software (Carl Zeiss).

Immunofluorescence Staining

After time-lapse microscopy, cells were washed twice with PBS and fixed for 10 min in 4% paraformaldehyde at room temperature or in ice-cold methanol containing 1 mM EGTA at –20 ^{o}C. After washing in PBS, cells were permeabilized using 0,15% Triton-X-100 for 10 min and blocked in blocking solution (1% BSA / 0,05% Tween-20 / PBS) for 45 min. Incubations with first (1/200) and secondary (1/500) antibody-mixtures were done for 1 h at room temperature in blocking solution. In between incubations cells were washed 3 times with PBS / 0,05% Tween-20. Thereafter cells were briefly washed in 70% and 100% ethanol respectively, air dried and mounted onto microscope slides using 10 µl of a 1:1 solution of VectaShield (Vector Laboratories) and DAPI-DABCO (Molecular Probes). Primary antibodies and antisera used: acetylated microtubules (Sigma-Aldrich), f-actin (Molecular Probes), EB1 (BD Biosciences), VASP (kindly provided by Dr. F. Gertler, Department of Biology, Massachusetts Institute of Technology, Cambridge, USA [32]), CLASP1 (#2292), CLASP2 (#2258), CLIP115/170 (#2221) and EB3 (#02-1005-07) have been described [25,33]. Secondary antibodies used: Alexa Fluor 488 or 594 (Molecular Probes) and FITC (Nordic) conjugated antibodies. Immunofluorescent images were taken using an Axiovert 100 M microscope with 40X/1.30 Oil-FLUAR objective lens (Carl Zeiss) and an ORCA II ER camera (C4742-98, Hamamatsu Photonics Systems). Image analysis was performed using Openlab 4.0 software (Improvision).

Visualization of MT dynamics using EB3-GFP

HUVEC were transiently transfected with EB3-GFP constructs [33] using SuperFect Transfection Reagent (Qiagen) and Nupherin Neuron (Biomol). Briefly, cells were grown till subconfluency and

transfection solutions containing DNA:Nupherin:SuperFect ratio of 1:3:6 were prepared according standard procedures. Transfection solutions were added to the cells; cells were centrifuged for 5 min at 100 g and incubated for 2.5 h at 37 ^{o}C. After overnight growing in standard medium cells were subcultured in Attofluor incubation chambers to facilitate live cell imaging during migration. Cell migration was induced for 24 h as described above and EB3-GFP positive cells were analyzed at 37 ^{o}C on an Axiovert 100 M microscope with 63X/1.4 Oil Plan-APOCHROMAT objective lens (Carl Zeiss) and an ORCA II ER camera (C4742-98, Hamamatsu Photonics Systems). Images were collected every second for 30 seconds.

RESULTS

Distinct EC migration patterns induced by bFGF and VEGF

The two major angiogenic factors known nowadays, bFGF and VEGF, are reported to induce chemokinetic and chemotactic migration respectively [30].

To analyse the migration pattern of EC upon treatment with these two factors we performed migration assays using the barrier assay [21]. HUVEC migration was monitored for 24 h and fibronectin was used as matrix (Fig. 1A). Control cells, with basal medium (BM) without addition of growth factors, showed random motility and at later time points some cells start to die. Both bFGF and VEGF induced HUVEC migration, but the patterns were very different. bFGF induced cells to migrate over long distances while VEGF-induced distance was only slightly increased as compared to BM (Fig. 1B). Moreover, when we quantified the directionality of cell movements (being the ratio of the shortest, linear distance from start to end point (D) and the total migrated track (T) of the cells) we observed an increased directionality induced by VEGF as compared to bFGF (Fig. 1C). The migration tracks of HUVEC treated with BM, bFGF and VEGF are depicted in Figure 1D, clearly showing the differences in migration patterns and directionality.

bFGF and VEGF induce different actin organization and VASP distribution

Actin cytoskeleton organization is a major aspect in determining cell morphology and migration response. Vasodilator-stimulated phosphoprotein (VASP) is known to be an essential regulator of actinfilament assembly, localizes to focal adhesions and sites of dynamic membrane activity in the leading edge and negatively regulates fibroblast migration [32,34,35]. Based on the observed differences shown in Figure 1, we examined actin cytoskeleton organization and VASP distribution in migrating EC (Fig. 2).

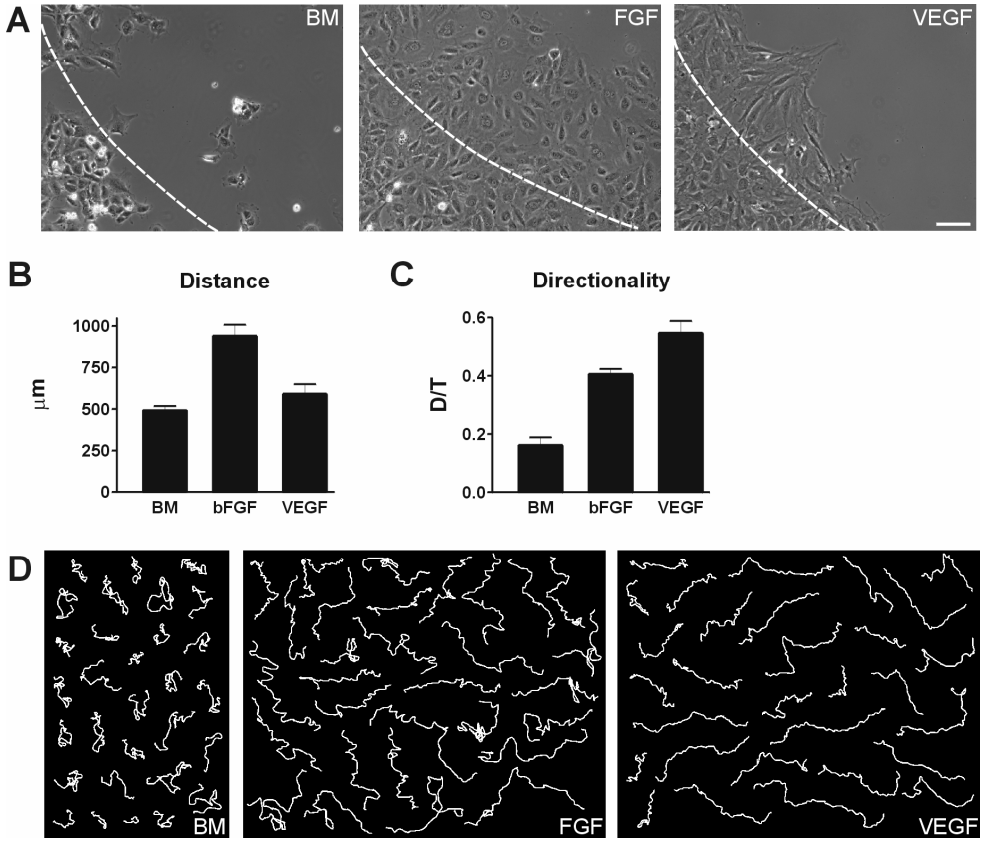

FIGURE 1. Distinct migration patterns induced by bFGF and VEGF in HUVEC.
A. HUVEC migration along fibronectin induced by BM (basal medium without addition of growth factors), bFGF (200 ng/ml) or VEGF (10 ng/ml). The white dashed line indicates the migration front at T=0 h. Pictures are at T=24 h and obtained from migration movies, Bar: 100 µm.
B. Total migrated distance of HUVEC in 24 h. Data represents mean ± SEM from at least three independent experiments.
C. Persistence of migratory directionality. D/T represents the ratio of the direct distance from start to end (D) divided by the total migrated track distance (T). Data represents mean ± SEM from at least three independent experiments.
D. Migration tracks of HUVEC migrating for 24 h. Migration tracks (n=30) from 3 independent experiments were copied and combined to create a single figure.

In BM-treated controls we observed some actin stress fibers mainly organized as dense peripheral bands and VASP primarily distributed throughout the cytoplasm and localized in focal adhesions. The differences between the two growth factors are very abundant. bFGF treated EC showed f-actin at the cell periphery (as dense peripheral bands) and in addition many actin was localized at a small rim, in the leading edges of the cells.

Interestingly, these cell areas stained also positive for VASP, which localized at the most distal site of the leading edge/cell membrane (see enlargement in Fig. 2B). We assume that at these sites there is an extensive actin polymerization to push the cell membrane forward. For VEGF the staining

patterns are different. F-actin is predominantly organized into stress-fibres throughout the cells and VASP was localised at the ends of these fibres in focal adhesion-like foci. When we analysed these staining patterns in more detail we observed also some leading edge/membrane actin-VASP staining but these patterns were very local in smaller segments of the cell periphery (see enlargement in Fig. 2B).

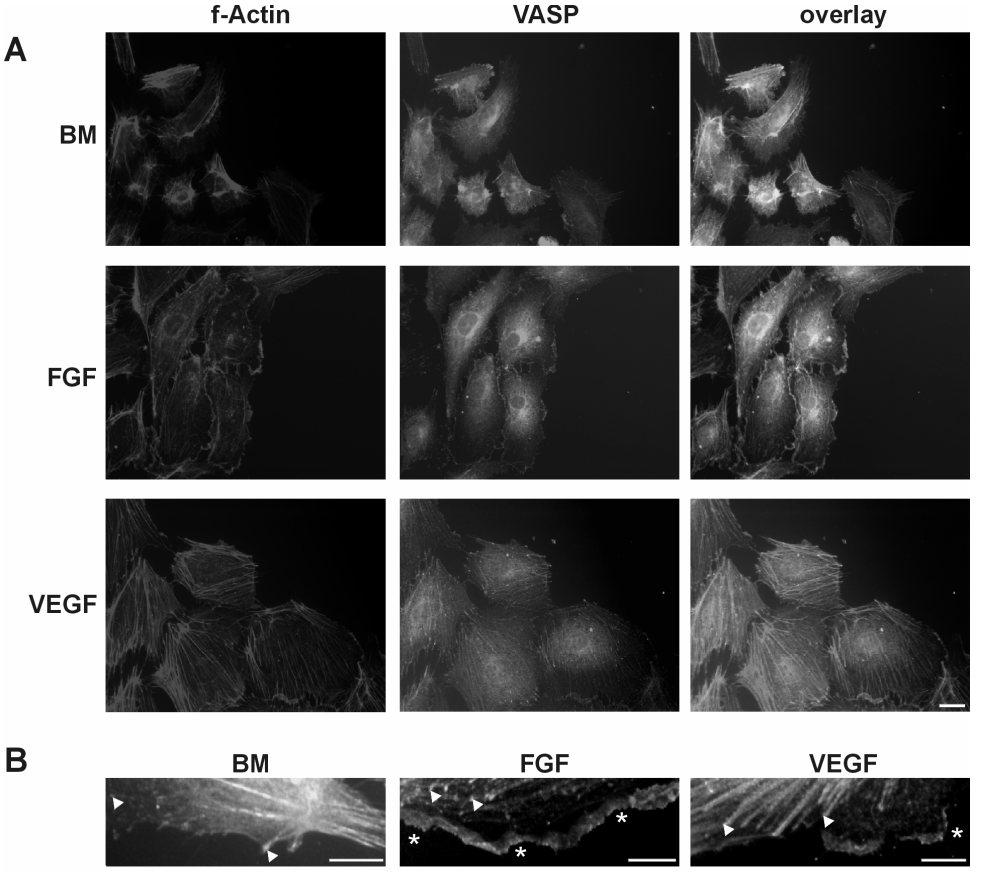

FIGURE 2. Actin and VASP distribution in migrating HUVEC **(CLR)**.
A. HUVEC were induced to migrate for 24 h, fixed and stained for f-Actin (red), Ena/VASP (green) and nuclei (blue). In basal medium controls the actin is mainly visible as dens peripheral bands and VASP is mainly cytoplasmic. Upon bFGF treatment, actin staining is observed at the edges of the cells and a positive VASP signal was found at the most distal site of this rim at the leading edge and cell rims. VEGF induced many stress fibers and VASP was mainly located in focal adhesions. Bar: 10 μm.
B. Enlargement of cell rims of HUVEC at migration fronts. Arrowheads point VASP located at ends of actin fibers as focal adhesions, Asterisks point membrane-expressed VASP. In bFGF treated we observed VASP along whole membranes while in VEGF treated cells this expression was locally. Bar: 5 μm.

Localization of MAP in cultured HUVEC

Next, we studied the distribution of stable MTs and MAP in cultured EC, growing in monolayer. Besides actin remodeling, MTs and their dynamics are crucial in migration and polarity [11]. We stained cultured HUVEC for stable MTs, CLIP-115/170, CLASP1, CLASP2, EB1, and EB3. Stainings for acetylated tubulin confirmed that a subset of MTs is stabilized in EC. CLIP-115/170 and both EB1 and EB3 localize at MT plus ends. For both CLASPs we observed cytoplasmic localization and, in contrast to other cell types like COS-1 [25], no positive MT plus ends were found (data not shown).

MT growth in EC during migration

To analyse the dynamic behaviour of growing MTs during EC migration we transfected growing HUVEC with EB3-GFP. EB3-GFP positive cells migrating into the cell free area and at the migration front were analysed after 24 h of treatment (BM, bFGF or VEGF) for MT dynamics. Velocity of EB3-GFP comets was measured to quantify MT growth rates. Average EB3-GFP velocities are shown in the table of Figure 3A. For BM and bFGF, MT growth rates were comparable (0.22 and 0.25 m/sec respectively). For VEGF, we observed a strongly increased MT growth rate of 0.35 μm/sec. Images of the migrating cells revealed also that VEGF-induced cells are much more spread out. In addition, this widespread cell body showed much more growing MT plus ends comets as compared to BM and bFGF treated cells (Fig. 3B).

A

Treatment	Average velocity[1] (number of dashes measured)
Basal Medium	0.22 ± 0.03 (22)
bFGF (200 ng/ml)	0.25 ± 0.04 (30)
VEGF (10 ng/ml)	0.35 ± 0.03 (30)

[1] μm/sec ± SEM, measured in 3 cells

B

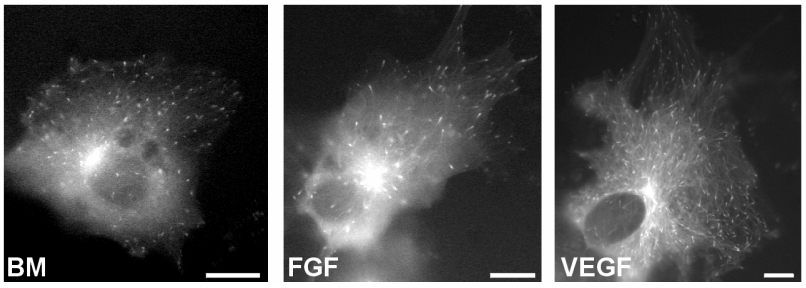

FIGURE 3. MT dynamics in migrating HUVEC.

A. Table showing the average MT growth velocities of BM, bFGF and VEGF treated migrating HUVEC transfected with EB3-GFP.
B. Pictures of EB3-GFP positive HUVEC at migration fronts. Cell free area is at upper right. VEGF cells are much more spread out, have more MT growing ends and MT growth rate is higher. Bar: 10 μm.

Cellular distribution of CLASP1 and CLASP2 during EC migration

Recently, we found that CLASP2 is involved in directional movement of embryonic fibroblasts (Drabek *et. al*., submitted and Fig. 4A).

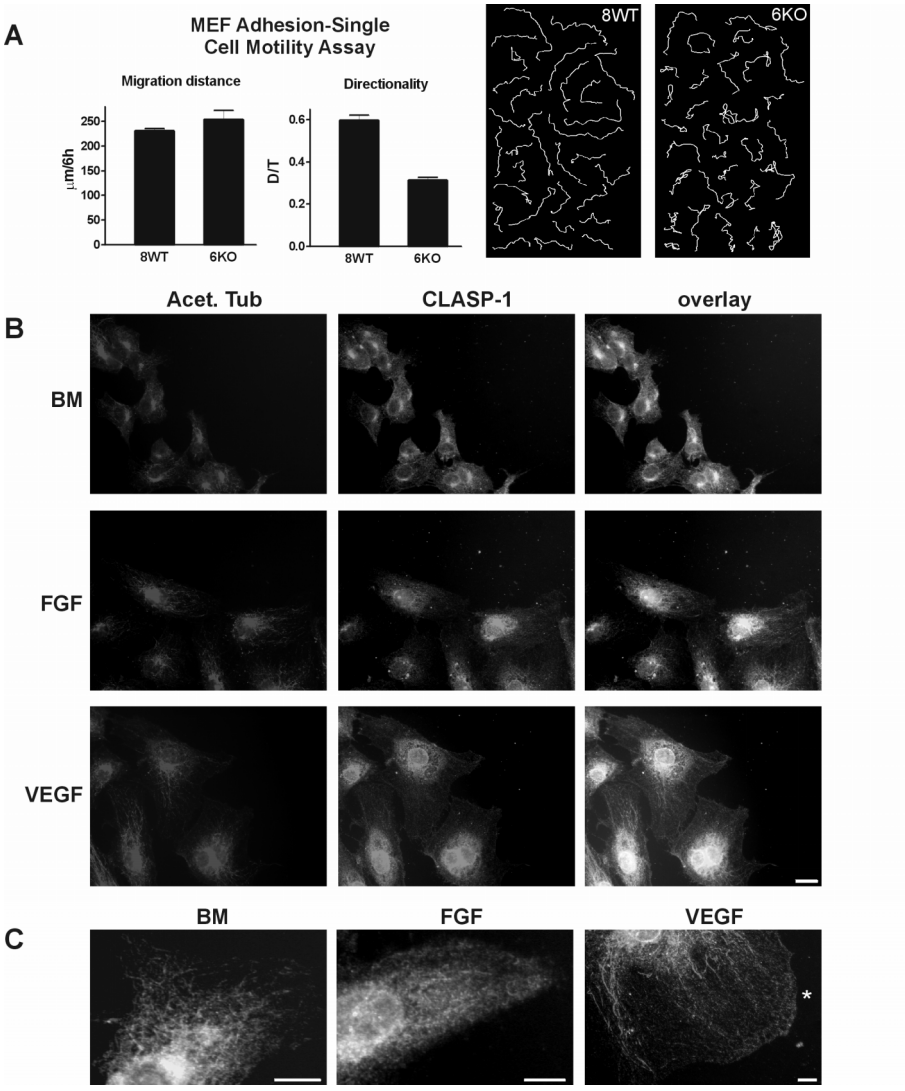

FIGURE 4. Role of CLASPs in directionality of cell movements **(CLR)**.

A. Mouse Embryonic Fibroblasts isolated from wild-type (8WT) and CLASP-2 knouckout mice (6KO) were allowed to adhere and single cell motility was measured under the microscope for 6h. No difference on migration distance was found while directionality was decreased in 6KO cells. Right part shows the migration tracks of 30 cells derived from 3 independent experiments.
B. HUVEC were induced to migrate for 24 h, fixed and stained for stable MTs (red), CLASP1 (green) and nuclei (blue). In BM cells we observed low amounts of stable MTs and CLASP1 was location was Golgi-associated and distributed throughout the cytoplasm. BFGF treatment did induce some nuclear CLASP1 and a mild increase in stable MTs. VEGF cells have slightly more stable MTs and s small accumulation of CLASP1 at local sites in the leading edge. Bar: 10 μm.
C. Enlargement of cell leading edges of BM, bFGF and VEGF treated HUVEC. Asterisk shows local CLASP1 accumulation. Bar: 5 μm.

Embryonic fibroblast isolated from CLASP2 knockout mice showed a much lower directionality of cell movements as compared with wild-type cells. We hypothesized that, given the migration patterns we observed for bFGF and VEGF induced migrating EC, that CLASPs might be involved in directed EC migration. To initiate evaluation of this hypothesis, we stained HUVEC for CLASP1 and CLASP2 in a co-staining with stable MTs after induction of migration (Figs. 4 B, C and 5). For CLASP1, we observed a Golgi-like and cytoplasmic staining pattern for BM treated EC. Nuclear staining was very low and in a subset of cells we also observed stable MTs. For both bFGF and VEGF treated EC, we found an increase in nuclear staining and CLASP1 located mainly around the nucleus. Furthermore, for bFGF the cytoplasmic CLASP1 staining was rather homogeneous and low. For VEGF, CLASP1 localisation in the cytoplasm is comparably low and diffuse but in a subset of cells at the migrating front, we also observed a small CLASP1 accumulation at local sites of the leading edge (see enlargement in Fig. 4C).

For CLASP2, in contrast to CLASP1, we did not observe this small accumulation at the cell periphery (Fig. 5). For bFGF, VEGF and BM controls we observed a rather diffuse staining pattern in the cytoplasm, no clear localisation around the nucleus, a Golgi-like staining and a much lower, or even absent, nuclear localisation of CLASP2. Also analysis at higher magnification did not reveal CLASP2 accumulation at sites of the leading edge (Fig. 5B). For stable MTs we did observe a small increase upon VEGF treatment, as we showed earlier [21]. However, this was not accompanied by leading edge localisation of CLASP2.

DISCUSSION

Directed cell migration is very important during the process of tumour-angiogenesis. Studies on directionality mechanisms involved in cell motility have provided ample knowledge on this complex process [8,9]. However, many of this and other studies are still performed in suitable cell systems, like astrocytes and fibroblasts. These cells are known to have intrinsic slow moving capacities. Other

cells, like tumour and endothelial cells are moving much faster, both *in vitro* and *in vivo* [3]. In the presented study we started to evaluate motility directionality using primary endothelial cells.

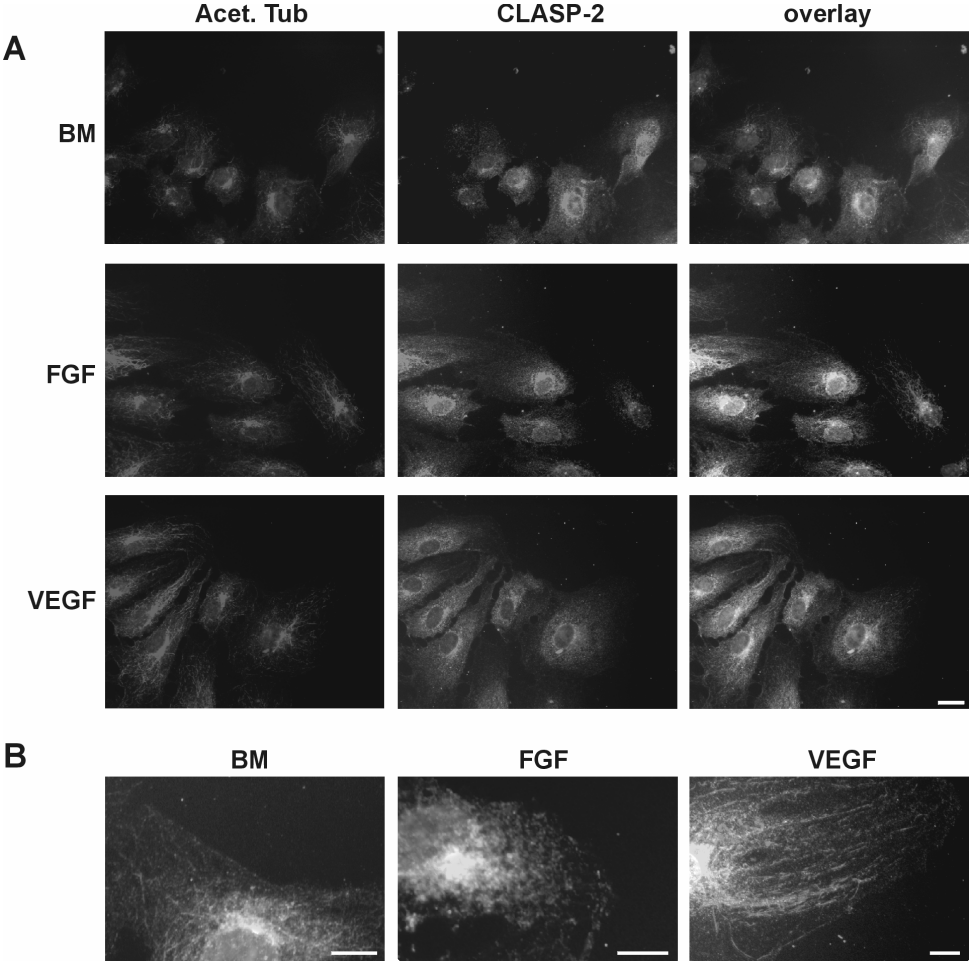

FIGURE 5. CLASP2 distribution in migrating HUVEC **(CLR)**.
A. HUVEC were induced to migrate for 24 h, fixed and stained for stable MTs (red), CLASP2 (green) and nuclei (blue). For the stable MTs staining again a small increase was observed for the VEGF treated cells. For CLASP2 no clear differences were observed between the different treatments. CLASP2 was found rather diffuse throughout the cytoplasm and no nuclear signal was seen. Bar: 100 μm.
B. Enlargement of cells at migration fronts. Bar: 5 μm.

Major drawbacks of these cells are the limited number of appropriate cell passages and therefore the restricted possibilities to genetically manipulate them. But because directed migration of endothelial cells is of crucial importance for angiogenesis, we have set up some initial experiments to study directionality and some proteins involved in its regulation.

The major findings of this preliminary study are that distinct directionality motility patterns induced by bFGF and VEGF are accompanied by differences in cytoskeleton organisation, MT dynamics and MAP localisation. More detailed, compared to bFGF, VEGF induced a more directed migration pattern of EC into a defined fibronectin-coated cell free area, built up of actin networks at the leading edge is much more local, MT growth is higher and CLASP1 tends to accumulate locally at the leading edge of migrating cells.

Recently, we showed that endothelial cells, in contrast to fibroblasts, have higher migratory capacities but a distinct MT stabilizing phenotype during migration [21]. This implies that the same fundamental processes do take place during (directed) migration of different cell types but these processes might be differentially organized and utilized. To further evaluate these processes in EC we studied two growth factors that induce a very distinct migration pattern. bFGF induced very high migration distances but directionality was lower as compared to VEGF that induced much lower migration distances (Fig. 1). These data correspond with earlier reports on chemo taxis [30]. Control cells, treated with basal medium without addition of growth factors, showed a typical random motility pattern. Using these three treatments we were able to study three important phenotypic migration profiles: random motility, fast migrating with moderate directionality and moderate migrating with high directionality.

Different morphology and dimensions of the cells accompanied these phenotypes. In BM-controls, cells were very small, upon bFGF the EC became somewhat bigger but after VEGF treatment the cells appeared broadly spread out. Actin cytoskeleton showed a very distinct organisation when bFGF and VEGF were compared (Fig. 2). Stress fibres are very abundant in the VEGF treated EC. These stress fibres may facilitate the rather sliding movement of these cells. We did not observe the stress fibres mainly oriented in the direction of migration, but both perpendicular and parallel. Using wound healing assays these features were also observed, but more separated in time after wounding instead of mixed [36]. The actin staining at the broad peripheral edges of the bFGF cells likely resembles the build up of a new actin network at cell edges during migration [35]. Striking was the difference between bFGF and VEGF. While for bFGF this staining pattern was observed in the whole cell edge, VEGF showed only local patterns. Whether this is has to do with the differences in directionality of the cell movements have to be determined in future experiments.

MTs are of crucial importance in directed cell migration and cell polarization. Staining for stable MTs and some MAP showed expression and localisation of these proteins in EC. For CLIPs and EB proteins, we observed comparable plus-end localisation as described for other cells [24]. Both

CLASP proteins however are distributed throughout the cytoplasm and nuclear staining has been ascribed to the role of CLASP in mitosis [37].

The differences we observed in MT growth rate between bFGF and VEGF migrating EC may imply that higher MT growth rate is accompanied by more directed migration and low MT growth rates by fast and less directed motility. However, the great differences in cell dimensions and spreading might also influence the number and velocity of growing MTs. As MTs do target substrates for adhesion turnover [19], more growing MTs might also mean more adhesions, but as well a higher turnover what rather is expected in bFGF cells. Clearly more research is needed to study the role of MT growth in directed EC migration. For example the rate between stable MTs and total tubulin will be studied in future experiments.

For CLASP2, novel data using knockout cells revealed that knockout cells show a lower directionality of movements after adherence (Drabek *et. al.,* submitted). For this reason we performed stainings for CLASPs in migrating EC upon treatment (Figs. 4 and 5). Surprisingly, for CLASP2 we did not observe major differences. CLASP2 remained within the cytoplasm and no localisation at leading edges was observed in contrast to fibroblast migrating into a wound (Drabek *et. al.,* submitted). For CLASP1 there were two remarkable observations. For both growth factors, CLASP1 accumulated around (and inside) the nucleus as compared to BM controls. For VEGF treated EC CLASP1 accumulated locally at the leading edge (Fig. 4C), suggesting that CLASP1 might be a specific signal regulating VEGF-induced directionality. Unexpectedly, at sites of accumulation there is no increase in stable MTs, a proposed function of CLASP2. Whether CLASP1 and CLASP2 are involved in directed migration and how they relate and/or cooperate remains to be elucidated in future experiments.

In conclusion, we provide initial data on MTs and MAP involved in directionality of EC movements induced by bFGF and VEGF. Future experiments, like CLASP-inhibition, relation of stable MTs and CLASP1, relation of MT growth rate and directionality, involvement of other actin polymerisation mediators and relation of CLASPs and VASP need to be set up to reveal and validate contribution of CLASP1, and possible other targets, in VEGF driven directed EC migration.

REFERENCES

1. Lauffenburger, D. A. and Horwitz, A. F. (1996). Cell migration: a physically integrated molecular process. *Cell* 84, 359-369.
2. Ridley, A. J., Schwartz, M. A., Burridge, K., Firtel, R. A., Ginsberg, M. H., Borisy, G., Parsons, J. T., and Horwitz, A. R. (2003). Cell migration: integrating signals from front to back. *Science.* 302, 1704-1709.
3. Condeelis, J. and Segall, J. E. (2003). Intravital imaging of cell movement in tumours. *Nat.Rev.Cancer* 3, 921-930.
4. Carmeliet, P. and Jain, R. K. (2000). Angiogenesis in cancer and other diseases. *Nature* 407, 249-57.

5. Folkman, J., Watson, K., Ingber, D., and Hanahan, D. (1989). Induction of angiogenesis during the transition from hyperplasia to neoplasia. *Nature* 339, 58-61.
6. Horwitz, A. R. and Parsons, J. T. (1999). Cell migration--movin' on. *Science* 286, 1102-1103.
7. Nobes, C. D. and Hall, A. (1999). Rho GTPases control polarity, protrusion, and adhesion during cell movement. *J Cell Biol* 144, 1235-1244.
8. Wittmann, T. and Waterman-Storer, C. M. (2001). Cell motility: can Rho GTPases and microtubules point the way? *J Cell Sci* 114, 3795-3803.
9. Pankov, R., Endo, Y., Even-Ram, S., Araki, M., Clark, K., Cukierman, E., Matsumoto, K., and Yamada, K. M. (2005). A Rac switch regulates random versus directionally persistent cell migration. *J.Cell Biol.* 170, 793-802.
10. Nabi, I. R. (1999). The polarization of the motile cell. *J Cell Sci* 112 (Pt 12), 1803-1811.
11. Small, J. V., Geiger, B., Kaverina, I., and Bershadsky, A. (2002). How do microtubules guide migrating cells? *Nat Rev Mol Cell Biol* 3, 957-964.
12. Palazzo, A. F., Joseph, H. L., Chen, Y. J., Dujardin, D. L., Alberts, A. S., Pfister, K. K., Vallee, R. B., and Gundersen, G. G. (2001). Cdc42, dynein, and dynactin regulate MTOC reorientation independent of Rho-regulated microtubule stabilization. *Curr Biol* 11, 1536-1541.
13. Gomes, E. R., Jani, S., and Gundersen, G. G. (2005). Nuclear movement regulated by Cdc42, MRCK, myosin, and actin flow establishes MTOC polarization in migrating cells. *Cell* 121, 451-463.
14. Etienne-Manneville, S. and Hall, A. (2001). Integrin-mediated activation of Cdc42 controls cell polarity in migrating astrocytes through PKCzeta. *Cell* 106, 489-498.
15. Desai, A. and Mitchison, T. J. (1997). Microtubule polymerization dynamics. *Annu.Rev.Cell Dev.Biol.* 13, 83-117.
16. Galjart, N. and Perez, F. (2003). A plus-end raft to control microtubule dynamics and function. *Curr Opin Cell Biol* 15, 48-53.
17. Kaverina, I., Krylyshkina, O., and Small, J. V. (1999). Microtubule targeting of substrate contacts promotes their relaxation and dissociation. *J Cell Biol* 146, 1033-1044.
18. Galbraith, C. G., Yamada, K. M., and Sheetz, M. P. (2002). The relationship between force and focal complex development. *J.Cell Biol.* 159, 695-705.
19. Small, J. V. and Kaverina, I. (2003). Microtubules meet substrate adhesions to arrange cell polarity. *Curr Opin Cell Biol* 15, 40-47.
20. Cook, T. A., Nagasaki, T., and Gundersen, G. G. (1998). Rho guanosine triphosphatase mediates the selective stabilization of microtubules induced by lysophosphatidic acid. *J.Cell Biol.* 141, 175-185.
21. Van Horssen, R., Galjart, N., Rens, J. A. P., Eggermont, A. M. M., and ten Hagen, T. L. M. (2006). Differential effects of matrix and growth factors on endothelial and fibroblast motility: Application of a modified cell migration assay. *J Cell Biochem* Epub 30 Jun (2006).
22. Gundersen, G. G., Kim, I., and Chapin, C. J. (1994). Induction of stable microtubules in 3T3 fibroblasts by TGF-beta and serum. *J.Cell Sci.* 107 (Pt 3), 645-659.
23. Sawin, K. E. (2000). Microtubule dynamics: the view from the tip. *Curr Biol* 10, R860-R862.
24. Akhmanova, A. and Hoogenraad, C. C. (2005). Microtubule plus-end-tracking proteins: mechanisms and functions. *Curr Opin.Cell Biol* 17, 47-54.
25. Akhmanova, A., Hoogenraad, C. C., Drabek, K., Stepanova, T., Dortland, B., Verkerk, T., Vermeulen, W., Burgering, B. M., De Zeeuw, C. I., Grosveld, F., and Galjart, N. (2001). Clasps are CLIP-115 and -170 associating proteins involved in the regional regulation of microtubule dynamics in motile fibroblasts. *Cell* 104, 923-935.
26. Komarova, Y., Lansbergen, G., Galjart, N., Grosveld, F., Borisy, G. G., and Akhmanova, A. (2005). EB1 and EB3 control CLIP dissociation from the ends of growing microtubules. *Mol Biol Cell* 16, 5334-5345.
27. Mimori-Kiyosue, Y., Grigoriev, I., Lansbergen, G., Sasaki, H., Matsui, C., Severin, F., Galjart, N., Grosveld, F., Vorobjev, I., Tsukita, S., and Akhmanova, A. (2005). CLASP1 and CLASP2 bind to EB1 and regulate microtubule plus-end dynamics at the cell cortex. *J Cell Biol* 168, 141-153.
28. Etienne-Manneville, S. and Hall, A. (2003). Cdc42 regulates GSK-3beta and adenomatous polyposis coli to control cell polarity. *Nature* 421, 753-756.
29. Gerhardt, H., Golding, M., Fruttiger, M., Ruhrberg, C., Lundkvist, A., Abramsson, A., Jeltsch, M., Mitchell, C., Alitalo, K., Shima, D., and Betsholtz, C. (2003). VEGF guides angiogenic sprouting utilizing endothelial tip cell filopodia. *J.Cell Biol.* 161, 1163-1177.
30. Yoshida, A., Anand-Apte, B., and Zetter, B. R. (1996). Differential endothelial migration and proliferation to basic fibroblast growth factor and vascular endothelial growth factor. *Growth Factors* 13, 57-64.
31. Jaffe, E. A., Nachman, R. L., Becker, C. G., and Minick, C. R. (1973). Culture of human endothelial cells derived from umbilical veins. Identification by morphologic and immunologic criteria. *J Clin Invest* 52, 2745-2756.
32. Bear, J. E., Loureiro, J. J., Libova, I., Fassler, R., Wehland, J., and Gertler, F. B. (2000). Negative regulation of fibroblast motility by Ena/VASP proteins. *Cell* 101, 717-728.
33. Stepanova, T., Slemmer, J., Hoogenraad, C. C., Lansbergen, G., Dortland, B., De Zeeuw, C. I., Grosveld, F., Van Cappellen, G., Akhmanova, A., and Galjart, N. (2003). Visualization of Microtubule Growth in Cultured Neurons via the Use of EB3-GFP (End-Binding Protein 3-Green Fluorescent Protein). *J Neurosci* 23, 2655-2664.

34. Brindle, N. P., Holt, M. R., Davies, J. E., Price, C. J., and Critchley, D. R. (1996). The focal-adhesion vasodilator-stimulated phosphoprotein (VASP) binds to the proline-rich domain in vinculin. *Biochem.J.* 318 (Pt 3), 753-757.
35. Pollard, T. D. and Borisy, G. G. (2003). Cellular motility driven by assembly and disassembly of actin filaments. *Cell* 112, 453-465.
36. Lee, T. Y. and Gotlieb, A. I. (1999). Early stages of endothelial wound repair: conversion of quiescent to migrating endothelial cells involves tyrosine phosphorylation and actin microfilament reorganization. *Cell Tissue Res.* 297, 435-450.
37. Maiato, H., Rieder, C. L., Earnshaw, W. C., and Sunkel, C. E. (2003). How do kinetochores CLASP dynamic microtubules? *Cell Cycle* 2, 511-514.

Chapter 4

E-cadherin status and breast cancer cell migration: mutant cell lines lack migration capacity while cell lines with hyper-methylated promoter are highly motile

Remco van Horssen[1]
Antoinette Hollestelle[2]
Joost Rens[1]
Alexander M. M. Eggermont[1]
Mieke Schutte[2]
Timo L.M. ten Hagen[1]

[1]Laboratory of Experimental Surgical Oncology, Department of Surgical Oncology, and [2]Department of Medical Oncology, Erasmus MC – Daniel den Hoed Cancer Centre, Rotterdam, The Netherlands.

In Preparation

ABSTRACT

Linking cell migration characteristics of tumour cells *in vitro* to metastasis formation *in vivo* is controversial. While inhibition of metastases can occur in all stages, the intrinsic features of tumour cells strongly determine the aggressiveness of the disease with respect to growth, invasion and metastasis. Using a novel barrier migration assay, we analysed the migratory capacity of several well-characterized human breast cancer cell lines (MDA-MB-231, MCF-7, CAMA-1, SUM-159PT, SUM52PE and SK-BR3). When comparing the various cell lines, the two hyper-methylated E-cadherin cell lines had the highest migration capacity, wild-type E-cadherin cell lines showed an intermediate migration capacity and breast cancer lines with mutant E-cadherin lacked migration capacity. Both tumour cell lines with wild-type E-cadherin genes did not respond to fibronectin (FN) while MDA-MB-231 cells, with hyper-methylated E-cadherin, showed a migration induction upon FN. Treatment with bFGF induced migration of cells with wild-type E-cadherin but not of cells with hyper-methylated E-cadherin. In contrast, both cell lines with mutant E-cadherin genes had no migration capacity and did not respond to FN, bFGF or both. Together, our results suggest a possible connection between E-cadherin gene status and migration capacities of breast cancer cells and justify more detailed research on E-cadherin involvement on cell motility.

INTRODUCTION

Tumour-metastases are the cause of death for most cancer patients. Metastases show certain organ specificity. For instance, breast and prostate cancer metastases are often found in bone [1,2], while melanoma metastases very frequently occur in the brain [3,4]. Metastasis formation is a multi step process. These steps include escape of the cancer cells from the primary tumour, migration to (tumour)vessels, entering the blood or lymphatic circulation, arrest in secondary sites, extravasation and migration into tissue, initiation of growth and vascularization of the metastatic tumour (reviewed in [5]).

Cell migration is one of these steps and recent *in vivo* evidence revealed that metastatic potential of a subset of tumour cells correlate with their migration capacity. In contrast to non-metastatic cells, metastatic cells exhibit polarization and migration towards blood vessels [6]. These metastatic tumour cells migrate along fibres of the extra cellular matrix (ECM) between primary tumours and blood vessels [7] and several motility genes have been shown to be upregulated in these migrating cells [8]. *In vivo* migration of (breast) tumour cells turned out to be amoeboid, while *in vitro* the same cells migrated with a fibroblast-like spindle morphology [9]. These intriguing

observations of intratumoural cell migration have shed new light on migration and invasion during metastasis formation. But next to *in vivo* models, application of (novel) *in vitro* cell migration assays will be very useful to identify and study specific elements involved in (cancer) cell migration [10].

Prior to initiation of cell motility, tumour cells undergo loss of intrinsic polarity, weaken their cell-cell junctions and change their morphology, called epithelial-mesenchymal transition (EMT) (reviewed in [11]). The molecular mechanisms underlying EMT turned out to be shared in tumour progression and morphogenesis [12]. Among many other regulators, E-cadherin is a mayor player in EMT, both in embryogenesis and tumour progression [13,14]. E-cadherin is the prototypic Type I cadherin, forming homophilic interaction in their extra cellular domains and are intracellular connected to the actin cytoskeleton intracellular indirectly via α- and β-catenin [15]. Recently it was shown that the exact linkage is very dynamic and regulated by α-catenin which serves as a switch between actin and the E-cadherin-β-catenin complex [16,17]. During EMT, E-cadherin is downregulated and transcriptional regulators have been identified from developmental biology studies (reviewed in [18]) with an important role for Snail transcription repressors [19].

During tumour progression E-cadherin is identified as a tumour suppressor [20] and E-cadherin protein levels inversely correlate with cancer grade [21]. In concordance with the reported effects of E-cadherin on cell-cell contact and invasion, downregulation of in E-cadherin have been reported to increase cell motility of breast tumour cells *in vitro* [22]. However, detailed data like morphology, migration pattern in relation to responsiveness to extracellular triggers are hardly available.

In this study we applied a novel cell migration approach to analyse cell migration parameters in various tumour cell lines in response to bFGF and/or fibronectin (FN). We describe the assay used and analysed a set of breast cancer cell lines with different characteristics. The data provide preliminary indications for a direct or indirect involvement of E-cadherin status in migration capacity of breast tumour cells.

MATERIALS AND METHODS

Cell culture and reagents

Human breast cancer cell lines (MDA-MB231, MCF-7, CAMA-1, SUM-159PT, SUM52PE, SK-BR3) [23] were cultured in RPMI 1640 medium (Biowhittaker) supplemented with 10% FCS and 100 U/ml penicillin/streptomycin (Life Technologies). The SUM cell lines were generated in the Ethier laboratory (available at http://www.asterand.com) and other cell lines were obtained from American Type Culture Collection (Manassas, VA). All tumour cells were maintained at 37 ^{o}C, 5% CO_2 in a

humidified incubator and routinely subcultured by removal from flasks using Trypsin-EDTA (Biowhittaker).

Cell migration assay

Barrier migration assays were performed as previously described [24] to obtain a reproducible and standardized method and to monitor cell movements real time (see also Fig. 1). A cover slip was placed in an Attofluor incubation chamber (Molecular Probes), which was subsequently sterilized. In this set up, a removable, sterile circular migration barrier was placed which fits tightly in the chamber and prevents cell growth into the middle of the coated cover slip. Cells were seeded around this barrier and grown until confluence. Subsequently, the migration barrier was removed; cells were washed twice and then incubated with the appropriate medium. Triggers for cell migration were none, FN (10 μg/ml, Roche), bFGF (200 ng/ml, PeproTech) or both. bFGF was diluted in the medium and Coated cover slips were obtianed by adding FN in serum-free medium to the cover slips and incubated for at least 1 h at 37 ^{o}C prior to cell seeding. The incubation chamber was placed on an inverted microscope and migration of cells was measured for 24 h.

Time-lapse microscopy

Time-lapse imaging of cell migration was done on Axiovert 100 M microscopes, equipped with either an AxioCam HRC digital camera or an AxioCam MRC digital camera (Carl Zeiss). Microscopes were controlled by AxioVision software, version 4.5. Cells in the incubation chamber were maintained at 37°C in a constantly humidified atmosphere, with controlled and heated CO_2-flow. Cells were imaged every 12 min with a 10X/0.30 PLAN-NEOFLUAR objective (Carl Zeiss).

Analysis of cell movements

Parameters of cell migration, including the total and average migration distance, migration velocity, effective migration distance, migration tracks and directionality (ratio of distance from start to end point and migrated track), were obtained from time-lapse movies, taking the nucleus as a reference. For each treatment, at least 10 migrating cells per experiment and at least 3 independent migration assays were performed. After cell division one of the daughter cells was followed. Migration velocity was calculated by dividing migration distance by migration time. Both the total distance (migrated track) and effective distance (reflecting directed migration towards the centre of the cover slip) were

calculated. All measurements were done using AxioVision 4.5 software. Images from the time-lapse analysis were processed to generate movies in Adobe Premiere.

RESULTS

Novel migration assay

Established models generally used for *in vitro* migration studies have important drawbacks, like lack of control of matrix composition, standardization of repeated assays and damage inflicted to the cells. To address these issues, we developed a novel "barrier" migration assay [24], to analyse migration capacities of cells. The setup and rationale for the barrier migration assay are depicted in Figure 1. Cell culture chambers containing cover glasses were coated with fibronectin (FN). Within the cell culture chamber a circular insert is positioned serving as barrier, thereby creating two compartments within the cell culture chamber. Cells are seeded in the large compartment around the barrier and grown till confluence. The small compartment is filled with culture medium.

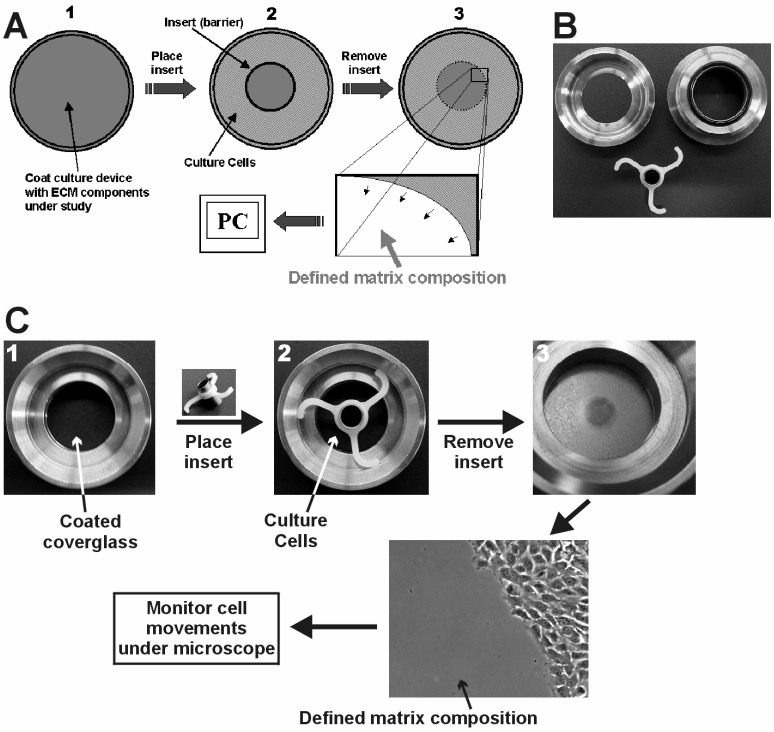

FIGURE 1. Setup of barrier migration assay.
A. Schematic representation of the novel cell migration assay to study unharmed cells migrating along a defined matrix in a real-time assay. Cell culture chambers are coated with fibronectin (1) and a so-called migration insert is placed in the middle of

the cell chamber (2). This insert serves as a barrier and generates two compartments in the cell chamber. Cells are seeded in the outer compartment around the barrier while the inner compartment is filled with medium alone. The barrier is removed when the cells have grown till confluence (3) and cell migration into the formerly inner compartment is imaged real-time under the microscope. The cell free area is controlled and has a defined matrix composition. In addition, the cells are left unharmed.
B. Cell chamber and migration barrier used to facilitate long time living cell imaging. Cells are grown on cover glasses, which are placed in the cell chamber.
C. Pictures of the barrier assay as depicted in the scheme of Fig. 1A. The same steps are depicted in A and C.

When the cells are grown as monolayer, the insert is removed, cells are incubated under specific conditions and the cell culture chamber is placed under the microscope to monitor cell movement into the cell free area with defined matrix composition. Figure 1A shows a schematic overview of this approach, the materials used for the cell culture chamber and insert are depicted in Figure 1B. Figure 1C shows the setup using the same steps as Figure 1A. Using this approach, both cells and matrix are untouched, the assay is standardized and quantifiable. Moreover, the composition of the matrix is controlled and cell movement and morphology are monitored in the same assay. Testing and validation of this assay was done by using endothelial cells and fibroblasts in a comparative analysis with 'scratch' migration assays [24] (see Chapter 2 of this thesis).

Breast cancer cells with wild-type E-cadherin show moderate migration capacity, respond to bFGF but not to FN

Using the barrier migration assay, we evaluated migration capacity of two human breast cell lines with wild-type E-cadherin expression (MCF-7 and SUM52PE). These epithelial cell lines showed a moderate migration capacity when no coating or growth factor was added (Fig. 2 A, none). Interestingly, when we studied migration capacity along a FN-coating we observed no differences. FN did not induce migration of these cell types (Fig. 2A, FN). When bFGF was added we observed an induction of migration both with and without FN-coating (Fig. 2A, right panels). Both cell lines exhibit morphology of epithelial sheets and when migration is induced, cells move forward as a sheet. It appears like a pushing movement of dividing and moving cells and no individual moving cells were observed. When we analysed the movies in more detail, we observed many cell divisions in the SUM-52PE cells without a visible forward movement of the migration front.

These observations suggest that the responses observed are migratory rather than proliferation dependent but this issue needs further investigations. Figure 2B shows the quantification of cell movements of the cell types studied under different conditions.

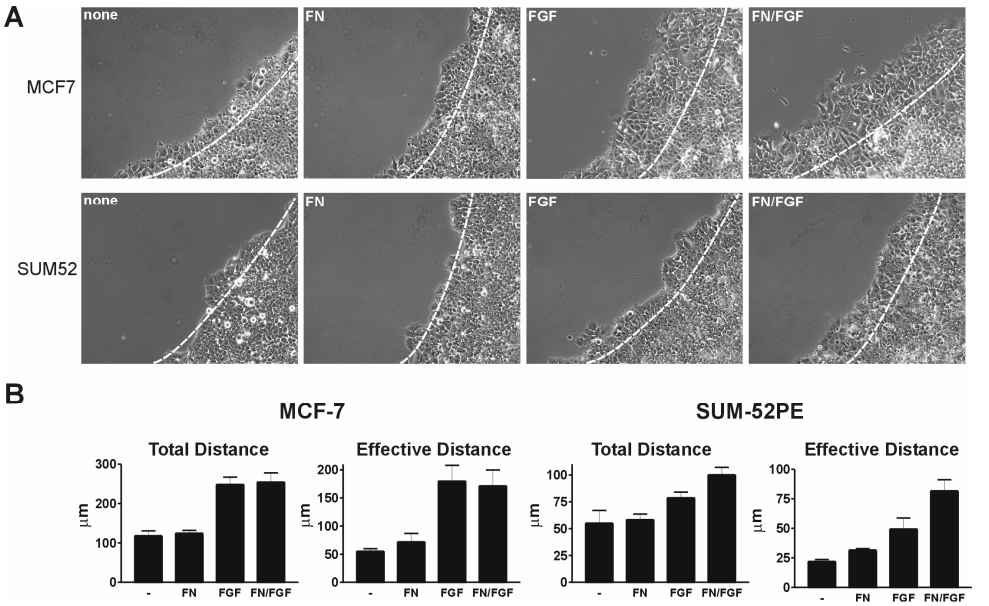

FIGURE 2. Migration capacities and response of wild-type E-cadherin breast cancer cells.
A. Pictures of migrating epithelial breast cancer cells after 24 h obtained from migration movies. White dashed lines indicate the migration front at T=0 h. Bar: 100 µm.
B. Total and effective migration distances of MCF-7 and SUM-52PE cells after 24 h with and without FN coating and with or without bFGF (200 ng/ml) treatment.

Breast cancer cells with hyper-methylated E-cadherin show high migration capacity and respond differentially to FN and bFGF

We then analysed the migration capacity of two breast cancer cell lines with undetectable E-cadherin protein expression due to hyper-methylation of the E-cadherin promoter (MDA-MB-231 and SUM-159PT) [25]. Both cell lines with hyper-methylated E-cadherin have a spindle-like morphology and exhibit a high migration capacity as observed in non-coated cell migration assays without growth factor treatment (Fig. 3A, none). For MDA-MB-231 cells, we observed cells moving individually ahead of the migration front, with the majority of cells remaining in the migration front. For the SUM-159PT cells however, all cells sticked together in moving monolayers, no single moving cells were observed but cell motility was very high. When MDA-MB-231 cells were allowed to migrate along FN-matrix, cell motility was increased whereas FN did not further induce migration of SUM-159PT cells (Fig. 3A, FN). Treatment with bFGF did not increase migration response in either of the two cell lines. The migration distances measured, both total and effective, are depicted in Figure 3B.

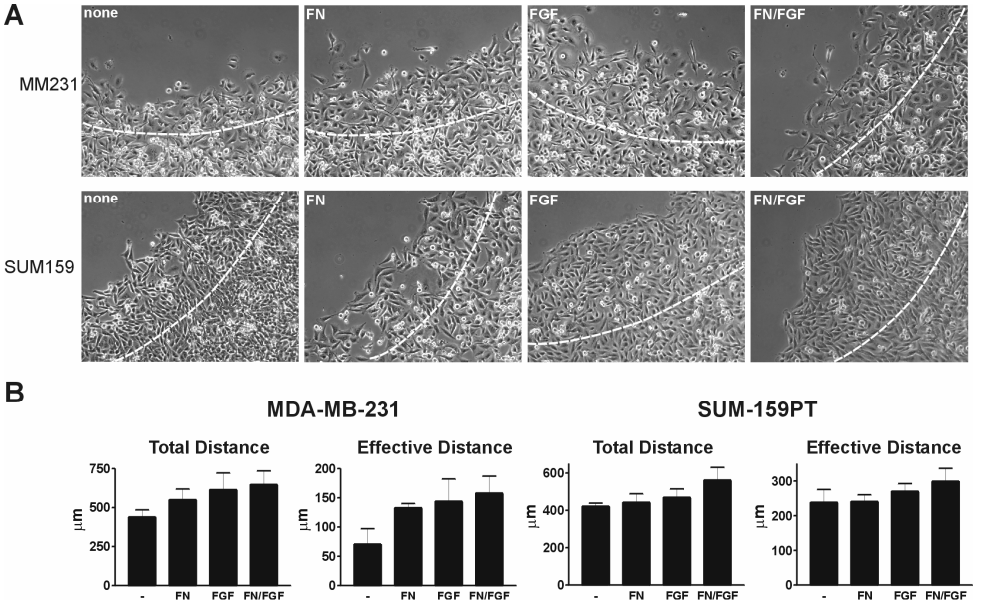

FIGURE 3. Migration capacities and response of breast cancer cells with hyper-methylated E-cadherin.
A. Pictures of migrating spindle-shaped breast cancer cells after 24 h obtained from migration movies. White dashed lines indicate the migration front at T=0 h. Bar: 100 µm.
B. Total and effective migration distances of MDA-MB-231 and SUM-159PT cells after 24 h with and without FN coating and with or without bFGF (200 ng/ml) treatment.

Breast cancer cells with mutant E-cadherin lack migration capacity and do not respond to FN or bFGF treatment

Next we examined the migration capacity of two breast cancer cell lines with biallelic mutations in E-cadherin (CAMA-1 and SB-BR3) [25]. These mutations resulted in aberrant or absent E-cadherin protein expression, but in both cases in a non-functional protein. The cells showed rounded cell morphology, consistent with abnormal E-cadherin mediated cell-cell junctions. Strikingly, both cell lines completely lacked capacity to migrate (Fig. 4A). During the 24 h of analysis, all cells remained at the same spot within the culture chamber. In addition, when we tried to induce migration by FN-coating, bFGF treatment or both, the cell lines still do not respond and showed no migration at all (Fig. 4A). All measurements show the same results, no migration capacity and no response to treatment as can be seen from the small scaling (Fig. 4B).

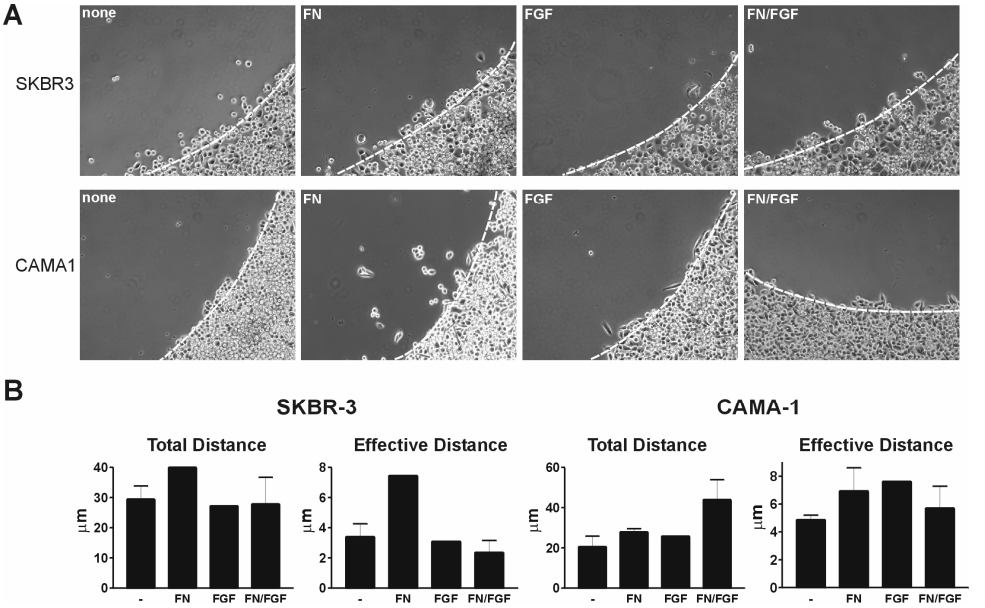

FIGURE 4. Migration capacities and response of breast cancer cells with mutant E-cadherin.
A. Pictures of migrating rounded breast cancer cells after 24 h obtained from migration movies. White dashed lines indicate the migration front at T=0 h. Bar: 100 µm.
B. Total and effective migration distances of SKBR-3 and CAMA-1 cells after 24 h with and without fibronectin coating and with or without bFGF (200 ng/ml) treatment.

Comparative analysis of different breast cancer cell lines

To compare the migratory capacities of the six cell lines studied, we plotted the migration distances of experiments without FN or bFGF in a single graph (Fig. 5).

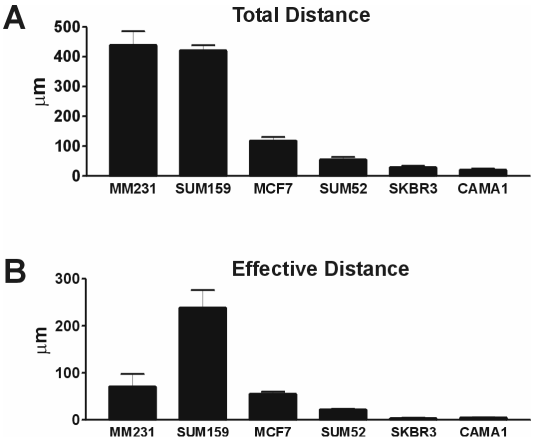

FIGURE 5. Migration capacities of 6 different breast cancer cell lines.
A. Total migration distances after 24 h.
B. Effective migration distances after 24 h.

The hyper-methylated E-cadherin cell lines have the highest migratory capacity. Strikingly, these two cell lines have comparable total distances but the effective distance of SUM-159PT cells is much higher. The epithelial wild-type E-cadherin cell lines show moderate migratory capacities, where MCF-7 is more migratory than SUM-52PE. The mutant E-cadherin cell lines both showed comparable low to absent migration.

DISCUSSION

In this study we show that various breast cancer cell lines with E-cadherin promoter-methylation and mutation have completely distinct cell motility capacities. These novel data suggest that mutation and hyper-methylation of E-cadherin are two separate entities as compared to wild-type E-cadherin.

Cell migration is one of the crucial steps of metastasis and recent studies directly link motility to metastasis [26]. We have used a novel barrier migration assay to analyse the migration potential of different breast cancer cell lines. This novel cell migration assay has been developed to obtain optimal control over the cells and the matrix along which the cells migrate [24]. Migration experiments are carried out real-time under the microscope to obtain a broad set of motility parameters like morphology, migration pattern, distances and velocity (see Fig. 1). In addition, cell divisions during migration can be analysed. Although cell migration *in vitro* is hard to translate to the *in vivo* situation of motility and metastasis formation, from *in vivo* experiments it has become clear that components of the ECM are of crucial importance for the process of cell motility within tumours [6].

We evaluated cell migration capacities of different breast cancer cell lines with reported differences in E-cadherin status. During breast tumour development E-cadherin acts as an invasion-suppressor and mutation or deregulation of protein expression results in an increase in invasiveness [27,28]. For a broad set of breast cancer cell lines E-cadherin status correlated with cell morphology (Hollestelle and Schutte, manuscript in preparation). Cells with wild-type E-cadherin showed an epithelial sheet morphology, cells with hyper-methylated E-cadherin promoter are spindle-shaped, while cells with E-cadherin mutations showed rounded cell morphology. We investigated the migration capacities of two cell lines out of each group. Strikingly, different cell lines with the same E-cadherin status were completely comparable (Figures 2-4). Three sets of two cell lines isolated from different patients, but with a similar E-cadherin gene status, showed the same migration capacity and responsiveness suggesting that E-cadherin status might directly or indirectly be involved in these processes. Our data suggests that E-cadherin, known to be a involved in tumour invasion [29], might

also act as a regulator of breast tumour cell migration. To justify this preliminary conclusion, more detailed genetic experiments on E-cadherin need to be done on the future.

For breast cancer cells with wild-type E-cadherin we observed a moderate migration capacity (Fig. 2). Cells with hyper-methylated E-cadherin promoter showed a strongly increased capacity (Fig. 3) while cells with E-cadherin mutations completely lacked the capacity to migrate. Moreover, the latter cells also did not respond to any trigger (Fig. 4). The reasons for big differences between mutation and hyper-methylation remain unclear and need to be addressed by future experiments. E-cadherin mutation might results in different secondary cellular effects as compared to hyper-methylation. Epithelial cells did not respond to FN-coating, while triggering with bFGF did induce motility. Epithelial cells moved as a sheet and future experiments need to address the exact contribution of cell proliferation to the migration responses to discriminate between the mitogenic and migration-inducing effects of bFGF (or other triggers).

We only tested one matrix component making drawing conclusions very preliminary. For the evaluation of matrix-component involvement in epithelial breast cancer cell lines more matrix components need to be evaluated. For epithelial cells one might speculate that these cells are hard to trigger by matrix components because the cell-cell contacts are very high and these cells can not move individually. For FN and collagen-IV an effect on motility of MCF-7 and MDA-MB-231 cells has been described [30]. However, these experiments were done using trans-well chemo tactic systems and in these responses different factors may be involved. One can imagine that crawling into/through a membrane and migrating along a defined matrix are dissimilar *in vitro* systems and differences may be observed for specific factors. One such difference was observed for MDA-MB-231 cells that showed a higher motility along FN-coating (Fig. 3). In addition, also for bFGF we observed different effects as reported previously when other assays (scratch and trans-well) were used. When bFGF expression was induced in MDA-MB-231 cells, the cells showed less malignant features, like a lower motility [31]. This effect on migration however, was transient and besides the different assays used, we added bFGF at higher concentrations. This again indicates the need for experiments to determine the proliferation dependent component of the observed effects.

When we analysed migration capacities of breast cancer cell lines with mutated E-cadherin, we unexpectedly observed that these cells completely lacked capacity to migrate and failed to respond to triggers as well (Fig. 4). These phenomena were observed in two cell lines. For a third cell line, MPE600, the same results were found (data not shown). These observations seem in contrast to an earlier study suggesting a motility increase upon E-cadherin mutation [22]. However, the cell line

used (MDA-MB-435S) is reported to have hyper-methylated E-cadherin promoter [32] with the wild-type gene (Hollestelle and Schutte, manuscript in preparation). Thus MDA-MB-435S is not a mutant cell lines but has hyper-methylation which is exactly in line with the presented migration data. These data show that breast cancer cells with mutated E-cadherin have completely lost the capacity to migrate and in addition also are not capable to gain this capacity when triggered. An interesting question is whether the loss of cell-cell contact and absence of migration capacity in those cells are linked or independent processes. Extra experiments need to be set up to confirm the observation and to allow statistical analysis of the differences in response. More breast cancer cell lines will be evaluated and mutant cell lines will be transfected with wild-type E-cadherin to further analyse the role of E-cadherin during breast tumour cell migration.

In conclusion, we show new data on breast cancer cell motility with a possible but complex role of E-cadherin. Both migration capacity and responsiveness of breast cancer cells might be linked E-cadherin status. However, on the exact involvement of E-cadherin and possible other factors, we can not make strong conclusions. For this purpose gene knock-in and knock-down experiments need to be done within one cell line to allow proper comparison. The use of a novel migration assay raised some new questions but also provided new data on motility of tumour cells, which might be useful for a future translation to *in vivo* migration and metastasis formation.

REFERENCES

1. Ruoslahti, E. (1996). How cancer spreads. *Sci.Am.* 275, 72-77.
2. Rusciano, D. and Burger, M. M. (1992). Why do cancer cells metastasize into particular organs? *Bioessays* 14, 185-194.
3. de la Monte, S. M., Moore, G. W., and Hutchins, G. M. (1983). Patterned distribution of metastases from malignant melanoma in humans. *Cancer Res.* 43, 3427-3433.
4. Amer, M. H., Al Sarraf, M., Baker, L. H., and Vaitkevicius, V. K. (1978). Malignant melanoma and central nervous system metastases: incidence, diagnosis, treatment and survival. *Cancer* 42, 660-668.
5. Chambers, A. F., Groom, A. C., and MacDonald, I. C. (2002). Dissemination and growth of cancer cells in metastatic sites. *Nat.Rev.Cancer* 2, 563-572.
6. Condeelis, J. and Segall, J. E. (2003). Intravital imaging of cell movement in tumours. *Nat.Rev.Cancer* 3, 921-930.
7. Yamaguchi, H., Wyckoff, J., and Condeelis, J. (2005). Cell migration in tumours. *Curr.Opin.Cell Biol.* 17, 559-564.
8. Wang, W., Goswami, S., Sahai, E., Wyckoff, J. B., Segall, J. E., and Condeelis, J. S. (2005). Tumour cells caught in the act of invading: their strategy for enhanced cell motility. *Trends Cell Biol.* 15, 138-145.
9. Wolf, K., Mazo, I., Leung, H., Engelke, K., von Andrian, U. H., Deryugina, E. I., Strongin, A. Y., Brocker, E. B., and Friedl, P. (2003). Compensation mechanism in tumour cell migration: mesenchymal-amoeboid transition after blocking of pericellular proteolysis. *J.Cell Biol.* 160, 267-277.
10. Friedl, P. and Wolf, K. (2003). Tumour-cell invasion and migration: diversity and escape mechanisms. *Nat.Rev.Cancer* 3, 362-374.
11. Thiery, J. P. (2002). Epithelial-mesenchymal transitions in tumour progression. *Nat.Rev.Cancer* 2, 442-454.
12. Savagner, P. (2001). Leaving the neighborhood: molecular mechanisms involved during epithelial-mesenchymal transition. *Bioessays* 23, 912-923.
13. Edelman, G. M., Gallin, W. J., Delouvee, A., Cunningham, B. A., and Thiery, J. P. (1983). Early epochal maps of two different cell adhesion molecules. *Proc.Natl.Acad.Sci.U.S.A* 80, 4384-4388.

14. Frixen, U. H., Behrens, J., Sachs, M., Eberle, G., Voss, B., Warda, A., Lochner, D., and Birchmeier, W. (1991). E-cadherin-mediated cell-cell adhesion prevents invasiveness of human carcinoma cells. *J.Cell Biol.* 113, 173-185.
15. Kemler, R. (1993). From cadherins to catenins: cytoplasmic protein interactions and regulation of cell adhesion. *Trends Genet.* 9, 317-321.
16. Drees, F., Pokutta, S., Yamada, S., Nelson, W. J., and Weis, W. I. (2005). Alpha-catenin is a molecular switch that binds E-cadherin-beta-catenin and regulates actin-filament assembly. *Cell* 123, 903-915.
17. Yamada, S., Pokutta, S., Drees, F., Weis, W. I., and Nelson, W. J. (2005). Deconstructing the cadherin-catenin-actin complex. *Cell* 123, 889-901.
18. Peinado, H., Portillo, F., and Cano, A. (2004). Transcriptional regulation of cadherins during development and carcinogenesis. *Int.J.Dev.Biol.* 48, 365-375.
19. Batlle, E., Sancho, E., Franci, C., Dominguez, D., Monfar, M., Baulida, J., and Garcia, D. H. (2000). The transcription factor snail is a repressor of E-cadherin gene expression in epithelial tumour cells. *Nat.Cell Biol.* 2, 84-89.
20. Berx, G., Cleton-Jansen, A. M., Nollet, F., de Leeuw, W. J., van, d., V, Cornelisse, C., and van Roy, F. (1995). E-cadherin is a tumour/invasion suppressor gene mutated in human lobular breast cancers. *EMBO J.* 14, 6107-6115.
21. Birchmeier, W. and Behrens, J. (1994). Cadherin expression in carcinomas: role in the formation of cell junctions and the prevention of invasiveness. *Biochim.Biophys.Acta* 1198, 11-26.
22. Handschuh, G., Candidus, S., Luber, B., Reich, U., Schott, C., Oswald, S., Becke, H., Hutzler, P., Birchmeier, W., Hofler, H., and Becker, K. F. (1999). Tumour-associated E-cadherin mutations alter cellular morphology, decrease cellular adhesion and increase cellular motility. *Oncogene* 18, 4301-4312.
23. Elstrodt, F., Hollestelle, A., Nagel, J. H., Gorin, M., Wasielewski, M., van den, O. A., Merajver, S. D., Ethier, S. P., and Schutte, M. (2006). BRCA1 mutation analysis of 41 human breast cancer cell lines reveals three new deleterious mutants. *Cancer Res.* 66, 41-45.
24. Van Horssen, R., Galjart, N., Rens, J. A. P., Eggermont, A. M. M., and ten Hagen, T. L. M. (2006). Differential effects of matrix and growth factors on endothelial and fibroblast motility: Application of a modified cell migration assay. *J Cell Biochem* Epub 30 Jun (2006).
25. van de, W. M., Barker, N., Harkes, I. C., van der, H. M., Dijk, N. J., Hollestelle, A., Klijn, J. G., Clevers, H., and Schutte, M. (2001). Mutant E-cadherin breast cancer cells do not display constitutive Wnt signaling. *Cancer Res.* 61, 278-284.
26. Jones, D. H., Nakashima, T., Sanchez, O. H., Kozieradzki, I., Komarova, S. V., Sarosi, I., Morony, S., Rubin, E., Sarao, R., Hojilla, C. V., Komnenovic, V., Kong, Y. Y., Schreiber, M., Dixon, S. J., Sims, S. M., Khokha, R., Wada, T., and Penninger, J. M. (2006). Regulation of cancer cell migration and bone metastasis by RANKL. *Nature* 440, 692-696.
27. Perl, A. K., Wilgenbus, P., Dahl, U., Semb, H., and Christofori, G. (1998). A causal role for E-cadherin in the transition from adenoma to carcinoma. *Nature* 392, 190-193.
28. Berx, G. and van Roy, F. (2001). The E-cadherin/catenin complex: an important gatekeeper in breast cancer tumourigenesis and malignant progression. *Breast Cancer Res.* 3, 289-293.
29. Vleminckx, K., Vakaet, L., Jr., Mareel, M., Fiers, W., and van Roy, F. (1991). Genetic manipulation of E-cadherin expression by epithelial tumour cells reveals an invasion suppressor role. *Cell* 66, 107-119.
30. Sisci, D., Aquila, S., Middea, E., Gentile, M., Maggiolini, M., Mastroianni, F., Montanaro, D., and Ando, S. (2004). Fibronectin and type IV collagen activate ERalpha AF-1 by c-Src pathway: effect on breast cancer cell motility. *Oncogene* 23, 8920-8930.
31. Korah, R. M., Sysounthone, V., Golowa, Y., and Wieder, R. (2000). Basic fibroblast growth factor confers a less malignant phenotype in MDA-MB-231 human breast cancer cells. *Cancer Res.* 60, 733-740.
32. Graff, J. R., Herman, J. G., Lapidus, R. G., Chopra, H., Xu, R., Jarrard, D. F., Isaacs, W. B., Pitha, P. M., Davidson, N. E., and Baylin, S. B. (1995). E-cadherin expression is silenced by DNA hypermethylation in human breast and prostate carcinomas. *Cancer Res.* 55, 5195-5199.

PART 2

Effects of EMAP-II on TNF antitumour activities - From molecule to patient

Chapter 5

TNF in Cancer Treatment: Molecular Insights, Anti-Tumour Effects and Clinical Utility

Remco van Horssen
Timo L. M. ten Hagen
Alexander M. M. Eggermont

Laboratory of Experimantal Surgical Oncology, Department of Surgical Oncology, Erasmus MC – Daniel den Hoed Cancer Center, Rotterdam, The Netherlands

The Oncologist 11(4): 397-408 (2006)

Note: This chapter contains figures that are also available in full colour (labeled with 'CLR'). These colour figures can be found in the Appendix of this book (page 209) and in the online version (via Medical Library, Erasmus MC).

ABSTRACT

Tumour necrosis factor alpha (TNF), isolated 30 years ago, is a multifunctional cytokine playing a key role in apoptosis and cell survival as well as in inflammation and immunity. Although named after its anti-tumour properties, TNF has been implicated in a wide spectrum of other diseases. The current use of TNF in cancer is regional treatment of locally advanced soft tissue sarcomas and metastatic melanomas and other irresectable tumours of any histology, to avoid amputation of the limb. It has been demonstrated in the isolated limb perfusion (ILP) setting that TNF acts synergistically with cytostatic drugs. The interaction of TNF with TNF Receptor-1 and -2 (TNF-R1, R2) activates several signal transduction pathways leading to the diverse functions of TNF. The signaling molecules of TNF-R1 have been elucidated quite well but regulation of the signaling remains unclear. Besides these molecular insights, laboratory experiments in past decade have shed light upon TNF action during tumour treatment. Besides extravasation of erythrocytes and lymphocytes leading to hemorrhagic necrosis, TNF targets the tumour-associated vasculature (TAV) by inducing hyper permeability and destruction of the vascular lining. This results in an immediate effect of selective accumulation of cytostatic drugs inside the tumour and a tardive effect of destruction of tumour vasculature. In this review, covering TNF from molecule to clinic, we provide an overview of the use of TNF in cancer starting with molecular insights of TNF-R1 signaling, cellular mechanisms of the anti tumour activities of TNF and we end with the clinical response. In addition possible factors modulating TNF actions will be discussed.

INTRODUCTION

Tumour necrosis factor alpha (TNF) is a multifunctional cytokine involved in apoptosis, cell survival, inflammation and immunity acting via two receptors [1,2]. Currently it is used in cancer treatment in an isolated limb perfusion (ILP) setting for soft tissue sarcomas (STS), irresectable tumours of various histological types, and melanoma in-transit metastases confined to the limb [3]. TNF was isolated in 1975 from serum of mice treated with bacterial endotoxin as the active component of "Coley's toxin" and shown to induce hemorrhagic necrosis of mice tumours [4,5]. It was almost a century ago that William Coley, a surgeon from New York, observed high fever and tumour necrosis in some cancer patients treated with his bacterial filtrate ("Coley's mixed toxins") [6]. A decade after its isolation TNF was also characterized as "cachectin" and as T-lymphocyte differentiation factor [7,8]. In 1984 the human TNF-gene was cloned [9,10] and a range of clinical experiments were set up

leading to a license from the European Medicine Evaluation Agency (EMEA) for the treatment of limb-threatening soft tissue sarcomas in an isolated perfusion setting [11].

TNF and TNF-R1 signaling

TNF is a 17-kDa protein consisting of 157 amino acids, which is a homotrimer in solution. In humans the gene is mapped on chromosome 6 [12]. Its bioactivity is mainly regulated by soluble TNF-binding receptors. TNF is mainly produced by activated macrophages, T-lymphocytes and NK-cells. Lower expression is known for a variety of other cells including fibroblasts, smooth muscle cells and tumour cells. In cells TNF is synthesized as pro-TNF (26 kDa) which is membrane-bound and upon cleavage of its pro-domain by TNF-converting enzyme (TACE) it is released (reviewed in [13]).

As mentioned above, TNF acts via two distinct receptors [14]. Although the affinity for TNF-R2 is 5 times higher compared to TNF-R1 [15], the latter initiates the majority of the biological activities of TNF. TNF-R1 (p60) is expressed on all cell types while TNF-R2 (p80) expression is mainly confined to immune cells [16]. The major difference between the two receptors is the Death Domain (DD) in TNF-R1 that is absent in TNF-R2. For this reason TNF-R1 is an important member of the death receptor family sharing the capability to induce apoptotic cell death [17]. Besides this apoptotic signaling TNF-R1 is widely studied because it is a dual role receptor: next to induction of apoptosis it also has the ability to transduce cell survival signals. Although signaling pathways are well defined nowadays, the life-death signaling regulation is still poorly understood [18,19].

The TNF-R1 signaling pathways are depicted in Figure 1. Upon binding of the homotrimer TNF, TNF-R1 trimerizes and silencer of death domain (SODD) protein is released [20]. TNFR-associated death domain (TRADD) binds to the DD of TNF-R1 and recruits the adaptor proteins receptor interacting protein (RIP), TNFR-associated factor 2 (TRAF-2) and Fas-associated death domain (FADD) [21]. In turn these adaptor proteins recruit key molecules, which are responsible for further intracellular signaling. When TNF-R1 signals to apoptosis FADD binds pro-Caspase-8, which is subsequently activated. This activation initiates a protease cascade leading to apoptosis, also involving the mitochondria and with caspases as key regulators [22]. The ultimate event in this apoptotic signaling is the activation of endonucleases, like EndoG, resulting in DNA fragmentation. Alternatively, when TNF-R1 signals to survival, TRAF-2 is recruited to the complex, which inhibits apoptosis via cytoplasmic inhibitor of apoptosis protein (cIAP). The binding of TRAF-2 initiates a pathway of phosphorylation steps resulting in the activation of cFos/cJun transcription factors via mitogen-activated protein kinase (MAPK) and cJun N-terminal kinase (JNK) [23]. The major signaling

event of TRAF-2 and RIP is the widely studied activation of Nuclear Factor Kappa B (NF-kB) transcription factor via NF-kB inducing kinase (NIK) and the Inhibitor of kB kinase (IKK)-complex [24].

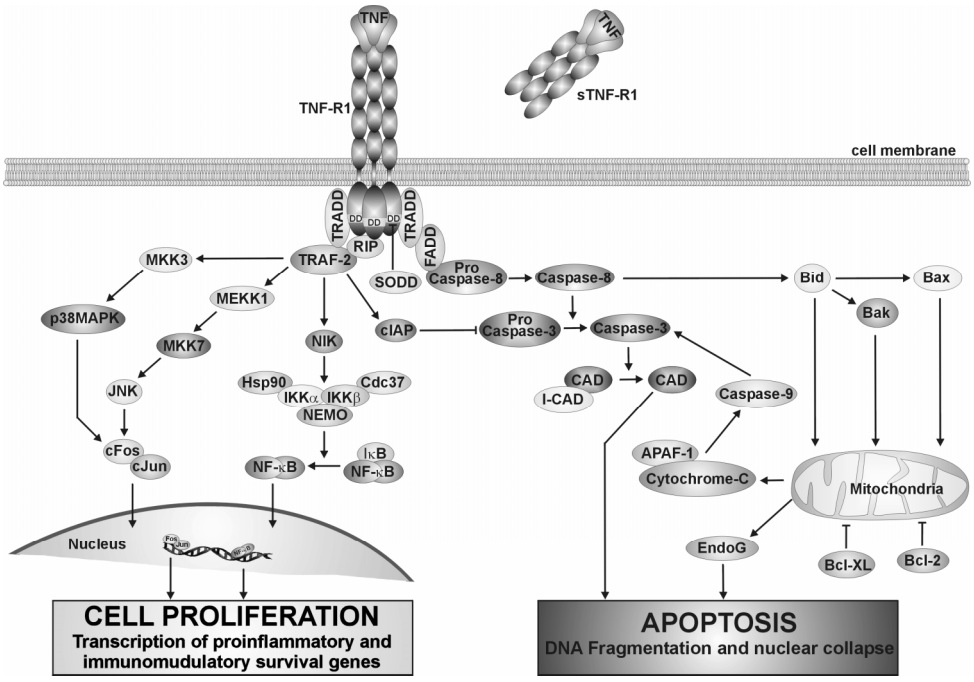

FIGURE 1. TNF-R1 signaling pathway **(CLR)**.
TNF activates both survival and proliferation pathways along with apoptotic pathways via TNF-R1. The separate pathways are well defined while the survival-death balance regulation remains unclear. Abbreviations: APAF-1: apoptosis protein activating factor-1, Bcl-2: B-cell lymphoma-2, Bid, Bak, Bax and Bcl-XL: mitochondrial proteins of the Bcl-2 family, CAD: caspase-activated DNAse, Caspase-3/8/9: cysteine aspartase (apoptotic protease) 3/8/9, Cdc37: co-chaperon of HSP90, cIAP: cytoplasmic inhibitor of apoptosis, cFos/cJun: transcription factors, DD: death domain, EndoG: mitochondrial DNAse, FADD: fas-associated DD, HSP90: heat shock protein-90, I-CAD: inhibitor of CAD, I-kB: inhibitor of NF- kB, IKKalpha/beta: I-kB kinase, JNK: cJun n-terminal kinase, MEKK1: MAPK/ERK kinase-1, MKK3/7: MAPK kinase 3/7, NEMO: NF-kB essential modulator, NF-kB: nuclear factor kappa B transcription factor, NIK: NF-kB inducing kinase, p38MAPK: p38 mitogen activated protein kinase, RIP: receptor interacting protein, SODD: silencer of DD, sTNF-R1: soluble TNF-R1, TNF: tumour necrosis factor alpha, TNF-R1: TNF receptor 1, TRADD: TNF receptor-associated DD, TRAF-2: TNF receptor-associated factor-2.

Both the NF-kB and cFos/cJun transcription factors induce transcription of anti-apoptotic, proliferation, immunomodulatory and inflammation genes. NF-kB is the major survival factor in preventing TNF-induced apoptosis and inhibition of this transcription factor may improve the efficacy of apoptosis-inducing cancer therapies [25]. NF-kB activation in many human malignancies is aberrant or consecutive and its role in regulation of the apoptosis-proliferation balance in tumour cells indicates its role in oncogenesis [26,27] For further details on the dual signaling of TNF-R1, see Figure 1.

Implications for cellular mechanisms underlying TNF effect during solid tumour treatment

It is widely known that TNF induces hemorrhagic necrosis in a certain set of tumour types. To investigate the underlying mechanisms of TNF action during ILP of solid tumours in humans we set up perfusion models in rats and reported that the hemorrhagic necrosis was strongly increased in tumours treated with TNF and chemotherapeutic drugs [28]. In addition we showed a synergistic anti tumour effect of the combination treatment with TNF and chemotherapeutic drugs [29]. In contrast, TNF alone induced only a mild central necrosis and there was no objective tumour response observed. The same rat models revealed as well that addition of TNF improved the accumulation of chemotherapeutic drugs selectively in the tumour up to 3 to 6 fold The augmented uptake of melphalan added to the molecular properties of this small molecule (distribution by gradient instead of convection) resulted in intra-tumoural concentrations close to the IC50 towards STS cells *in vitro* [30,31]. These levels results in tumour cell kill in the ILP-setting and melphalan can distribute within the well-perfused parts of the tumour although the intra-tumoural pressure is high. This selective uptake of melphalan by the tumour was also observed when other vaso-active drugs were used in the ILP-setting (see below). It is important to note that the cell lines we used were not sensitive to TNF *in vitro*, which is in accordance with other reports describing a lack of effect of TNF and no synergism with cytotoxic drugs on cell lines [32,33]. Next to these ILP data, studies in mice and rat showed that a systemic low dose of TNF augments the anti tumour activity of Doxil [34,35]. These observations are comprehensible clues that mechanisms underlying the TNF effect during solid tumour treatment cannot be caused by a direct cytotoxic or cytostatic effect of TNF towards the tumour cells. It was suggested that rather than tumour cells itself, cells of the tumour-stroma may be responsible for the observed anti tumour effect of TNF in patients. This hypothesis was confirmed by data from mice experiments revealing that TNF had a cytotoxic effect against tumour vasculature [36].

Angiogenesis and tumour-associated vasculature

Angiogenesis, the formation of new blood vessels from pre-existing ones, has become a major field of research, mainly in cancer [37]. Angiogenesis is essential for a tumour to provide the tumour cells with oxygen and essential nutrients for growth and to metastasize hematogenically [38]. A growing tumour activates surrounding vessels by secreting angiogenic factors thereby changing the dormant tumour-phenotype towards an angiogenic one, the so-called ‘angiogenic switch’ [39]. Activated endothelial cells have to migrate towards the tumour along a newly formed matrix, of which the

components are synthesized by themselves, tumour cells and other cells like macrophages and fibroblasts [40]. Figure 2 shows schematically the process of tumour angiogenesis that can be divided into 4 different stages. A small dormant, tumour (stage 1) can, depending on the nature of the tumour and its microenvironment, make the 'angiogenic switch' to ensure exponential growth. The tumour is secreting growth factors, to activate endothelial cells of surrounding vessels (stage 2). Upon activation these endothelial cells start to migrate and proliferate towards the tumour. Only one endothelial cell starts an angiogenic sprout and develops into an endothelial tip cell migrating along the extra cellular matrix (ECM) and guiding the following so-called stalk endothelial cells (stage 3) [41]. Finally, the growing tumour is connected to the vasculature (stage 4). Besides growth and proliferation the tumour can metastasize. Malignant tumour cells now have access to the vessels, by invasion of the vessels, ECM degradation, attachment and homing to target sites distal metastasis can be formed [42]. The process of tumour angiogenesis results in a tumour associated vasculature (TAV), which is rather chaotic, both in structure and function. In comparison with normal vessels the tumour vessels have a non-continuous endothelium, an enlarged basal membrane and a aberrant pericyte coverage [43].

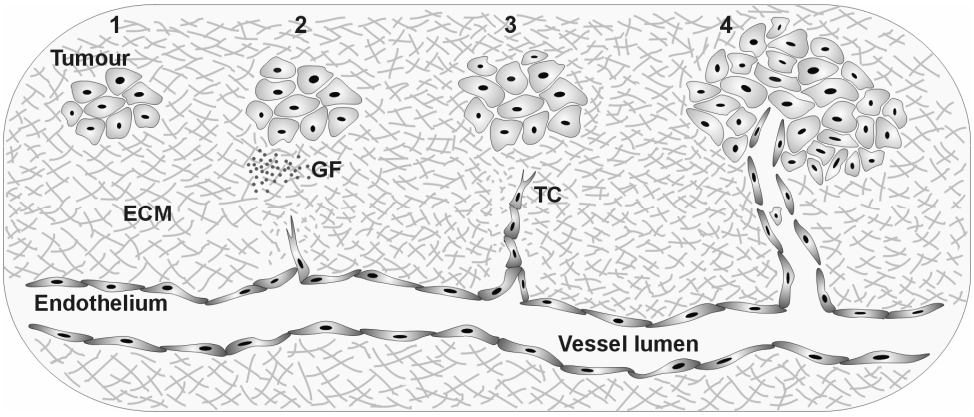

FIGURE 2. The sequential steps during tumourangiogenesis **(CLR)**.
The dormant tumour in stage 1 starts to secrete angiogenic growth factors (GF) after its 'angiogenic switch', which is accomplished by an imbalance in pro- and anti-angiogenic factors. These GF activate endothelial cells of surrounding vessels and these cells start to migrate (stage 2) and proliferate towards the tumour. An endothelial tip cell (TC) is guiding this sprouting process (stage 3). In stage 4 the novel sprout has formed a lumen and the tumour is connected to the vasculature thereby ensuring its growth and enabling itself to metastasize hematogenically.

Frequently, in tumours the vascular hierarchy of arterioles, capillaries and venules is absent resulting in loosely associated pericytes [44]. From animal experiments it is known that pericytes are present in small tumours and more abundant in large tumours [45]. The contribution of pericytes to (anti)-angiogenic therapies is currently an attractive focus of research. On one hand, these characteristics impair tumour blood flow, delivery of oxygen and therapeutics to the tumour cells and vessel functionality but on the other hand these differences may be used as a target. The solid tumours treated by ILP with TNF have a massive vascular structure consisting of vessels with the phenotype specific for tumour vessels although detailed study needs to clarify exact contribution of the TAV to observed anti-tumour responses.

Activities of TNF in solid tumours: hypothetical mechanism

The vascular differences mentioned above are depicted in Figure 3A. These differences are responsible for a more leaky vasculature in the tumour with average intra-endothelial gaps of 400 nm depending on tumour type [46].

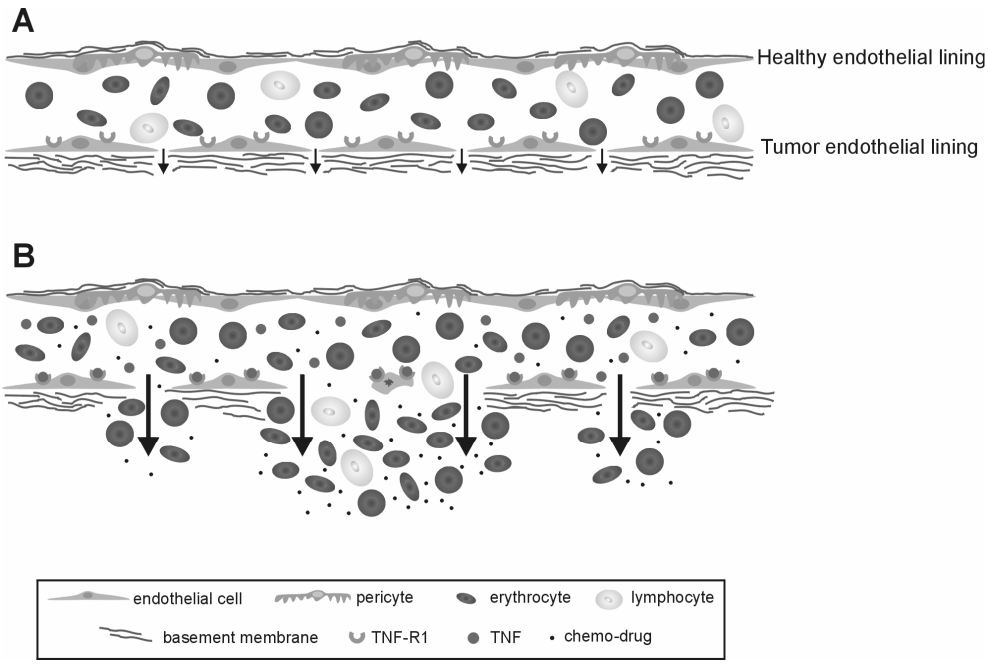

FIGURE 3. Differences between healthy and tumour endothelium and a proposed mechanism of the TNF effect **(CLR)**.

A. Schematic representation of a vessel with healthy endothelial lining (upper) and tumour endothelial lining (lower). Healthy endothelium is a continuous lining of endothelial cells, covered with pericytes and with a thin basement membrane. The permeability is low and extravasation is tightly organized. In contrast, tumour endothelium does not consist of a continuous lining of endothelial cells, it lacks pericyte coverage and the basement membrane is thickened. This phenotype results in an increased permeability of tumour vessel (small arrows). We hypothesize that the tumour endothelium exhibits a higher TNF-R1 expression due to TNF-R1 upregulating factors produced by vessel-surrounding cells.
B. Upon TNF treatment in an ILP the healthy endothelium stays intact because it is TNF-insensitive by lacking TNF-R1 expression on the membrane. Tumour endothelium binds TNF, which affects endothelial phenotype and induces apoptosis in some endothelial cells. These two processes result in an enormous induction of vessel permeability (big arrows). As a result the chemo-drug is well distributed throughout the tumour and a strong extravasation of erythrocytes results in a massive hemorrhagic tumour necrosis. The selectively targeted tumour vessels are non-functional anymore and regress.

Blood cells like lymphocytes and monocytes easily adhere and extravasate into the tumour. We speculate that the endothelial cells of the tumour vessels compared to normal vessels have an upregulation of TNF-R1 on their membrane, which may be dependent on TNF-R1 upregulating factors produced by vessel-surrounding cells like tumour cells and macrophages. This upregulation along with the specific architecture of the endothelial lining defines the tumour vessels as a specific target for TNF treatment (Fig. 3B). When TNF is administered via an ILP to treat solid tumours it binds soluble receptors and because of the high dosage TNF-R1 on tumour endothelial cells are occupied. Healthy endothelium in contrast, does bind TNF however due to a lower amount of membrane-bound TNF-R1, most TNF-R1 is stored in the golgi-apparatus [47], there is no toxicity. We propose that this TNF-TNF-R1 binding results in a hyper permeability of the tumour vessels and erythrocytes and other blood cells extravasate. The strong extravasation of erythrocytes results in massive hemorrhagic necrosis of the tumour. Due to the direct cytotoxicity of high dose TNF to endothelial cells, some of these cells will undergo apoptosis and this process will strongly enhance the induced hyper permeability (Fig. 3B). Several studies have shown that a lower dose of TNF results in comparable responses [48,49], suggesting that a lower dose still may induce these anti-vascular effects. The healthy vessels however stay intact no apoptosis and no extravasation occurs. The observed synergistic activity of TNF and chemotherapeutic drugs are a consequence of this double induced hyper permeability. This hyper permeability throughout the tumour facilitates augmented accumulation and distribution of the drug in the tumour, resulting in an improved exposure of the tumour cells to the cytostatic agent [30]. This double induced hyper permeability along with the dual targeting, the TAV (by TNF) and the tumour cells (by the chemo-drug), might be

an explanation for the observed synergistic response of tumours to TNF and chemo resulting in high response rates in patients.

Clinical Efficacy of TNF-based isolated limb perfusion

The use of TNF in the ILP setting was pioneered by Lejeune and Lienard [50]. In 19 melanoma patients and a few STS cases impressive and very rapid responses were observed. This observation was followed by multicenter trials in patients with locally advanced STS and melanoma. In Table 1 we present an overview of the multicenter trials in Europe that lead to the approval of TNF by the European Medicine Evaluation Agency (EMEA) in 1998 for its application in ILP for the treatment of high grade (2-3) STS. In these multicenter trials an overall response rate of 76% and a median limb salvage rate of 82% was observed. Moreover this table lists the largest single center studies in STS that confirm the results of the multicenter experience [49,51-67]. We observe strikingly consistent major response rates, with a median of 76 % (range 58% -91%), with a median limb salvage rate of 84% (range: 58-97). The TNF-based ILP is now performed in 35 cancer centers in Europe with national referral patterns for limb salvage.

ILP with melphalan alone for melanoma in-transit metastases (IT-mets) is reported in the literature to result in about 50 % CR rate and a 80% overall response rate [68]. The introduction of TNF in this setting was reported to increase CR rates to 70-90% and overall response rates to 95-100%. These results are summarized in Table 2 [50,69-78].

Early on however it was observed that ILP with TNF+Melphalan (TM-ILP) is especially effective against bulky tumours such as STS, where ILP with Melphalan alone [79] or Doxorubicine alone [79, 80] fails. It should also be noted of course that both drugs have no activity against melanoma in the systemic setting and that melfalan has no activity agains STS in the systemic setting. TNF-based ILP with Melphalan or Doxorubicin results in similar tumour response rates, but because of less locoregional toxicity Melphalan is preferred over Doxorubicin in the ILP setting [65, 66, 67] In our own series of 50 ILPs in patients with bulky in-transit melanoma the CR rate was still 58% [73], identical to the CR rate that was seen in a interim analysis of a randomized trial by Fraker et al., [74] where TNF-based ILP showed to be of significant benefit in patients with a high tumour load, increasing the CR rate from 19% for M-ILP to 58% in TM-ILP. Apart from bulky melanoma a further indication for TNF-based ILP is failure to a prior ILP since excellent response rates have been reported in this situation [76,77]. Similarly high response rates have been reported for TNF-based ILP for non-melanoma locally advanced skin cancers [78].

Table 1:

Principle Studies on TNF-based ILP for Irresectable Soft Tissue Sarcomas

ILP Studies Drugs	Pts n	CR %	PR %	NC/PD %	Limb Salvage %	Ref Year	Ref #
Pivotal Multicenter Studies							
TNF+IFN+M	20	55[1]	40[1]	5[1]	90	1993	51
TNF+IFN+M	59	18[1] 36[2]	64[1] 51[2]	18[1] 13[2]	84	1996	52
TNF±IFN+M	195	18[1] 29[2]	57[1] 53[2]	25[1] 18[2]	82	1996	53
TNF±IFN+M	270 196[4]	28[3] 17[3]	48[3] 48[2]	24[3] 35[2]	76 71[4]	1999	54
Single Center Studies (>20 Pts)							
TNF±IFN+M	35	37[2]	54[2]	9[2]	85	1997	55
TNF±IFN+M	34	35[2]	59[2]	6[2]	85	1998	56
TNF+Dox	20	26[5]	64[5]	10[5]	85	1999	57
TNF±IFN+M	22	18[2]	64[2]	18[2]	77	2000	58
TNF±IFN+M	55	-	-	-	84	2001	59
TNF±IFN+M	49	8[2]	55[2]	37[2]	58	2003	60
TNF±IFN+M[10]	29	38[2]	38[2]	18[2]	76	2003	61
TNF±IFN+M[9]	64	42[2]	45[2]	13[2]	82	2005	62
TNF±IFN+M[11]	29	20[2]	50[2]	30[2]	65	2005	63
TNF±IFN+M[8]	37	16[2]	68[2]	16[2]	97	2005	64
TNF+Dox[7]	21	5[1] 55[2]	57[1] 35[2]	38[1] 10[2]	71	2005	65
TNF±IFN+M	217	18[1] 26[2]	51[1] 49[2]	31[1] 25[2]	87	2005	66
TNF+M[7]	100	49[6] 35[6]	17[6] 22[6]	34[6] 43[6]	87	2005	49
TNF±IFN+M[7]	240	24[2]	50[2]	26[2]	82	2005	67

Pts = patients; n = number of patients; CR = complete remission; PR = partial remission rate; NC = no change; PD = progressive disease
1 Objective Clinical Response Rate By WHO criteria.
2 CR: clinical CR or 100% necrosis; PR: clinical PR or >50-99% necrosis.
3 CR only recognized by EMEA when histopathology showed 100% necrosis.
4 Independent committee recognized 196 patients as pure amputation candidates.
5 No clinical response data; CR: >90% necrosis; PR: radiological and/or histopathological >50% necrosis.
6 CR/PR: loss of vasculature on Ultrasound/MRI; lower panel CR: >90% necrosis on histopathology
7 low dose TNF of 1mg, or Various doses of TNF (Bonvalot: 0.5 mg – 4 mg); (Grünhagen: 1mg – 4 mg) STS patients.
8 Patients with metastatic disease.
9 Patients with multiple tumors in extremity.
10 Patients >75 years old.
11 Patients with recurrent sarcomas in 60-70 Gray irradiated fields.

As TNF acts primarily on the tumour vasculature, these observations make sense and the propensity to respond to a TNF-based ILP is assumed to depend more on tumour vasculature than on the histologic type of tumours.

Table 2:

TNF-based ILP in Melanoma and Non-Melanoma Skin Cancer Patients

ILP	Pts n	CR %	PR %	Overall RR	TTLP Median mo	Ref Year	Ref #
All Melanoma Patients	19	89	11	100*	8+	1992	50
	44	90	10	100*	18+	1993	69
	58	88	12	100*	26	1995	70
	26	76	16	92*	ns	1996	71
	32	78	22	100*	14	1999	72
	32	69	22	91	14	1999	72
	100	69	26	95	16+	2004	73
Bulky Melanoma only	39	59	16	75	ns	2002	74
	20	70	25	95	ns	2004	75
	50	58	34	83	8	2004	73
Repeat ILP for Melanoma	17	65	29	94	6	1997	76
	26	75	25	100	14	2005	77
Non Melanoma Skin Cancers	15	60	27	87	20+	1999	78

Pts = patients; n = number of patients; CR = complete remission; PR = partial remission rate; Overall RR = Overall (CR+PR) Response Rate; TTLP = time to local progression; mo = months; ns = not specified ; * TNF + IFN

Response of STS to TNF-based ILP is shown in Figure 4A. MRI of a patient with six-seven high-grade leiomyosarcoma in the upper leg shows before ILP clear dark tumour masses with high gadolinium uptake. Five weeks after ILP all tumour masses are gadolinium-negative. Along the distal femur only small tumour remnants are visible, but at the proximal femur a large, but gadolinium negative, tumour mass without signs of regressions is visible. All lesions were resected and found to be 100% necrotic. Thus the response was classified as a histopathologic CR.

Targeting by TNF of the tumour vasculature is revealed in patients by angiographies before and after ILP. The TAV was selectively destructed by the TNF-based ILP; the TAV is gone while normal vessels of the limbs are still intact after ILP (Fig. 4B). TNF targets the vasculature of tumours with completely different histologies but as the TAV is well developed in all these tumours the combination therapy in the ILP-setting is very effective for the distinct tumours treated. Synergistic and high response rates are achieved in sarcomas consisting of a broad range of subtypes as well as in melanomas.

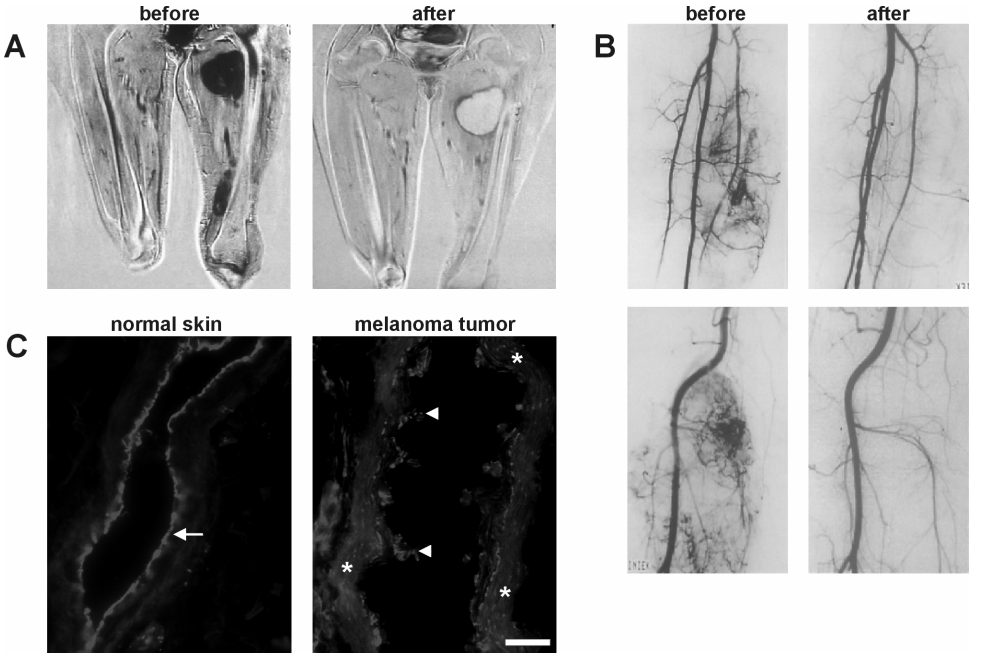

FIGURE 4. Anti-tumour and anti-vascular effects of TNF upon ILP treatment of sarcoma and melanoma patients **(CLR)**.
A. MRI of a patient with a high-grade leiomyosarcoma in the upper leg showing tumour mass before treatment (left) while 5 weeks after ILP with TNF and melphalan there is no gadolinium uptake in the tumour remnants (right). Tumour remnants were resected and all necrotic.
B. Angiographies of 2 patients with rapidly growing sarcomas in the leg before (left) and after (right) ILP with TNF and melphalan. Angiographies clearly show the well-developed tumour vasculature before ILP, which is selectively destructed after treatment while the normal vessel are still present and intact. Both patients were classified as complete responders.
C. Endothelial lining of tumour vessels is destructed. Endothelial staining (CD-31) of vessels in normal skin (left) and melanoma (right) in biopsies of a melanoma patient taken after ILP. Vessels in the normal skin show a continuous endothelial lining (arrow) while in the melanoma-associated vessel this lining is disrupted and the endothelial cells detach from the basement membrane (arrowheads). The elastic fibers (asterisks, stained aspecific) in the thickened basement membrane are also visible in the melanoma vessel. Scale bar: 50 μm.

At the histopathological level a massive hemorrhagic necrosis is observed inside melanomas treated with ILP [81] an effect likely caused by the TNF-induced coagulation and extravasation of erythrocytes [82]. In accordance with the angiographies of STS, the vascular lining of melanoma tumour vessels is destructed (Fig. 4C). Staining for endothelial cells reveals that upon treatment in skin vessels the endothelium is intact and continuous while this lining is heavily disrupted and the cells detach from the underlying basement membrane in melanoma-associated vessels. These anti-

vascular TNF-effects are achieved by the high concentration reached during ILP. At these high levels TNF acts anti-vascular and anti-angiogenic while at lower concentration TNF is known to promote angiogenesis [83]. In addition to the direct TAV-mediated effects, TNF reduces the blood flow in tumours in a dose-dependent fashion [84]. These set of anti-vascular TNF-effects were recently confirmed by experiments revealing that the tumour response to TNF correlates whit the degree of tumour vascularity [85]. Along with this dual role in angiogenesis, TNF is also known for its dual role in cancer treatment, anti-TNF therapy is also used for several cancers. The anti-neoplastic and tumour-promoting effects of TNF are discussed in a recent review [86].

Approaches to modulate TNF action in cancer treatment

High response rates in ILP-setting do not avoid the search for factors that modulate the TNF effect in solid tumours. Besides the possible application of TNF in other settings (for example systemic treatment) and for other tumours-types, the non-responding patients in the ILP-setting may also benefit from TNF sensitizers. Some of these approaches are mentioned below. An obvious target is inhibition of the NF-kB survival pathway. Inactivation of NF-kB is known to sensitize several tumours to TNF [87]. NF-kB can be blocked in several ways, overexpression of its inhibitor I-kB and selective NF-kB inhibitors have shown to increase TNF-induces apoptosis of tumour cells [88,89]. One such inhibitor, bortezomib, has by now entered the clinic as a combination therapy with chemotoxic drugs for prostate cancer and myeloma [90].

Nitric oxide (NO) is involved in survival of TNF treated cells through NF-kB induced expression of inducible NO synthase (iNOS) [91,92]. We have previously shown that inhibition of NOS by addition of L-NAME during TNF-based ILP resulted in an increased tumour response in rats bearing STS [93]. These observations are confirmed by a recent study showing that NOS inhibition in endothelial cells reduces their sensitivity to TNF *in vitro* leading to the hypothesis that tumour vessels exhibit a higher level of NOS which might explain the higher TNF-sensitivity [94]. These studies justify further evaluation of NOS inhibition in tumours of patients treated by an ILP to stimulate the anti-TAV activities of TNF.

Apoptosis induced by TNF is also associated with the generation of reactive oxygen species (ROS). It is shown that the key-survival factor NF-kB induces ROS neutralizing enzymes like superoxide dismutase [95]. Induction of the ROS production or an inhibition of the NF-kB pathway by cyclooxygenase-2 (COX-2) inhibitors are reported to be successful in sensitizing tumour cells to TNF-induced apoptosis [96].

Procedures with liposomal encapsulation of TNF to elongate its circulation time and to achieve effective TNF concentrations in the tumour showed to be effective in systemic treatment in combination with chemotherapeutic drugs in rats [97].

Another experimental approach is the development of TNF analogues like TNF-mutants selectively binding to TNF-R1 [98] and mutants affecting the pharmacokinetics of TNF-TNFR1 interactions at tumour vascular level [99]. In animal models these approaches have shown promising results compared to wild type TNF but this research is still too experimental and no TNF-analogues have reached clinical studies yet.

A more physiological and therefore potent way is the role of other cytokines that serve as TNF sensitizers. Interferon gamma (IFN) is one of the widely studied cytokines and although in the ILP setting for melanomas and sarcomas no beneficial effects and some levels of toxicity were observed, for other cancers IFN might be very suitable because of its reported actions on TNF-R1 and caspase-8 thereby regulating TNF-induced apoptosis [100]. Endothelial monocyte-activating polypeptide II (EMAP-II) is a cytokine produced by tumour cells so a local production is suggested thereby facilitating TNF anti-tumour activities. EMAP-II can sensitize reported TNF-resistant tumours sensitive to TNF, which was shown by upregulation of EMAP-II resulting in an increased TNF effect [101]. Underlying mechanisms for this effect remain unclear although it is postulated that an upregulation of TNF-R1 on endothelial cells might be an explanation [102]. Besides TNF modulating effects EMAP-II exhibits other anti-tumour effects like anti-angiogenic and immunosuppressive activities [103,104]. Combining these cytokines with TNF and investigation of expression patterns and local protein production might be very promising in modulating TNF activities in cancer treatment.

Besides modulating TNF actions other TAV manipulating agent are tested in ILP as well. Recently we showed that both histamine (via its own vascular activity) and Interleukin-2 (via upregulation of TNF production) have strong synergistic anti-tumour effects when combined with melphalan. Importantly, with both these agents an augmented accumulation of melphalan in the tumour specifically was observed, confirming TAV as effective target in solid tumour treatment [105,106].

CONCLUSIONS

The use of high dose of TNF locally administered in combination with melphalan for patients with metastatic in-transit melanoma and soft tissue sarcoma confined to the limb is a well-established treatment modality nowadays. Furthermore the modulation of tumour pathophysiology by low dose

TNF indicates that in combination with liposomal drugs systemic therapy should be investigated in the clinic. Besides understanding of the molecular events of TNF-R1 signaling taking place during tumour treatment, these studies likely will expand the use of TNF for other cancer types and for non-responding ILP-patients as well. The multifunctional properties of TNF may well result in a more varied application of this cytokine.

REFERENCES

1. Bazzoni, F. and Beutler, B. (1996). The tumour necrosis factor ligand and receptor families. *N Engl J Med* 334, 1717-1725.
2. Locksley, R. M., Killeen, N., and Lenardo, M. J. (2001). The TNF and TNF receptor superfamilies: integrating mammalian biology. *Cell* 104, 487-501.
3. Eggermont, A. M., de Wilt, J. H., and ten Hagen, T. L. (2003). Current uses of isolated limb perfusion in the clinic and a model system for new strategies. *Lancet Oncol.* 4, 429-437.
4. Carswell, E. A., Old, L. J., Kassel, R. L., Green, S., Fiore, N., and Williamson, B. (1975). An endotoxin-induced serum factor that causes necrosis of tumours. *Proc Natl Acad Sci U S A* 72, 3666-3670.
5. Old, L. J. (1985). Tumour necrosis factor (TNF). *Science.* 230, 630-2.
6. NAUTS, H. C., FOWLER, G. A., and BOGATKO, F. H. (1953). A review of the influence of bacterial infection and of bacterial products (Coley's toxins) on malignant tumours in man; a critical analysis of 30 inoperable cases treated by Coley's mixed toxins, in which diagnosis was confirmed by microscopic examination selected for special study. *Acta Med.Scand.Suppl* 144, 1-103.
7. Beutler, B., Greenwald, D., Hulmes, J. D., Chang, M., Pan, Y. C., Mathison, J., Ulevitch, R., and Cerami, A. (1985). Identity of tumour necrosis factor and the macrophage-secreted factor cachectin. *Nature* 316, 552-554.
8. Takeda, K., Iwamoto, S., Sugimoto, H., Takuma, T., Kawatani, N., Noda, M., Masaki, A., Morise, H., Arimura, H., and Konno, K. (1986). Identity of differentiation inducing factor and tumour necrosis factor. *Nature* 323, 338-340.
9. Shirai, T., Yamaguchi, H., Ito, H., Todd, C. W., and Wallace, R. B. (1985). Cloning and expression in Escherichia coli of the gene for human tumour necrosis factor. *Nature* 313, 803-806.
10. Marmenout, A., Fransen, L., Tavernier, J., Van der, H. J., Tizard, R., Kawashima, E., Shaw, A., Johnson, M. J., Semon, D., Muller, R., and . (1985). Molecular cloning and expression of human tumour necrosis factor and comparison with mouse tumour necrosis factor. *Eur.J.Biochem.* 152, 515-522.
11. Lejeune, F. J., Ruegg, C., and Lienard, D. (1998). Clinical applications of TNF-alpha in cancer. *Curr.Opin.Immunol.* 10, 573-580.
12. Muller, U., Jongeneel, C. V., Nedospasov, S. A., Lindahl, K. F., and Steinmetz, M. (1987). Tumour necrosis factor and lymphotoxin genes map close to H-2D in the mouse major histocompatibility complex. *Nature* 325, 265-267.
13. Bemelmans, M. H., van Tits, L. J., and Buurman, W. A. (1996). Tumour necrosis factor: function, release and clearance. *Crit Rev.Immunol.* 16, 1-11.
14. Vandenabeele, P., Declercq, W., Beyaert, R., and Fiers, W. (1995). Two tumour necrosis factor receptors: structure and function. *Trends Cell Biology* 5, 392-399.
15. Tartaglia, L. A. and Goeddel, D. V. (1992). Two TNF receptors. *Immunol Today* 13, 151-153.
16. Aggarwal, B. B. (2003). Signalling pathways of the TNF superfamily: a double-edged sword. *Nat.Rev.Immunol.* 3, 745-756.
17. Ashkenazi, A. and Dixit, V. M. (1998). Death receptors: signaling and modulation. *Science.* 281, 1305-1308.
18. Baker, S. J. and Reddy, E. P. (1998). Modulation of life and death by the TNF receptor superfamily. *Oncogene* 17, 3261-3270.
19. Muppidi, J. R., Tschopp, J., and Siegel, R. M. (2004). Life and death decisions: secondary complexes and lipid rafts in TNF receptor family signal transduction. *Immunity.* 21, 461-465.
20. Takada, H., Chen, N. J., Mirtsos, C., Suzuki, S., Suzuki, N., Wakeham, A., Mak, T. W., and Yeh, W. C. (2003). Role of SODD in regulation of tumour necrosis factor responses. *Mol.Cell Biol.* 23, 4026-4033.
21. Rath, P. C. and Aggarwal, B. B. (1999). TNF-induced signaling in apoptosis. *J Clin Immunol* 19, 350-364.
22. Degterev, A., Boyce, M., and Yuan, J. (2003). A decade of caspases. *Oncogene* 22, 8543-8567.
23. Natoli, G., Costanzo, A., Ianni, A., Templeton, D. J., Woodgett, J. R., Balsano, C., and Levrero, M. (1997). Activation of SAPK/JNK by TNF receptor 1 through a noncytotoxic TRAF2-dependent pathway. *Science.* 275, 200-203.

24. Devin, A., Cook, A., Lin, Y., Rodriguez, Y., Kelliher, M., and Liu, Z. (2000). The distinct roles of TRAF2 and RIP in IKK activation by TNF-R1: TRAF2 recruits IKK to TNF-R1 while RIP mediates IKK activation. *Immunity.* 12, 419-429.
25. Beg, A. A. and Baltimore, D. (1996). An essential role for NF-kappaB in preventing TNF-alpha-induced cell death. *Science* 274, 782-784.
26. Dolcet, X., Llobet, D., Pallares, J., and Matias-Guiu, X. (2005). NF-kB in development and progression of human cancer. *Virchows Arch.* 446, 475-482.
27. Lin, A. and Karin, M. (2003). NF-kappaB in cancer: a marked target. *Semin.Cancer Biol.* 13, 107-114.
28. Manusama, E. R., Stavast, J., Durante, N. M., Marquet, R. L., and Eggermont, A. M. (1996). Isolated limb perfusion with TNF alpha and melphalan in a rat osteosarcoma model: a new anti-tumour approach. *Eur.J.Surg.Oncol.* 22, 152-157.
29. Manusama, E. R., Nooijen, P. T., Stavast, J., Durante, N. M., Marquet, R. L., and Eggermont, A. M. (1996). Synergistic antitumour effect of recombinant human tumour necrosis factor alpha with melphalan in isolated limb perfusion in the rat. *Br.J.Surg.* 83, 551-555.
30. van der Veen, A. H., de Wilt, J. H., Eggermont, A. M., van Tiel, S. T., Seynhaeve, A. L., and ten Hagen, T. L. (2000). TNF-alpha augments intratumoural concentrations of doxorubicin in TNF-alpha-based isolated limb perfusion in rat sarcoma models and enhances anti-tumour effects. *Br.J.Cancer* 82, 973-980.
31. de Wilt, J. H., ten Hagen, T. L., de Boeck, G., van Tiel, S. T., de Bruijn, E. A., and Eggermont, A. M. (2000). Tumour necrosis factor alpha increases melphalan concentration in tumour tissue after isolated limb perfusion. *Br.J.Cancer* 82, 1000-1003.
32. Ruggiero, V., Latham, K., and Baglioni, C. (1987). Cytostatic and cytotoxic activity of tumour necrosis factor on human cancer cells. *J.Immunol.* 138, 2711-2717.
33. Watanabe, N., Niitsu, Y., Yamauchi, N., Ohtsuka, Y., Sone, H., Neda, H., Maeda, M., and Urushizaki, I. (1988). Synergistic cytotoxicity of recombinant human TNF and various anti-cancer drugs. *Immunopharmacol.Immunotoxicol.* 10, 117-127.
34. Brouckaert, P., Takahashi, N., van Tiel, S. T., Hostens, J., Eggermont, A. M., Seynhaeve, A. L., Fiers, W., and ten Hagen, T. L. (2004). Tumour necrosis factor-alpha augmented tumour response in B16BL6 melanoma-bearing mice treated with stealth liposomal doxorubicin (Doxil) correlates with altered Doxil pharmacokinetics. *Int.J.Cancer* 109, 442-448.
35. ten Hagen, T. L., van der Veen, A. H., Nooijen, P. T., van Tiel, S. T., Seynhaeve, A. L., and Eggermont, A. M. (2000). Low-dose tumour necrosis factor-alpha augments antitumour activity of stealth liposomal doxorubicin (DOXIL) in soft tissue sarcoma-bearing rats. *Int.J.Cancer* 87, 829-837.
36. Watanabe, N., Niitsu, Y., Umeno, H., Kuriyama, H., Neda, H., Yamauchi, N., Maeda, M., and Urushizaki, I. (1988). Toxic effect of tumour necrosis factor on tumour vasculature in mice. *Cancer Res.* 48, 2179-2183.
37. Carmeliet, P. (2003). Angiogenesis in health and disease. *Nat.Med.* 9, 653-660.
38. Folkman, J. (1971). Tumour angiogenesis: therapeutic implications. *N Engl J Med* 285, 1182-1186.
39. Bergers, G. and Benjamin, L. E. (2003). Tumourigenesis and the angiogenic switch. *Nat.Rev.Cancer* 3, 401-410.
40. Bussolino, F., Mantovani, A., and Persico, G. (1997). Molecular mechanisms of blood vessel formation. *Trends Biochem Sci* 22, 251-256.
41. Gerhardt, H., Golding, M., Fruttiger, M., Ruhrberg, C., Lundkvist, A., Abramsson, A., Jeltsch, M., Mitchell, C., Alitalo, K., Shima, D., and Betsholtz, C. (2003). VEGF guides angiogenic sprouting utilizing endothelial tip cell filopodia. *J.Cell Biol.* 161, 1163-1177.
42. Chambers, A. F., Groom, A. C., and MacDonald, I. C. (2002). Dissemination and growth of cancer cells in metastatic sites. *Nat.Rev.Cancer* 2, 563-572.
43. Carmeliet, P. and Jain, R. K. (2000). Angiogenesis in cancer and other diseases. *Nature* 407, 249-57.
44. Baluk, P., Hashizume, H., and McDonald, D. M. (2005). Cellular abnormalities of blood vessels as targets in cancer. *Curr.Opin.Genet.Dev.* 15, 102-111.
45. Morikawa, S., Baluk, P., Kaidoh, T., Haskell, A., Jain, R. K., and McDonald, D. M. (2002). Abnormalities in pericytes on blood vessels and endothelial sprouts in tumours. *Am.J.Pathol.* 160, 985-1000.
46. Hashizume, H., Baluk, P., Morikawa, S., McLean, J. W., Thurston, G., Roberge, S., Jain, R. K., and McDonald, D. M. (2000). Openings between defective endothelial cells explain tumour vessel leakiness. *Am.J.Pathol.* 156, 1363-1380.
47. Bradley, J. R., Thiru, S., and Pober, J. S. (1995). Disparate localization of 55-kd and 75-kd tumour necrosis factor receptors in human endothelial cells. *Am J Pathol* 146, 27-32.
48. Hill, S., Fawcett, W. J., Sheldon, J., Soni, N., Williams, T., and Thomas, J. M. (1993). Low-dose tumour necrosis factor alpha and melphalan in hyperthermic isolated limb perfusion. *Br.J.Surg.* 80, 995-997.
49. Bonvalot, S., Laplanche, A., Lejeune, F., Stoeckle, E., Le Pechoux, C., Vanel, D., Terrier, P., Lumbroso, J., Ricard, M., Antoni, G., Cavalcanti, A., Robert, C., Lassau, N., Blay, J. Y., and Le Cesne, A. (2005). Limb salvage with isolated perfusion for soft tissue sarcoma: could less TNF-alpha be better? *Ann Oncol* 16, 1061-1068.

50. Lienard, D., Ewalenko, P., Delmotte, J. J., Renard, N., and Lejeune, F. J. (1992). High-dose recombinant tumour necrosis factor alpha in combination with interferon gamma and melphalan in isolation perfusion of the limbs for melanoma and sarcoma. *J.Clin.Oncol.* 10, 52-60.
51. Eggermont, A. M. M., Lienard, D., Schraffordt Koops, H., Rosenkaimer, F., and Lejeune, F. J. (1993). Treatment of irresectable soft tissue sarcomas of the limbs by isolation perfusion with high dose TNF-alpha in combination with interferon-gamma and melphalan. *In* "Tumour Necrosis Factor: Molecular and cellular biology and clinical relevance." (W. Fiers and W. A. Buurman, Eds.), Karger, Basel.
52. Eggermont, A. M., Schraffordt, K. H., Lienard, D., Kroon, B. B., van Geel, A. N., Hoekstra, H. J., and Lejeune, F. J. (1996). Isolated limb perfusion with high-dose tumour necrosis factor-alpha in combination with interferon-gamma and melphalan for nonresectable extremity soft tissue sarcomas: a multicenter trial. *J.Clin.Oncol.* 14, 2653-2665.
53. Eggermont, A. M., Schraffordt, K. H., Klausner, J. M., Kroon, B. B., Schlag, P. M., Lienard, D., van Geel, A. N., Hoekstra, H. J., Meller, I., Nieweg, O. E., Kettelhack, C., Ben Ari, G., Pector, J. C., and Lejeune, F. J. (1996). Isolated limb perfusion with tumour necrosis factor and melphalan for limb salvage in 186 patients with locally advanced soft tissue extremity sarcomas. The cumulative multicenter European experience. *Ann.Surg.* 224, 756-764.
54. Eggermont, A. M., Schraffordt Koops, H., Klaase, J. M., Schlag, P. M., Kroon, B. B., Gustafson, P., Steinmann, G., and Lejeune, F. (1999). Limb Salvage by Isolated Limb Perfusion with Tumour Necrosis Factor Alpha and melphalan for locally advanced extremity soft tissue sarcomas: results of 270 perfusions in 246 patients. *Proc Am Soc Clin Oncol* 11, 497-508.
55. Gutman, M., Inbar, M., Lev-Shlush, D., Abu-Abid, S., Mozes, M., Chaitchik, S. X. M. I., and Klausner, J. M. (1997). High dose tumour necrosis factor-alpha and melphalan administered via isolated limb perfusion for advanced limb soft tissue sarcoma results in a >90% response rate and limb preservation. *Cancer* 79, 1129-1137.
56. Olieman, A. F. T., Pras, E., van Ginkel, R. J., Molenaar, W. M., Schraffordt Koops, H., and Hoekstra, H. J. (1998). Feasibility and efficacy of external beam radiotherapy after hyperthermic isolated limb perfusion with TNF-alpha and melphalan for limb-saving treatment in locally advanced extremity soft- tissue sarcoma. *Int.J.Radiat.Oncol.Biol.Phys.* 40, 807-814.
57. Rossi, C. R., Foletto, M., Di Filippo, F., Vaglini, M., Anza', M., Azzarelli, A., Pilati, P., Mocellin, S., and Lise, M. (1999). Soft tissue limb sarcomas: Italian clinical trials with hyperthermic antiblastic perfusion. *Cancer* 86, 1742-1749.
58. Lejeune, F. J., Pujol, N., Lienard, D., Mosimann, F., Raffoul, W., Genton, A., Guillou, L., Landry, M., Chassot, P. G., Chiolero, R., Bischof-Delaloye, A., Leyvraz, S., Mirimanoff, R. O., Bejkos, D., and Leyvraz, P. F. (2000). Limb salvage by neoadjuvant isolated perfusion with TNFalpha and melphalan for non-resectable soft tissue sarcoma of the extremities. *Eur.J Surg.Oncol.2000.Nov.;26.(7.):669.-678.* 26, 669-678.
59. Hohenberger P., Kettelhack, C., Hermann A., and Schlag, P. M. (2001). Functional outcome after preoperative isolated limb perfusion with rhTNFalpha/Melphalan for high-grade extremity sarcoma. *Eur J Cancer* 37, S34-35.
60. Noorda EM, Vrouwenraets BC, Nieweg, O. E., Slooten GW, and Kroon, B. B. (2003). Isolated limb perfusion with TNFalpha and Melphalan for Irresectable Soft Tissue Sarcoma of the Extremities. *Ann Surg Oncol* 10, S36.
61. van Etten, B., van Geel, A. N., de Wilt, J. H. W., and Eggermont, A. M. M. (2003). Fifty tumour necrosis factor-based isolated limb perfusions for limb salvage in patients older than 75 years with limb-threatening soft tissue sarcomas and other extremity tumours. *Ann.Surg.Oncol.* 10, 32-37.
62. Grunhagen, D. J., Brunstein, F., Graveland, W. J., van Geel, A. N., de Wilt, J. H., and Eggermont, A. M. (2005). Isolated limb perfusion with tumour necrosis factor and melphalan prevents amputation in patients with multiple sarcomas in arm or leg. *Ann Surg Oncol* 12, 473-479.
63. Lans, T. E., Grunhagen, D. J., de Wilt, J. H., van Geel, A. N., and Eggermont, A. M. (2005). Isolated limb perfusions with tumour necrosis factor and melphalan for locally recurrent soft tissue sarcoma in previously irradiated limbs. *Ann Surg Oncol* 12, 406-411.
64. Grunhagen, D. J., de Wilt, J. H., Graveland, W. J., van Geel, A. N., and Eggermont, A. M. (2005). Palliative Value of TNF-based ILP in metastatic melanoma and sarcoma patients. *Cancer* in press.
65. Rossi, C. R., Mocellin, S., Pilati, P., Foletto, M., Campana, L., Quintieri, L., De Salvo, G. L., and Lise, M. (2005). Hyperthermic isolated perfusion with low-dose tumour necrosis factor alpha and doxorubicin for the treatment of limb-threatening soft tissue sarcomas. *Ann Surg Oncol* 12, 398-405.
66. Grunhagen, D. J., Brunstein, F., Verhoef C., Graveland, W. J., van Geel, A. N., de Wilt, J. H., and Eggermont, A. M. (2005). Outcome and Prognostic Factor Analysis of 217 Consecutive Isolated Limb Perfusions with TNFalpha and Melphalan for Limb-threatening Soft Tissue Sarcoma. *Cancer* in press.
67. Grunhagen, D. J., de Wilt, J. H., van Geel, A. N., Graveland, W. J., Verhoef, C., and Eggermont, A. M. (2005). TNF dose reduction in isolated limb perfusion. *Eur J Surg Oncol*.
68. Eggermont, A. M. (1996). Treatment of melanoma in-transit metastases confined to the limb. *Cancer Surv.* 26:335-49., 335-349.
69. Lejeune, F. J., Lienard, D., Leyvraz, S., and Mirimanoff, R. O. (1993). Regional therapy of melanoma. *Eur.J.Cancer* 29A, 606-612.

70. Eggermont, A. M., Lienard, D., Schraffordt Koops, H., Kroon, B. B., Rosenkaimer, F., Klaase, J. M., Schmitz, P., and Lejeune, F. (1995). High Dose TNFalpha in Isolated Perfusion of the Limb: Highly Effective Treatment for Melanoma in transit Metastases or Unresectable Sarcoma. *Reg Canc Treat* 7, 32-36.
71. Fraker, D. L., Alexander, H. R., Andrich, M., and Rosenberg, S. A. (1996). Treatment of patients with melanoma of the extremity using hyperthermic isolated limb perfusion with melphalan, tumour necrosis factor, and interferon gamma: results of a tumour necrosis factor dose-escalation study. *J Clin Oncol* 14, 479-489.
72. Lienard, D., Eggermont, A. M., Koops, H. S., Kroon, B., Towse, G., Hiemstra, S., Schmitz, P., Clarke, J., Steinmann, G., Rosenkaimer, F., and Lejeune, F. J. (1999). Isolated limb perfusion with tumour necrosis factor-alpha and melphalan with or without interferon-gamma for the treatment of in-transit melanoma metastases: a multicentre randomized phase II study. *Melanoma.Res.* 9, 491-502.
73. Grunhagen, D. J., Brunstein, F., Graveland, W. J., van Geel, A. N., de Wilt, J. H., and Eggermont, A. M. (2004). One hundred consecutive isolated limb perfusions with TNF-alpha and melphalan in melanoma patients with multiple in-transit metastases. *Ann.Surg.* 240, 939-947.
74. Fraker, D. L., Alexander, H. R., and Ross, R. (2002). A Phase III Trial of Isolated Limb Perfusion For Extremity Melanoma Comparing Melphalan Alone versus Melpahlan plus TNFalpha plus IFNgamma. *Ann Surg Oncol* 9, S8.
75. Rossi, C. R., Foletto, M., Mocellin, S., Pilati, P., and Lise, M. (2004). Hyperthermic isolated limb perfusion with low-dose tumour necrosis factor-alpha and melphalan for bulky in-transit melanoma metastases. *Ann Surg Oncol* 11, 173-177.
76. Bartlett, D. L., Ma, G., Alexander, H. R., Libutti, S. K., and Fraker, D. L. (1997). Isolated limb reperfusion with tumour necrosis factor and melphalan in patients with extremity melanoma after failure of isolated limb perfusion with chemotherapeutics. *Cancer* 80, 2084-2090.
77. Grunhagen, D. J., van Etten, B., Brunstein, F., Graveland, W. J., van Geel, A. N., de Wilt, J. H., and Eggermont, A. M. (2005). Efficacy of repeat isolated limb perfusions with tumour necrosis factor alpha and melphalan for multiple in-transit metastases in patients with prior isolated limb perfusion failure. *Ann Surg Oncol* 12, 609-615.
78. Olieman, A. F., Lienard, D., Eggermont, A. M., Kroon, B. B., Lejeune, F. J., Hoekstra, H. J., and Koops, H. S. (1999). Hyperthermic isolated limb perfusion with tumour necrosis factor alpha, interferon gamma, and melphalan for locally advanced nonmelanoma skin tumours of the extremities: a multicenter study. *Arch.Surg.* 134, 303-307.
79. Klaase, J. M., Kroon, B. B., Benckhuijsen C. et al. (1989). Results of regional isolation perfusion with cytostatics in patients with soft tissue tumours of the extremities, *Cancer* 64, 616-621
80. Feig B. W., Ross M. I., Cornieer J. et al. (2004). Prospective evaluation of isolated limb perfusion with Doxorubicin in patients with unresectable extremity sarcomas. *Ann.Surg.Oncol* 11, S80
81. Nooijen, P. T., Manusama, E. R., Eggermont, A. M., Schalkwijk, L., Stavast, J., Marquet, R. L., de Waal, R. M., and Ruiter, D. J. (1996). Synergistic effects of TNF-alpha and melphalan in an isolated limb perfusion model of rat sarcoma: a histopathological, immunohistochemical and electron microscopical study. *Br.J.Cancer* 74, 1908-1915.
82. Shimomura, K., Manda, T., Mukumoto, S., Kobayashi, K., Nakano, K., and Mori, J. (1988). Recombinant human tumour necrosis factor-alpha: thrombus formation is a cause of anti-tumour activity. *Int.J.Cancer* 41, 243-247.
83. Fajardo, L. F., Kwan, H. H., Kowalski, J., Prionas, S. D., and Allison, A. C. (1992). Dual role of tumour necrosis factor-alpha in angiogenesis. *Am.J.Pathol.* 140, 539-544.
84. Naredi, P. L., Lindner, P. G., Holmberg, S. B., Stenram, U., Peterson, A., and Hafstrom, L. R. (1993). The effects of tumour necrosis factor alpha on the vascular bed and blood flow in an experimental rat hepatoma. *Int.J.Cancer* 54, 645-649.
85. van Etten, B., de Vries, M. R., van Ijken, M. G., Lans, T. E., Guetens, G., Ambagtsheer, G., van Tiel, S. T., de Boeck, G., de Bruijn, E. A., Eggermont, A. M., and ten Hagen, T. L. (2003). Degree of tumour vascularity correlates with drug accumulation and tumour response upon TNF-alpha-based isolated hepatic perfusion. *Br.J.Cancer* 88, 314-319.
86. Mocellin, S., Rossi, C. R., Pilati, P., and Nitti, D. (2005). Tumour necrosis factor, cancer and anticancer therapy. *Cytokine Growth Factor Rev.* 16, 35-53.
87. Orlowski, R. Z. and Baldwin, A. S., Jr. (2002). NF-kappaB as a therapeutic target in cancer. *Trends Mol.Med.* 8, 385-389.
88. Wang, C. Y., Cusack, J. C., Jr., Liu, R., and Baldwin, A. S., Jr. (1999). Control of inducible chemoresistance: enhanced anti-tumour therapy through increased apoptosis by inhibition of NF-kappaB. *Nat.Med.* 5, 412-417.
89. Lee, K. Y., Chang, W., Qiu, D., Kao, P. N., and Rosen, G. D. (1999). PG490 (triptolide) cooperates with tumour necrosis factor-alpha to induce apoptosis in tumour cells. *J.Biol.Chem.* 274, 13451-13455.
90. Richardson, P. G., Barlogie, B., Berenson, J., Singhal, S., Jagannath, S., Irwin, D., Rajkumar, S. V., Srkalovic, G., Alsina, M., Alexanian, R., Siegel, D., Orlowski, R. Z., Kuter, D., Limentani, S. A., Lee, S., Hideshima, T., Esseltine, D. L., Kauffman, M., Adams, J., Schenkein, D. P., and Anderson, K. C. (2003). A phase 2 study of bortezomib in relapsed, refractory myeloma. *N.Engl.J.Med.* 348, 2609-2617.
91. Ganster, R. W., Taylor, B. S., Shao, L., and Geller, D. A. (2001). Complex regulation of human inducible nitric oxide synthase gene transcription by Stat 1 and NF-kappa B. *Proc.Natl.Acad.Sci.U.S.A* 98, 8638-8643.

92. Binder, C., Schulz, M., Hiddemann, W., and Oellerich, M. (1999). Induction of inducible nitric oxide synthase is an essential part of tumour necrosis factor-alpha-induced apoptosis in MCF-7 and other epithelial tumour cells. *Lab Invest* 79, 1703-1712.
93. de Wilt, J. H., Manusama, E. R., van Etten, B., van Tiel, S. T., Jorna, A. S., Seynhaeve, A. L., and ten Hagen, T. L. (2000). Nitric oxide synthase inhibition results in synergistic anti-tumour activity with melphalan and tumour necrosis factor alpha-based isolated limb perfusions [In Process Citation]. *Br J Cancer* 83, 1176-82.
94. Mocellin, S., Provenzano, M., Rossi, C. R., Pilati, P., Scalerta, R., Lise, M., and Nitti, D. (2004). Induction of endothelial nitric oxide synthase expression by melanoma sensitizes endothelial cells to tumour necrosis factor-driven cytotoxicity. *Clin.Cancer Res.* 10, 6879-6886.
95. Delhalle, S., Deregowski, V., Benoit, V., Merville, M. P., and Bours, V. (2002). NF-kappaB-dependent MnSOD expression protects adenocarcinoma cells from TNF-alpha-induced apoptosis. *Oncogene* 21, 3917-3924.
96. Totzke, G., Schulze-Osthoff, K., and Janicke, R. U. (2003). Cyclooxygenase-2 (COX-2) inhibitors sensitize tumour cells specifically to death receptor-induced apoptosis independently of COX-2 inhibition. *Oncogene* 22, 8021-8030.
97. ten Hagen, T. L., Seynhaeve, A. L., van Tiel, S. T., Ruiter, D. J., and Eggermont, A. M. (2002). Pegylated liposomal tumour necrosis factor-alpha results in reduced toxicity and synergistic antitumour activity after systemic administration in combination with liposomal doxorubicin (Doxil) in soft tissue sarcoma-bearing rats. *Int.J.Cancer* 97, 115-120.
98. Ameloot, P. and Brouckaert, P. (2004). Production and characterization of receptor-specific TNF muteins. *Methods Mol.Med.* 98, 33-46.
99. Curnis, F., Sacchi, A., and Corti, A. (2002). Improving chemotherapeutic drug penetration in tumours by vascular targeting and barrier alteration. *J.Clin.Invest* 110, 475-482.
100. Fulda, S. and Debatin, K. M. (2002). IFNgamma sensitizes for apoptosis by upregulating caspase-8 expression through the Stat1 pathway. *Oncogene* 21, 2295-2308.
101. Gnant, M. F., Berger, A. C., Huang, J., Puhlmann, M., Wu, P. C., Merino, M. J., Bartlett, D. L., Alexander, H. R., Jr., and Libutti, S. K. (1999). Sensitization of tumour necrosis factor alpha-resistant human melanoma by tumour-specific in vivo transfer of the gene encoding endothelial monocyte-activating polypeptide II using recombinant vaccinia virus. *Cancer Res* 59, 4668-74.
102. Berger, A. C., Alexander, H. R., Wu, P. C., Tang, G., Gnant, M. F., Mixon, A., Turner, E. S., and Libutti, S. K. (2000). Tumour necrosis factor receptor I (p55) is upregulated on endothelial cells by exposure to the tumour-derived cytokine endothelial monocyte- activating polypeptide II (EMAP-II). *Cytokine* 12, 992-1000.
103. Schwarz, M. A., Kandel, J., Brett, J., Li, J., Hayward, J., Schwarz, R. E., Chappey, O., Wautier, J. L., Chabot, J., Lo Gerfo, P., and Stern, D. (1999). Endothelial-monocyte activating polypeptide II, a novel antitumour cytokine that suppresses primary and metastatic tumour growth and induces apoptosis in growing endothelial cells. *J Exp Med* 190, 341-54.
104. Murray, J. C., Symonds, P., Ward, W., Huggins, M., Tiga, A., Rice, K., Heng, Y. M., Todd, I., and Robins, R. A. (2004). Colorectal cancer cells induce lymphocyte apoptosis by an endothelial monocyte-activating polypeptide-II-dependent mechanism. *J.Immunol.* 172, 274-281.
105. Brunstein, F., Hoving, S., Seynhaeve, A. L., van Tiel, S. T., Guetens, G., de Bruijn, E. A., Eggermont, A. M., and ten Hagen, T. L. (2004). Synergistic antitumour activity of histamine plus melphalan in isolated limb perfusion: preclinical studies. *J.Natl.Cancer Inst.* 96, 1603-1610.
106. Hoving, S., Brunstein, F., aan, d. W.-A., van Tiel, S. T., de Boeck, G., de Bruijn, E. A., Eggermont, A. M., and ten Hagen, T. L. (2005). Synergistic antitumour response of interleukin 2 with melphalan in isolated limb perfusion in soft tissue sarcoma-bearing rats. *Cancer Res.* 65, 4300-4308.

Chapter 6

Endothelial Monocyte-Activating Polypetide-II and its functions in (patho)physiological processes

Remco van Horssen
Alexander M. M. Eggermont
Timo L.M. ten Hagen.

Laboratory of Experimental Surgical Oncology, Department of Surgical Oncology, Erasmus MC – Daniel den Hoed Cancer Center, Rotterdam, The Netherlands.

Cytokine & Growth Factor Reviews (2006): 17(5) in press

ABSTRACT

Endothelial Monocyte-Activating Polypeptide-II (EMAP-II) is a pro-inflammatory cytokine with anti-angiogenic properties. Its precursor, proEMAP, is identical to the p43 auxiliary component of the tRNA multisynthetase complex and therefore involved in protein translation. Although most of the activities have been ascribed to the active form EMAP-II, also p43 has reported cytokine properties. ProEMAP/p43 and EMAP-II act on many levels and on many cell types including endothelial cells, immune cells and fibroblasts. In this review we summarize all available data on isolation, expression and functions of EMAP-II both in physiological processes as well as in pathological settings, like cancer. We also discuss the different reported mechanisms for processing of proEMAP/p43 into EMAP-II. Finally, we speculate on the possible applications of this cytokine for (cancer) therapy.

Discovery and isolation

The history and discovery of EMAP-II are closely related to that of Tumour Necrosis Factor-α (TNF). TNF, discovered in the mid 70-ties but cloned almost ten years later, was named after the observation that it can induce hemorrhagic necrosis in murine tumours [1-4]. After its cloning, research focused mainly on the TNF-induced vascular response. *In vitro*, TNF exerts procoagulant activity and modulates haemostatic activity of endothelial cells (EC) [5,6]. *In vivo* however, comparable TNF-concentrations induced severe tissue damage and a septic shock-like syndrome [7]. In addition, tumour-bearing mice turned out to be more susceptible to TNF-induced toxic side effects than to TNF anti-tumour activity, thus limiting the applicability of TNF [8]. Within this context it is remarkable that relatively low concentrations of TNF administered to methylcholanthrene A (Meth A) fibrosarcoma-bearing mice induced fibrin formation throughout the tumour vascular bed [9]. This interesting finding, and the TNF-sensitivity of Meth A sarcomas, initiated the search for Meth A sarcoma-produced factors that might enhance the procoagulant response to TNF.

In 1990, a polypeptide was purified from Meth A-conditioned medium capable of enhancing TNF-induced Tissue Factor (TF) upregulation on EC. This tumour-derived TNF-mediator had an estimated molecular weight of 44 kD and was called Meth A factor [10]. Meth A factor induced TF, together with TNF, in a more than additive way. Subsequently, this polypeptide was called Endothelial Monocyte-Activating Polypeptide–I due to its procoagulant activity of EC and to prevent confusion with the afterwards identified EMAP-II. The same group of researchers isolated a second factor from Meth A supernatants of approximately 46 kD. This factor had a lower TF inducing capacity, but also induced monocyte activation [11]. This second factor turned out to be identical to

Vascular Permeability Factor, isolated earlier as an angiogenic mitogen [12,13]. This factor was renamed and is nowadays known as Vascular Endothelial Growth Factor (VEGF) [14] and still is considered the key angiogenic factor, with essential roles in development, inflammation, differentiation and tumour growth (for reviews see [15,16]).

Two years later, in 1992, another factor was isolated from Meth A conditioned medium, a polypeptide of approximately 22 kD. This factor had a unique amino-terminal sequence, induced TF expression to modulate coagulant responses, was chemotactic for monocytes and granulocytes and induced inflammation upon injection [17]. Based on its properties, this factor was named EMAP-II and was suggested to manipulate the tumour microenvironment, especially the vasculature. The precursor of this protein, proEMAP, turned out to be identical to another protein, namely the p43 auxiliary protein of the aminoacyl tRNA synthetase (ARS) complex, discussed in more detail below [18].

Again two years later the human EMAP-II gene was cloned and reported to activate EC and monocytes *in vitro* and induce thrombo-hemorrhagic effects and tumour regression when injected intratumourally into Meth A sarcomas [19].

Currently, EMAP-II proteins have been identified in a broad set of organisms. Figure 1 shows EMAP-II protein sequence and alignment of a selection of species. Homology is the highest among vertebrates, mainly in both the N- and the C-terminal part. For the mature protein part of the sequence (C-terminal) also some homology with fly EMAP-II is present. As to be expected, the homologues domains overlap – in part – with the functional domains, which are discussed below. Except for the yeast homologue, all EMAP-II proteins share a C-terminal lysine residue.

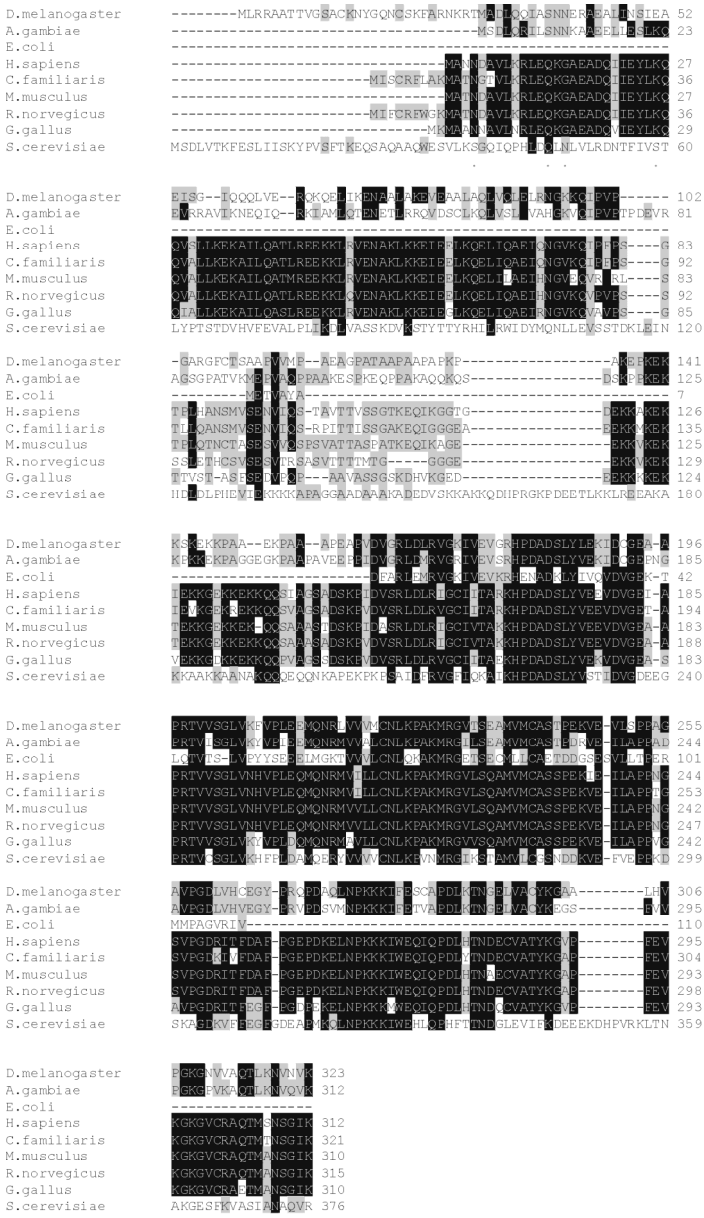

FIGURE 1. Homology of proEMAP/p43 protein sequence between different species. Alignment of protein sequence of a selection of species in which EMAP-II protein is found using ClustalW software. Amino acids present in at least five species are indicated by black boxes, when present in less than five, similar amino acid residues are indicated by gray boxes. Accession numbers of the protein sequences are: D. melanogaster (NP_610426), A.gambiae (XP_314551), E. coli (NP_289648), H. sapiens (NP_004748), C. familiaris (XP_545016), M. musculus (NP_031952), R.norvegicus (NP_446209), G.gallus (XP_420496) and S.cerevisiae (P46672).

Gene structure and protein characteristics

EMAP-II is known in literature by several synonyms: SCYE1, small inducible cytokine subfamily E member 1; p43, multisynthetase complex auxiliary component p43; MCA1, multisynthetase complex auxiliary component 1; AIMP1, ARS-interacting multifunctional protein 1. For clarity we will use EMAP-II (for the active protein) and proEMAP/p43 (for its precursor) in this review.

The human EMAP-II gene is located on chromosome 4q24 and spans approximately 31.2 kb. The EMAP-II gene contains 7 exons and the ATG start site is located in the second exon. Gene transcription results in a 1057 bp mRNA transcript of which 118 bp are untranslated divided between 5' and 3' into 49 and 69 bp respectively. The human EMAP-II mRNA sequence and the gene structure are depicted in Figure 2.

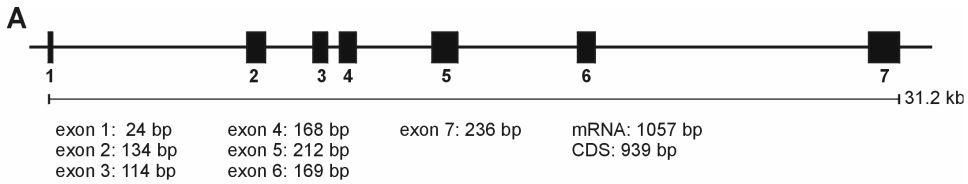

B

```
   1 GGAACCCGTG GTCCTCCGCT TCATGATTTT CTGCCGTCTC TTGGCAAAA***A*** ***TG***GCAAATAA
  61 TGATGCTGTT CTGAAGAGAC TGGAGCAGAA GGGTGCAGAG GCAGATCAAA TCATTGAATA
 121 TCTTAAGCAG CAAGTTTCTC TACTTAAGGA GAAAGCAATT TTGCAGGCAA CTTTGAGGGA
 181 AGAGAAGAAA CTTCGAGTTG AAAATGCTAA ACTGAAGAAA GAAATTGAAG AACTGAAACA
 241 AGAGCTAATT CAGGCAGAAA TTCAAAATGG AGTGAAGCAA ATAGCATTTC CATCTGGTAC
 301 TCCACTGCAC GCTAATTCTA TGGTTTCTGA AAATGTGATA CAGTCTACAG CAGTAACAAC
 361 CGTATCTTCT GGTACCAAAG AACAGATAAA AGGAGGAACA GGAGACGAAA AGAAAGCGAA
 421 AGAGAAAATT GAAAAGAAAG GAGAGAAGAA GGAGAAAAAA CAGCAATCAA TAGCTGGAAG
 481 TGCCGACTCT AAGCCAATAG ATGTTTCCCG TCTGGATCTT CGAATTGGTT GCATCATAAC
 541 TGCTAGAAAA CACCCTGATG CAGATTCTTT GTATGTGGAA GAAGTAGATG TCGGAGAAAT
 601 AGCCCCAAGG ACAGTTGTCA GTGGCCTGGT GAATCATGTT CCTCTTGAAC AGATGCAAAA
 661 TCGGATGGTG ATTTTACTTT GTAACCTGAA ACCTGCAAAG ATGAGGGGAG TATTATCTCA
 721 AGCAATGGTC ATGTGTGCTA GTTCACCAGA GAAAATTGAA ATCTTGGCTC CTCCAAATGG
 781 GTCTGTTCCT GGAGACAGAA TTACTTTTGA TGCTTTCCCA GGAGAGCCTG ACAAGGAGCT
 841 GAATCCTAAG AAGAAGATTT GGGAGCAGAT CCAGCCTGAT CTTCACACTA ATGATGAGTG
 901 TGTGGCTACA TACAAAGGAG TTCCCTTTGA GGTGAAAGGG AAGGGAGTAT GTAGGGCTCA
 961 AACCATGAGC AACAGTGGAA TCAAA***TAA***AA TGCTTCCACT ACCAAAAGAC ATTAGAGAAA
1021 ACCTTAAAAG TAATAAAGAG AAATATATTT GTCACTT
```

FIGURE 2. Structure of the human EMAP-II gene.
A. Schematic representation of the human EMAP-II gene. Transcription of the EMAP-II gene results in a 1057 bp mRNA (Accession number U10117) and the coding sequence (CDS) is 939 bp. The human EMAP-II gene contains 7 exons spanning approximately 31.2 kb on chromosome 4q24. For gene structure information GENATLAS was used.
B. mRNA sequence of EMAP-II transcript. The CDS is depicted in *italic* and the start and stop codon are depicted in ***bold italic***.

Because of its function as auxiliary protein within the ARS complex, proEMAP/p43 is expressed in virtually all tissues and can be considered as a housekeeping gene and marker for protein

synthesis [20,21]. Although proEMAP/p43 is universally expressed, the level of expression varies and is abundant at sites of apoptosis and tissue remodeling [21,22].

Protein translation is a very complex biological process. Besides mRNA and tRNA, many proteins, co-factors and enzymes are involved. As translation is one of the basic processes in every cell, many of these factors are considered to be housekeeping proteins. In higher eukaryotic organisms nine ARS (specific for amino acids Arg, Asp, Gln, Glu, Ile, Leu, Lys, Met, Pro) are assembled in a 1-1.5 x 10^6 Da multi protein complex [23]. Within this multi-enzyme complex also three auxiliary proteins are associated, initially named for their apparent molecular weight, p18, p38 and p43 [24]. These three auxiliary proteins share functions in maintenance of the stability of the ARS complex, but also have different other properties. The p18 protein is suggested to be involved in association with the ARS complex with elongation factor 1H and p38 is reported to contribute to the protein-protein interactions within the complex [25,26]. Many more functions have been described for the p43 subunit. P43 is a tRNA binding protein, suggesting a role in tRNA trafficking [27]. Strikingly, p43 also has a variety of biological functions, corresponding with the observation that p18 and p38 are always found as components of the ARS complex, while p43 and p43-like proteins are distributed widely within different species. Besides in vertebrates, p43 or p43-like domains have been found in bacteria (Trpb), in yeast (Arc1p) and in protozoan and metazoan species [28-31]. Within this context the isolation of EMAP-II (described above) from tumour-derived culture medium is remarkable, because the observation that proEMAP and p43 were the same proteins was made several years later. This link between protein synthesis and cell signaling has also been found in other tRNA synthetases (RS), like tyrosyl-RS and tryptophanyl-RS [32,33]. The biological functions of proEMAP/p43 and EMAP-II are very abundantly described and widely studied.

Functional domains

By peptide-sequence analysis and deletion fragment studies within the proEMAP/p43 sequence, several functional domains are identified. Figure 3 summarizes the different motifs and domains found. The division of p43 and EMAP-II (being the C-terminal part, residue 147-312 based on cleavage after Asp^{146}) is also depicted in Figure 3. The first functional domain, the peptide responsible for induction of monocyte and leukocyte migration, inflammatory response and binding to a monocyte-derived protein, was identified as the N-terminal region of EMAP-II mature protein [34]. This peptide corresponds to amino acids 152-166 within the proEMAP/p43 protein. Interestingly, this

peptide contains a so-called RIGRIIT motif, also present in tyrosyl-RS and corresponding to residue 158-164, that was later identified as being responsible for monocyte and leukocyte migration [35]. The tRNA binding domain is the most prominent domain within the protein and is mapped to the EMAP-II part of the protein [31,36]. This domain encompasses amino acid 151-252. Three other functional domains were described recently using deletion fragments of proEMAP/p43 [37]. Both the regions which regulate fibroblast proliferation and EC apoptosis are located in the proEMAP/p43 part of the protein, corresponding with observations that several cell types secrete proEMAP/p43 [38,39], which has also several biological activities (discussed below).

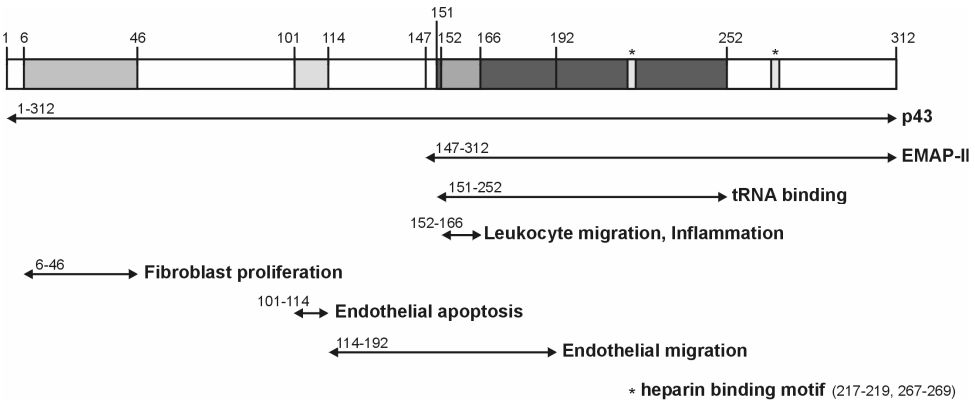

FIGURE 3. Functional domains within the proEMAP/p43-EMAP-II protein.
Different domains identified in literature as functional domains are depicted. Numbers refer to the amino acid sequence of human EMAP-II. In this figure Asp^{147} is depicted as cleavage-site to process proEMAP/p43 into mature EMAP-II. Different domains and motifs are derived from different studies using different experimental setups. For references, see text.

The fibroblast proliferation region corresponds with amino acid 6-46 and the EC apoptosis region with amino acid 101-114. A relatively large region of the protein appeared to have a function in EC migration (residue 114-192). This region overlaps the peptide involved in leukocyte migration and thus also contains the RIGRIIT motif. Finally, EMAP-II contains two heparin-binding motifs, both located in the mature protein (residues 217-219 and 267-269). These motifs were shown to be involved in the anti-angiogenic activities of EMAP-II at acidic pH [40].

Features and biological functions of proEMAP/p43 and EMAP-II

As mentioned above, proEMAP/p43 (and its cleavage product EMAP-II) exhibits a broad spectrum of biological activities. One of the synonyms (AIMP1) underlines these multifunctional properties of EMAP-II [41]. Both for the mature cytokine EMAP-II and for its precursor proEMAP/p43 multiple

functions have been described in literature. Table 1 summarizes thus far identified activities and shows whether activity has been documented for EMAP-II, proEMAP/p43 or both.

Biological function, feature	proEMAP/p43	EMAP-II	Ref
Manipulation of EC coagulation properties		X	17
Upregulation of TF expression		X	17
Monocyte/macrophage, granulocyte chemotaxis		X	17
Proinflammatory response (footpad)		X	17
Directed leucocyte migration		X	34
Increase intracellular calcium levels		X	34
Release of von Willebrand Factor by EC		X	19
Upregulation of E- and P-selectin by EC		X	19
Induction of TNF production by monocytes		X	19
Thrombohemorrhage in Meth A (i.t.)		X	19
Induction of TNF-sensitivity (i.v.) of MC-2 (i.t.)		X	19
Induction of TNF-sensitivity (i.v.) of B16, HT-1080 (i.t.)		X	43
Auxiliary component of multi RS complex	X		31
Induction of TNF-sensitivity (i.v.) of TAV in human melanoma (EMAP-gene transfer)	X	X	44,45
Association with (autoimmune) brain diseases, injury	X	X	59-63
Neovascularization during lung development	X	X	65,66
High serum levels during pregnancy	X	X	69
Inhibition of primary and metastatic tumor growth		X	52,53
Antiangiogenic, apoptosis of growing EC		X	52,54
Association with apoptosis-induced influx of leucocytes into reperfused kidneys		X	71
Apoptosis of corneal EC after transplantation		X	67
Position in multi RS complex near midpoint	X		42
Upregulation of TNF-R1 mRNA in EC		X	79
Improvement of photodynamic therapy effects		X	55
mRNA expression related to TNF-SAM2 effectively in glioblastoma patients		X	68
Induction of proinflammatory genes (like TNF)	X		39,75
Reduction of keratitis via anti-angiogenesis		X	56
Binding to αATP synthase on tumor cells	X	X	84
Expression negatively regulated by PGE(2)	X		70
Dose-dependent role in angiogenesis	X		57
Induction of TNF-sensitivity (ILP) of BN175 (EMAP-gene transfer)	X	X	49,50
Marker for microglial cells in brain		X	64
Association with macrophages in uveal melanoma		X	72
Affects EC actin cytoskeleton (at high dose)		X	82
Induction of lymphocyte apoptosis in solid tumors		X	73,74
Involved in rapamycin decreased inflammation		X	76,77
Induction of vasodilatation via NOS		X	85
Induction of fibroblast proliferation, wound repair	X		78
Binds to heparan sulphate at low pH		X	40
Induction of DOC1 gene expression in EC		X	80
Binding to $\alpha 5\beta 1$ integrin, blocks adhesion of EC to FN		X	83
TNF-R1 and TRADD mobilization in EC		X	81
Correlation with response of melanoma patients to TNF-based ILP		X	51

TABLE 1. Summary of all reported biological functions and features of EMAP-II.
All published features from EMAP-II isolation till now are listed and the table indicates whether activity has been described for proEMAP/p43, EMAP-II or both and their corresponding references are given. For a detailed description, see text. Abbreviations: EC, endothelial cells; TF, tissue factor; TNF, tumour necrosis factor-α; RS, tRNA synthetase; TAV, tumour-associated vasculature; i.v., intravenous; i.t., intratumoural, PGE(2), prostaglandin E(2); ILP, isolated limb perfusion; NOS, nitric oxide synthase; DOC1, downregulated in ovarian cancer 1; FN, fibronectin; TRADD, TNFR associated death domain.

Effects on cells and function of proEMAP/p43

Right after its isolation (see above) the first EMAP-II functions were reported. These include manipulation of the procoagulant properties of EC, likely through upregulation of TF, and the chemotactic effects towards monocytes and granulocytes. These *in vitro* observations correspond with the observed proinflammatory response after EMAP-II injection in footpads of mice [17]. A couple of years after its isolation these functions were mapped to the amino terminus of EMAP-II (see also Figure 3). Leukocyte migration was shown to be directed by EMAP-II and in addition, an increase in intra cellular calcium levels was found to be involved in this cellular activation [34]. These activities towards monocytes and EC were analyzed in more detail to point out the molecular players involved. In EC, EMAP-II induces E- and P-selectin expression, release of von Willebrand Factor and TNF production by monocytes [19].

One of the most intriguing findings with respect to EMAP-II was done in 1997 when the p43 auxiliary component of the RS multi-enzyme complex turned out to be homologous to the precursor of EMAP-II [31]. This finding led to naming the precursor of EMAP-II proEMAP/p43. The fact that p43 and proEMAP were actually the same proteins linked cytokine properties and basic functions in protein translation to one and the same protein. Structural analysis of the multi RS complex revealed that proEMAP/p43 occupies a central position within the complex [42].

Anti-tumour and anti-angiogenic properties

When injected intra-tumourally into Meth A fibrosarcoma-bearing mice, EMAP-II induced a TNF-like thrombo-hemorrhage and for the mammary carcinoma MC-2 the same treatment induced sensitivity to systemic TNF treatment [19]. For mouse melanoma (B16) and human fibrosarcoma (HT-1080) similar observations were made [43]. Consistent with its initially described functions and relation to TNF anti-cancer therapy experiments using retroviral gene transfer revealed that TNF-resistant human melanomas (Pmel) were rendered sensitive to systemic TNF therapy when the tumour cells were transfected to increase proEMAP/p43 and EMAP-II protein expression [44,45]. This enhancing effect of EMAP-II on TNF anti-cancer therapy was suggested to expand the clinical use of TNF (for recent review see [46]).

In the clinic, TNF is used in isolated perfusion settings for sarcoma and melanoma patients [47,48]. To investigate the role of EMAP-II in isolated limb perfusion (ILP) the same retroviral gene transfer approach was used to generate soft tissue sarcomas with different proEMAP/p43 and EMAP-II protein levels. These sarcomas were treated with a TNF-based ILP in rats and also in this

ILP-setting EMAP-II increased sensitivity towards TNF [49,50]. Recently, upregulated EMAP-II expression after ILP in melanoma biopsies from TNF-based ILP treated patients was found to correlate with a complete response to ILP treatment [51]. Next to contribution to TNF therapy, EMAP-II is shown to be capable to inhibit primary and metastatic tumour growth of lung carcinoma (LLC) and mammary tumours (MDA-MB-468) in mice [52] and primary tumour growth of glioma in rats [53]. These anti-tumour effects were suggested to be angiogenesis mediated because EMAP-II showed anti-angiogenic activities and was capable of inducing apoptosis in growing EC [52,54].

The anti-angiogenic activities of EMAP-II have been investigated in several settings. In mice bearing mammary carcinomas, pre-treatment with EMAP-II enhanced the effectiveness of photodynamic therapy, which was mediated by a decrease in VEGF expression [55]. Anti-angiogenic properties of EMAP-II are also implicated in stromal keratitis. Via anti-angiogenic activities like induction of EC apoptosis a decrease in infection and inflammation was observed resulting in a reduction in severity of keratitis [56]. Interestingly, besides EMAP-II also for proEMAP/p43 a role in angiogenesis has been described. This role turned out to be biphasic and dose-dependent; low concentrations are pro-angiogenic while high concentrations are anti-angiogenic [57]. These properties are very comparable to other cytokines, like TNF [58].

Brain disease, embryogenesis and serum levels studies

Beside anti-tumour activities, EMAP-II is also reported to be involved in a broad set of brain diseases and injury. More specific, EMAP-II is associated with macrophages in several autoimmune inflammatory lesions, spinal cord injury, virus induced inflammation of the nervous system, hippocampal brain damage, and traumatic brain injury [59-63]. Based on these findings during brain damage, injury and inflammation EMAP-II is considered to be a marker for microglial cells in these lesions [64].

During embryogenesis, a role for proEMAP/p43 and EMAP-II has been found in lung development. This function is linked to the manipulation of neovascularisation by EMAP-II during embryonic development [65,66].

Some other studies have been performed to evaluate EMAP-II protein and mRNA expression in patient samples. In a search for proteins involved in corneal transplant rejection, EMAP-II was found in serum and appeared capable of inducing corneal EC apoptosis, which was suggested to be involved in corneal decompensation after transplantation [67]. In slides of glioblastoma tumours from patients treated with TNF-SAM2 and chemotherapy, EMAP-II mRNA expression did correlate with the

outcome of the treatment. Patients with high EMAP-II expression tended to have a longer progression free survival [68]. Interestingly, also during pregnancy proEMAP/p43 and EMAP-II serum levels are increased, while there was no evidence that EMAP-II is involved in endothelial activation during preeclampsia [69]. Next to pregnancy, also during the menstrual cycle a temporal EMAP-II expression pattern is observed. The gene coding for the proEMAP/p43 protein, is negatively regulated by prostaglandin E2 [70].

Apoptosis and inflammation

The initially described function of EMAP-II as chemo attractant for leukocytes and macrophages has been translated to a set of disease settings. In areas of apoptosis in ischemia-reperfused kidneys, high EMAP-II expression correlated with sites of leukocytes-infiltrated inflamed tissue. When apoptosis was inhibited, inflammation was also declined [71]. In primary uveal melanoma, areas of high EMAP-II expression correlate with tumour-associated macrophages accumulation [72]. Comparable correlation was found in experiments with melanoma biopsies of ILP treated patients [51]. A more detailed function of EMAP-II in solid tumours has been described recently, showing that EMAP-II expressing tumour cells (producing EMAP-II as membrane-bound protein or secreted cytokine) can induce apoptosis of lymphocytes in solid tumours. This function in the tumour microenvironment suggests an immunosuppressive role of EMAP-II in growing solid tumours [73,74].

The proinflammatory role of EMAP-II, as observed during protein characterization right after EMAP-II identification [17] is also further investigated. For proEMAP/p43 a proinflammatory role has been described, in line with the initial finding for EMAP-II, resulting in upregulation of proinflammatory genes like TNF [75,76]. The mature EMAP-II is reported to be one of the mediators of the anti-proliferative and anti-inflammatory action of rapamycin, both after injury and neointima formation [77,78].

Mechanistic studies on proEMAP/p43 and EMAP-II effects

Unexpectedly, given the many functions of proEMAP/p43 and EMAP-II, including its presence as a component of the multi RS complex, Park *et al*. succeeded to make proEMAP/p43 knockout mice. The fact that these mice survive without proEMAP/p43 put its vital function in protein translation in another perspective. Apparently, due to the crucial importance of protein translation, there is a kind of rescue by other (unknown) proteins and mechanisms. The major defect reported in these knockouts is a retarded wound closure due to a decrease in fibroblast proliferation [79].

Recently, besides describing the many roles of EMAP-II, more details are being published about mechanistic processes underlying the functions. As EC are still considered as the mayor target, several mechanisms have been proposed for these cells. For the TNF sensitizing properties initially a very straightforward mechanism was suggested: an upregulation of TNF-R1 mRNA expression [80]. Protein data, however, were less convincing and in a recent broad micro array study of EMAP-II induced genes by EC no TNF-R1 was found. In contrast, DOC1 (downregulated in ovarian cancer 1) came out as one of most abundantly regulated genes [81]. Apparently in line with this micro array study are novel data on TNF-R1 and TRADD protein showing redistribution, rather than upregulation in EC upon EMAP-II treatment [82]. As other possible targets of EMAP-II in EC, two proteins involved in actin dynamics, Hsp27 and cofilin, were found in a broader study with angiogenesis inhibitors [83]. Interestingly, for the apoptotic features of EMAP-II in growing EC the mechanisms involved include inhibition of EC adhesion and spreading on fibronectin via direct binding of EMAP-II to integrin 5 1 [84]. For the anti-proliferative properties of EMAP-II and proEMAP/p43 towards EC, binding to the - subunit of ATP synthase was found as mechanistic explanation [85]. In a more detailed study this interaction turned out to be mediated by heparan sulfate and strongly enhanced at low pH [86].

For vasodilatation occurring during EMAP-II induced inflammation, NO is suggested to be involved as revealed by studies using pulmonary artery rings. When NO was repressed via NOS inhibition with L-NAME, the EMAP-II induced vasodilatation was decreased [87].

The many function described above and summarized in Table 1 for proEMAP/p43 and EMAP-II show the complexity of involvement in both protein translation and cytokine effects. This fascinating link of protein translation and cytokine function is gained in higher organisms: present in mammals while absent in yeast and bacteria [88]. Based on this very broad range of functions and features EMAP-II is referred to as a pro-inflammatory cytokine with anti-angiogenic properties.

From proEMAP/p43 to EMAP-II

Although many functions of EMAP-II are also reported for its precursor proEMAP/p43 (see Table 1) still the majority of activities are ascribed to the mature cytokine EMAP-II.

ProEMAP/p43 is proteolytically cleaved to produce the mature cytokine EMAP-II under conditions of cellular stress like apoptosis, hypoxia and treatment with chemotherapeutic agents [21,38,89]. The mechanism(s) of proEMAP/p43 cleavage and especially which proteases are involved turned out to be very complex and are still under debate. First indications on proEMAP/p43 cleavage arose from studies with full-length tyrosyl-tRNA synthetase (TyrRS). This TyrRS is secreted

under apoptotic conditions and cleaved into mini TyrRS and a COOH-terminal domain known to be EMAP-II-like [35]. These two fragments with cytokine activities can be generated by leukocyte elastase, an extra cellular protease [32]. This implies that the precursor is secreted, as described later also for proEMAP/p43. For EMAP-II comparable cleavage has been suggested.

When proEMAP/p43 is incubated with elastase-2, the cleavage products did not include the EMAP-II part (amino acid 147-312), which still is considered to be the mature EMAP-II cytokine [90]. This EMAP-II cytokine is based on *in vitro* cleavage experiments using recombinant mouse proEMAP/p43. These experiments identified caspase-7, and to a lesser extend caspase-3, as proteases capable of proEMAP/p43 cleavage [91]. The cleavage site within the proEMAP/p43 sequence was mapped at the critical aspartate residue (Asp-144) in the ASTD-motif. Although this motif is absent in humans, Asp-146 has been suggested to be critical in cleavage of human proEMAP/p43 [92]. In line with these findings is the fact that caspase-7 is capable of cleaving EMAP-II out of the whole murine multi tRNA synthethase complex [93]. Noteworthy, these findings were made in *in vitro* cleavage assays with recombinant mouse proteins.

Experiments with human proteins show very different results and question the suggested similarity on cleavage mechanisms. Data on recombinant human proEMAP/p43 show that human caspase-3 and –7 are not capable of proEMAP/p43 cleavage in an *in vitro* assay, and in lysates of human tumour cell lines triggered with apoptosis-inducers no EMAP-II was found [94]. In another study in which mouse melanoma tumour cells were used, EMAP-II release was induced by hypoxia, this induction was also shown to be independent of caspase-3 and -7 activation [95]. The involvement of caspases in proEMAP/p43 cleavage is very contradictive and at least very dependent on experimental setting. For translation to the *in vivo* situation the mechanisms of proEMAP/p43 cleavage might very well be microenvironment dependent and different mature EMAP-II forms still might retain their cytokine activities. Using different tumour cell lines, we recently found no involvement of caspase-3 and –7 in proEMAP/p43 cleavage and show data on matrix metalloprotease-7 contribution [96].

In conclusion, the cleavage of proEMAP/p43 varies strongly between different settings, species and likely even between tumour types. The exact mechanisms, cleavage sites and whether this affects the cytokine properties and activity of EMAP-II are still unknown.

CONCLUSIONS

The plethora of properties of proEMAP/p43 and EMAP-II shows that this protein is an important player in cell functionality and may be a very attractive target for therapy. Because of its close relation with TNF, one of the first applications might be manipulation of TNF effectiveness in ILP settings or expression analysis during treatment and follow-up of patients with solid tumours. Novel data on molecular mechanisms involved in EMAP-II actions towards EC and inflammation-related infiltrated cells (like macrophages and lymphocytes) may expand the use of EMAP-II but clearly more research, using both *in vitro* and *in vivo* experimental models, need to be conducted.

As EMAP-II is considered a marker for microglial cells and macrophages in brain diseases [97] the proEMAP/p43 and EMAP-II distribution in tissue biopsies might serve as a diagnostic marker for specific disease settings, possibly in combination with other markers [98].

In conclusion, the multifunctional properties, many pathological settings in which EMAP-II is involved and the interesting novel molecular data might in the future result in more wide-ranging applications in several therapeutic settings.

ACKNOWLEDGEMENTS

This study was supported by research grants from Mrace Translational Research Fund of the Erasmus University MC and Foundation “Heelkundig Kanker Onderzoek”.

REFERENCES

1. Carswell, E. A., Old, L. J., Kassel, R. L., Green, S., Fiore, N., and Williamson, B. (1975). An endotoxin-induced serum factor that causes necrosis of tumours. *Proc Natl Acad Sci U S A* 72, 3666-3670.
2. Shirai, T., Yamaguchi, H., Ito, H., Todd, C. W., and Wallace, R. B. (1985). Cloning and expression in Escherichia coli of the gene for human tumour necrosis factor. *Nature* 313, 803-806.
3. Marmenout, A., Fransen, L., Tavernier, J., Van der, H. J., Tizard, R., Kawashima, E., Shaw, A., Johnson, M. J., Semon, D., Muller, R., and . (1985). Molecular cloning and expression of human tumour necrosis factor and comparison with mouse tumour necrosis factor. *Eur.J.Biochem.* 152, 515-522.
4. Old, L. J. (1985). Tumour necrosis factor (TNF). *Science.* 230, 630-2.
5. Nawroth, P. P. and Stern, D. M. (1986). Modulation of endothelial cell hemostatic properties by tumour necrosis factor. *J.Exp.Med.* 163, 740-745.
6. Bevilacqua, M. P., Pober, J. S., Majeau, G. R., Fiers, W., Cotran, R. S., and Gimbrone, M. A., Jr. (1986). Recombinant tumour necrosis factor induces procoagulant activity in cultured human vascular endothelium: characterization and comparison with the actions of interleukin 1. *Proc.Natl.Acad.Sci.U.S.A* 83, 4533-4537.
7. Tracey, K. J., Beutler, B., Lowry, S. F., Merryweather, J., Wolpe, S., Milsark, I. W., Hariri, R. J., Fahey, T. J., III, Zentella, A., Albert, J. D., and . (1986). Shock and tissue injury induced by recombinant human cachectin. *Science* 234, 470-474.
8. Asher, A., Mule, J. J., Reichert, C. M., Shiloni, E., and Rosenberg, S. A. (1987). Studies on the anti-tumour efficacy of systemically administered recombinant tumour necrosis factor against several murine tumours in vivo. *J.Immunol.* 138, 963-974.
9. Nawroth, P., Handley, D., Matsueda, G., de Waal, R., Gerlach, H., Blohm, D., and Stern, D. (1988). Tumour necrosis factor/cachectin-induced intravascular fibrin formation in meth A fibrosarcomas. *J.Exp.Med.* 168, 637-647.

10. Clauss, M., Murray, J. C., Vianna, M., de Waal, R., Thurston, G., Nawroth, P., Gerlach, H., Bach, R., Familletti, P. C., and Stern, D. (1990). A polypeptide factor produced by fibrosarcoma cells that induces endothelial tissue factor and enhances the procoagulant response to tumour necrosis factor/cachectin. *J Biol Chem* 265, 7078-83.
11. Clauss, M., Gerlach, M., Gerlach, H., Brett, J., Wang, F., Familletti, P. C., Pan, Y. C., Olander, J. V., Connolly, D. T., and Stern, D. (1990). Vascular permeability factor: a tumour-derived polypeptide that induces endothelial cell and monocyte procoagulant activity, and promotes monocyte migration. *J Exp Med* 172, 1535-45.
12. Senger, D. R., Galli, S. J., Dvorak, A. M., Perruzzi, C. A., Harvey, V. S., and Dvorak, H. F. (1983). Tumour cells secrete a vascular permeability factor that promotes accumulation of ascites fluid. *Science.* 219, 983-985.
13. Connolly, D. T., Heuvelman, D. M., Nelson, R., Olander, J. V., Eppley, B. L., Delfino, J. J., Siegel, N. R., Leimgruber, R. M., and Feder, J. (1989). Tumour vascular permeability factor stimulates endothelial cell growth and angiogenesis. *J.Clin.Invest* 84, 1470-1478.
14. Leung, D. W., Cachianes, G., Kuang, W. J., Goeddel, D. V., and Ferrara, N. (1989). Vascular endothelial growth factor is a secreted angiogenic mitogen. *Science.* 246, 1306-1309.
15. Dvorak, H. F., Brown, L. F., Detmar, M., and Dvorak, A. M. (1995). Vascular permeability factor/vascular endothelial growth factor, microvascular hyperpermeability, and angiogenesis. *Am.J Pathol.* 146, 1029-1039.
16. Ferrara, N., Gerber, H. P., and LeCouter, J. (2003). The biology of VEGF and its receptors. *Nat.Med.* 9, 669-676.
17. Kao, J., Ryan, J., Brett, G., Chen, J., Shen, H., Fan, Y. G., Godman, G., Familletti, P. C., Wang, F., Pan, Y. C., and et al. (1992). Endothelial monocyte-activating polypeptide II. A novel tumour-derived polypeptide that activates host-response mechanisms. *J Biol Chem* 267, 20239-47.
18. Shalak, V., Kaminska, M., Mitnacht-Kraus, R., Vandenabeele, P., Clauss, M., and Mirande, M. (2001). The EMAPII cytokine is released from the mammalian multisynthetase complex after cleavage of its p43/proEMAPII component. *J Biol Chem* 276, 23769-23776.
19. Kao, J., Houck, K., Fan, Y., Haehnel, I., Libutti, S. K., Kayton, M. L., Grikscheit, T., Chabot, J., Nowygrod, R., Greenberg, S., and et al. (1994). Characterization of a novel tumour-derived cytokine. Endothelial-monocyte activating polypeptide II. *J Biol Chem* 269, 25106-19.
20. Lee, S. W., Cho, B. H., Park, S. G., and Kim, S. (2004). Aminoacyl-tRNA synthetase complexes: beyond translation. *J.Cell Sci.* 117, 3725-3734.
21. Knies, U. E., Behrensdorf, H. A., Mitchell, C. A., Deutsch, U., Risau, W., Drexler, H. C., and Clauss, M. (1998). Regulation of endothelial monocyte-activating polypeptide II release by apoptosis. *Proc Natl Acad Sci U S A* 95, 12322-7.
22. Tas, M. P. and Murray, J. C. (1996). Endothelial-monocyte-activating polypeptide II. *Int J Biochem Cell Biol* 28, 837-41.
23. Yang, D. C. (1996). Mammalian aminoacyl-tRNA synthetases. *Curr.Top.Cell Regul.* 34, 101-136.
24. Mirande, M. (1991). Aminoacyl-tRNA synthetase family from prokaryotes and eukaryotes: Structural domains and their implications.
25. Quevillon, S. and Mirande, M. (1996). The p18 component of the multisynthetase complex shares a protein motif with the beta and gamma subunits of eukaryotic elongation factor 1. *FEBS Lett.* 395, 63-67.
26. Quevillon, S., Robinson, J. C., Berthonneau, E., Siatecka, M., and Mirande, M. (1999). Macromolecular assemblage of aminoacyl-tRNA synthetases: identification of protein-protein interactions and characterization of a core protein. *J.Mol.Biol.* 285, 183-195.
27. Wolin, S. L. and Matera, A. G. (1999). The trials and travels of tRNA. *Genes Dev.* 13, 1-10.
28. Morales, A. J., Swairjo, M. A., and Schimmel, P. (1999). Structure-specific tRNA-binding protein from the extreme thermophile Aquifex aeolicus. *EMBO J.* 18, 3475-3483.
29. Simos, G., Sauer, A., Fasiolo, F., and Hurt, E. C. (1998). A conserved domain within Arc1p delivers tRNA to aminoacyl-tRNA synthetases. *Mol.Cell* 1, 235-242.
30. Tan, M., Heckmann, K., and Brunen-Nieweler, C. (1999). The micronuclear gene encoding a putative aminoacyl-tRNA synthetase cofactor of the ciliate Euplotes octocarinatus is interrupted by two sequences that are removed during macronuclear development. *Gene* 233, 131-40.
31. Quevillon, S., Agou, F., Robinson, J. C., and Mirande, M. (1997). The p43 component of the mammalian multi-synthetase complex is likely to be the precursor of the endothelial monocyte-activating polypeptide II cytokine. *J Biol Chem* 272, 32573-9.
32. Wakasugi, K. and Schimmel, P. (1999). Two distinct cytokines released from a human aminoacyl-tRNA synthetase [see comments]. *Science.* 284, 147-51.
33. Yang, X. L., Schimmel, P., and Ewalt, K. L. (2004). Relationship of two human tRNA synthetases used in cell signaling. *Trends Biochem.Sci.* 29, 250-256.
34. Kao, J., Fan, Y. G., Haehnel, I., Brett, J., Greenberg, S., Clauss, M., Kayton, M., Houck, K., Kisiel, W., Seljelid, R., and et al. (1994). A peptide derived from the amino terminus of endothelial-monocyte-activating polypeptide II modulates mononuclear and polymorphonuclear leukocyte functions, defines an apparently novel cellular interaction site, and induces an acute inflammatory response. *J Biol Chem* 269, 9774-9782.

35. Wakasugi, K. and Schimmel, P. (1999). Highly differentiated motifs responsible for two cytokine activities of a split human tRNA synthetase. *J Biol Chem* 274, 23155-9.
36. Kim, Y., Shin, J., Li, R., Cheong, C., Kim, K., and Kim, S. (2000). A novel anti-tumour cytokine contains an RNA binding motif present in aminoacyl-tRNA synthetases. *J Biol Chem* 275, 27062-8.
37. Han, J. M., Park, S. G., Lee, Y., and Kim, S. (2006). Structural separation of different extracellular activities in aminoacyl-tRNA synthetase-interacting multi-functional protein, p43/AIMP1. *Biochem.Biophys.Res.Commun.* 342, 113-118.
38. Barnett, G., Jakobsen, A. M., Tas, M., Rice, K., Carmichael, J., and Murray, J. C. (2000). Prostate adenocarcinoma cells release the novel proinflammatory polypeptide EMAP-II in response to stress. *Cancer Res* 60, 2850-7.
39. Ko, Y. G., Park, H., Kim, T., Lee, J. W., Park, S. G., Seol, W., Kim, J. E., Lee, W. H., Kim, S. H., Park, J. E., and Kim, S. (2001). A cofactor of tRNA synthetase, p43, is secreted to upregulate proinflammatory genes. *J Biol Chem* 276, 23028-23033.
40. Chang, S. Y., Ko, H. J., Heo, T. H., and Kang, C. Y. (2005). Heparan sulfate regulates the antiangiogenic activity of endothelial monocyte-activating polypeptide-II at acidic pH. *Mol.Pharmacol.* 67, 1534-1543.
41. Park, S. G., Ewalt, K. L., and Kim, S. (2005). Functional expansion of aminoacyl-tRNA synthetases and their interacting factors: new perspectives on housekeepers. *Trends Biochem.Sci.* 30, 569-574.
42. Norcum, M. T. and Warrington, J. A. (2000). The cytokine portion of p43 occupies a central position within the eukaryotic multisynthetase complex. *J Biol Chem* 275, 17921-4.
43. Marvin, M. R., Libutti, S. K., Kayton, M., Kao, J., Hayward, J., Grikscheit, T., Fan, Y., Brett, J., Weinberg, A., Nowygrod, R., LoGerfo, P., Feind, C., Hansen, K. S., Schwartz, M., Stern, D., and Chabot, J. (1996). A novel tumour-derived mediator that sensitizes cytokine-resistant tumours to tumour necrosis factor. *J Surg Res* 63, 248-55.
44. Wu, P. C., Alexander, H. R., Huang, J., Hwu, P., Gnant, M., Berger, A. C., Turner, E., Wilson, O., and Libutti, S. K. (1999). In vivo sensitivity of human melanoma to tumour necrosis factor (TNF)-alpha is determined by tumour production of the novel cytokine endothelial-monocyte activating polypeptide II (EMAPII). *Cancer Res* 59, 205-12.
45. Gnant, M. F., Berger, A. C., Huang, J., Puhlmann, M., Wu, P. C., Merino, M. J., Bartlett, D. L., Alexander, H. R., Jr., and Libutti, S. K. (1999). Sensitization of tumour necrosis factor alpha-resistant human melanoma by tumour-specific in vivo transfer of the gene encoding endothelial monocyte-activating polypeptide II using recombinant vaccinia virus. *Cancer Res* 59, 4668-74.
46. Van Horssen, R., ten Hagen, T. L. M., and Eggermont, A. M. M. (2006). TNF in cancer treatment: Molecular insights, antitumour effects and clinical utility. *The Oncologist* 11(4) 397-408.
47. Eggermont, A. M., Schraffordt, K. H., Lienard, D., Kroon, B. B., van Geel, A. N., Hoekstra, H. J., and Lejeune, F. J. (1996). Isolated limb perfusion with high-dose tumour necrosis factor-alpha in combination with interferon-gamma and melphalan for nonresectable extremity soft tissue sarcomas: a multicenter trial. *J.Clin.Oncol.* 14, 2653-2665.
48. Grunhagen, D. J., Brunstein, F., Graveland, W. J., van Geel, A. N., de Wilt, J. H., and Eggermont, A. M. (2004). One hundred consecutive isolated limb perfusions with TNF-alpha and melphalan in melanoma patients with multiple in-transit metastases. *Ann.Surg.* 240, 939-947.
49. Lans, T. E., ten Hagen, T. L., Van Horssen, R., Wu, P. C., van Tiel, S. T., Libutti, S. K., Alexander, H. R., and Eggermont, A. M. (2002). Improved antitumour response to isolated limb perfusion with tumour necrosis factor after upregulation of endothelial monocyte-activating polypeptide II in soft tissue sarcoma. *Ann.Surg.Oncol.* 9, 812-819.
50. Lans, T. E., Van Horssen, R., Eggermont, A. M., and ten Hagen, T. L. (2004). Involvement of endothelial monocyte activating polypeptide II in tumour necrosis factor-alpha-based anti-cancer therapy. *Anticancer Res.* 24, 2243-2248.
51. Van Horssen, R., Rens, J. A. P., Brunstein, F., Guns, V., van Gils, M., ten Hagen, T. L. M., and Eggermont, A. M. M. (2006). Intratumoural expression of TNF-R1 and EMAP-II in relation to response of patients treated with TNF-based isolated limb perfusion. *Int J Cancer* Epub 13 Apr.
52. Schwarz, M. A., Kandel, J., Brett, J., Li, J., Hayward, J., Schwarz, R. E., Chappey, O., Wautier, J. L., Chabot, J., Lo Gerfo, P., and Stern, D. (1999). Endothelial-monocyte activating polypeptide II, a novel antitumour cytokine that suppresses primary and metastatic tumour growth and induces apoptosis in growing endothelial cells. *J Exp Med* 190, 341-54.
53. Schwarz, R. E. and Schwarz, M. A. (2004). In vivo therapy of local tumour progression by targeting vascular endothelium with EMAP-II. *J.Surg.Res.* 120, 64-72.
54. Berger, A. C., Alexander, H. R., Tang, G., Wu, P. S., Hewitt, S. M., Turner, E., Kruger, E., Figg, W. D., Grove, A., Kohn, E., Stern, D., and Libutti, S. K. (2000). Endothelial monocyte activating polypeptide II induces endothelial cell apoptosis and may inhibit tumour angiogenesis. *Microvasc Res* 60, 70-80.
55. Ferrario, A., von Tiehl, K. F., Rucker, N., Schwarz, M. A., Gill, P. S., and Gomer, C. J. (2000). Antiangiogenic treatment enhances photodynamic therapy responsiveness in a mouse mammary carcinoma. *Cancer Res* 60, 4066-9.

56. Zheng, M., Schwarz, M. A., Lee, S., Kumaraguru, U., and Rouse, B. T. (2001). Control of stromal keratitis by inhibition of neovascularization. *Am J Pathol* 159, 1021-1029.
57. Park, S. G., Kang, Y. S., Ahn, Y. H., Lee, S. H., Kim, K. R., Kim, K. W., Koh, G. Y., Ko, Y. G., and Kim, S. (2002). Dose-dependent biphasic activity of tRNA synthetase-associating factor, p43, in angiogenesis. *J.Biol.Chem.* 277, 45243-45248.
58. Fajardo, L. F., Kwan, H. H., Kowalski, J., Prionas, S. D., and Allison, A. C. (1992). Dual role of tumour necrosis factor-alpha in angiogenesis. *Am.J.Pathol.* 140, 539-544.
59. Schluesener, H. J., Seid, K., Zhao, Y., and Meyermann, R. (1997). Localization of endothelial-monocyte-activating polypeptide II (EMAP II), a novel proinflammatory cytokine, to lesions of experimental autoimmune encephalomyelitis, neuritis and uveitis: expression by monocytes and activated microglial cells. *Glia* 20, 365-72.
60. Mueller, C. A., Schluesener, H. J., Conrad, S., Meyermann, R., and Schwab, J. M. (2003). Spinal cord injury induces lesional expression of the proinflammatory and antiangiogenic cytokine EMAP II. *J.Neurotrauma* 20, 1007-1015.
61. Wege, H., Schluesener, H., Meyermann, R., Barac-Latas, V., Suchanek, G., and Lassmann, H. (1998). Coronavirus infection and demyelination. Development of inflammatory lesions in Lewis rats. *Adv Exp Med Biol* 440, 437-44.
62. Brabeck, C., Michetti, F., Geloso, M. C., Corvino, V., Goezalan, F., Meyermann, R., and Schluesener, H. J. (2002). Expression of EMAP-II by activated monocytes/microglial cells in different regions of the rat hippocampus after trimethyltin-induced brain damage. *Exp.Neurol.* 177, 341-346.
63. Mueller, C. A., Schluesener, H. J., Conrad, S., Meyermann, R., and Schwab, J. M. (2003). Lesional expression of a proinflammatory and antiangiogenic cytokine EMAP II confined to endothelium and microglia/macrophages during secondary damage following experimental traumatic brain injury. *J.Neuroimmunol.* 135, 1-9.
64. Mueller, C. A., Richt, J. A., Meyermann, R., Deininger, M., and Schluesener, H. (2003). Accumulation of the proinflammatory cytokine endothelial-monocyte-activating polypeptide II in ramified microglial cells in brains of Borna virus infected Lewis rats. *Neurosci.Lett.* 339, 215-218.
65. Schwarz, M., Lee, M., Zhang, F., Zhao, J., Jin, Y., Smith, S., Bhuva, J., Stern, D., Warburton, D., and Starnes, V. (1999). EMAP II: a modulator of neovascularization in the developing lung. *Am J Physiol* 276, 365-75.
66. Warburton, D., Schwarz, M., Tefft, D., Flores-Delgado, G., Anderson, K. D., and Cardoso, W. V. (2000). The molecular basis of lung morphogenesis. *Mech Dev* 92, 55-81.
67. Liu, S. H. and Gottsch, J. D. (1999). Apoptosis induced by a corneal-endothelium-derived cytokine. *Invest Ophthalmol Vis Sci* 40, 3152-9.
68. Yamamoto, M., Fukushima, T., Ueno, Y., Hayashi, S., Kimura, H., Soma, G., and Tomonaga, M. (2000). Clinical significance of the expression of endothelial-monocyte activating polypeptide II (EMAPII) in the treatment of glioblastoma with recombinant mutant human tumour necrosis factor-alpha (TNF-SAM2). *Anticancer Res* 20, 4081-4086.
69. Wellings, R. P., Lash, G. E., Murray, J. C., Tas, M., Ward, W., Trew, A. J., and Baker, P. N. (1999). Endothelial monocyte-activating polypeptide-2 is increased in pregnancy but is not further increased in preeclampsia. *J Soc Gynecol Investig* 6, 142-6.
70. Battersby, S., Boddy, S. C., Critchley, H. O., and Jabbour, H. N. (2002). Expression and localization of endothelial monocyte-activating polypeptide II in the human endometrium across the menstrual cycle: regulation of expression by prostaglandin E(2). *J.Clin.Endocrinol.Metab* 87, 3928-3935.
71. Daemen, M. A., van 't Veer, C., Denecker, G., Heemskerk, V. H., Wolfs, T. G., Clauss, M., Vandenabeele, P., and Buurman, W. A. (1999). Inhibition of apoptosis induced by ischemia-reperfusion prevents inflammation. *J Clin Invest* 104, 541-9.
72. Clarijs, R., Schalkwijk, L., Ruiter, D. J., and de Waal, R. M. (2003). EMAP-II expression is associated with macrophage accumulation in primary uveal melanoma. *Invest Ophthalmol.Vis.Sci.* 44, 1801-1806.
73. Murray, J. C., Symonds, P., Ward, W., Huggins, M., Tiga, A., Rice, K., Heng, Y. M., Todd, I., and Robins, R. A. (2004). Colorectal cancer cells induce lymphocyte apoptosis by an endothelial monocyte-activating polypeptide-II-dependent mechanism. *J.Immunol.* 172, 274-281.
74. Murray, J. C., Heng, Y. M., Symonds, P., Rice, K., Ward, W., Huggins, M., Todd, I., and Robins, R. A. (2004). Endothelial monocyte-activating polypeptide-II (EMAP-II): a novel inducer of lymphocyte apoptosis. *J.Leukoc.Biol.* 75, 772-776.
75. Ko, Y. G., Park, H., Kim, T., Lee, J. W., Park, S. G., Seol, W., Kim, J. E., Lee, W. H., Kim, S. H., Park, J. E., and Kim, S. (2001). A cofactor of tRNA synthetase, p43, is secreted to upregulate proinflammatory genes. *J Biol Chem* 276, 23028-23033.
76. Park, H., Park, S. G., Kim, J., Ko, Y. G., and Kim, S. (2002). Signaling pathways for TNF production induced by human aminoacyl-tRNA synthetase-associating factor, p43. *Cytokine* 20, 148-153.
77. Nuhrenberg, T. G., Voisard, R., Fahlisch, F., Rudelius, M., Braun, J., Gschwend, J., Kountides, M., Herter, T., Baur, R., Hombach, V., Baeuerle, P. A., and Zohlnhofer, D. (2005). Rapamycin attenuates vascular wall inflammation and progenitor cell promoters after angioplasty. *FASEB J.* 19, 246-248.

78. Zohlnhofer, D., Nuhrenberg, T. G., Neumann, F. J., Richter, T., May, A. E., Schmidt, R., Denker, K., Clauss, M. A., Schomig, A., and Baeuerle, P. A. (2004). Rapamycin effects transcriptional programs in smooth muscle cells controlling proliferative and inflammatory properties. *Mol.Pharmacol.* 65, 880-889.
79. Park, S. G., Shin, H., Shin, Y. K., Lee, Y., Choi, E. C., Park, B. J., and Kim, S. (2005). The novel cytokine p43 stimulates dermal fibroblast proliferation and wound repair. *Am.J.Pathol.* 166, 387-398.
80. Berger, A. C., Alexander, H. R., Wu, P. C., Tang, G., Gnant, M. F., Mixon, A., Turner, E. S., and Libutti, S. K. (2000). Tumour necrosis factor receptor I (p55) is upregulated on endothelial cells by exposure to the tumour-derived cytokine endothelial monocyte- activating polypeptide II (EMAP-II). *Cytokine* 12, 992-1000.
81. Tandle, A. T., Mazzanti, C., Alexander, H. R., Roberts, D. D., and Libutti, S. K. (2005). Endothelial monocyte activating polypeptide-II induced gene expression changes in endothelial cells. *Cytokine* 30, 347-358.
82. Van Horssen, R., Rens, J. A. P., Schipper, D., Eggermont, A. M. M., and ten Hagen, T. L. M. (2006). EMAP-II facilitates TNF-R1 apoptotic signaling in endothelial cells via TRADD mobilization. *Submitted*.
83. Keezer, S. M., Ivie, S. E., Krutzsch, H. C., Tandle, A., Libutti, S. K., and Roberts, D. D. (2003). Angiogenesis inhibitors target the endothelial cell cytoskeleton through altered regulation of heat shock protein 27 and cofilin. *Cancer Res.* 63, 6405-6412.
84. Schwarz, M. A., Zheng, H., Liu, J., Corbett, S., and Schwarz, R. E. (2005). Endothelial-monocyte activating polypeptide II alters fibronectin based endothelial cell adhesion and matrix assembly via alpha5 beta1 integrin. *Exp.Cell Res.*
85. Chang, S. Y., Park, S. G., Kim, S., and Kang, C. Y. (2002). Interaction of the C-terminal domain of p43 and the alpha subunit of ATP synthase. Its functional implication in endothelial cell proliferation. *J Biol Chem* 277, 8388-8394.
86. Chang, S. Y., Ko, H. J., Heo, T. H., and Kang, C. Y. (2005). Heparan sulfate regulates the antiangiogenic activity of endothelial monocyte-activating polypeptide-II at acidic pH. *Mol.Pharmacol.* 67, 1534-1543.
87. Tsai, B. M., Wang, M., Clauss, M., Sun, P., and Meldrum, D. R. (2004). Endothelial monocyte-activating polypeptide II causes NOS-dependent pulmonary artery vasodilation: a novel effect for a proinflammatory cytokine. *Am.J.Physiol Regul.Integr.Comp Physiol* 287, R767-R771.
88. Liu, J., Yang, X. L., Ewalt, K. L., and Schimmel, P. (2002). Mutational switching of a yeast tRNA synthetase into a mammalian-like synthetase cytokine. *Biochemistry* 41, 14232-14237.
89. Matschurat, S., Knies, U. E., Person, V., Fink, L., Stoelcker, B., Ebenebe, C., Behrensdorf, H. A., Schaper, J., and Clauss, M. (2003). Regulation of EMAP II by hypoxia. *Am.J.Pathol.* 162, 93-103.
90. Han, J. M., Park, S. G., Lee, Y., and Kim, S. (2006). Structural separation of different extracellular activities in aminoacyl-tRNA synthetase-interacting multi-functional protein, p43/AIMP1. *Biochem.Biophys.Res.Commun.* 342, 113-118.
91. Behrensdorf, H. A., van de Craen, M., Knies, U. E., Vandenabeele, P., and Clauss, M. (2000). The endothelial monocyte-activating polypeptide II (EMAP II) is a substrate for caspase-7. *FEBS Lett* 466, 143-7.
92. Berger, A. C., Tang, G., Alexander, H. R., and Libutti, S. K. (2000). Endothelial monocyte-activating polypeptide II, a tumour-derived cytokine that plays an important role in inflammation, apoptosis, and angiogenesis [In Process Citation]. *J Immunother* 23, 519-27.
93. Shalak, V., Kaminska, M., Mitnacht-Kraus, R., Vandenabeele, P., Clauss, M., and Mirande, M. (2001). The EMAPII cytokine is released from the mammalian multisynthetase complex after cleavage of its p43/proEMAPII component. *J Biol Chem* 276, 23769-23776.
94. Zhang, F. R. and Schwarz, M. A. (2002). Pro-EMAP II is not primarily cleaved by caspase-3 and -7. *Am.J.Physiol Lung Cell Mol.Physiol* 282, L1239-L1244.
95. Matschurat, S., Knies, U. E., Person, V., Fink, L., Stoelcker, B., Ebenebe, C., Behrensdorf, H. A., Schaper, J., and Clauss, M. (2003). Regulation of EMAP II by hypoxia. *Am.J.Pathol.* 162, 93-103.
96. Van Horssen, R., Rens, J. A. P., Schipper, D., Eggermont, A. M. M., and ten Hagen, T. L. M. (2006). MMP-7 is involved in EMAP-II release of tumour cells by cleavage of proEMAP/p43. *Submitted*.
97. Mueller, C. A., Richt, J. A., Meyermann, R., Deininger, M., and Schluesener, H. (2003). Accumulation of the proinflammatory cytokine endothelial-monocyte-activating polypeptide II in ramified microglial cells in brains of Borna virus infected Lewis rats. *Neurosci.Lett.* 339, 215-218.
98. Guo, L. H., Trautmann, K., and Schluesener, H. J. (2005). Expression of P2X4 receptor by lesional activated microglia during formalin-induced inflammatory pain. *J.Neuroimmunol.* 163, 120-127.

Chapter 7

MMP-7 is involved in EMAP-II release of tumour cells by cleavage of proEMAP/p43

Remco van Horssen[1]
Joost A. P. Rens[1]
Debby Schipper[1]
Theo M. Luider[2]
Alexander M. M. Eggermont[1]
Timo L. M. ten Hagen[1]

[1]Laboratory of Experimental Surgical Oncology, Department of Surgical Oncology and [2]Department of Neurology and Centre for Biomics, Erasmus MC – Daniel den Hoed Cancer Center, Rotterdam, The Netherlands

Submitted to Journal of Biological Chemistry

ABSTRACT

Endothelial monocyte-activating polypeptide-II (EMAP-II) is a proinflammatory cytokine with antiangiogenic properties and released by cells in response to cellular stress. Its precursor (proEMAP/p43), identical to the p43 component of the mammalian multi tRNA synthetase complex, is involved in protein translation. The mechanism of conversion of proEMAP/p43 into EMAP-II is still under debate. As EMAP-II was initially isolated from tumour cell derived medium, we studied the cleavage of proEMAP/p43 by tumour cells. We found that caspase-7 activation kinetics did not overlap the kinetics of proEMAP/p43 cleavage. Recombinant caspase-3, and –7 did not cleave proEMAP/p43 in cell lysates either. In addition, inhibition of caspase-3 and –7 did not result in a decline in EMAP-II release by tumour cells. Next we investigated the involvement of different matrix metalloproteinases (MMPs) in proEMAP/p43 cleavage. In contrast to MMP-2, 3, and –9, MMP-7 cleaved proEMAP/p43 in cell lysates into a product corresponding to EMAP-II. Involvement of MMP-7 was confirmed by mass spectrometry and recombinant protein cleavage. Inhibition of MMP-7 with a broad range inhibitor and specific RNAi resulted in a decreased EMAP-II release by tumour cells. Finally, we showed that the kinetics of MMP-7 activation overlap with EMAP-II release by triggered tumour cells. In conclusion, we provide evidence that in tumour cells MMP-7 is involved in the conversion of proEMAP/p43 into EMAP-II and suggest that MMP-7 may attribute to EMAP-II activities at specific sites in the tumour microenvironment.

INTRODUCTION

Endothelial monocyte-activating polypeptide-II (EMAP-II) is a multifunctional cytokine that was first isolated from supernatants of cultured murine fibrosarcoma and human melanoma cells [1,2]. Initially described functions of EMAP-II are proinflammatory properties, chemotaxis of neutrophils and monocytes/macrophages and induction of von Willebrand Factor, E- and P-selectin and Tissue Factor in endothelial cells (EC) [3,4]. In addition, EMAP-II is highly expressed at sites of epithelial mesenchymal junctions and angiogenesis during embryonic development [5,6] and exhibits antiangiogenic activities by inducing EC apoptosis and suppression of tumour growth [7,8]. It inhibits EC proliferation, which is suggested to be mediated by binding of EMAP-II to -adenosine triphosphate synthase [9]. Recently, the antiangiogenic activity of EMAP-II is shown to be regulated by heparan sulphate [10] and EMAP-II is shown to bind alpha5 integrins thereby inhibiting the adhesion of EC to fibronectin matrix [11]. Furthermore, a cancer cell dependent novel immunosuppressive role of EMAP-II has been described by inducing lymphocyte apoptosis [12,13].

For both human and mouse, the sequence of EMAP-II [4,14] shows that it is produced as a precursor protein (proEMAP) that was shown to be identical to the p43 subunit of the mammalian multi tRNA synthetase complex and thereby involved in protein translation [15-17]. ProEMAP/p43 (~ 35 kDa) is proteolytically cleaved to produce the mature polypeptide of 18-20 kDa, however no secretion signal peptide is present in the sequence [18]. Inducers of the release of mature EMAP-II by tumour cells *in vitro* are apoptosis [19] and cellular stress, like hypoxia and treatment with chemotherapeutic agents [20].

The mechanisms of proEMAP cleavage, however, are still under debate and contradicting papers have been published on this issue. Using *in vitro* cleavage experiments with recombinant mouse proEMAP/p43, caspase-7, and to a lesser extend caspase-3, were identified as proteases capable of proEMAP/p43 cleavage [21]. The cleavage site within the proEMAP/p43 sequence was mapped at the critical aspartate residue (Asp-144) in the ASTD-motif. Although this motif is absent in humans, Asp-146 has been suggested to be critical in this cleavage [22], but supportive experimental data is missing. Apparently in line with these findings is the fact that caspase-7 is capable of cleaving EMAP-II out of the whole murine multi tRNA synthetase complex [15]. In contrast, data on recombinant human proEMAP/p43 show that human caspase-3 and –7 are not capable to cleave proEMAP/p43 in an *in vitro* cleavage assay and in lysates of human tumour cell lines triggered with apoptosis-inducers, no EMAP-II was found [23]. In another report, where EMAP-II release was induced in mouse melanoma cells by hypoxia, this induction was shown to be independent of caspase-3 and -7 activation [24]. Recently, proEMAP isolated from endothelial cells was shown to be cleaved by Cathepsin L and a 44 amino acid region of proEMAP was identified as being susceptible to protease cleavage [25].

To address the conflicting data we set up experiments to identify a protease that cleaves proEMAP/p43 in tumour cells. Based on kinetics of EMAP-II release and caspase-7 activation in tumour cells, inhibition experiments and *in vitro* cleavage experiments we excluded caspase-7 from proEMAP/p43 cleavage. Because matrix metalloproteinases (MMPs) are known for their protein cleavage activities we studied MMP-2, -3, -7 and –9 for their contribution to proEMAP/p43 cleavage. We identified MMP-7 as being capable of cleaving proEMAP/p43 and confirmed this by mass spectrometry, recombinant protein cleavage, inhibition experiments and kinetics studies. Our results show that in tumour cells MMP-7 rather than caspase-7 is involved in the cleavage of proEMAP/p43 into EMAP-II and justifies more research on MMP-7 expression in relation to EMAP-II cleavage by tumours.

MATERIALS AND METHODS

Cell culture

B16BL6 (mouse melanoma) and BLM (human melanoma, kindly provided by drs. R.M.W. de Waal and W.P.Leenders, University Medical Center St Radboud, Nijmegen, The Netherlands) cells were cultured in DMEM medium (Biowhittaker) and BN175 (rat syngeneic soft tissue sarcoma), Meth A (methylcholanthrene A-transformed mouse fibrosarcoma) and PG-WU (Gibbon Ape ecotropic packaging kidney cell line, kindly provided by drs. P.C. Wu and S.K. Libutti, National Cancer Institute, NIH, Bethesda, USA) cells were cultured in RPMI 1640 medium (Biowhittaker) supplemented with 10% Fetal Calf Serum (FCS) and 100 U/ml penicillin/streptomycin (Life Technologies). PG-WU cells were cultured under selection of neomycin (800 μg/ml, Sigma-Aldrich). Tumour cells were maintained at 37 ^{o}C, 5% CO_2 in a humidified incubator and routinely subcultured by removal from flasks using Trypsin-EDTA (Sigma-Aldrich).

Generation and analysis of high EMAP-expressing cell lines

The packaging cell line PG-WU, producing a retrovirus encoding for the human EMAP-II gene [26], was used to transfect B16BL6, BN175 and BLM cells. To prepare virus-containing conditioned medium 5x10^{6} PG-WU cells were grown for at least 48 h, viral supernatants were briefly centrifuged, filtered across a 0.45 μm membrane (Corning) and SequaBrene (1 μl/ml supernatant, Sigma-Aldrich) was added. Tumour cells, grown till 40-50% confluence, were transfected with freshly prepared viral supernatants for 5 h on 3 subsequent days and in between incubated with standard medium. For each cell line 12 different clones were expanded under neomycin selection (800 μg/ml, Sigma-Aldrich) and checked for viral human EMAP-II gene incorporation by PCR and Western blotting. DNA was extracted from the cells using QiaAmp DNA Mini columns (Qiagen). For PCR the following primers were used: 5'-AATCGGATGGTGATTTTACTTTGTA-3' (forward, within EMAP-II sequence) paired with either 5'-CATTTTATTTGATTCCACTGTTGC-3' (reverse, within EMAP-II sequence) or 5'-GAATGCTCGTCAAGAAGACAG-3' (reverse, within IRES vector sequence). Amplification was performed using a T-Gradient thermocycler (Biometra) using 35 cycles of a 94 ^{o}C denaturation step (45 s), a 55 ^{o}C annealing step (45 s) and a 72 ^{o}C elongation step (60 s) followed by 72 ^{o}C (7 min) and soaked at 4 ^{o}C. Amplified PCR products were analyzed on agarose gels.

Treatment of tumour cells to induce EMAP-II production

B16BL6, BN175, BLM, their high EMAP-expressing clones (B16-E, BN-E, BLM-E) and Meth A cells

were treated with a set of chemotherapeutic drugs, apoptosis inducers, hypoxia, hypoxia mimicker, cytokines and starvation. The different treatments were: Actinomycin D (100 ng/ml, Sigma-Aldrich), Cyclohexamide/TNF-α (3 μg/ml / 250 ng/ml, Sigma-Aldrich, TNFα was a generous gift of Boehringer-Ingelheim GmbH), Mevinolin/Etoposide (20-40 μg/ml each, Sigma-Aldrich), Ionomycin (20 μg/ml, MP Biomedicals), IFN-β (500 U/ml, Biosource), hypoxia (1% O_2) or starvation. Treatments were tested for the different cell lines and for different time points to identify the optimal trigger for EMAP-II production. For inhibition experiments caspase-3 and –7 inhibitor DEVD-CHO, cell permeable (1 μM, BioSource) or MMP-1, -3, -7, -9 inhibiting MMP-inhibitor-II (10 μg/ml, Calbiochem) was added.

Western Blot analysis

At several time points medium samples were taken, protease inhibitor cocktail (Roche) added, protein concentration determined with Coomassie Plus Reagent (Pierce) and normalized by protein content. Equal amounts of supernatant proteins were precipitated with ice-cold acetone and resuspended in 50 μl Laemmli Sample Buffer (BioRad). Samples were heated at 95 °C for 8 min, electrophoresed by SDS-PAGE on 15% gels and transferred onto polyvinylidene difluoride (PVDF) membranes (BioRad). Membranes were blocked for at least 1 h at room temperature with 5% nonfat dried milk (BioRad) in PBS/0,05% Tween-20 and incubated with anti-EMAP-II (0,2 μg/ml, BioSource) or anti-MMP-7 (0,2 μg/ml, Abcam) diluted in 5% nonfat dried milk in PBS/0,05% Tween-20 overnight at 4 °C. After washing with PBS/0,05% Tween-20 and incubation with biotinylated goat anti-rabbit IgG for 1 h at room temperature, proteins were made visible by amplified alkaline phosphatase (BioRad). Membranes were incubated with alkaline phosphatase-streptavidin complex (BioRad) for 1 h at room temperature, washed and stained with NBT-BCIP substrate (Roche) until staining was optimal. The substrate reaction was stopped by washing several times with AD, membranes were dried and scanned for analysis. To confirm equal protein loading afterwards, all PVDF membranes were stained with Ponceau S solution (Sigma-Aldrich) for total protein. An abundantly present protein was used as loading control to show equal protein loading.

Caspase-7 activity assay

To measure caspase-7 activity Caspase-7 Activity Assay Kit (Cell Signaling) was used according to manufactures protocol. Briefly, after treatment cells were washed once with ice-cold PBS, scraped,

resuspended in ice-cold Cell Extraction Buffer (50 mM Pipes/KOH (pH 6.5), 2 mM EDTA, 0,1% Chaps, 5 mM DTT, 20 μg/ml leupeptin, 10 μg/ml pepstatin A, 10 μg/ml aprotinin) and subjected to 3 freeze-thaw cycles. After centrifugation for 10 min at 4 °C, caspase-7 was immunoprecipitated by Caspase-7 Antibody (Cell Signaling) and protein A sepharose beads (Amersham). The precipitate was washed with Reaction Buffer (50 mM Hepes (pH 7.5), 75 mM NaCl, 5 mM DTT, 0,1% Chaps) and incubated with 0.4 mM caspase-7 substrate (Ac-DEVD-AFC) in Reaction Buffer overnight at 37 °C. AFC fluorescence was measured at excitation of 400 nm and emission of 510 nm.

In vitro cleavage assay

B16BL6, BN175 and their high EMAP-expressing clones were grown in 75 cm^2 flasks and lysed in Lysis Buffer (50 mM Tris-HCl (pH 7.5), 150 mM NaCl, 0.2% NP-40, 10% glycerol) and 1:1 diluted in MMP Reaction Buffer (50 mM Tris-HCl (pH 7.5), 10 mM $CaCl_2$, 0.05% tween-20, 0.02% NaN_3). A control (t=0 h) sample was taken, recombinant active MMP-2, -3 (trypsin-activated proMMP-3), (Oncogene) -7, -9 (Calbiochem) (0,1 μg/ml) was added and samples were incubated at 37 °C for several time points. Alternatively, tumour cell lysates were diluted in 2X Reaction Buffer, recombinant active caspase-3, -7 (respectively 100 and 10 U/sample, Calbiochem) was added and samples were incubated at 37 °C for several time points. ProEMAP/p43 cleavage was analyzed by Western blotting. To confirm activity of added recombinant caspases and MMPs in tumour cell lysates, we performed activity assays. For caspase-3 and -7, Enzolyte AnaRed Caspase-7 activity assay and for MMP-2, -3, -7, and -9, Enzolyte 520 MMP activity assays with the corresponding specific substrates (Anaspec) were used. B16-E and BN-E cell lysates were 1:1 diluted in assay buffer, caspase-3 (100 U), -7 (10 U) or 25 ng MMP was added, samples were incubated at 37 °C for several time points and the caspase and MMP activity was measured by adding the corresponding specific substrates.

Recombinant protein cleavage

Recombinant human GST-tagged proEMAP/p43 (100 ng, Abnova) and recombinant human MMP-7 (100 ng) were incubated in 200 l MMP assay buffer at 37 °C for 1 and 2 h. ProEMAP/p43 cleavage was analyzed by Western blotting using antibodies against EMAP-II and GST.

Mass spectrometry

In vitro cleavage assays with MMP-7 were repeated and control samples (t=0 h) and t=6 h (B16-E) or t=24 h (BN-E) were both stained by Coomassie Brilliant Blue (Pierce) and analyzed by Western

blotting. Bands of interest were cut out of the gel, destained, lyophilized and digested by Trypsin (ultra-grade, Promega) in 50 mM Tris-HCl (pH 8.8) overnight at room temperature. Acetonitrile/0.1% TFA (1:2) solution (7 μl) was added to the gel plugs and 0.5 μl of a matrix-sample (0.5 μl:2.5μl) solution was spotted on a MALDI-TOF MS target plate. ACCA (2 mg in 1 ml acetonitrile) was used as matrix. Mass spectra were obtained on a Bruker Apex Q 9.4 Tesla Fourier transform mass spectrometer (FTMS), using a broadband MS scan (m/z 800-4000 at 125,000 resolution at m/z 2000) [27]. Mass spectra of complex peptide mixtures were screened for human EMAP-specific peptides obtained from the GenBank protein database by using MASCOT software (www.matrixscience.com).

MMP-7 inhibition by siRNA

For the inhibition of MMP-7 we used double stranded 25-nt RNA duplex, stealth RNA interference, to mouse MMP-7 (sequence: 5'-GCCAGAUGUUGCAGAAUACUCACUA-3') and their scrambled control RNA interference duplexes (Invitrogen). Duplexes were transfected into B16-E cells in a triple transfection setup using Lipofectamine 2000 (Invitrogen) according to the manufacturer's protocol. Two RNAi duplexes were tested for their ability to down regulate MMP-7 (checked by Western blotting). The RNAi duplex with optimal inhibition was used in consecutive experiments to evaluate the effects of MMP-7 inhibition on proEMAP/p43 cleavage. Inhibition was quantified by densitometric analysis using ImageJ Software (NCI) and expression ratios were calculated.

MMP-7 activity assay

MMP-7 activity was measured using MMP-7 assay kit (Enzolyte, Anaspec) according to manufacturer's protocol. Briefly, after treatment in phenol red-free medium, conditioned medium was concentrated and incubated with APMA (1 mM) for 15 minutes at 37 ^{o}C. MMP-7 substrate (5-FAM/QXL-520 FRET peptide) was added, samples were incubated for 60 minutes at room temperature and fluorescence was measured at excitation of 490 nm and emission of 520 nm.

RESULTS

Generation of high EMAP-expressing cell lines

To study the cleavage of proEMAP/p43 by tumour cells we generated cell lines with an upregulated EMAP-II expression as described in the materials and methods section and published before [26,28]. By retroviral transfection we made B16-E, BN-E and BLM-E cell lines, checked clones for

incorporation of viral human EMAP-II cDNA by PCR and selected clones based on proEMAP/p43 protein production (data not shown).

Optimal trigger for tumour cells to produce EMAP-II is cell type dependent

It is well documented in literature that some tumour cells *in vitro* can produce active EMAP-II at low levels in the culture medium, either with or without treatment, while other tumour cells do not [12,20]. In Meth A, B16BL6, B16-E, BN175, BN-E, BLM and BLM-E cell lines cellular stress was induced with a set of triggers to prompt the cells to produce active EMAP-II. Except for Meth A, none of these cell lines produced detectable amounts of EMAP-II before treatment. For B16BL6, B16-E, BN175 and BN-E the optimal treatment conditions are depicted in Fig. 1A.

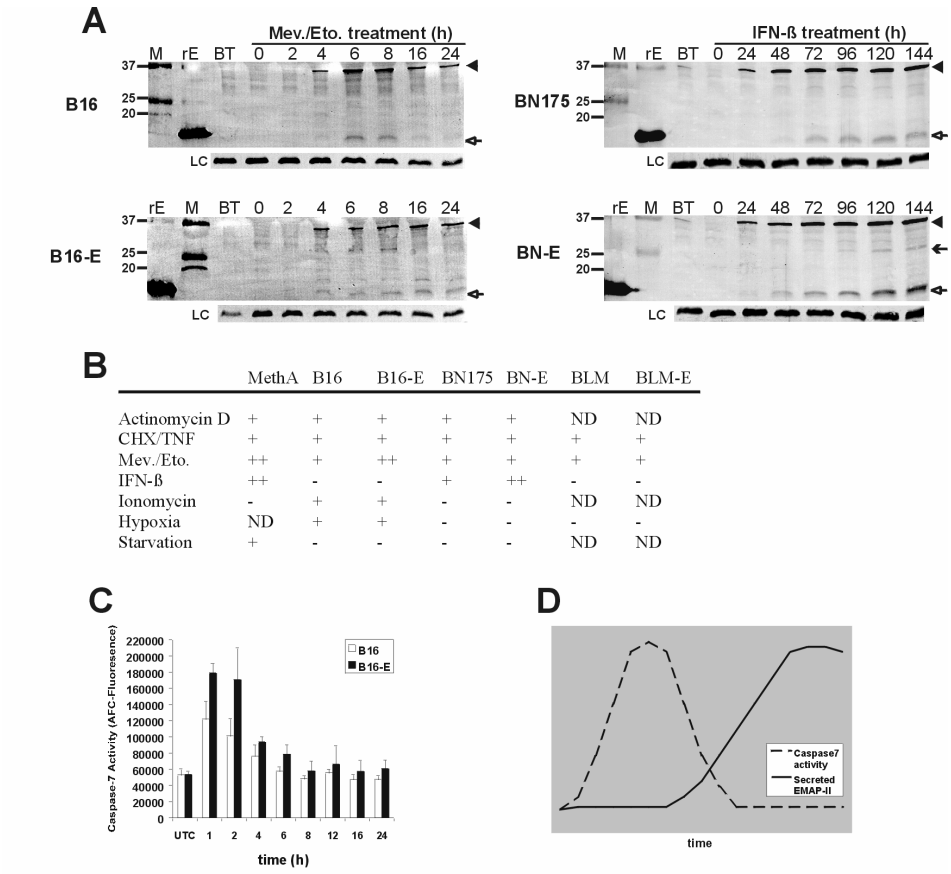

FIGURE 1. ProEMAP/p43 cleavage induction is cell type dependent and does not correspond to caspase-7 activation.

A. Western blot analysis for proEMAP/p43 and EMAP-II in the culture medium of B16, B16-E, BN175 and BN-E tumour cells. B16 and B16-E cells were treated with Mevinolin/Etoposide combination for 0-24 h, BN175 and BN-E cells were triggered by IFN-β for 0-144 h. For B16 and BN175 cells the high proEMAP/p43 expressing clones show more EMAP-II in the culture medium. Arrowhead points proEMAP/p43, open arrow points EMAP-II and small arrows intermediate form. (M) protein kD marker, (rE) recombinant EMAP-II, 50 ng. (BT) Before treatment, (LC) Loading control.
B. Table summarizes all different treatments tested on different tumour cell lines to find the optimal trigger for proEMAP/p43 cleavage as tested by Western blot analysis for EMAP-II in the culture medium. (-) no EMAP-II detected, (+) low amounts of EMAP-II, (++) high amounts of EMAP-II, (ND) Not determined.
C. Caspase-7 activity during proEMAP/p43 cleavage in B16 and B16-E cells triggered by Mevinolin/Etoposide combination for 0-24 h. Caspase-7 is activated at much earlier time points compared to EMAP-II production. (UTC) untreated control. Graph represents mean activity ± SD of three independent experiments.
D. Schematic representation of caspase-7 and proEMAP/p43 cleavage kinetics over time. At time points that EMAP-II is detected caspase-7 activity is decreased to background levels.

Upon treatment all cells produced EMAP-II, although there were cell-type dependent differences in intermediates formed and the EMAP-II production was higher in the transfected clones compared to the wild-type tumour cells. For all tumour cells also proEMAP/p43 was detected in the culture medium, a feature described earlier by others [19]. Noteworthy is the fact that the observed active EMAP-II form appeared to have a lower mass than the recombinant EMAP-II standard, also found by Murray *et al.* [12]. The sequence of the recombinant EMAP-II protein is based on the suggested cleavage of proEMAP/p43 by caspase-7 [21]. The different triggers tested together with the production of EMAP-II are listed in the table of Fig. 1B.

Kinetics of caspase-7 activity and proEMAP/p43 cleavage by B16BL6 tumour cells

Using immunoprecipation and a specific caspase-7 substrate we determined the activity of caspase-7 in the culture medium of B16BL6 and B16-E melanoma cells treated with Mevinolin/Etoposide to trigger EMAP-II production. The caspase-7 activity over time is presented in Fig. 1C. For both B16BL6 and B16-E cells we found an optimal caspase-7 activity after 1-2 h. However, when at later time points caspase-7 activity decreased to control levels, the EMAP-II production still increased as can be seen from the Western blots in Fig. 1A. For BN175 and BN-E we found comparable results (data not shown). Caspase-7 activation appeared at much earlier time points than EMAP-II production. We concluded that activation of caspase-7 and production of EMAP-II do not overlap and that still EMAP-II is produced when no caspase-7 activity can be detected. This is depicted in a schematic graph in Fig. 1D.

Active caspase-3 and -7 do not cleave proEMAP/p43 in tumour cell lysate

Concerning the involvement of caspase-3 and -7 in proEMAP/p43 cleavage contradictive reports are published in the literature. Active caspase-3 or –7, have not been added to cell lysates. Instead,

recombinant proteins (mouse proEMAP/p43 and caspase-3 or –7) were used in recombinant protein cleavage assays or EMAP-II and caspase-3 and -7 detected in human tumour cell lysates [21,23].

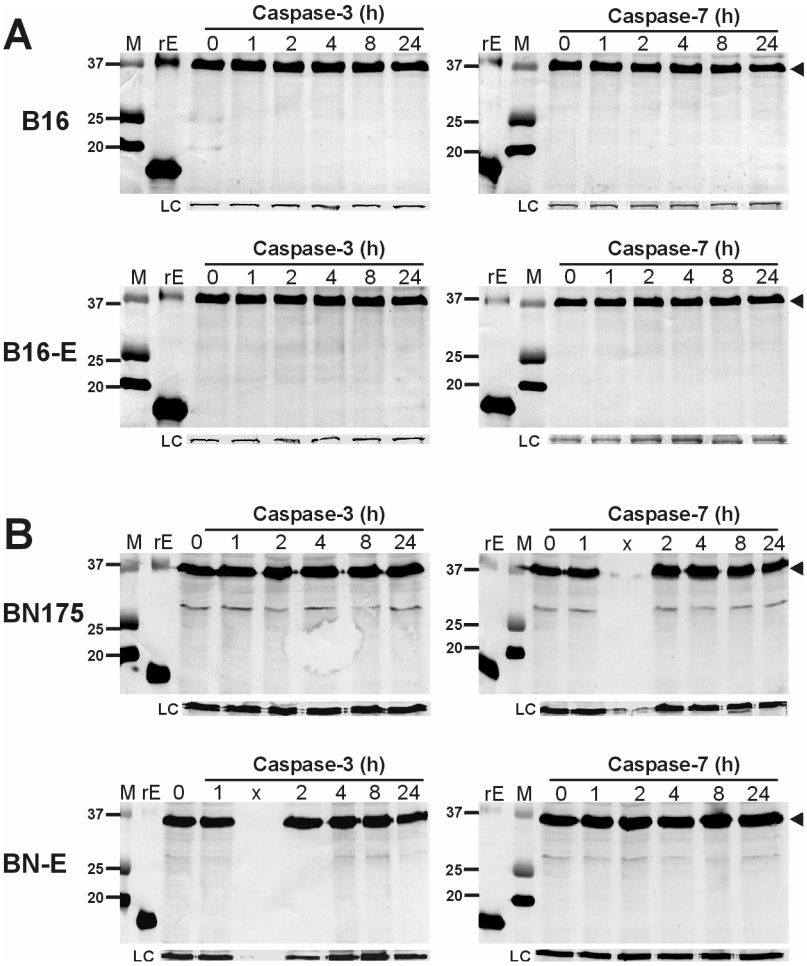

FIGURE 2. ProEMAP/p43 is not cleaved by caspase-3 or -7 in cell lysates.
A. B16 and B16-E cell lysate with recombinant caspase-3 and -7 (100 U/sample) added.
B. BN175 and BN-E cell lysate with recombinant caspase-3 and -7 (100 U/sample) added. ProEMAP/p43 cleavage in cell lysate was evaluated over time by Western blot analysis. Arrowhead points proEMAP/p43. (M) Protein kD marker, (rE) recombinant EMAP-II, 50 ng, (x) Empty lane, (LC) Loading control.

When we incubated cell lysate of B16BL6, B16-E (Fig. 2A) and BN175, BN-E (Fig. 2B) with active recombinant human caspase-3 and -7 in optimal cleavage buffer, we observed no cleavage of proEMAP/p43 over time. Even after 24 h no change was observed in the amount of proEMAP/p43. The activity of recombinant caspases in cell lysates was validated with specific substrates (see Fig.

5A, B). Both caspase-3 and -7 were still active in cell lysates as compared to controls used in the activity assay. We conclude that these data correspond with the caspase-7 kinetics shown in Fig. 1C and that caspase-3 and -7 do not cleave proEMAP/p43 in the cell lines studied.

Inhibition of caspase-3 and -7 does not abolish EMAP-II production by tumour cells

To evaluate the effect of caspase-3 and -7 on production of active EMAP-II we treated B16BL6, B16-E, BN175 and BN-E cells with the optimal trigger for EMAP-II production with or without addition of specific caspase inhibitor.

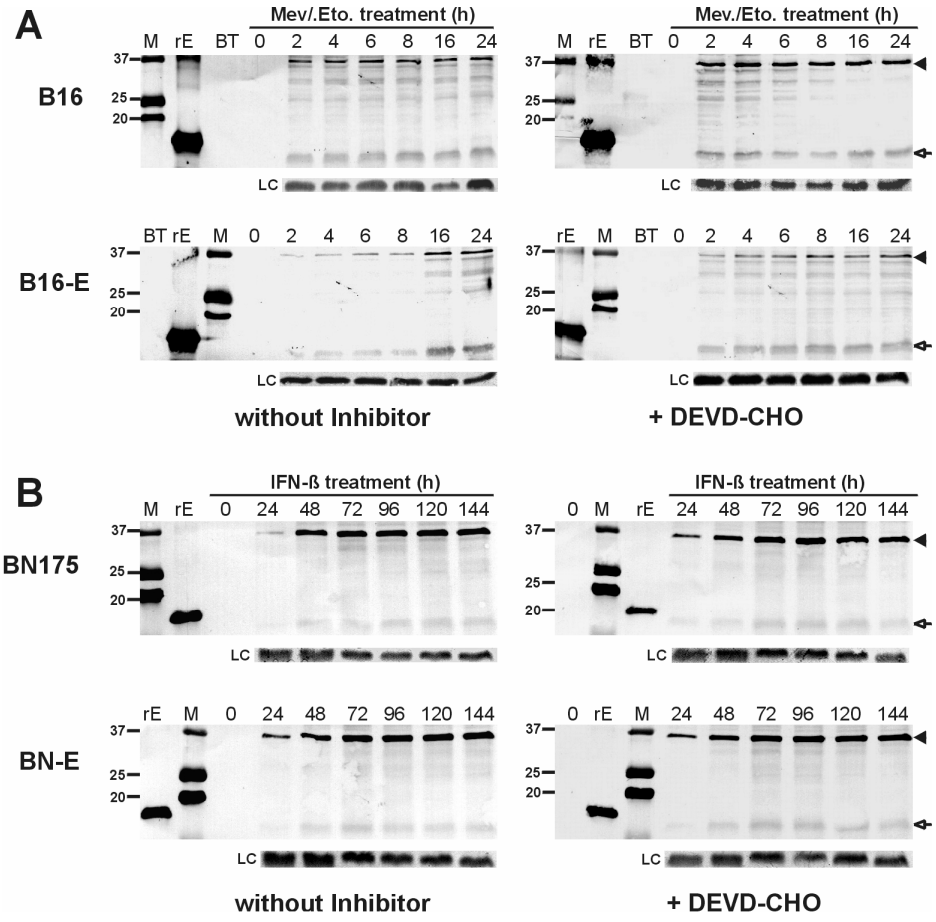

FIGURE 3. Inhibition of caspase-7 does not prevent proEMAP/p43 cleavage by tumour cells.
A. B16 and B16-E cells treated with Mevinolin/Etoposide combination for 0-24 h with (left) and without (right) caspase-3 and -7 inhibitor.

B. BN175 and BN-E cells treated with IFN-β for 0-144h with (left) and without (right) caspase-3 and -7 inhibitor. ProEMAP/p43 cleavage in culture medium was evaluated over time by Western blot analysis. Arrowhead points proEMAP/p43, open arrow points EMAP-II. (M) Protein kD marker, (rE) recombinant EMAP-II, 50 ng, (BT) Before treatment, (LC) Loading control.

Fig. 3A shows the treatment of B16 and B6-E with Mevinolin/Etoposide (40 μg/ml each, 0-24 h) with (right) and without (left) DEVD-CHO. Addition of this specific inhibitor to the cells did not abolish the formation of EMAP-II, although for some time points we observed differences in the amount of EMAP-II. For BN175 and BN-E (triggered with IFN-β, 500 U/ml, 0-144 h) we also observed no effect of the caspase inhibitor DEVD-CHO (Fig. 3B). Activity of DEVD-CHO was confirmed in a caspase-cleavage assay (data not shown). Taken together, we provide several clues that caspase-3 and -7 are not involved in proEMAP/p43 cleavage in tumour cells.

MMP-7, in contrast to MMP-2,-3, and -9, cleaves proEMAP/p43 in tumour cell lysate

Matschurat *et al.,* showed that EMAP-II release is regulated by hypoxia in B16 and Meth A cells [24] and suggested that hypoxia-regulated proteases might be possible candidates for proEMAP/p43 cleavage. Because it is known that MMPs are in part regulated by hypoxia, that they cleave matrix-components as well as a number of other proteins, and that within the proEMAP/p43 sequence some putative MMP-sites are present [29,30], we tested MMPs for their ability to cleave proEMAP/p43.

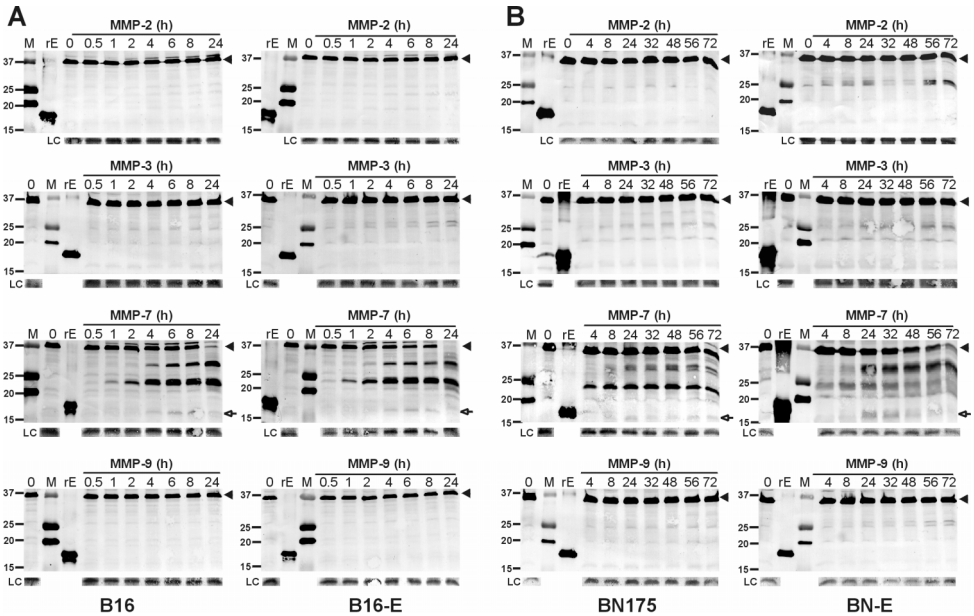

FIGURE 4. MMP-7, in contrast to MMP-2, -3, -9, cleaves proEMAP/p43 in B16 and BN175 cell lysates.
A. B16 and B16-E cell lysate incubated with MMP-2, -3, -7, -9 (0,1 μg/ml) for 0-24 h.
B. BN175 and BN-E cell lysate incubated with MMP-2, -3, -7, -9 (0,1 μg/ml) for 0-72 h. ProEMAP/p43 cleavage in cell lysate was evaluated over time by Western blot analysis. Arrowhead points proEMAP/p43, open arrow points EMAP-II. (M) Protein kD marker, (rE) recombinant EMAP-II, 50 ng, (LC) Loading control.

MMP-2, -3, -7 and –9 were tested in an *in vitro* cleavage assay with lysates of B16BL6 and B16-E (Fig. 4A) and BN175 and BN-E cells (Fig. 4B). In contrast to MMP-2, -3, and -9, MMP-7 appeared capable of cleaving proEMAP/p43 into two major intermediate forms and a cleavage-product of about 17-18 kD, comparable with the apparent size of EMAP-II in our other experiments. For B16BL6 and B16-E the cleavage happened much faster and was optimal at 6-8 h. In contrast, for BN175 and BN-E we found an optimal time point at 32 h. For both cell lines EMAP-II levels were very low and decreased at later time points, indicating that EMAP-II is very unstable. For the other MMPs tested no change in proEMAP/p43 was observed over time. The activity of recombinant MMPs in cell lysates was validated with specific substrates (see Fig. 5A, B). All MMPs were active after 4 h and even after 24 h we detected substantial activities. For MMP-3 (the only activated proMMP) the activity in cell lysate is even higher as compared to the control used in the activity assay. Fig. 4 shows that within tumour cell lysate MMP-7 is capable of cleaving proEMAP/p43 in both mouse melanoma and rat sarcoma cells.

Identification of EMAP-specific peptide in cleavage products

To confirm MMP-7 involvement in EMAP-II generation, we performed mass spectrometry analysis on different bands in MMP-7 treated B16-E cell lysates. Based on Western blot analysis, several bands were cut out of a Coomassie stained gel and analyzed by MALDI-FTMS. (Fig. 5C, D). A zoom-in on the 1534.82 peak of the mass spectra is shown in Fig. 5C. This EMAP-specific peptide (obtained from the GenBank database) was found in the recombinant protein, proEMAP, intermediate and EMAP-II cleavage product bands. For the EMAP-II cleavage product however no significance was found by the software. Other samples ('EMAP-II' band close to cleavage product, negative control (empty lane) and marker protein) did not contain the specific peptide. For BN-E cell lysate treated with MMP-7 the EMAP-peptide was identified in the proEMAP-band (data not shown). Because the proEMAP-band is being processed, intermediate and EMAP-II cleavage product are formed by MMP-7 and these same bands contained EMAP-specific peptide we conclude that proEMAP is cleaved by MMP-7.

Additional evidence for this conclusion is shown in Fig. 5E where recombinant proEMAP was incubated with recombinant MMP-7. After 1 and 2 h incubation both intermediate and EMAP-II cleavage products were observed. Staining for the N-terminal GST-tag confirmed the cleavage of GST-proEMAP and showed the N-terminal fragments as well (Fig. 5E).

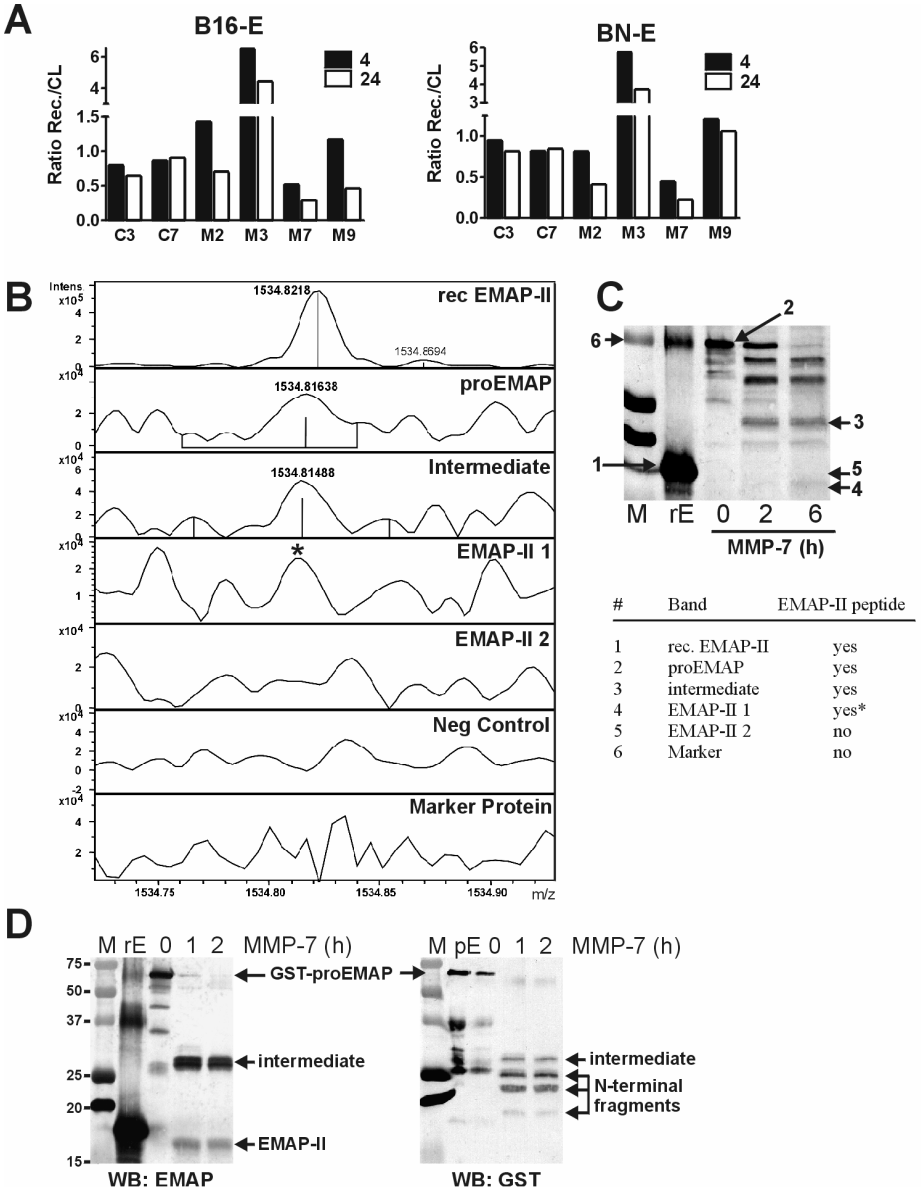

FIGURE 5. ProEMAP/p43 is cleaved by MMP-7

A. Activity measurements of recombinant proteases in tumour cell lysates. B16-E (left) and BN-E (right) cell lysates were incubated with caspase-3, -7 (100, 10 U) or MMP-2, -3, -7, -9 (25 ng) and activity was measured after 4 and 24 h and compared to positive controls (fresh recombinant protease). All proteases used were still active after incubation in cell lysates. In time the activity decreases while for MMP-3 the activity increased. (CL) Cell lysate, (C) Caspase, (M) MMP.
B. MALDI-FTMS analysis of different peptide mixtures derived from protein bands migrating at indicated spots (D). B16-E cell lysate was incubated with MMP-7 and samples were loaded on two gels, one stained with Coomassie and one analyzed by Western blotting. An EMAP-II specific peptide peak (1534.82) was found in recombinant EMAP-II, proEMAP and intermediate product. For EMAP-II cleavage product the peak seemed present but too low to be separated from the background (indicated by the asterisk). A band migrating close to EMAP-II ('EMAP-II 2'), the negative control and a protein from the marker did not contain the peptide.
C. Western blot of the same cleavage reaction as used for mass spectrometry analysis. Six isolated bands are indicated and the table shows where EMAP-II peptide was found. Asterisk means present but not significant. A spot from an empty lane was used as negative control.
D. Recombinant proEMAP/p43 cleavage by MMP-7. Recombinant human proEMAP/p43 with a N-terminal GST-tag was incubated with recombinant human MMP-7 for 1 and 2 h. At both time points EMAP-II and intermediate forms were detected. GST-antibodies showed N-terminal fragments. All proEMAP/p43 was processed by MMP-7 within 2 h.

MMP inhibition interferes with proEMAP/p43 cleavage in tumour cells

To validate the MMP-7 cleavage data we induced B16BL6, B16-E and BN175, BN-E cells to produce EMAP-II with and without addition of a broad range MMP-Inhibitor (inhibits MMP-1, -3, -7, -9). For B16BL6 melanoma cells we observed inhibition of EMAP-II cleavage when MMP-Inhibitor was present, active EMAP-II was absent in medium when inhibitor was added (Fig. 6A). For BN175 and BN-E cells the observed effects were less pronounced indicating that in these cells proEMAP cleavage might be more complex (data not shown). We conclude that inhibition of MMP by a broad range inhibitor prevented B16 melanoma cells from proEMAP/p43 cleavage.

To specifically study the role of MMP-7 in proEMAP/p43 cleavage by tumour cells we performed RNAi inhibition experiments with B16-E tumour cells. Firstly, two designed RNAi duplexes were tested for their ability to inhibit MMP-7 production. Fig. 6B shows the RNAi inhibition of MMP-7 in B16-E cells. MMP-7 RNAi induced a down regulation of MMP-7 protein production, mainly reflected by the decrease of its active form (~18 kD). We continued with the RNAi (number 2) with the highest inhibition. B16-E cells, transfected with RNAi or the scrambled control, were triggered to produce EMAP-II. We observed a decrease in proEMAP/p43 cleavage when MMP-7 was inhibited resulting in lower amounts of EMAP-II and intermediate form in the culture medium (Fig. 6C). From repeated experiments inhibition was quantified and depicted as ratio RNAi/scrambled (Fig. 6D). For proEMAP and the loading control (LC) the expression was comparable while for intermediate and EMAP-II cleavage products a significant inhibition was found.

Kinetics of MMP-7 activity and proEMAP/p43 cleavage

In Figure 1 we showed that the kinetics of caspase-7 activation and proEMAP/p43 cleavage did not correspond. Using a specific MMP-7 activity measurement, we determined the MMP-7 activity during triggering of proEMAP/p43 cleavage. In contrast to caspase-7 we detected MMP-7 activity increasing in time along with EMAP-II production. Time points of proEMAP/p43 cleavage overlapped with those of MMP-7 activation. For both B16-E and BN-E tumour cells we observed MMP-7 activity increasing along with increasing incubation times (Fig. 6E, F).

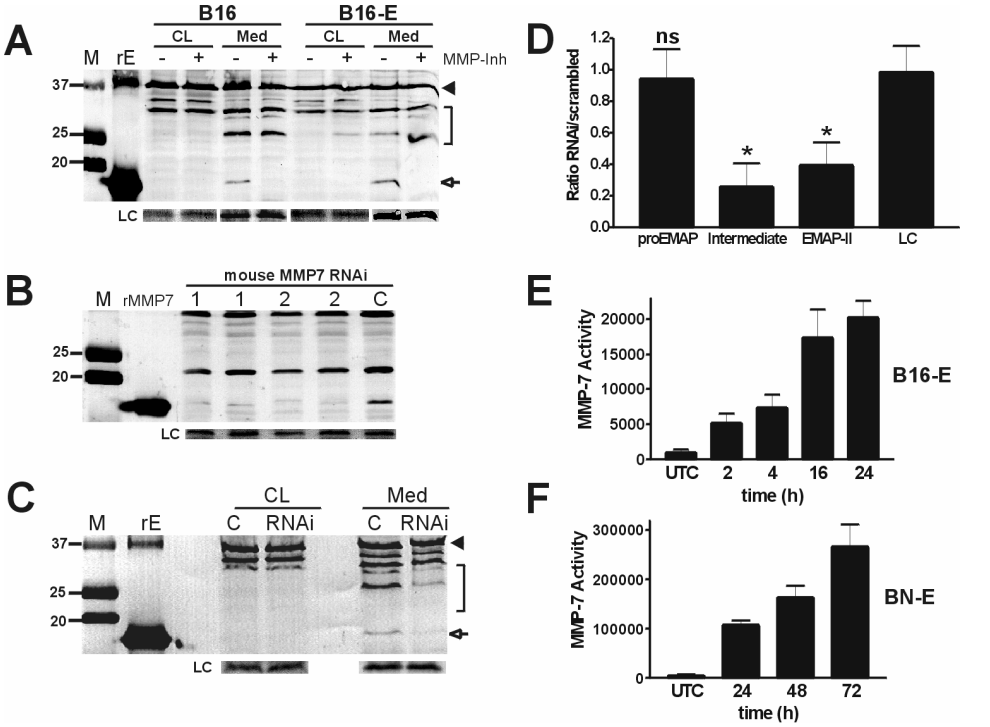

FIGURE 6. Inhibition of MMP prevents B16 tumour cells from release of EMAP-II in the culture medium.
A. B16 and B16-E cells treated with Mevinolin/Etoposide combination for 24 h with and without broad range MMP-inhibitor. Arrowhead points proEMAP/p43, open arrow points EMAP-II, brace indicated intermediate forms. (M) Protein kD marker, (rE) recombinant EMAP-II, 50 ng, (CL) Cell lysate, (Med) culture medium, (LC) Loading control.
B. Western blot analysis of MMP-7 levels in B16-E cells after triple transfection of two different MMP-7 RNAi duplexes (1 and 2, in duplo) or their scrambled control (C). We observed MMP-7 inhibition, mainly represented by its active form. (LC) Loading control.
C. B16-E cells treated with Mevinolin/Etoposide combination for 24 h after RNAi inhibition of MMP-7 compared to the control. When MMP-7 is inhibited, less EMAP-II is secreted in the medium. ProEMAP/p43 and EMAP-II were detected by Western blotting in cell lysate and culture medium. Arrowhead points proEMAP/p43, open arrow points EMAP-II, brace indicated intermediate forms. (M) Protein kD marker, (rE) recombinant EMAP-II, 50 ng, (CL) Cell lysate, (Med) culture medium, (LC) Loading control.
D. Quantification of RNAi experiments. Seven repeated experiments were quantified for expression levels of proEMAP, intermediate form, EMAP-II and the LC. Graph shows ratio RNAi/scrambled control. For intermediate and EMAP-II a significant decrease was found (* $p<0.0001$ and $p=0.0002$ respectively). n.s. not significant as compared to LC.

E. MMP-7 activity during proEMAP/p43 cleavage of B16-E cells triggered with Mevinolin/Etoposide for 0-24 h.
F. MMP-7 activity during proEMAP/p43 cleavage of BN-E cells triggered with IFN-
for 0-72 h. For both cell lines (Fig. E and F) time points of MMP-7 activation and proEMAP/p43 overlap. (UTC) Untreated control. Graph represents mean activity ± SD of three independent experiments.

Noteworthy, the absolute measured activity values for MMP-7 are about 10-fold higher in BN-E tumour cells as compared to B16-E cells. These measurements are in accordance with our other experiments on the involvement of MMP-7 in proEMAP/p43 cleavage and we conclude that MMP-7 is a protease capable of and involved in the cleavage of proEMAP/p43 into EMAP-II in tumour cells.

DISCUSSION

In the presented study we provide evidence that MMP-7 is involved in the cleavage of proEMAP/p43 into EMAP-II by tumour cells. In literature contradictory reports and theories are published concerning the mechanism of proEMAP/p43 cleavage. This accounts especially for capsase-7, which is claimed to be responsible for proEMAP/p43 cleavage but also excluded [21,23]. EMAP-II has been described to have a number of activities such as, cytokine properties, anti-angiogenic, embryonic development, apoptosis, proliferation, adhesion, TNF-sensitivity of tumours, protein translation [3,6,7,11,13,31-33]. Given these many functions and the controversy on proEMAP/p43 cleavage knowledge on this cleavage will be very useful.

We initiated to evaluate the role of caspase-7 in the cleavage of proEMAP/p43 by tumour cells. To induce active EMAP-II production we triggered mouse, rat and human tumour cells with a set of cellular stress inducers. From other reports it is known that different tumour cell types differ in their production of active EMAP-II [12,20]. In line with these reports, we did observe differences between the cell lines (Fig. 1B). In addition, we observed very low amount of active EMAP-II in the culture medium, which is due to the high instability of this polypeptide in conditioned medium. Mature EMAP-II may either be broken down or further processed [18]. Noteworthy is also the small differences we observed in the apparent molecular weight and gel-mobility of EMAP-II between the cell lines. Recently, we published that indeed active EMAP-II differs in gel-mobility when comparing different species [34]. This may imply that besides the differences in optimal treatment for proEMAP/p43 cleavage, also the mechanisms involved are (in part) different within different species.

In our experiments we excluded caspase-7 from cleavage of proEMAP/p43 by tumour cells. We provide multiple clues to justify this conclusion: kinetics of caspase-7 activation does not overlap with proEMAP/p43 cleavage, caspase-7 inhibition does not prevent tumour cells from cleaving proEMAP/p43, and in an *in vitro* assay using cell lysate and recombinant caspase-7 we did not

observe proEMAP/p43 cleavage (Figs. 1-3). These data are in line with Zhang *et al.* but in contrast with Behrensdorf *et al.* [21,23]. We speculate that the discrepancy may result from the assays used. We used for the first time tumour cells in culture for proEMAP/p43 cleavage studies. In addition, we used tumour cell lysate to add recombinant caspases, instead of detecting them in the lysate. We feel that by using tumour cells, we obtained a more physiological setup. Processes and proteins within the cell may therefore be overlooked in previous studies, which only used recombinant protein cleavage assays. Because we present multiple findings based on different types of experiments, which are supported by others, we consider caspase-7 not to be involved in proEMAP/p43 cleavage by tumour cells.

To identify a protease involved in proEMAP/p43 cleavage we focused on MMPs as these proteases are well known for their ability to cleave and activate proteins, besides matrix components, like plasminogen, TNF-α, CD95 and TGF-β [35-38]. We initially chose to test MMP-2, -7 and -9 based on their reported cleavage effects and because we found putative cleavage sites within the proEMAP/p43 sequence. However, these putative sites are very speculative and the consensus sequence for MMP cleavage varies extensively between substrates [30]. We studied MMP-3 as well, which is known to activate MMP-7, as we wanted to exclude a possible cleavage of proEMAP/p43 directly by MMP-3. Using an *in vitro* cleavage assay with cell lysates we found MMP-7 capable of cleaving proEMAP/p43, while MMP-2, -3 and -9 did not cleave proEMAP-p43 (Fig. 4). MMP-7 is an extra cellular MMP mainly produced by carcinoma and stroma cells, known to cleave many proteins and involved in tumour cell invasion [39,40]. Interestingly, with this *in vitro* assay the optimal time point for proEMAP/p43 cleavage differs between B16BL6 melanoma and BN175 sarcoma cells. This is another indication that the exact mechanism of cleavage differs between the cell types studied. Different cell types likely differentially regulate activity of MMPs via other MMPs and inhibitors (like TIMPs). This was confirmed by activity assays which showed that all MMPs (and caspases) were active in tumour cell lysates but for some MMP we observed differences in activity levels (Fig. 5A, B). The fact that there is one product in B16BL6 and probably two products in BN175, appearing as a rather broad band, confirms this cell type dependency. However, the cleaved EMAP-II appears at comparable molecular weights as shown in earlier experiments. To exactly map the cleavage site in these different cell types the cleaved EMAP-II, both from *in vitro* cleavage experiments as well from cell culture experiments, should be isolated and sequenced. Very interesting will be whether there are differences in the biological properties of this tumour cell produced EMAP-II. Isolation and testing of these small amounts of EMAP-II is focus of ongoing research.

To further confirm the involvement of MMP-7 in proEMAP/p43 cleavage we performed mass spectrometry analysis on different cleavage products (Fig. 5C). Mass spectra from different bands, containing multiple proteins, were compared against known EMAP-II peptides. For the bands corresponding to recombinant EMAP-II, proEMAP, intermediate and EMAP-II cleavage product we found the EMAP-II peptide present (Fig. 5D shows the corresponding Western blot of B16-E cell lysate treated with MMP-7). This peptide was absent in negative control, marker protein and a band migrating next to EMAP-II. These data confirm that proEMAP/p43 indeed is cleaved by MMP-7 in B16-E cell lysates. Additional recombinant protein cleavage again confirmed MMP-7 induced proEMAP/p43 cleavage. By using GST-tagged proEMAP/p43 also the N-terminal fragments were shown (Fig. 5E).

To validate our findings in cells we inhibited MMPs during treatment of B16BL6 and BN175 cells to produce EMAP-II. Using a broad range inhibitor the cleavage of proEMAP/p43 was prevented and no EMAP-II appeared in the culture medium of B16BL6 cells (Fig. 6A). For BN175 cells we did not observe this effect (data not shown). These differences again confirm the cell type dependent cleavage mechanisms. In addition, using the broad range MMP inhibitor we observed more intermediate forms, which might indicate a broader involvement of MMPs in this process. Specific inhibition of MMP-7 by RNAi confirmed the involvement of MMP-7 in proEMAP/p43 cleavage (Fig. 6B, C). The cleaved EMAP-II product appeared to run somewhat higher as compared to Fig. 1. This might indicate that MMP-7 influences/activate other proteases (like caspases and other MMPs), which are also involved in (further) proEMAP/p43 cleavage. Whether this is true needs to be addressed in future experiments. Quantification of the MMP-7 RNAi inhibited cleavage revealed that both intermediate and EMAP-II were significantly decreased while proEMAP and the loading controls were comparable. The absence of an effect on proEMAP/p43 might be due to the huge differences in amounts of secreted proEMAP/p43 and EMAP-II. For all cell experiments proEMAP/p43 was more abundantly detected in conditioned medium as compared to EMAP-II. MMP-7 involvement is further emphasized by the kinetics of MMP-7 activation and proEMAP/p43 cleavage.

The proposed role of MMP-7 is summarized in a schematic drawing in Fig. 7. We hypothesize that upon cellular stress proEMAP/p43 protein is ‘secreted’ during apoptotic cell death. Because proEMAP/p43 has no signal peptide, this is likely an undirected process. In the extra cellular space proEMAP/p43 is cleaved by MMP-7. Alternatively proEMAP/p43 cleavage occurs on the membrane during other stress signals like hypoxia. In this case proEMAP/p43 and MMP-7 are docked in a

membrane complex, probably with other unknown proteins. What happens to the multi tRNA synthetase complex (a conformational change or release of some subunits) is unclear.

For some tumour cells membrane expression of EMAP-II is detected and MMP-7 is known to cleave other membrane bound proteins [12,37,41]. Strikingly, in a recent study on protease involvement in proEMAP/p43 cleavage this membrane bound phenotype was also found for fibroblasts [25]. Upon production of EMAP-II, macrophages are recruited to the sites of cell death and membrane bound EMAP-II is involved in lymphocyte apoptosis (Fig. 7).

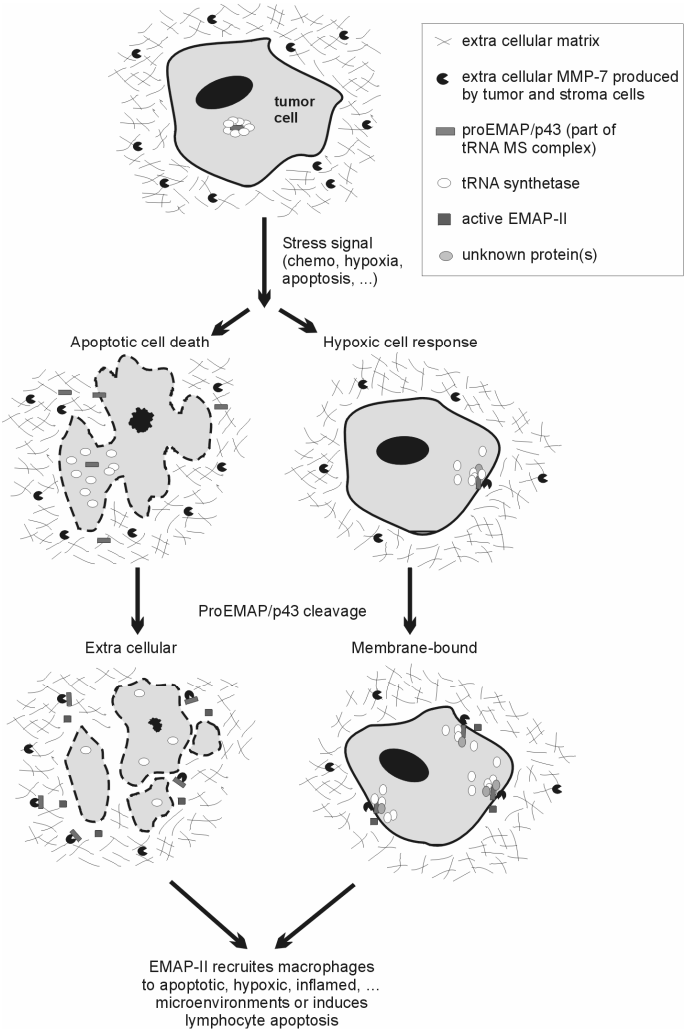

FIGURE 7. Schematic representation of the proposed involvement of MMP-7 in proEMAP/p43 cleavage and EMAP-II production. Within tumour cells proEMAP/p43 is present as part of the tRNA multisynthetase (MS) complex and MMP-7 is

stored extra cellular. Upon cellular stress signals we propose two ways of proEMAP/p43 cleavage. During apoptotic cell death, protein synthesis is inhibited and the tRNA MS complex falls apart, proEMAP/p43 is undirected secreted and becomes available as MMP-7 substrate and EMAP-II is formed. The active EMAP-II recruits macrophages to clear cellular debris after apoptotic cell death. Alternatively, upon other signals the tRNA MS complex is (in part) directed to the cell membrane, after a conformational change and/or binding of other proteins, proEMAP/p43 becomes available for cleavage at the cell membrane. MMP-7 is present in the same complex. The formed membrane-bound EMAP-II can induce lymphocyte apoptosis.

In conclusion we provide several indications that MMP-7, instead of caspase-7, is involved in the cleavage of proEMAP/p43 by tumour cells. These novel findings justify more research on the exact mechanisms of this cleavage and point out implications for the manipulation of EMAP-II activities both in tumours as in other diseases and normal processes.

ACKNOWLEDGEMENTS

The authors would like to thank V. Guns for her valuable contribution to this project and the testing of several MMP activity experiments. We thank Boehringer Ingelheim GmbH for the generous supply of TNF. The presented work was financially supported by grants from Mrace Translational Research Fund from the Erasmus MC and Foundation “Vanderes”.

REFERENCES

1. Kao, J., Ryan, J., Brett, G., Chen, J., Shen, H., Fan, Y. G., Godman, G., Familletti, P. C., Wang, F., Pan, Y. C., and et al. (1992). Endothelial monocyte-activating polypeptide II. A novel tumour-derived polypeptide that activates host-response mechanisms. *J Biol Chem* 267, 20239-47.
2. Murray, J. C., Clauss, M., Denekamp, J., and Stern, D. (1991). Selective induction of endothelial cell tissue factor in the presence of a tumour-derived mediator: a potential mechanism of flavone acetic acid action in tumour vasculature. *Int.J.Cancer* 49, 254-259.
3. Kao, J., Fan, Y. G., Haehnel, I., Brett, J., Greenberg, S., Clauss, M., Kayton, M., Houck, K., Kisiel, W., Seljelid, R., and et al. (1994). A peptide derived from the amino terminus of endothelial-monocyte-activating polypeptide II modulates mononuclear and polymorphonuclear leukocyte functions, defines an apparently novel cellular interaction site, and induces an acute inflammatory response. *J Biol Chem* 269, 9774-9782.
4. Kao, J., Houck, K., Fan, Y., Haehnel, I., Libutti, S. K., Kayton, M. L., Grikscheit, T., Chabot, J., Nowygrod, R., Greenberg, S., and et al. (1994). Characterization of a novel tumour-derived cytokine. Endothelial-monocyte activating polypeptide II. *J Biol Chem* 269, 25106-19.
5. Zhang, F. and Schwarz, M. A. (2000). Temporo-spatial distribution of endothelial-monocyte activating polypeptide II, an anti-angiogenic protein, in the mouse embryo. *Dev Dyn* 218, 490-8.
6. Schwarz, M., Lee, M., Zhang, F., Zhao, J., Jin, Y., Smith, S., Bhuva, J., Stern, D., Warburton, D., and Starnes, V. (1999). EMAP II: a modulator of neovascularization in the developing lung. *Am J Physiol* 276, 365-75.
7. Schwarz, M. A., Kandel, J., Brett, J., Li, J., Hayward, J., Schwarz, R. E., Chappey, O., Wautier, J. L., Chabot, J., Lo Gerfo, P., and Stern, D. (1999). Endothelial-monocyte activating polypeptide II, a novel antitumour cytokine that suppresses primary and metastatic tumour growth and induces apoptosis in growing endothelial cells. *J Exp Med* 190, 341-54.
8. Berger, A. C., Alexander, H. R., Tang, G., Wu, P. S., Hewitt, S. M., Turner, E., Kruger, E., Figg, W. D., Grove, A., Kohn, E., Stern, D., and Libutti, S. K. (2000). Endothelial monocyte activating polypeptide II induces endothelial cell apoptosis and may inhibit tumour angiogenesis. *Microvasc Res* 60, 70-80.
9. Chang, S. Y., Park, S. G., Kim, S., and Kang, C. Y. (2002). Interaction of the C-terminal domain of p43 and the alpha subunit of ATP synthase. Its functional implication in endothelial cell proliferation. *J Biol Chem* 277, 8388-8394.
10. Chang, S. Y., Ko, H. J., Heo, T. H., and Kang, C. Y. (2005). Heparan sulfate regulates the antiangiogenic activity of endothelial monocyte-activating polypeptide-II at acidic pH. *Mol.Pharmacol.* 67, 1534-1543.

11. Schwarz, M. A., Zheng, H., Liu, J., Corbett, S., and Schwarz, R. E. (2005). Endothelial-monocyte activating polypeptide II alters fibronectin based endothelial cell adhesion and matrix assembly via alpha5 beta1 integrin. *Exp.Cell Res.*
12. Murray, J. C., Symonds, P., Ward, W., Huggins, M., Tiga, A., Rice, K., Heng, Y. M., Todd, I., and Robins, R. A. (2004). Colorectal cancer cells induce lymphocyte apoptosis by an endothelial monocyte-activating polypeptide-II-dependent mechanism. *J.Immunol.* 172, 274-281.
13. Murray, J. C., Heng, Y. M., Symonds, P., Rice, K., Ward, W., Huggins, M., Todd, I., and Robins, R. A. (2004). Endothelial monocyte-activating polypeptide-II (EMAP-II): a novel inducer of lymphocyte apoptosis. *J.Leukoc.Biol.* 75, 772-776.
14. Tas, M. P., Houghton, J., Jakobsen, A. M., Tolmachova, T., Carmichael, J., and Murray, J. C. (1997). Cloning and expression of human endothelial-monocyte-activating polypeptide 2 (EMAP-2) and identification of its putative precursor. *Cytokine* 9, 535-9.
15. Shalak, V., Kaminska, M., Mitnacht-Kraus, R., Vandenabeele, P., Clauss, M., and Mirande, M. (2001). The EMAPII cytokine is released from the mammalian multisynthetase complex after cleavage of its p43/proEMAPII component. *J Biol Chem* 276, 23769-23776.
16. Quevillon, S., Agou, F., Robinson, J. C., and Mirande, M. (1997). The p43 component of the mammalian multi-synthetase complex is likely to be the precursor of the endothelial monocyte-activating polypeptide II cytokine. *J Biol Chem* 272, 32573-9.
17. Norcum, M. T. and Warrington, J. A. (2000). The cytokine portion of p43 occupies a central position within the eukaryotic multisynthetase complex. *J Biol Chem* 275, 17921-4.
18. Tas, M. P. and Murray, J. C. (1996). Endothelial-monocyte-activating polypeptide II. *Int J Biochem Cell Biol* 28, 837-41.
19. Knies, U. E., Behrensdorf, H. A., Mitchell, C. A., Deutsch, U., Risau, W., Drexler, H. C., and Clauss, M. (1998). Regulation of endothelial monocyte-activating polypeptide II release by apoptosis. *Proc Natl Acad Sci U S A* 95, 12322-7.
20. Barnett, G., Jakobsen, A. M., Tas, M., Rice, K., Carmichael, J., and Murray, J. C. (2000). Prostate adenocarcinoma cells release the novel proinflammatory polypeptide EMAP-II in response to stress. *Cancer Res* 60, 2850-7.
21. Behrensdorf, H. A., van de Craen, M., Knies, U. E., Vandenabeele, P., and Clauss, M. (2000). The endothelial monocyte-activating polypeptide II (EMAP II) is a substrate for caspase-7. *FEBS Lett* 466, 143-7.
22. Berger, A. C., Tang, G., Alexander, H. R., and Libutti, S. K. (2000). Endothelial monocyte-activating polypeptide II, a tumour-derived cytokine that plays an important role in inflammation, apoptosis, and angiogenesis [In Process Citation]. *J Immunother* 23, 519-27.
23. Zhang, F. R. and Schwarz, M. A. (2002). Pro-EMAP II is not primarily cleaved by caspase-3 and -7. *Am.J.Physiol Lung Cell Mol.Physiol* 282, L1239-L1244.
24. Matschurat, S., Knies, U. E., Person, V., Fink, L., Stoelcker, B., Ebenebe, C., Behrensdorf, H. A., Schaper, J., and Clauss, M. (2003). Regulation of EMAP II by hypoxia. *Am.J.Pathol.* 162, 93-103.
25. Liu, J. and Schwarz, M. A. (2006). Identification of protease-sensitive sites in Human Endothelial-Monocyte Activating Polypeptide II protein. *Exp.Cell Res.* Epub, Apr 3.
26. Gnant, M. F., Berger, A. C., Huang, J., Puhlmann, M., Wu, P. C., Merino, M. J., Bartlett, D. L., Alexander, H. R., Jr., and Libutti, S. K. (1999). Sensitization of tumour necrosis factor alpha-resistant human melanoma by tumour-specific in vivo transfer of the gene encoding endothelial monocyte-activating polypeptide II using recombinant vaccinia virus. *Cancer Res* 59, 4668-74.
27. Nellist, M., Burgers, P. C., van den Ouweland, A. M., Halley, D. J., and Luider, T. M. (2005). Phosphorylation and binding partner analysis of the TSC1-TSC2 complex. *Biochem.Biophys.Res.Commun.* 333, 818-826.
28. Lans, T. E., ten Hagen, T. L., Van Horssen, R., Wu, P. C., van Tiel, S. T., Libutti, S. K., Alexander, H. R., and Eggermont, A. M. (2002). Improved antitumour response to isolated limb perfusion with tumour necrosis factor after upregulation of endothelial monocyte-activating polypeptide II in soft tissue sarcoma. *Ann.Surg.Oncol.* 9, 812-819.
29. Canning, M. T., Postovit, L. M., Clarke, S. H., and Graham, C. H. (2001). Oxygen-mediated regulation of gelatinase and tissue inhibitor of metalloproteinases-1 expression by invasive cells. *Exp.Cell Res.* 267, 88-94.
30. Turk, B. E., Huang, L. L., Piro, E. T., and Cantley, L. C. (2001). Determination of protease cleavage site motifs using mixture-based oriented peptide libraries. *Nat.Biotechnol.* 19, 661-667.
31. Park, S. G., Shin, H., Shin, Y. K., Lee, Y., Choi, E. C., Park, B. J., and Kim, S. (2005). The novel cytokine p43 stimulates dermal fibroblast proliferation and wound repair. *Am.J.Pathol.* 166, 387-398.
32. Kayton, M. L. and Libutti, S. K. (2001). Endothelial monocyte activating polypeptide II (EMAP II) enhances the effect of TNF on tumour-associated vasculature. *Curr Opin Investig Drugs* 2, 136-138.
33. Lee, S. W., Cho, B. H., Park, S. G., and Kim, S. (2004). Aminoacyl-tRNA synthetase complexes: beyond translation. *J.Cell Sci.* 117, 3725-3734.
34. Van Horssen, R., Rens, J. A. P., Brunstein, F., Guns, V., van Gils, M., ten Hagen, T. L. M., and Eggermont, A. M. M. (2006). Intratumoural expression of TNF-R1 and EMAP-II in relation to response of patients treated with TNF-based isolated limb perfusion. *Int J Cancer* Epub 13 Apr.

35. Patterson, B. C. and Sang, Q. A. (1997). Angiostatin-converting enzyme activities of human matrilysin (MMP-7) and gelatinase B/type IV collagenase (MMP-9). *J.Biol.Chem.* 272, 28823-28825.
36. Haro, H., Crawford, H. C., Fingleton, B., Shinomiya, K., Spengler, D. M., and Matrisian, L. M. (2000). Matrix metalloproteinase-7-dependent release of tumour necrosis factor-alpha in a model of herniated disc resorption. *J.Clin.Invest* 105, 143-150.
37. Strand, S., Vollmer, P., van den, A. L., Gottfried, D., Alla, V., Heid, H., Kuball, J., Theobald, M., Galle, P. R., and Strand, D. (2004). Cleavage of CD95 by matrix metalloproteinase-7 induces apoptosis resistance in tumour cells. *Oncogene* 23, 3732-3736.
38. Yu, Q. and Stamenkovic, I. (2000). Cell surface-localized matrix metalloproteinase-9 proteolytically activates TGF-beta and promotes tumour invasion and angiogenesis. *Genes Dev.* 14, 163-176.
39. Wielockx, B., Libert, C., and Wilson, C. (2004). Matrilysin (matrix metalloproteinase-7): a new promising drug target in cancer and inflammation? *Cytokine Growth Factor Rev.* 15, 111-115.
40. Chang, C. and Werb, Z. (2001). The many faces of metalloproteases: cell growth, invasion, angiogenesis and metastasis. *Trends Cell Biol.* 11, S37-S43.
41. Yu, W. H., Woessner, J. F., Jr., McNeish, J. D., and Stamenkovic, I. (2002). CD44 anchors the assembly of matrilysin/MMP-7 with heparin-binding epidermal growth factor precursor and ErbB4 and regulates female reproductive organ remodeling. *Genes Dev.* 16, 307-323.

Chapter 8

EMAP-II facilitates TNF-R1 apoptotic signalling in endothelial cells and induces TRADD mobilization

Remco van Horssen
Joost A. P. Rens
Debby Schipper
Alexander M. M. Eggermont
Timo L. M. ten Hagen

Laboratory of Experimental Surgical Oncology, Department of Surgical Oncology, Erasmus MC – Daniel den Hoed Cancer Center, Rotterdam, The Netherlands

Submitted

Note: This chapter contains figures that are also available in full colour (labeled with 'CLR'). These colour figures can be found in the Appendix of this book (page 209) and in the online version (via Medical Library, Erasmus MC).

ABSTRACT

Endothelial monocyte-activating polypeptide-II (EMAP-II), a proinflammatory cytokine with antiangiogenic properties, renders tumours sensitive to tumour necrosis factor-alpha (TNF) treatment. The exact mechanisms for this effect remain unclear. Here we show that human endothelial cells (EC) are insensitive to TNF-induced apoptosis but after a short pre-treatment with EMAP-II, EC quickly undergo TNF-induced apoptosis. EMAP-II treatment did not increase TNF-R1 protein expression but rather induced TNF-R1 redistribution from Golgi storage pools to cell membranes. In addition, we observed EMAP-II induced mobilization and membrane expression of the TNF-R1-Associated Death Domain (TRADD) protein. Immunofluorescence co-staining experiments revealed that these two effects occurred at the same time in the same cell but TNF-R1 and TRADD were localized in different vesicles. These findings suggest that EMAP-II sensitises EC to apoptosis by facilitating TNF-R1 apoptotic signalling via TRADD mobilization and introduce a molecular and antiangiogenic explanation for the TNF sensitising properties of EMAP-II in tumours.

INTRODUCTION

Endothelial monocyte-activating polypeptide-II (EMAP-II) is a proinflammatory cytokine with antiangiogenic properties and isolated from supernatants of cultured tumour cells [1,2]. EMAP-II is a chemo attractant for monocytes/macrophages and neutrophils, induces von Willebrand Factor, E- and P-selectin and Tissue Factor on endothelial cells (EC) and suppresses tumour growth [3]. For its antiangiogenic activities inhibition of EC proliferation and a role for heparan sulphate and pH have been suggested. EMAP-II was shown to bind alpha5 integrins thereby inhibiting the adhesion of EC to fibronectin matrix [4,5]. In addition, tumour-produced EMAP-II can be immunosuppressive by inducing lymphocyte apoptosis and tumours with an upregulated EMAP-II expression are rendered sensitive to tumour necrosis factor-alpha (TNF) therapy [6,7]. This was confirmed by retroviral transfer of the EMAP-II gene in both subcutaneous mice models and isolated limb perfusions in rats [8,9]. An upregulation of TNF-R1 by EMAP-II in EC *in vitro* has been presented as possible explanation for the EMAP-II induced TNF-sensitivity [10]. However, data on mRNA and protein level were not consistent and in a recent gene array study of EMAP-II-induced genes in EC no TNF-R1 was found leaving the exact underlying mechanisms unclear [11].

TNF exerts pleiotropic effects in immunity, inflammation, cell proliferation, differentiation and apoptosis [12]. TNF acts via two distinct receptors, TNF-R1 and TNF-R2, with TNF-R1 being member of the death receptor family containing a Death Domain (DD) [13]. Upon TNF binding TNF-R1

signalling can lead to survival and apoptotic pathways both initiated by the recruitment of TNF-R1-Associated Death Domain (TRADD) [14]. Subsequently, TNFR-Associated Factor 2 (TRAF-2) and Receptor Interacting Protein 1 (RIP-1) bind and are involved in the survival signalling while Fas-Associated Death Domain (FADD) and caspase-8 mediate apoptotic signalling [15].

Recent data showed how these signalling complexes act mechanistically. Survival pathways are activated by the formation of complex I, including TNF-R1, TRADD, TRAF-2 and RIP-1. During apoptotic signalling complex II or Death Inducing Signalling Complex (DISC) is formed, which includes TRADD, FADD and RIP-1 and is able to bind caspase-8 [16]. Besides formation of distinct complexes, also regulation by intracellular compartmentalization of so-called TNF-receptosomes has been reported [17]. These data show that TNF-R1 signalling is very complex and besides the proteins themselves, also the way in which they are involved is being unravelled. Although exact mechanisms remain unresolved, FADD/caspase-8, in contrast to TRADD, is not recruited to the membrane [18].

In this report we investigated the effects of EMAP-II on early TNF-R1 signalling in EC. We found that EC are insensitive to short TNF treatment, but when pre-treated with EMAP-II EC became very responsive to TNF-induced apoptosis. Our data confirm that EMAP-II does not change the TNF-R1 protein expression but rather induces TNF-R1 redistribution from Golgi storage pools to the cell membrane. In addition, we observed an EMAP-II-induced membrane expression of TRADD, which was confirmed by immunofluorescence showing small fractions of mobilized TRADD. Finally, we observed that although these two effects occurred at the same time in the same cell, TNF-R1 and TRADD were localized in different vesicles.

MATERIALS AND METHODS

Cell culture and reagents

Human Umbilical Vein Endothelial Cells (HUVEC) were used between passage 3 and 7 and maintained in Human Endothelial-SFM Medium supplemented with 10% New Born Calf Serum, 5% Human Serum (Invitrogen), 20 ng/ml bFGF and 100 ng/ml EGF (PeproTech), in gelatin-coated flasks. Cells were cultured at 37 ^{o}C, 5% CO_2 in a humidified incubator. Human recombinant TNF and EMAP-II were kindly provided by Boehringer-Ingelheim, GmbH.

Apoptosis Assay

HUVEC were treated for 1 h with TNF with and without 1 h pre-treatment of EMAP-II at various concentrations. After 2 h treatment the medium was replaced by medium containing 0,5 μM of the apoptotic death cell marker Yo-Pro-1 iodide (491/509) (Molecular Probes) and cells were incubated 20 minutes at 37 °C in the dark. Bright field and immunofluorescent images were taken using an Axiovert 100 M microscope using a 10X/0.30 PLAN-NEOFLUAR objective lens and AxioCam HRC digital camera using AxioVision software (Carl Zeiss).

Immunoprecipitation and Western Blotting

HUVEC were grown till confluence, treated with EMAP-II (concentration range, 1h), washed twice with ice-cold PBS and lysed in ice-cold Lysis Buffer (50 mM Tris-HCl (pH 7,4), 150 mM NaCl, 1 mM EDTA, 1% NP-40, protein inhibitor cocktail) for 30 min on ice. Lysates were cleared from cellular debris by centrifugation for 10 min at 0 °C, 12000g. In the meantime Protein A Sepharose Beads were washed twice with Lysis Buffer. Protein concentration was determined with Coomassie Plus Reagent (Pierce) in samples of conditioned medium, cell lysate and cell lysate of membrane biotinylated cells and samples were normalized by protein content. Samples were pre-cleared with 20 μl Protein A Sepharose Beads for 1 h at 4 °C and incubated with 10 μl of polyclonal goat-anti human TNF-R1 antibody (R&D Systems) for 4 h at 4 °C using an upright rotator. The Sepharose Beads were washed twice in Lysis Buffer and twice in Lysis Buffer lacking NP-40. Precipitates were resuspended in Laemmli Sample Buffer, electrophoresed by SDS-PAGE on 10% gels and transferred onto polyvinylidene difluoride membranes (BioRad). Membranes were blocked for at least 1 h at room temperature with 5% nonfat dried milk in PBS/0,05% Tween-20 and incubated with mouse anti-TNF-R1 antibody (0,2 μg/ml, R&D Systems), mouse anti-TRADD antibody (0,5 μg/ml, Pharmingen) or mouse anti-FADD antibody (0,5 μg/ml, Pharmingen) overnight at 4 °C. After washing with PBS/0,05% Tween-20 and incubation with biotinylated goat anti-mouse IgG for 1 h at room temperature, proteins were made visible by amplified alkaline phosphatase (BioRad). Membranes were incubated with alkaline phosphatase-streptavidin complex for 1 h at room temperature, washed and stained with NBT-BCIP substrate (Roche) until staining was optimal. The substrate reaction was stopped by washing several times with AD, membranes were dried and scanned for analysis.

Membrane Biotinylation

To detect membrane-bound TNF-R1, EMAP-II treated HUVEC were washed twice with ice-cold PBS. Before lysis, cells were incubated with S-NHS-biotin (0,5 mg/ml, Sigma-Aldrich) dissolved in ice-cold PBS for 1 h at 4 ^{o}C. For detection of membrane-bound TNF-R1, TNF-R1 precipitates of cell lysates of membrane biotinylated cells were blotted and stained directly with alkaline phosphatase-streptavidin. For detection of membrane-bound TRADD and FADD, membranes of membrane biotinylated cells were isolated by precipitation with streptavidin labeled Sepharose beads (Amersham) and anti-TRADD or FADD incubated immunoblots were incubated with alkaline-phosphatase labeled secondary antibodies.

Immunofluorescence Staining

After treatment, HUVEC were washed twice with PBS, fixed in 4% formalin at room temperature for 10 min, washed and permeabilized using 0,15% Triton-X-100 for 2 min. After blocking for 45 min in blocking solution (1% BSA / 0,05% Tween-20 / PBS) fixed cells were incubated with first (1/200) and secondary (1/500) antibody-mixtures for 2 h at room temperature in blocking solution. In between incubations cells were washed 3 times with PBS / 0,05% Tween-20. Thereafter cells were briefly washed in 70% and 100% ethanol respectively, air dried and mounted onto microscope slides using 10 μl of a 1:1 solution of VectaShield (Vector Laboratories) and DAPI-DABCO (Molecular Probes). Primary antibodies used: mouse anti-human TRADD (BD Transduction Laboratories), rabbit anti-human TNF-R1 (PeproTech), sheep anti-human TGN46 (Serotec). Alexa Fluor 594 and Alexa Fluor 488 (Molecular Probes) labelled secondary antibodies were used. Immunofluorescent images were taken using an Axiovert 100 M microscope with 40X/1.30 Oil-FLUAR or 63X/1.4 Oil Plan-APOCHROMAT objective lens (Carl Zeiss) and an ORCA II ER camera (C4742-98, Hamamatsu Photonics Systems).

RESULTS

The observed anti-tumour activities of TNF when administered via an isolated limb perfusion (ILP) have been ascribed to be vasculature-mediated. When used in combination with chemotherapeutic drugs, TNF affects the EC and the drug kills the tumour cells [19,20]. However, EC *in vitro* appeared insensitive to (short) high dose TNF treatment. When we treated EC for 1 h with low (10 ng/ml) and high (10 μg/ml) dose TNF we did not observe any effects. Both morphology and apoptosis data

showed no difference (Fig. 1A). In contrast, when we pre-treated EC for 1 h with EMAP-II (10 μg/ml) and afterwards with TNF, at high dose TNF all EC underwent apoptosis within 1 h (Fig. 1B).

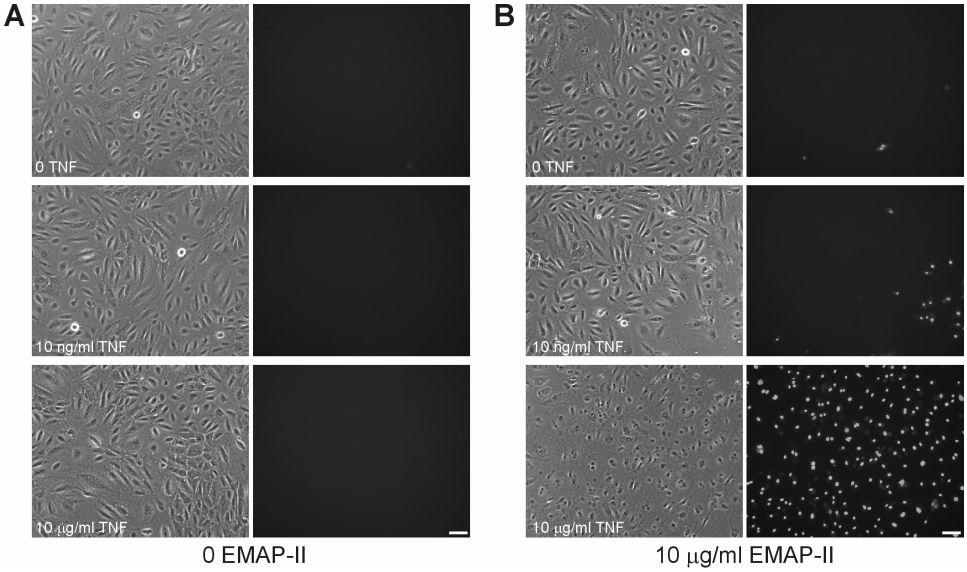

FIGURE 1. EMAP-II sensitises HUVEC towards TNF-induced apoptosis **(CLR)**.
A. HUVEC were treated with 0, 10 ng/ml or 10 μg/ml TNF for 1 h after 1 h pre-treatment with standard culture medium (control). Pictures were taken to show monolayer morphology (left) and apoptotic cells (right). No TNF effect was observed. Bar, 100 μm.
B. HUVEC were treated with 0, 10 ng/ml or 10 μg/ml TNF for 1 h after a 1 h pre-treatment with 10 μg/ml EMAP-II. High dose TNF induced massive apoptotic cell death after EMAP-II pre-treatment. At low dose some EC undergo apoptosis. Bar, 100 μm.

After 1 h pre-treatment with EMAP-II the cells still look healthy, as can be seen in the 0 TNF controls. This apoptosis sensitising effect was very fast and complete.

To further study this EMAP-II sensitising effect we determined TNF-R1 protein expression in EC upon EMAP-II treatment (1 h, concentration course) and did not observe an increase. However, when we isolated cell membranes from EMAP-II treated EC, we did observe a concentration dependent upregulation of membrane-bound TNF-R1 (Fig. 2A).

This redistribution, rather than upregulation, might be an explanation for the observed TNF-sensitising properties of EMAP-II and also explains the apparently contradictive reports in literature. To confirm the observed TNF-R1 redistribution we stained EC for TGN (trans-Golgi network) and TNF-R1. In untreated controls TNF-R1 is mainly located in the Golgi storage pool. Almost all Golgi and TNF-R1 overlapped as shown in the merged image (Fig. 2B).

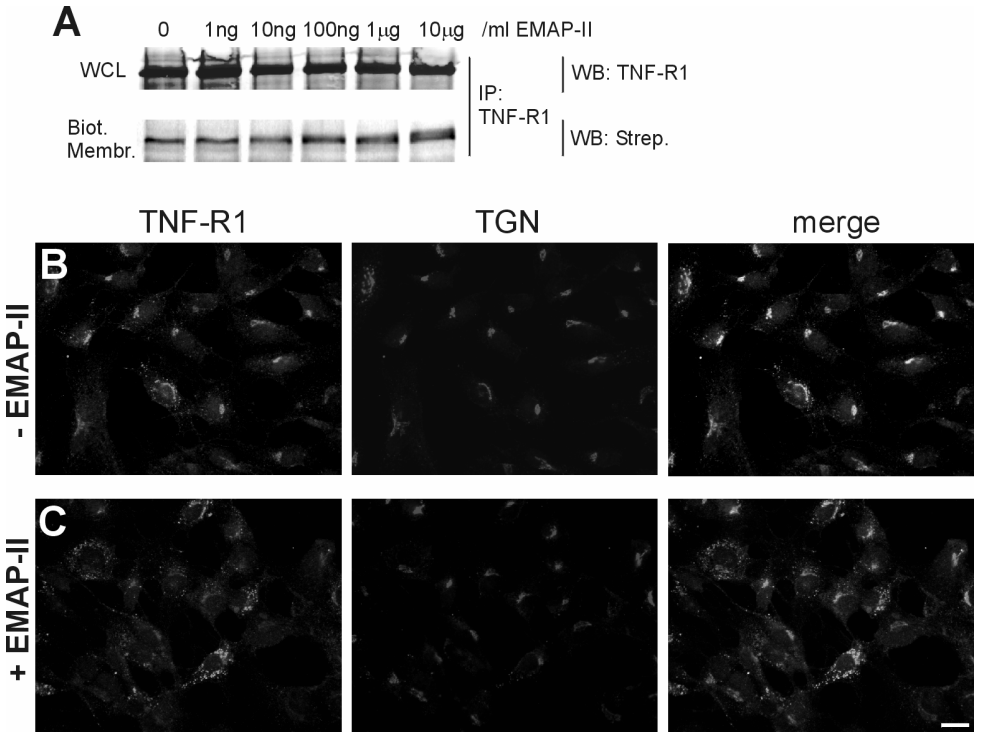

FIGURE 2. EMAP-II induces TNF-R1 redistribution in HUVEC **(CLR)**.
A. Immunoprecipitation and western blot analysis of TNF-R1 in whole cell lysate (WCL) and cell membranes upon 1 h EMAP-II treatment. Total TNF-R1 expression was not altered, while the membrane-bound TNF-R1 fraction was increased at increasing EMAP-II concentrations.
B. Immunofluorescent staining for TNF-R1 and TGN (trans-Golgi network) of non-treated HUVEC. TNF-R1 expression is mainly Golgi-associated (merged image).
C. Immunofluorescent staining for TNF-R1 and TGN after 1 h EMAP-II (10 g/ml) treatment. The Golgi-associated TNF-R1 expression was clearly decreased. The overlapping yellow staining is almost completely absent indicating TNF-R1 redistribution out of Golgi storage pools. Bar, 20 μm.

Upon 1 h EMAP-II treatment we observed that fractions of TNF-R1 were redistributed out of the Golgi, probably towards the cell membrane. The Golgi-associated TNF-R1 staining was decreased in treated EC (Fig. 2C). The Golgi were stained red in the merged image indicating loss of TNF-R1 (green) signal. We conclude that within 1 h EMAP-II induced a redistribution of TNF-R1 out of the Golgi storage pools and subsequently enhanced the membrane-expression of TNF-R1 in EC.

TRADD is one of the major mediators of TNF-R1 signal transduction so we tested whether EMAP-II also might affect TRADD expression and cellular distribution. We treated EC with low (10 ng/ml) and high (10 μg/ml) dose EMAP-II for 1 h and determined TRADD and FADD protein expression in the cell lysate and membrane fractions.

For TRADD, in contrast to FADD in the same sample, we observed membrane expression of a small fraction of the protein; while in the cell lysate no differences for TRADD were seen (Fig. 3A).

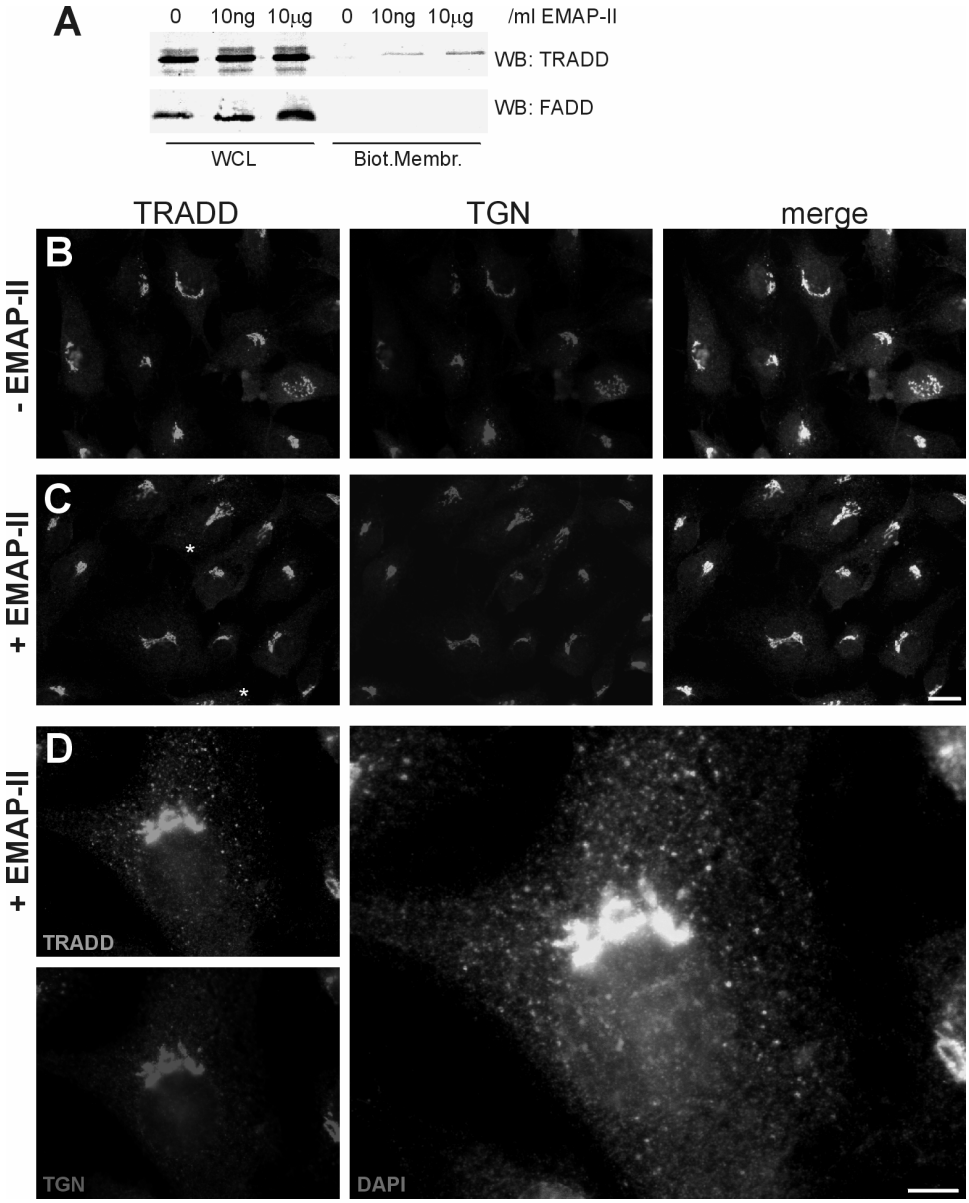

FIGURE 3. EMAP-II induces mobilization and membrane-expression of TRADD in HUVEC **(CLR)**.
A. Western blot analysis of TRADD and FADD in whole cell lysate (WCL) and cell membranes in HUVEC treated with 0, 10 ng/ml, 10 μg/ml EMAP-II for 1 h. EMAP-II induced small amounts of TRADD membrane-expression. FADD expression was upregulated in the cell lysate.

B. Immunofluorescent staining for TRADD and TGN (trans-Golgi network) of non-treated HUVEC. TRADD expression is almost exclusively within the Golgi apparatus.
C. Immunofluorescent staining for TRADD and TGN after 1 h EMAP-II (10 μg/ml) treatment. TRADD expression appeared mainly Golgi-associated as shown by the yellow overlap in the merged image. In addition some TRADD-containing vesicles were observed (asterisks). Bar, 20 μm.
D. High magnification image of a treated EC showing TRADD mobilization in small vesicles, staining positive for TRADD (green) and negative for TGN (red). Bar, 5 μm.

For FADD, we observed a small increase in the cell lysate upon EMAP-II treatment. Using immunofluorescence for TRADD and TGN, we observed a strong Golgi-associated expression of TRADD in both the untreated (Fig. 3B) and treated (Fig. 3C) EC. The clear decline of co-staining (as found for TGN and TNF-R1, see Fig. 2) was not observed. However, when we made images at high magnification, a subset of treated EC showed small vesicles staining positive for TRADD, and negative for TGN. This phenomenon was not observed in the untreated EC. Fig. 3D shows an example of a treated EC, co-stained for TRADD and TGN that mobilized small fractions of TRADD (green) via small vesicles into the cell periphery

To search for a possible connection between the two observed EMAP-II effects in EC we set up a co-staining of TNF-R1 and TRADD. In untreated EC TNF-R1 mainly was expressed in the Golgi apparatus and sporadically some high TNF-R1 expressing cells were found. For TRADD the localization was in the Golgi and overlap in the merged image revealed localization of these two proteins at the same compartment within the cells (Fig. 4A). Upon EMAP-II treatment, the Golgi-expression of TNF-R1 was clearly declined and more high TNF-R1 expressing cells were observed. For TRADD its location was still mainly in the Golgi but some TRADD-containing vesicles were also seen (Fig. 4B, arrows). Strikingly, in the merged image the overlap between TNF-R1 and TRADD was gone for the Golgi storage pools, only Golgi-associated TRADD (red) was observed. Moreover, we observed that EMAP-II treated cells, showing TNF-R1 redistribution, also stained positive for TRADD-containing vesicles (arrowheads in Fig. 4C).

These TRADD-containing vesicles were clearly other vesicles than the TNF-R1-containing vesicles. We did not observe co-staining for any vesicle and the size of the vesicles is also very different. For non-treated EC that sometimes showed TNF-R1 redistribution, no positive stain for TRADD-containing vesicles was observed (asterisk, Fig. 4A). From these observations we conclude that there are two possible explanations for the sensitising properties of EMAP-II: it induces TNF-R1 redistribution and TRADD mobilization. These two effects occur at the same time in the same cell.

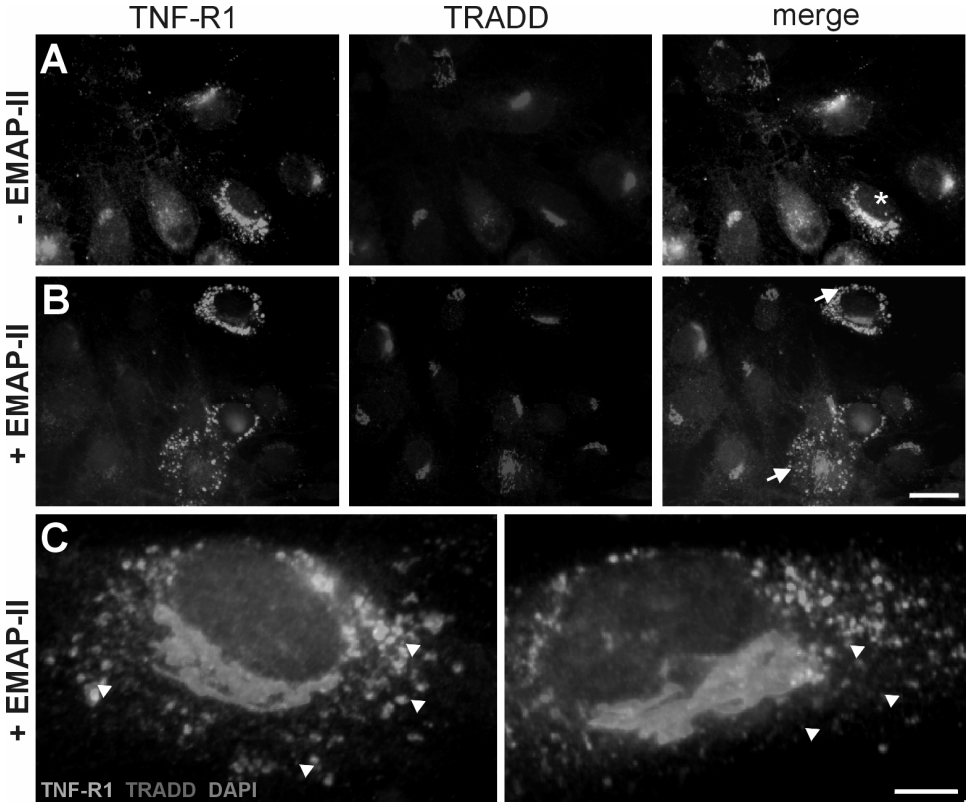

FIGURE 4. TNF-R1 and TRADD are transported in different vesicles within the same cell **(CLR)**.
A. Immunofluorescent staining for TNF-R1 and TRADD of non-treated HUVEC. Both proteins were mainly expressed in the Golgi. Also in sporadically observed EC with TNF-R1 redistribution, the Golgi showed co-staining and no TRADD-positive vesicles were seen (asterisk).
B. Immunofluorescent staining for TRADD and TGN after 1 h EMAP-II (10 μg/ml) treatment. TNF-R1 expression in the Golgi is decreased while TRADD expression was still Golgi-associated. Merged images did not show co-localization (yellow) in Golgi anymore. Cells with TNF-R1 redistribution stained positive for TRADD-containing vesicles as well (arrows), Bar, 20 μm.
C. High magnification images of two EMAP-II treated EC showing TNF-R1 redistribution and TRADD mobilization. The small amounts of mobilized TRADD (red, arrow-heads) located in different vesicles as compared to the abundantly present TNF-R1 (green). Bar, 5 μm.

DISCUSSION

In this report we describe an explanation for the TNF-sensitising properties of EMAP-II. The use of TNF in the clinic is restricted to isolated perfusion settings due to severe systemic toxicity when administered systemically [19]. Therefore studies aimed to understand and improve TNF therapy are very useful. EMAP-II is shown to determine TNF sensitivity of tumours *in vivo*, both in systemic and isolated treatment modalities [7-9]. Supportive mechanistic data however are limited and not confirmative. An upregulation of TNF-R1 on mRNA level in EC has been reported [10] but in a gene array study no TNF-R1 was picked up [11]. In a recent study using patient biopsies we also observed

no correlation between TNF-R1 protein levels and response to TNF treatment [21]. Recently, more detailed knowledge has become available on TNF-R1 signalling. For the regulation of this signalling, compartmentalization and formation of specific complexes is crucial [16,17]. We set up experiments to evaluate the effects of EMAP-II on TNF-R1 and TRADD localization and distribution in EC.

EMAP-II is shown to induce EC apoptosis of growing EC under subconfluent conditions in a long-term (12-48 h) treatment [3,22]. When we treated confluent EC with EMAP-II for 1 h we did not observe apoptosis or virtual morphological changes. However, this 1 h treatment was sufficient to render EC sensitive to TNF-induced apoptosis. This sensitising effect was very fast and absolute (Fig. 1B). In patients, TNF-induced tumour necrosis seemed at least partially mediated by anti-vascular effects and in mice the involvement of TNF-R1 expressing EC of the tumour vasculature has been suggested [23]. We speculate that local upregulation of EMAP-II in the tumour microenvironment may enhance the sensitivity of tumour vessels to TNF.

Interestingly, when we evaluated the TNF-R1 protein expression of EMAP-II treated EC we did not observe an upregulation. In contrast, TNF-R1 was redistributed out of Golgi storage pools towards the cell membrane (Fig. 2). This finding might explain the contradictive reports in literature and also illustrates that TNF-sensitising properties of EMAP-II do involve TNF-R1 protein redistribution. For some cells we did not observe TNF-R1 expression neither in the Golgi nor in other cellular compartments. Because TNF-R1 signalling is a very dynamic process (within minutes) only a small fraction will be present on the cell membrane and many receptors are shedded to regulate TNF activities.

The priming effect of EMAP-II on EC also involved TRADD mobilization. TRADD is know to be recruited to the membrane upon TNF-binding to TNF-R1 [14]. Recently, for PAK4 a facilitating effect on TRADD-TNF-R1 binding properties was reported [24]. To our knowledge EMAP-II is the first reported cytokine to exhibit comparable activities, while the TNF-R1 signalling outcome is the opposite.

Although not excluded we do not expect a direct binding of EMAP-II to TNF-R1. Sequence and domain analysis only located a tRNA binding domain within the EMAP-II protein. Exact underlying mechanisms for this EMAP-II effect remain unclear. Small fractions of mobilized TRADD become membrane-bound and based on its properties, this fraction is likely bound to TNF-R1. In co-immunoprecipitation experiments we did not detect TNF-R1 bound TRADD, probably due to the very low amounts that will be TNF-R1 bound as compared to TNF-treated cells. Nevertheless the two observed EMAP-II effects on early TNF-R1 signalling suggests a ‘priming-effect’ of the EC by EMAP-

II for TNF-induced apoptosis. In addition, when we co-stained for TRADD and TNF-R1 the two effects seemed to take place at the same time in the same cell. In non-treated cells, we sporadically observed TNF-R1 redistribution but no effect on TRADD was seen. For EMAP-II treated EC we observed that virtually all cells with TNF-R1 redistribution also showed a TRADD mobilization (Fig. 4). The EMAP-II induced TNF-R1 redistribution may induce TRADD mobilizing or vice versa. The sum of these effects might be an explanation for the sensitising properties of EMAP-II for inducing EC apoptosis as we showed in Fig. 1.

Evidently more detailed research needs to be conducted to elucidate the exact molecular regulation of the EMAP-II effects on TNF-R1 apoptotic signalling induced by TNF. For example, what happens to the distribution of TNF-R1 and TRADD upon TNF-treatment? Will there be an effect on the survival signalling of TNF? Are there EMAP-II interacting proteins? And how are these involved in the EMAP-II activities towards EC? These and other questions are open avenues of future research. In conclusion, we provide data that EMAP-II is capable to affect TNF-R1 apoptotic signalling in EC and suggest a molecular and antiangiogenic mechanism for the TNF sensitising properties of EMAP-II. A more detailed knowledge of the EMAP-II-TNF axis may result in a more directed and widespread utility of TNF in the treatment of cancer patients.

CONCLUSION

TNF-R1 induced apoptosis is a very complex process and for EC little is known about the regulation. When TNF is used to treat solid tumours its activities are vasculature mediated.[19] In contrast, EC *in vitro* are insensitive to TNF. EMAP-II is known to be able to enhance TNF-induced tumour regression in mouse models.[7,8] Mechanistic data for this effect, however, are very contradictive.

The data presented in this study suggest that indeed the underlying mechanisms might be more complex than anticipated earlier. We also observed no effect of EMAP-II on TNF-R1 protein levels. In contrast, TNF-R1 membrane localisation on EC was induced by EMAP-II treatment. In addition, TRADD was mobilized out of the Golgi. These data show that prior to addition of TNF, its apoptotic signalling can be manipulated by EMAP-II. Both TNF-R1 and TRADD are mobilized within the same cell. This very quick mobilisation was observed before addition of TNF. Pre-treatment of EC with EMAP-II thereby facilitates TNF-induced EC apoptosis.

ACKNOWLEDGEMENTS

The authors would like to thank Boehringer Ingelheim GmbH for the generous supply of TNF and EMAP-II. The presented work was financially supported by grant from Mrace Translational Research Fund from the Erasmus MC.

REFERENCES

1. Murray, J. C., Clauss, M., Denekamp, J., and Stern, D. (1991). Selective induction of endothelial cell tissue factor in the presence of a tumour-derived mediator: a potential mechanism of flavone acetic acid action in tumour vasculature. *Int.J.Cancer* 49, 254-259.
2. Kao, J., Ryan, J., Brett, G., Chen, J., Shen, H., Fan, Y. G., Godman, G., Familletti, P. C., Wang, F., Pan, Y. C., and et al. (1992). Endothelial monocyte-activating polypeptide II. A novel tumour-derived polypeptide that activates host-response mechanisms. *J Biol Chem* 267, 20239-47.
3. Schwarz, M. A., Kandel, J., Brett, J., Li, J., Hayward, J., Schwarz, R. E., Chappey, O., Wautier, J. L., Chabot, J., Lo Gerfo, P., and Stern, D. (1999). Endothelial-monocyte activating polypeptide II, a novel antitumour cytokine that suppresses primary and metastatic tumour growth and induces apoptosis in growing endothelial cells. *J Exp Med* 190, 341-54.
4. Chang, S. Y., Ko, H. J., Heo, T. H., and Kang, C. Y. (2005). Heparan sulfate regulates the antiangiogenic activity of endothelial monocyte-activating polypeptide-II at acidic pH. *Mol.Pharmacol.* 67, 1534-1543.
5. Schwarz, M. A., Zheng, H., Liu, J., Corbett, S., and Schwarz, R. E. (2005). Endothelial-monocyte activating polypeptide II alters fibronectin based endothelial cell adhesion and matrix assembly via alpha5 beta1 integrin. *Exp.Cell Res.*
6. Murray, J. C., Symonds, P., Ward, W., Huggins, M., Tiga, A., Rice, K., Heng, Y. M., Todd, I., and Robins, R. A. (2004). Colorectal cancer cells induce lymphocyte apoptosis by an endothelial monocyte-activating polypeptide-II-dependent mechanism. *J.Immunol.* 172, 274-281.
7. Wu, P. C., Alexander, H. R., Huang, J., Hwu, P., Gnant, M., Berger, A. C., Turner, E., Wilson, O., and Libutti, S. K. (1999). In vivo sensitivity of human melanoma to tumour necrosis factor (TNF)-alpha is determined by tumour production of the novel cytokine endothelial-monocyte activating polypeptide II (EMAPII). *Cancer Res* 59, 205-12.
8. Gnant, M. F., Berger, A. C., Huang, J., Puhlmann, M., Wu, P. C., Merino, M. J., Bartlett, D. L., Alexander, H. R., Jr., and Libutti, S. K. (1999). Sensitization of tumour necrosis factor alpha-resistant human melanoma by tumour-specific in vivo transfer of the gene encoding endothelial monocyte-activating polypeptide II using recombinant vaccinia virus. *Cancer Res* 59, 4668-74.
9. Lans, T. E., ten Hagen, T. L., Van Horssen, R., Wu, P. C., van Tiel, S. T., Libutti, S. K., Alexander, H. R., and Eggermont, A. M. (2002). Improved antitumour response to isolated limb perfusion with tumour necrosis factor after upregulation of endothelial monocyte-activating polypeptide II in soft tissue sarcoma. *Ann.Surg.Oncol.* 9, 812-819.
10. Berger, A. C., Alexander, H. R., Wu, P. C., Tang, G., Gnant, M. F., Mixon, A., Turner, E. S., and Libutti, S. K. (2000). Tumour necrosis factor receptor I (p55) is upregulated on endothelial cells by exposure to the tumour-derived cytokine endothelial monocyte- activating polypeptide II (EMAP-II). *Cytokine* 12, 992-1000.
11. Tandle, A. T., Mazzanti, C., Alexander, H. R., Roberts, D. D., and Libutti, S. K. (2005). Endothelial monocyte activating polypeptide-II induced gene expression changes in endothelial cells. *Cytokine* 30, 347-358.
12. Ashkenazi, A. and Dixit, V. M. (1998). Death receptors: signaling and modulation. *Science.* 281, 1305-1308.
13. Tartaglia, L. A. and Goeddel, D. V. (1992). Two TNF receptors. *Immunol Today* 13, 151-153.
14. Jones, S. J., Ledgerwood, E. C., Prins, J. B., Galbraith, J., Johnson, D. R., Pober, J. S., and Bradley, J. R. (1999). TNF recruits TRADD to the plasma membrane but not the trans-Golgi network, the principal subcellular location of TNF-R1. *J.Immunol.* 162, 1042-1048.
15. Baud, V. and Karin, M. (2001). Signal transduction by tumour necrosis factor and its relatives. *Trends Cell Biol.* 11, 372-377.
16. Micheau, O. and Tschopp, J. (2003). Induction of TNF receptor I-mediated apoptosis via two sequential signaling complexes. *Cell* 114, 181-190.
17. Schneider-Brachert, W., Tchikov, V., Neumeyer, J., Jakob, M., Winoto-Morbach, S., Held-Feindt, J., Heinrich, M., Merkel, O., Ehrenschwender, M., Adam, D., Mentlein, R., Kabelitz, D., and Schutze, S. (2004). Compartmentalization of TNF receptor 1 signaling: internalized TNF receptosomes as death signaling vesicles. *Immunity.* 21, 415-428.
18. Harper, N., Hughes, M., MacFarlane, M., and Cohen, G. M. (2003). Fas-associated death domain protein and caspase-8 are not recruited to the tumour necrosis factor receptor 1 signaling complex during tumour necrosis factor-induced apoptosis. *J.Biol.Chem.* 278, 25534-25541.

19. Eggermont, A. M., de Wilt, J. H., and ten Hagen, T. L. (2003). Current uses of isolated limb perfusion in the clinic and a model system for new strategies. *Lancet Oncol.* 4, 429-437.
20. Lejeune, F. J., Lienard, D., Eggermont, A. M. M., Schraffordt Koops, H., Rosenkaimer, F., Gerain, J., Klaase, J. M., Kroon, B. B. R., Vanderveken, J., and Schmitz, P. (1994). Rationale for using TNF alpha and chemotherapy in regional therapy of melanoma. *J.Cell Biochem.* 56, 52-61.
21. Van Horssen, R., Rens, J. A. P., Brunstein, F., Guns, V., van Gils, M., ten Hagen, T. L. M., and Eggermont, A. M. M. (2006). Intratumoural expression of TNF-R1 and EMAP-II in relation to response of patients treated with TNF-based isolated limb perfusion. *Int J Cancer* Epub 13 Apr.
22. Berger, A. C., Alexander, H. R., Tang, G., Wu, P. S., Hewitt, S. M., Turner, E., Kruger, E., Figg, W. D., Grove, A., Kohn, E., Stern, D., and Libutti, S. K. (2000). Endothelial monocyte activating polypeptide II induces endothelial cell apoptosis and may inhibit tumour angiogenesis. *Microvasc Res* 60, 70-80.
23. Stoelcker, B., Ruhland, B., Hehlgans, T., Bluethmann, H., Luther, T., and Mannel, D. N. (2000). Tumour necrosis factor induces tumour necrosis via tumour necrosis factor receptor type 1-expressing endothelial cells of the tumour vasculature. *Am J Pathol* 156, 1171-1176.
24. Li, X. and Minden, A. (2005). Pak4 functions in TNFalpha induced survival pathways by facilitating TRADD binding to the TNF receptor. *J.Biol.Chem.*

Chapter 9

Improved response to TNF-based ILP of EMAP-II transfected soft-tissue sarcoma in rats

Titia E. Lans[1]
Remco van Horssen[1]
Peter C. Wu[2]
Sandra T. van Tiel[1]
Steve K. Libutti[2]
H. Richard Alexander[2]
Alexander M.M. Eggermont[1]
Timo L.M. ten Hagen[1]

[1]Laboratory of Experimental Surgical Oncology, Department of Surgical Oncology, Erasmus MC – Daniel den Hoed Cancer Centre, Rotterdam, The Netherlands and [2]Surgery Branch, Centre for Cancer Research, National Cancer Institute, Bethesda, MD, USA

Adapted from:
Ann Surg Oncol (2002) 9(8): 812-819 and Anticancer Res (2004) 24(4): 2243-2248

Note: This chapter contains figures that are also available in full colour (labeled with 'CLR'). These colour figures can be found in the Appendix of this book (page 209) and in the online version (via Medical Library, Erasmus MC).

ABSTRACT

Tumour Necrosis Factor-alpha (TNF) is a proinflammatory cytokine with potent anti-tumour activities. Its clinical use in cancer treatment is limited by considerable toxicity after systemic administration, and is currently confined to isolated limb and organ perfusion settings. The high dose administered via these settings can lead to hemorrhagic necrosis in solid tumours. The novel tumour-derived cytokine, Endothelial Monocyte-Activating Polypeptide II (EMAP-II) has been demonstrated to render a TNF-resistant tumour sensitive to TNF therapy. We demonstrate here that *in vitro* stable transfection of rat sarcoma cells led to higher levels of proEMAP/p43 protein and supernatants of transfected cells did induce an increase of Tissue Factor activity by endothelial cells. This gene transfer resulted in improved response rates of soft-tissue sarcoma to subsequent regional TNF treatment by means of an isolated limb perfusion (ILP) in rats. In order to confirm that this was an EMAP-II related effect, wild-type tumour bearing rats were pre-treated with an intravenous injection of recombinant EMAP-II followed by an ILP with TNF. These experiments resulted in a comparable tumour response as was observed in rats bearing EMAP-II transfected sarcoma treated by TNF-ILP. These results indicate that induction of EMAP-II production by sarcoma tumours in rats via gene transfer, improves the response to ILP with TNF.

INTRODUCTION

Studies of the anti-tumour activities of systemically administered TNF in humans have been hampered by severe dose-limiting toxicity at relatively low doses of the cytokine which are insufficient for an antitumour response [1]. This situation changed when TNF was applied in the isolated limb perfusion (ILP) setting. The efficacy of the application of TNF in combination with cytostatic agents in ILP for treatment of patients with in transit melanoma metastases or locally advanced soft tissue sarcomas has now been well established [1-3]. This treatment can be used as a limb-saving neoadjuvant therapy when it is followed by local excision of residual tumour. TNF became a registered cancer drug in Europe based on results of multicenter studies in which clinical response rates of 75% and limb salvage rates of 71% were observed in 196 patients who had been classified as having unresectable solid tumours that could only have been managed by amputation. Approval by the EMEA was given for the use of TNF in the setting of an ILP for locally advanced extremity grade II-III soft tissue sarcomas (STS) [4]. However, up to 25% of the patients do not respond to TNF-based ILP with a sufficient anti-tumour effect for limb preservation. Underlying reasons and mechanisms for this non-responding patient group is not known.

There is evidence that the mechanism of action of TNF is not directly on tumour cells but acts indirectly by destruction of tumour associated vasculature [5]. This destruction may eventually lead to death of tumour cells when used in combination with an anti-tumour drug. The anti-tumour effects after TNF-based ILP can be very rapid, indicating that the TNF-mediated collapse of the tumour vascular bed may play an essential role in the anti-tumour mechanism. The selective destructive effects of TNF-based ILP on tumour associated vessels have been illustrated in the clinic by means of pre- and post perfusion angiographies (see also Chapter 5 of this thesis). Severe hemorrhagic necrosis, accompanied with vascular destruction was observed after ILP with TNF in combination with Melphalan. Our laboratory has developed ILP models with different tumour types in rats to study prerequisites for improving efficacy of different treatments and to study mechanisms of synergy [6,7]. These models mimic the clinical setting closely with respect to response rates and histopathology. The crucial observation has been that TNF selectively and highly significantly enhances the uptake of Melphalan and doxorubicin in the tumours[8].

Endothelial Monocyte-Activating Polypeptide II (EMAP-II) is a pro-inflammatory cytokine with anti-angiogenic properties. EMAP-II induces chemo taxis of neutrophils and monocytes/macrophages and an induction of von Willebrand Factor, E- and P-selectin and Tissue Factor in endothelial cells [9,10]. In addition, EMAP-II exhibits antiangiogenic activities by inducing endothelial cell apoptosis and can inhibit tumour growth [11]. For TNF-resistant tumours, EMAP-II is shown to sensitise those tumours towards systemic TNF treatment. These sensitising properties were not seen on tumour cells *in vitro* suggesting an anti-tumour effect at vascular level. Wu et al [12] defined a way to upregulate EMAP-II production by means of retroviral transfection of a human melanoma cell line. We used this same method using a TNF-resistant rat soft tissue sarcoma, BN175. Here we describe application of EMAP-II gene transfer, subsequent regional TNF treatment and its effects on *in vivo* tumour growth in a rat ILP model.

MATERIALS AND METHODS

Animals

Inbred male Brown Norway rats, weighing 200 to 300 grams, were obtained from Harlan-CPB, Austerlitz, The Netherlands. All animals were kept at standard laboratory conditions and were fed a standard laboratory diet (Hope Farms, Woerden, the Netherlands). The experimental protocols adhered to the rules laid down in the “Dutch Animal Experimentation Act” (1977) and the published

"Guidelines on the protection of Experimental Animals" by the council of the EC (1986). All animal studies were done in accordance with protocols approved by the Animal Care Committee of the Erasmus University of Rotterdam, the Netherlands.

Tumour model

BN-175 is a non-immunogenic, rapidly growing soft tissue sarcoma syngeneic in Brown Norway rats, with a tumour doubling time of approximately 2 to 3 days. This tumour was implanted into the flank of donor rats and passaged serially. For this study we used small tumour fragments (± 1 mm^2) that were subcutaneous implanted into the right hind limb just above the ankle. All surgical interventions were performed at a tumour diameter between 5 and 10 mm, at least 7 days after implantation. Rats were sacrificed if tumour diameter exceeded 25 mm.

Drugs

Recombinant human Tumour Necrosis Factor-α, recombinant human EMAP-II and antibodies directed to human EMAP-II were provided as a kind gift by Dr. G. Adolf (Boehringer Ingelheim GmbH, Germany).

Transfection of BN-175 tumour cells with the EMAP II gene

Viral supernatants from the Gibbon Ape ecotropic packaging cell line PG-WU was used to transfect the BN-175 tumour cell line. To prepare virus-containing conditioned medium $5x10^6$ PG-WU cells were grown for at least 48 h, viral supernatants were briefly centrifuged, filtered across a 0.45 μm membrane (Corning) and SequaBrene (1 μl/ml supernatant, Sigma-Aldrich) was added. Tumour cells, grown till 40-50% confluence, were washed twice with PBS and transfected with freshly prepared viral supernatants for 6 h on 3 subsequent days and in between incubated with standard medium in an incubator at 37 ^oC and 5% CO_2. After 5 to 7 days the transfected tumour cells (named BN-E) were subcultured into 75 cm^2 flasks and expanded under Neomycin selection (800 μg/ml, Sigma).

Analysis of EMAP-II transfected cells

Transfected tumour cells were trypsinated and pelleted. DNA was extracted using the QIamp DNA mini kit (Qiagen Inc.) and amplified by PCR using primers specific for the EMAP-II insert and the downstream retroviral IRES region of the vector to selectively amplify retroviral derived EMAP-II. For

EMAP-II the following primers were used: 5'-AATCGGATGGTGATTTTACTTTGTA-3' (EF-1) as the forward primer in both PCR reactions and backward: 5'-CATTTTATTTGATTCCACTGTTGC-3' (ER-1) with a PCR product of 333 bp for the EMAP-II part, and backward for IRES and EMAP-II: 5'-GAATGCTCGTCAAGAAGACAG-3' (ER-2), resulting in a 577 bp PCR product. PCR amplification was performed under the following conditions: 5 minutes at 95 ^{o}C, 35 cycles (94 ^{o}C for 45 seconds, 55 ^{o}C for 45 seconds, 72 ^{o}C for 60 seconds), and 7 minutes at 72 ^{o}C, soak at 4 ^{o}C. Amplified PCR-products were subjected to gel electrophoresis on a 1% agarose gel containing ethidium bromide.

Western blot analysis

After transfection, tumour cells were harvested, washed and centrifuged. Cell pellets were lysed at 4 ^{o}C in 50 mM TrisCl (pH 8.0); 150 mM NaCl; 0.02% Na-azide; 0.1 % SDS; 1 μg/ml aprotinine; 5% Na-deoxycholate; 1 % Nonidet P-40; 10 ng/ml DNAse I and 100 μg/ml PMSF for 10 min. Samples were vortexed and debris was pelleted by centrifugation at 15,000 *g* for 10 minutes. Protein contents were determined by BCA protein assay (Pierce) to correct for equal loading and 120 μg protein per sample was loaded on SDS-gels. Lysates were mixed with Laemmli buffer containing 5% β-mercaptoethanol, boiled for 5 minutes and electrophoresed on a 15 % Acrylamide-gel using SDS-PAGE. Membranes were subsequently blocked for non-specific binding overnight at 4 ^{o}C with PBS/ 5 % nonfat dry milk/ 0.05 % Tween-20 and incubated for 2 hours with EMAP-II polyclonal rabbit antiserum (diluted 1:2000 in PBS/ 5 % nonfat dry milk/ 0.05 % Tween-20) at 4 ^{o}C. After washing thoroughly, the membranes were incubated for 1 hour with biotinylated goat-anti-rabbit IgG antiserum (diluted 1:3000 in PBS/ 5 % nonfat dry milk/ 0.05 % Tween-20) at room temperature. Membranes were incubated with alkaline phosphatase-streptavidin complex for 1 h at room temperature, washed and stained with NBT-BCIP substrate (Roche) until staining was optimal. The substrate reaction was stopped by washing several times with AD, membranes were dried and scanned for analysis.

Coagulation Assay

Conditioned medium from wild type BN-175 and BN-E tumour cell lines was tested for procoagulant activity using a two-stage coagulation assay. HUVEC (Biowhittaker) were grown to ~80% confluence in 6-well plates in complete EGM-2 media (Clonetics). Cells were washed twice with sterile PBS. Tumour conditioned medium was produced by growing ~5x10^{6} tumour cells per 75-cm^{2} tissue culture flask in 15 ml of serum-free medium. After 24 hr, conditioned medium was collected and vacuum filtered across a 0.45 μm membrane to remove cellular debris and used directly. HUVEC were

treated with conditioned medium of tumour cells. Normal HUVEC and tumour cell medium were used as a negative control and TNF at a concentration of 1 μg/ml as a positive control. The samples were incubated for 6 hours at 37 ^{o}C in a 5% CO_2 incubator and assayed for procoagulant activity. Medium was removed from the treated HUVEC and cells were washed with Ca/Mg free PBS. After 10 min incubation with 1 ml 25 mM Tris/EDTA (pH 7.4) per well, cells were gently removed from the wells and subsequently collected and centrifuged at 14,000 *g* for 10 minutes at room temperature. Supernatants were carefully removed and the resultant cell pellets were resuspended in 100 μl assay buffer (25 mM Tris, pH 7.4; 150 mM NaCl; 0.1% BSA) and shortly vortexed. Cell pellets were added to 100 μl human citrated plasma (Biopool), mixed well and incubated at 37 ^{o}C degrees for 3 minutes in a clinical fibrometer. The coagulation reaction was catalyzed by adding 100 μl 30 mM $CaCl_2$ and clotting time was measured. Standard curves were generated using recombinant human Tissue Factor (American Diagnostica, Greenwich, CT) to calculate Tissue Factor concentrations.

Immunohistochemistry

Approximately 2 x 10^6 BN175 or BN-E tumour cells were injected subcutaneously in the flank region of syngeneic Brown Norway (BN) rats. When tumours reached 10 mm in diameter they were resected from the animal, immediately fixated in 4 % formalin and embedded in paraffin. Assessment of tumour histology was done on 5 to 8 μm hematoxylin-eosin stained sections. Before staining for EMAP-II, sections were dewaxed with xyleen and rehydrated by passing through a graded series of alcohol followed by PBS. Sections were micro waved two times for 5 min in 0.01 M citrate buffer (2.1 g/l citric acid and 1g/l Sodium hydroxide) to enhance immunoreactivity. All incubations were carried out in a humidified chamber at room temperature. Sections were incubated in 5 % normal goat serum for 30 min to block nonspecific binding of antibodies. Sections were rinsed with PBS/0,05% Tween-20 and rabbit polyclonal antibodies against human EMAP-II was added at a 1:100 dilution. Polyclonal rabbit IgG (Santa Cruz Biotechnology) was used as a negative control. Slides were incubated for 1 hour, washed three times with PBS and subsequently incubated with goat-anti-rabbit secondary antibodies conjugated to peroxidase for 1 h. After washing three times in PBS, slides were incubated with avidin-biotin complex reagent, followed by diaminobenzidine substrate. Thereafter the slides were rinsed with distilled water and counter stained with hematoxylin. Finally, slides were dehydrated with graded alcohol, xyleen and covered with Enthalan. Slides were examined with a Leica DM-RXA microscope and images were made using a Sony DXC950 digital camera.

Isolated Limb Perfusion (ILP) model

The perfusion technique was performed as described previously [7,13]. In our laboratory Manusama et al. modified the technique of ILP in rats, originally described by Benckhuijsen [14]. In this model, using the BN-175 soft tissue sarcoma, it was shown that only when TNF was combined with Melphalan or Doxorubicin a tumour response could be reached. We used the BN-175 soft tissue sarcoma to set up an experimental model to study the response rate to TNF-based ILP. Briefly, small fragments (3-5 mm) of tumour were implanted subcutaneous into the right hind limb of the rat. About 7 to 8 days after implantation tumours reached an average diameter of 8-12 mm and ILP-treatment was performed. Animals were anaesthetized with Hypnorm (Janssen Pharmaceutica, Tilburg, The Netherlands) and Ketamine (Apharmo BV, Arnhem, The Netherlands). Heparin (50 IU) was injected intravenously to prevent coagulation. To keep the hind limb at a constant temperature, a warm water mattress was applied. Temperature was measured with a temperature probe on the skin covering the tumour and was maintained between 38 and 39 ^{o}C. The femoral artery and vein were cannulated with silastic tubing (0.012 inch ID, 0.025 inch OD; 0.025 inch ID, 0.047 inch OD respectively, Dow Corning, Michigan, USA). Collaterals were occluded by a groin tourniquet and time of isolation started when the tourniquet was tightened. An oxygenation reservoir and a roller pump were included into the circuit. The perfusion solution consisted of 5 ml Haemaccel (Behring Pharma, Amsterdam, the Netherlands) in the sham perfusions, and TNF (50 μg) was added to the oxygenation reservoir as a bolus in the treatment group. A roller pump (Watson Marlow, Falmouth, UK; type 505 U) recirculated the perfusate at a flow rate of 2.4 ml/ min. A washout with 5 ml oxygenated Haemaccel was performed at the end of the perfusion. After the perfusion, the cannulas were removed and the femoral vessels of the perfused limb were ligated. The extensive collateral circulation was capable to restore the blood supply of the perfused leg. In other experiments, 16 hours before ILP, 50 μg recombinant EMAP-II, dissolved in 200 μl PBS, was injected intravenously. Rats were closely monitored afterwards and moderate but reversible toxicity was observed after EMAP-II administration. Subsequent tumour growth was daily recorded by calliper measurement. Tumour volume was calculated as 0.4 x (A^2 x B), where B represents the longest diameter and A the diameter perpendicular to B.

RESULTS

Transfection of BN-175 cells with EMAP-II

BN-175 (rat soft tissue sarcoma) cells were transfected with retroviral particles containing EMAP-II gene and appeared resistant to continuous exposure to 800 μg/ml neomycin, demonstrating successful transfection with the construct (data not shown). After 2 weeks of growing in selection medium, genomic DNA was extracted from the transfected tumour cell lines to confirm incorporation of the human EMAP-II gene. PCR analysis showed human EMAP-II in BN-E cell line in contrast to BN175 wild-type cells (Fig. 1A).

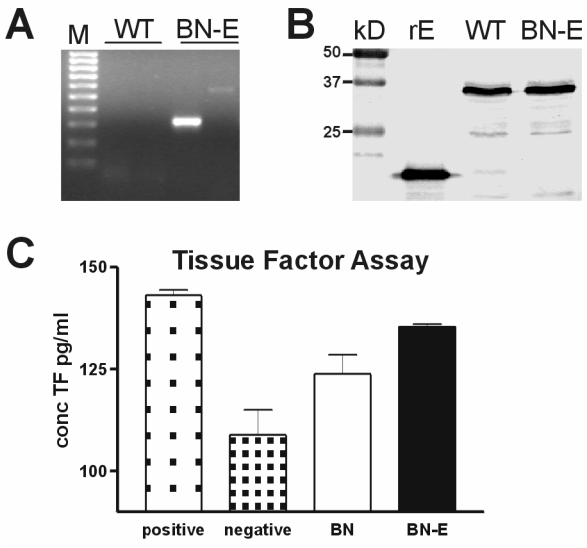

FIGURE 1. Validation of EMAP-II transfected cell lines.
A. PCR analysis of wild-type BN-175 and EMAP-II transfected cell lines (BN-E). Viral derived human EMAP-II is only present in the BN-E cells.
B. Western blots analysis of BN-175 and BN-E cell lysate (120 μg) for EMAP-II. kD: protein marker, rE: recombinant human EMAP-II (100 ng).
C. Tissue Factor Assay. positive control: medium of HUVEC treated with 1 μg TNF; negative: medium of untreated cells; wild type tumour medium; transfected tumour medium. For detailed methods, see materials and methods section.

Western Blot analysis of wild type and transfected tumour cell lysates demonstrated that the band corresponding to the size of proEMAP/p43, ~35 kDa (Fig. 1B) did not visually increase in the BN-E cells. We only show the results with normal growing tumour cells. In our ongoing experiments we would like to demonstrate the generation of active EMAP-II and intermediate cleavage products by inducing apoptosis or other triggers like hypoxia in the tumour cells.

Coagulation Assay

We wanted to test whether the EMAP-II transfected cell line, BN-E, produced functional protein. We determined EMAP-II activity based on the induction of Tissue Factor expression on human endothelial cells. HUVECs were treated with conditioned medium of transfected and wild-type tumour cells. As shown in Fig. 1C, 6 hour exposure of HUVECs to medium conditioned by tumour transfected with EMAP-II (BN-E) induced a 20 % increase in the production of Tissue Factor by these cells, as compared to treatment with conditioned medium from wild type cells. Non-conditioned medium and recombinant TNF were used as negative and positive controls respectively.

Immunohistochemical analysis for EMAP in tumours

The tumour model used for our *in vivo* studies was generated by injection of $2x10^6$ tumour cells subcutaneous in the hind limb of a syngeneic Brown Norway rat.

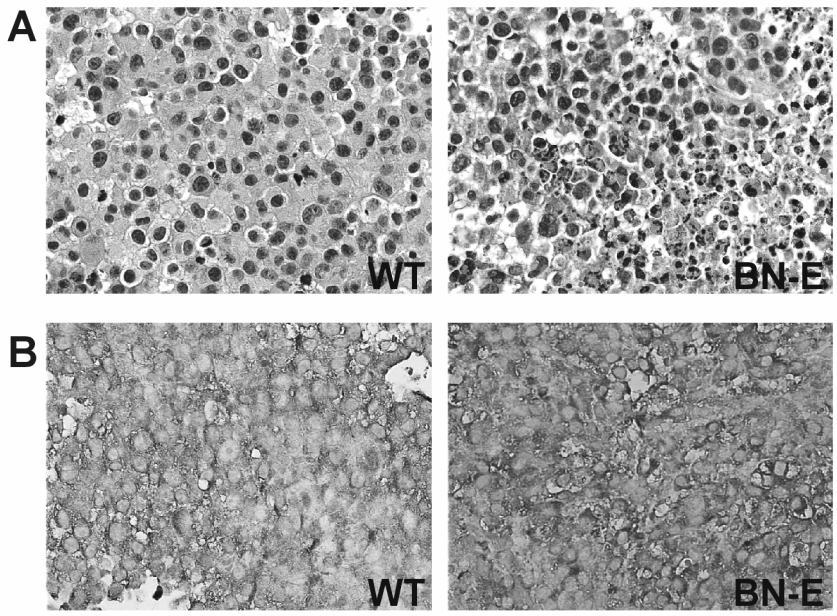

FIGURE 2. Histological and immunohistochemical analysis of wild-type and BN-E tumours **(CLR)**.
A. H&E staining.
B. Immunohistichemical staining for EMAP-II. Transfected tumour cells look somewhat smaller. EMAP-II is expressed by all cells and staining patterns are comparable.

Tumours were grown to an average diameter of 8-12 mm and we observed comparable growth rates between wild-type and EMAP transfected tumours (data not shown). Figure 2 shows

histological H&E staining (A) and immunohistochemistry for EMAP-II (B) for wild-type and BN-E tumours. Both images showed morphological differences, with smaller BN-E cells, but because the antibody recognizes both endogenous and exogenous EMAP-II no differences were observed. EMAP-II is expressed by all cells.

TNF-ILP in rats with wild-type and BN-E tumours

In Figure 3A results of TNF-ILP in rats bearing the BN-E tumour compared to the wild-type tumour are shown. Perfusion with Haemaccel alone resulted in progressive disease in all animals. Although ILP with TNF resulted in a slight inhibition of tumour growth of the wild type tumour compared with the sham control, there was no significant difference in tumour response. As can be seen in this graph the EMAP-II transfected tumour BN-E responded significantly better to ILP with 50 μg TNF. We saw macroscopically a more profound necrosis in the BN-E tumour that led to a significant slower outgrowth of tumour after the perfusion. In animals with transfected tumours a small rim of viable tumour cells survived. However, as can be seen at day nine, the overall observed response rate still implied a decline in tumour dimension, while profound recurrent tumour growth was demonstrated in all animals from day eleven. Tumour volumes are shown in the table of Figure 3B.

A

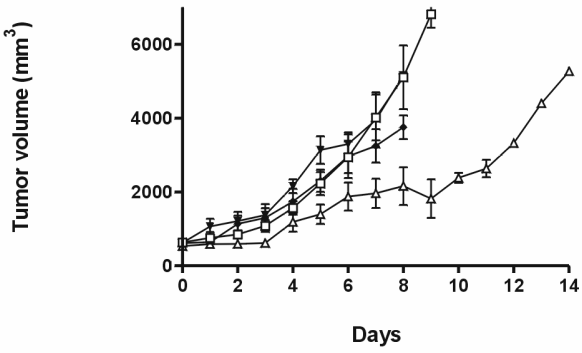

B

Day	0	2	4	6	8	10	12	14
WT								
Sham	622	1210	2156	3299				
TNF	617	1134	1740	2967	3752			
BN-E								
Sham	713	846	1569	2941	5107			
TNF	532	589	1184	1877	2159	2381	3322	5220

FIGURE 3. A. Growth curves of BN wild-type tumour after ILP with sham (▼) n=5 and TNF (♦) n=7 and BN-E tumour after ILP with sham (□) n=7 and TNF (Δ) n=5.
B. Tumour volumes of wild-type and BN-E tumours in rats on consecutive days after sham or TNF-ILP.

TNF-ILP rats with wild-type tumours preceded by EMAP-II injection

Recombinant human EMAP-II (50 μg) was injected intravenously in rats 16 hours prior to TNF perfusion. Rats showed a moderate toxic response immediately after injection, which was reversible within 4 hours. Figure 4 shows the growth curves of wild-type tumours of animals treated with TNF perfusion after pre-treatment with i.v. EMAP-II.

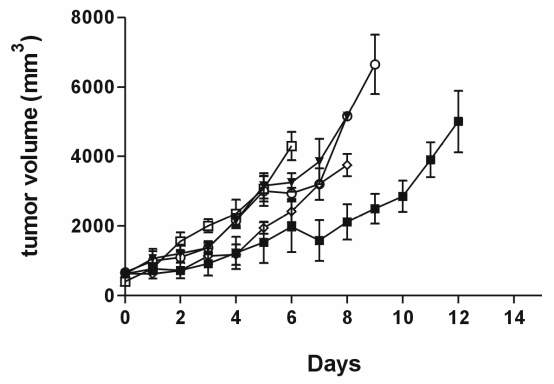

FIGURE 4. Results of ILP in wild type BN tumour with and without pre-treatment with IV EMAP-II. Control tumour with no treatment (□) n=6, sham perfusion alone (▼) n=5, TNF-ILP alone (♦) n=7, IV EMAP-II treatment followed by sham perfusion (o), and IV EMAP-II followed by TNF-ILP (■) n=6.

Sham perfusions after EMAP-II injection were also performed. Wild-type tumours treated with sham perfusion or TNF-ILP alone continued to grow, the EMAP-II pre-treated animals showed a delay in tumour growth only after TNF-ILP. This difference was observed until the ninth day, when both groups started to develop the same growth rate.

DISCUSSION

The results presented in this study show that transfection of the TNF resistant tumour BN-175 with EMAP-II can render this tumour TNF sensitive during TNF-based ILP treatment. This approach could provide clues for further study to enhance efficacy in the clinical setting where 25 % of patients with locally advanced limb threatening extremity soft tissue sarcoma do not respond to TNF and chemotherapy in the ILP setting.

By introducing the isolated perfusion as a mode to apply TNF in patients we have been able to achieve effective concentrations of TNF in the tumour region. Antitumour effects after TNF containing ILP can be extremely rapid. TNF mediated collapse of the tumour vascular bed plays an essential

role in the antitumour mechanism as has been illustrated in publications on clinical studies by pre and post perfusion angiography [11]. Moreover, in studies in sarcoma patients with magnetic resonance spectrometry we have clearly shown that the metabolic shut down of the tumour is virtually complete within 16 hours after the perfusion, confirming the likelihood of TNF mediating its most important effects on the vasculature of the tumour. At the histopathological level these intravascular effects such as thrombocyte aggregation, erythrostasis, endothelial and vascular destruction have been described for the early stage changes after ILP which resembles closely to observations made in experimental tumour systems. Because TNF is known to act on the tumour endothelium, a range of cytotoxic agents have been used in combination to have an additional anti-tumour effect. After the initial destruction of tumour vessels these agents can exert their toxic effect on the tumour cells.

Here we used a gene-transfer approach to improve the effect of TNF therapy. Based on distinct responsiveness of different tumours to TNF, a cytokine that contributes to these distinct responses was isolated. This cytokine, EMAP-II, is produced by tumours and capable of rendering a TNF insensitive tumour sensitive to TNF treatment [12]. This may be an important finding regarding the clinical use of TNF as anti cancer therapy in ILP. Therefore, we investigated whether we could enhance the TNF-sensitivity during ILP of a non-responding rat sarcoma *in vivo* by transfecting the tumour with EMAP II, in order to increase EMAP-II levels.

EMAP-II is a tumour-derived cytokine with pro-inflammatory properties, inducing procoagulant activity on the surface of endothelial cells and chemo taxis of monocytes/macrophages [15]. High expression levels are found in association with tissues that display high turnover and high levels of protein synthesis, like tumour tissue [16]. It was first isolated from the conditioned medium of the murine Meth-A fibrosarcoma. This tumour responds well to TNF therapy and investigators identified EMAP-II in the supernatant of cultured tumour cells. Studies have shown that EMAP-II is capable of sensitizing resistant tumours to the anti tumour effects of TNF and led us to hypothesize that EMAP-II could be of additional benefit in the TNF-ILP setting. By gene-transfer we created a more sensitive tumour to TNF therapy, without the toxic side effects of systemic EMAP-II application. In our next experiments we injected recombinant EMAP-II in rats that were 16 hours later subjected to a TNF-ILP. In a dose of 50 μg rEMAP per rat combined with 50 μg TNF we saw a significant decrease of growth of the tumours, with an immediate, although moderate and reversible, toxic reaction to the injected EMAP-II. These results were comparable with the effect seen in the transfected tumour and suggest that this effect is mediated by EMAP-II rather than an effect created by transfection of the

tumour. Currently we are making control cell lines transfected with empty-vector containing viruses to confirm this.

ILP might be an interesting method for new treatment modalities such as adenoviral-vector mediated gene therapy [17,18]. In our laboratory we have shown that ILP is a good and selective method for effective homogeneous transvascular local gene-delivery by using adenoviral vectors. Experiments in our soft tissue sarcoma and osteosarcoma ILP models have clearly shown this by making use of luciferase-marker gene and LacZ gene methodology [19]. Moreover, we have shown that ILP with adenoviral-vector gene delivery of the cytokine IL-3 is the only method in these tumour models to achieve good tumour responses in contrast to other methods such as IV administration, intra-arterial administration or intra-tumour administration [18]. It demonstrates that ILP is a valuable method to treat advanced limb tumours and to develop new treatment modalities.

The possibility of manipulating the sensitivity for TNF in a tumour *in vivo* also leaves a window for systemic application of TNF in future settings. If viral vectors can be used to increase tumour sensitivity in a way that the TNF dose can be lowered, we might be able to save patients in the future the invasive perfusion procedure and be able to administer TNF systemically in patients.

REFERENCES

1. Asher, A., Mule, J. J., Reichert, C. M., Shiloni, E., and Rosenberg, S. A. (1987). Studies on the anti-tumour efficacy of systemically administered recombinant tumour necrosis factor against several murine tumours in vivo. *J.Immunol.* 138, 963-974.
2. Lienard, D., Eggermont, A. M., Koops, H. S., Kroon, B., Towse, G., Hiemstra, S., Schmitz, P., Clarke, J., Steinmann, G., Rosenkaimer, F., and Lejeune, F. J. (1999). Isolated limb perfusion with tumour necrosis factor-alpha and melphalan with or without interferon-gamma for the treatment of in-transit melanoma metastases: a multicentre randomized phase II study. *Melanoma.Res.* 9, 491-502.
3. Vaglini, M., Belli, F., Ammatuna, M., Inglese, M. G., Manzi, R., Prada, A., Persiani, L., Santinami, M., Santoro, N., and Cascinelli, N. (1994). Treatment of primary or relapsing limb cancer by isolation perfusion with high-dose alpha-tumour necrosis factor, gamma-interferon, and melphalan. *Cancer* 73, 483-492.
4. Eggermont, A. M., Schraffordt, K. H., Lienard, D., Kroon, B. B., van Geel, A. N., Hoekstra, H. J., and Lejeune, F. J. (1996). Isolated limb perfusion with high-dose tumour necrosis factor-alpha in combination with interferon-gamma and melphalan for nonresectable extremity soft tissue sarcomas: a multicenter trial. *J.Clin.Oncol.* 14, 2653-2665.
5. Berger, A. C., Alexander, H. R., Wu, P. C., Tang, G., Gnant, M. F., Mixon, A., Turner, E. S., and Libutti, S. K. (2000). Tumour necrosis factor receptor I (p55) is upregulated on endothelial cells by exposure to the tumour-derived cytokine endothelial monocyte- activating polypeptide II (EMAP-II). *Cytokine* 12, 992-1000.
6. de Wilt, J. H., Manusama, E. R., van Tiel, S. T., van Ijken, M. G., ten Hagen, T. L., and Eggermont, A. M. (1999). Prerequisites for effective isolated limb perfusion using tumour necrosis factor alpha and melphalan in rats. *Br.J.Cancer* 80, 161-166.
7. Manusama, E. R., Stavast, J., Durante, N. M., Marquet, R. L., and Eggermont, A. M. (1996). Isolated limb perfusion with TNF alpha and melphalan in a rat osteosarcoma model: a new anti-tumour approach. *Eur.J.Surg.Oncol.* 22, 152-157.
8. Olieman, A. F., Lienard, D., Eggermont, A. M., Kroon, B. B., Lejeune, F. J., Hoekstra, H. J., and Koops, H. S. (1999). Hyperthermic isolated limb perfusion with tumour necrosis factor alpha, interferon gamma, and melphalan for locally advanced nonmelanoma skin tumours of the extremities: a multicenter study. *Arch.Surg.* 134, 303-307.

9. Kao, J., Ryan, J., Brett, G., Chen, J., Shen, H., Fan, Y. G., Godman, G., Familletti, P. C., Wang, F., Pan, Y. C., and et al. (1992). Endothelial monocyte-activating polypeptide II. A novel tumour-derived polypeptide that activates host-response mechanisms. *J Biol Chem* 267, 20239-47.
10. Kao, J., Houck, K., Fan, Y., Haehnel, I., Libutti, S. K., Kayton, M. L., Grikscheit, T., Chabot, J., Nowygrod, R., Greenberg, S., and et al. (1994). Characterization of a novel tumour-derived cytokine. Endothelial-monocyte activating polypeptide II. *J Biol Chem* 269, 25106-19.
11. Schwarz, M. A., Kandel, J., Brett, J., Li, J., Hayward, J., Schwarz, R. E., Chappey, O., Wautier, J. L., Chabot, J., Lo Gerfo, P., and Stern, D. (1999). Endothelial-monocyte activating polypeptide II, a novel antitumour cytokine that suppresses primary and metastatic tumour growth and induces apoptosis in growing endothelial cells. *J Exp Med* 190, 341-54.
12. Wu, P. C., Alexander, H. R., Huang, J., Hwu, P., Gnant, M., Berger, A. C., Turner, E., Wilson, O., and Libutti, S. K. (1999). In vivo sensitivity of human melanoma to tumour necrosis factor (TNF)-alpha is determined by tumour production of the novel cytokine endothelial-monocyte activating polypeptide II (EMAPII). *Cancer Res* 59, 205-12.
13. Nooijen, P. T., Manusama, E. R., Eggermont, A. M., Schalkwijk, L., Stavast, J., Marquet, R. L., de Waal, R. M., and Ruiter, D. J. (1996). Synergistic effects of TNF-alpha and melphalan in an isolated limb perfusion model of rat sarcoma: a histopathological, immunohistochemical and electron microscopical study. *Br.J.Cancer* 74, 1908-1915.
14. Benckhuijsen, C., Varossieau, F. J., Hart, A. A., Wieberdink, J., and Noordhoek, J. (1986). Pharmacokinetics of melphalan in isolated perfusion of the limbs. *J.Pharmacol.Exp.Ther.* 237, 583-588.
15. Berger, A. C., Alexander, H. R., Tang, G., Wu, P. S., Hewitt, S. M., Turner, E., Kruger, E., Figg, W. D., Grove, A., Kohn, E., Stern, D., and Libutti, S. K. (2000). Endothelial monocyte activating polypeptide II induces endothelial cell apoptosis and may inhibit tumour angiogenesis. *Microvasc Res* 60, 70-80.
16. Murray, J. C., Barnett, G., Tas, M., Jakobsen, A., Brown, J., Powe, D., and Clelland, C. (2000). Immunohistochemical Analysis of Endothelial-Monocyte-Activating Polypeptide-II Expression in Vivo. *Am J Pathol* 157, 2045-2053.
17. de Roos, W. K., de Wilt, J. H., Der Kaaden, M. E., Manusama, E. R., de Vries, M. W., Bout, A., ten Hagen, T. L., Valerio, D., and Eggermont, A. M. (2000). Isolated limb perfusion for local gene delivery: efficient and targeted adenovirus-mediated gene transfer into soft tissue sarcomas. *Ann.Surg.* 232, 814-821.
18. de Wilt, J. H., Bout, A., Eggermont, A. M., van Tiel, S. T., de Vries, M. W., ten Hagen, T. L., de Roos, W. K., Valerio, D., and van der Kaaden, M. E. (2001). Adenovirus-mediated interleukin 3 beta gene transfer by isolated limb perfusion inhibits growth of limb sarcoma in rats. *Hum.Gene Ther.* 12, 489-502.
19. Manusama, E. R., de Wilt, J. H., ten Hagen, T. L., Marquet, R. L., and Eggermont, A. M. (1999). Toxicity and antitumour activity of interferon gamma alone and in combinations with TNFalpha and melphalan in isolated limb perfusion in the BN175 sarcoma tumour model in rats. *Oncol.Rep.* 6, 173-177.

Chapter 10

Intratumoural expression of TNF-R1 and EMAP-II in relation to response of patients treated with TNF-based isolated limb perfusion

Remco van Horssen
Joost A. P. Rens
Flavia Brunstein
Veronique Guns
Marjon van Gils
Timo L. M. ten Hagen
Alexander M. M. Eggermont

Laboratory for Experimental Surgical Oncology, Department of Surgical Oncology, Erasmus MC – Daniel den Hoed Cancer Centre, Rotterdam, The Netherlands.

International Journal of Cancer (2006): 119(6) 1481-1490

Note: This chapter contains figures that are also available in full colour (labeled with 'CLR'). These colour figures can be found in the Appendix of this book (page 209) and in the online version (via Medical Library, Erasmus MC).

ABSTRACT

Tumour necrosis factor-alpha (TNF) has been used in the clinic for more than 10 years in an isolated limb perfusion (ILP). However, intra-tumoural expression of TNF receptor-1 (TNF-R1) and TNF-R1 upregulating factors are unknown. We determined the expression of TNF-R1, proEMAP and EMAP-II before and after ILP and evaluated this against clinical response. Tumour biopsies were taken before and after ILP of patients (N=27) with advanced sarcoma or metastatic melanoma. Biopsies were randomly analysed by western blotting for proEMAP/EMAP-II and TNF-R1 expression. Appropriate melanoma biopsies were stained for EMAP-II, TNF-R1, CD31 and CD68. For melanomas we found that an up-regulation of EMAP-II, in contrast to proEMAP or TNF-R1, directly after ILP significantly correlated with a complete tumour response. No correlation was found for sarcoma patients. In a comparative analysis we found that the overall proEMAP and EMAP-II expression was higher in melanoma as compared to sarcoma cases and measurements in cell lines revealed high proEMAP expression by melanoma cells. We report high EMAP-II expression by endothelial cells and association with macrophages. In addition, macrophages are recruited to vessel-remnants after ILP. An upregulation of EMAP-II directly after ILP of melanoma patients correlates with and might predict a complete response to TNF-based ILP. The association of macrophages with EMAP-II expression and vascular damage suggests a role for EMAP-II in regulating the TNF-based anti-tumour effects observed with an ILP. Analysis of EMAP-II expression in melanoma biopsies should be implemented in the ILP procedure.

INTRODUCTION

In the clinic, TNF is currently used in an ILP setting and is registered in Europe since 1998 [1]. Patients with soft tissue sarcoma (STS) or in transit melanoma metastases in the extremities treated by an ILP with TNF and Melphalan respond very well and 75% limb salvage is achieved with up to 80% response rates in patients with limb threatening locally advanced STS [2,3] whilst a 70% or higher complete response rate is achieved in patients with melanoma in transit metastases [4,5]. Responding tumours show hemorrhagic necrosis and the TNF effect seems tumour associated vasculature-dependent [1]. Molecular data on intra-tumoural expression of TNF-R1 and TNF-R1 upregulating factors however do not exist.

Endothelial monocyte-activating polypeptide-II (EMAP-II) is a multifunctional cytokine that was first isolated from supernatants of cultured murine fibrosarcoma and human melanoma cells [6,7]. Even before it was named, its enhancing effects on tumour necrosis factor-alpha (TNF)-induced

hemorrhagic tumour response were reported [8]. EMAP-II induces chemo taxis of neutrophils and monocytes/macrophages and an induction of von Willebrand Factor, E- and P-selectin and Tissue Factor in endothelial cells [9,10]. In addition, EMAP-II exhibits antiangiogenic activities by inducing endothelial cell apoptosis and suppression of tumour growth [11]. Recently, a cancer cell dependent novel immunosuppressive role of EMAP-II by inducing lymphocyte apoptosis has been described [12]. EMAP-II is transcribed in all cells as proEMAP and involved in protein translation as component of the tRNA synthase complex [13].

For TNF-resistant tumours EMAP-II is shown to sensitise those tumours towards TNF upon EMAP-II gene transfer. These sensitising properties were not seen on tumour cells *in vitro* suggesting an anti-tumour effect at vascular level. This was confirmed by a strong increase in Tissue Factor induction by high EMAP-II expressing tumours compared to wild type [14,15]. Another relation between TNF and EMAP-II was found in endothelial cells in which EMAP-II was capable of inducing an up-regulation of TNF-R1 mRNA expression [16]. However, this up-regulation on mRNA level did not correspond to protein levels and in a recent gene array study no records on EMAP-II-altered TNF-R1 expression were found [17] suggesting that the relation between EMAP-II and TNF-R1 is more complex. In a rat model we showed that high EMAP-expressing tumours show a better response to TNF in an isolated limb perfusion (ILP) [18]. This TNF-sensitising effect of EMAP-II initiated studies on the role of EMAP-II in the clinical application of TNF in cancer treatment.

In the current study we show data on TNF-R1 and EMAP-II protein expression in tumours from patients treated with a TNF-melphalan ILP. In a double blind set-up we evaluated and quantified proEMAP, EMAP-II and TNF-R1 protein expression both before and after ILP of sarcoma and melanoma patients (total N=27). In addition, comparative analysis, histology and immunofluorescence stainings of melanoma to locate these proteins were done. The TNF-R1 and EMAP-II distribution within tumour tissue before and after ILP treatment indicates possible underlying mechanisms of the observed anti tumour effects of an ILP treatment.

MATERIALS AND METHODS

Patients

At the Erasmus MC-Daniel den Hoed Cancer Centre more than 350 TNF-based ILPs were performed between 1991 and 2002 in soft tissue sarcoma and melanoma bearing patients. Because of the multifocality of the tumours and impossibility of surgical resection all patients were potential candidates for amputation. Tumour material from these patients was stored in a tumour bank.

Corresponding tumour biopsies before and after ILP were available for 11 patients. Only two melanoma patients received a melphalan alone ILP and no appropriate biopsies were available from these patients. Patients were included when a standardized taken biopsy was available both pre- and post-ILP. To expand this group extra biopsies were taken from patients treated between 2001-2004. In total 27 patients (14 suffering from sarcoma and 13 suffering from melanoma) were included in this study. Due to the nature of the biopsies, sarcomas and melanomas were used for western blotting experiments and appropriate melanomas were used for immunofluorescence as well. TNF-based ILP with TNF and melphalan is a registered treatment modality for patients with limb threatening tumours, the protocols are approved by the Medical Ethical Committee of the Erasmus University Medical Centre and an informed consent form was obtained from all patients. Patients and tumour characteristics are listed in Table I.

Isolated limb perfusion

TNF-based ILP procedure has been described previously [2,3]. Besides lymph node dissection, (for melanoma patients undergoing an iliac perfusion or with palpable lymph nodes) a tumour biopsy was taken directly before and directly after (within 1-2 minutes) the ILP procedure. The biopsies were directly frozen and stored at –80 ^{o}C until analysis. Response rates were reported according to WHO criteria [19] in which a complete response (CR) is disappearance of all lesions with no new areas of disease appearing in the ILP regions. Partial response (PR) is defined as a reduction of 50-99 % of the total tumour size and a stable disease (SD) is defined as no change after ILP treatment. The final outcome of the ILP consists of the clinical and histological response.

Tissue lysis and Western blotting

Tumour lysates were prepared in freshly made Lysis Buffer (50 mM Pipes/KOH, pH 6.5, 2 mM EDTA, 0,1% Chaps, 5 mM DTT, protease inhibitor cocktail (Roche Diagnostics)), 100 μl per 25 mg tumour-tissue and the samples were subjected to 3 freeze-thaw cycles. Cultured tumour cells were lysed as described below. Samples were centrifuged for 10 minutes at 14000 rpm at 4 ^{o}C and within the clear supernatant the protein concentration was determined using Coomassie Reagent (Uptima). 100 μg of tumour lysate or 150 μg of total protein from cultured cells was resolved by SDS-PAGE, transferred to polyvinylidene difluoride membranes (BioRad) and analysed by Western blotting using rabbit anti-human EMAP-II (BioSource) or mouse anti-human TNF-R1 (R&D Systems). Expression was quantified by densitometric analysis using ImageJ Software (NIH) and compared to positive control

(recombinant protein) for EMAP-II (BioSource) or expressed as absolute total density (averaged pixel value times the number of pixels) for TNF-R1.

Cell Culture

B16BL6 (mouse melanoma), BLM (human melanoma) and Mel57 (human melanoma) cells were cultured in DMEM medium (Biowhittaker), BN175 (rat syngeneic soft tissue sarcoma) cells were cultured in RPMI 1640 medium (Biowhittaker), ROS-1 (rat osteo sarcoma) cells were cultured in EMEM medium supplemented with 10% Fetal Calf Serum (FCS) and 100 U/ml penicillin/streptomycin (Life Technologies). Tumour cells were maintained at 37 ^{o}C, 5% CO_2 in a humidified incubator and routinely subcultured by removal from flasks using Trypsin-EDTA (Sigma-Aldrich). Human Umbilical Vein Endothelial Cells (HUVEC) were used between passage 3 and 7 and maintained in Human Endothelial-SFM Medium supplemented with 10% New Born Calf Serum, 5% Human Serum (Invitrogen), 20 ng/ml bFGF and 100 ng/ml EGF (PeproTech), in gelatin-coated flasks.

ELISA

Total EMAP concentrations were determined in tumour cell lysates. Tumour cells were counted and lysed in 75 μl/1.10^6 cells Lysis Buffer (50 mM Tris-HCl (pH 7,4), 150 mM NaCl, 1 mM EDTA, 1% NP-40, protein inhibitor cocktail) for 30 min on ice. Cell lysates were cleared from cellular debris by centrifugation for 10 min at 0 ^{o}C, 14000 rpm and stored at –80 ^{o}C until analysis. ELISA was performed using the Accucyte Human EMAP-2 Kit for detection of total EMAP-2 (CytImmune) using the provided reagents according to the manufacturers instructions.

Immunofluorescence stainings

Cryosections (5 μm) of Tissue-Tek (Sakura) embedded melanoma biopsies were fixed on polylysine-coated slides with acetone, air-dried and rehydrated with PBS. Tissue sections were incubated in blocking solution (1% BSA / 0,05% Tween-20 / PBS) for at least 30 minutes and subsequently incubated with primary antibodies (rabbit anti-human TNF-R1, R&D Systems, mouse anti-human TNF-R1, Alexis, rabbit anti-human EMAP-II, BioSource, sheep anti-human CD31, R&D Systems, mouse anti-human CD68, DaKo Cytomation) for 1 hour at room temperature (CD31, CD68) or overnight at 4 ^{o}C (EMAP-II, TNF-R1) followed by green (488) and red (594) labelled Alexa Fluor secondary antibodies (Molecular Probes) for 1 hour at room temperature. Specificity of the antibodies used was checked by staining with secondary antibodies alone. Slides were mounted using a 1:1

solution of VectaShield (Vector Laboratories) and DAPI-DABCO (Molecular Probes). Immunofluorescent images were taken using an Axiovert 100 M microscope with 40X/1.30 Oil-Plan-NEOFLUAR objective lens (Carl Zeiss) and an ORCA II ER camera (C4742-98, Hamamatsu Photonics Systems) with Openlab 3.1.5 software (Improvision).

HE staining

The same tumour biopsies of melanoma patients used for western blot analysis were used for histological analysis. 5 μm cryosections of Tissue-Tek (Sakura) embedded melanoma biopsies were fixed on polylysine-coated slides with acetone, air-dried and rehydrated with PBS. Sections were stained with haematoxylin and eosin using standard procedures. Slides were examined on a Leica DM-RXA microscope and photographed using a Sony 3CCD DXC 950 camera.

Statistical analysis

ProEMAP, EMAP-II and TNF-R1 expression were divided in up- and down regulated after ILP treatment. Expression threshold was set at > 5% compared to control and an upregulation was considered relevant when it was at least 1.2 times higher compared to before treatment. ProEMAP and EMAP-II were compared to TNF-R1 expression and clinical outcome using cross tabulation and Chi-Square tests. All tests were two sided and the cutoff level for statistical significance was set at $p < 0.05$.

RESULTS

Patients

Twenty-seven patients were included in this study, divided in 14 suffering from sarcoma and 13 suffering from melanoma confined to leg or arm. All patients were treated with an ILP with a combination of TNF and melphalan. Patients were included when a standardized taken tumour biopsy was available from just before and immediately after ILP. From one patient (no. 21) also normal skin biopsies were taken. From one patient (no. 16) no response data were available because this patient died 4 days after a leakage-free ILP due to a myocardial infarction and was known with a previous cardiac history. Patient characteristics are summarized in Table I.

Pat No.	Sex	Age (y)	Tumor type	Subtype sarcoma	Number of tumors	Site	Grade	Stage	ILP type	Response to ILP
1	F	65	S	Pleiomorphic	>10	Lower leg	High	PT	Fem	SD
2	M	74	S	Kaposi	>10	Lower leg/foot	Low	PT	Fem	CR
3	M	74	S	Pleiomorphic	1	Upper arm	High	PT	Axil	SD
4	M	41	S	Lipo	4	Upper/lower leg, knee	High	LR	Iliac	PR
5	M	73	S	Leiomyo	>10	Upper arm	High	LR	Axil	PR
6	M	54	S	Pleiomorphic	1	Upper leg	High	PT	Iliac	PR
7	F	68	S	Leiomyo	1	Lower leg	High	PT	Fem	PR
8	M	88	S	Angio	6	Ankle/foot	Med	LR	Fem	CR
9	M	50	S	Neuro	1	Upper leg	Med	Met	Iliac	PR
10	M	20	S	Aggressive fibro	8	Upper/lower leg	Low	LR	Iliac	PR
11	F	73	S	Clear	1	Upper leg	High	Met	Iliac	PR
12	F	82	S	Mal fibr histiocyt	1	Upper leg	High	PT	Iliac	PR
13	M	51	S	Pleiomorphic	1	Upper arm	High	LR	Axil	PR
14	F	45	S	Stuart-Treves	>100	Upper leg	Med	PT	Iliac	PR
15	F	82	M	-	>50	Lower leg	-	Met, PLN	Iliac	PR
16	F	77	M	-	>100	Total leg	-	Met. PLN	Iliac	- *
17	M	78	M	-	>100	Lower leg, foot	-	PT, Dmet	Iliac	PR
18	F	62	M	-	<10	Lower arm	-	Met, PLN	Axil	CR
19	M	25	M	-	>100	Lower leg, foot	-	PT, Dmet	Iliac	PR
20	F	57	M	-	>50	Total leg	-	Met, PLN	Iliac	CR
21	M	64	M	-	>20	Lower leg	-	Met, PLN	Fem	CR
22	F	83	M	-	>50	Lower leg	-	Met, PLN	Fem	CR
23	F	66	M	-	<10	Lower leg, foot	-	Met	Fem	CR
24	F	65	M	-	>100	Total leg	-	Met, PLN	Iliac	SD
25	F	77	M	-	<10	Lower leg, foot	-	Met, PLN	Iliac	PR
26	F	76	M	-	>50	Total leg	-	Met	Iliac	CR
27	F	46	M	-	>20	Total leg	-	Met, PLN	Iliac	SD

TABLE I. Patient and tumour characteristics. The 14 sarcoma and 13 melanoma patients consist of 15 females (56%) and 12 males (44%), the average age is 63 (range 20-88). * Patient no. 16 died 4 days after ILP due to a myocardial infarction. This patient was included for expression studies but excluded from statistical analysis. Abbreviations: F, female; M, male; S, sarcoma; M, melanoma; Med, medium; PT, primary tumour; LR, local recurrence; Met, metastases; PLN, positive lymph nodes; Dmet, distal metastases; Fem, femoral ILP; Axil, axilar ILP; Iliac, Iliac ILP; SD, stable disease, CR, complete response; PR, partial response.

EMAP-II and TNF-R1 expression before and after ILP in sarcoma patients

Fig. 1*a* shows protein expression of EMAP-II and TNF-R1 in 14 sarcoma patients before (b) and after (a) ILP. All sarcoma patients show proEMAP expression although in patient 3 and 14 the expression is very low. The mature cytokine EMAP-II was also observed in nearly all sarcoma biopsies although it was very low in a number of patients. In addition some intermediate forms were observed which is in accordance with previous reports [20,21]. Also TNF-R1 expression was found in almost all sarcoma patients. For proEMAP, EMAP-II and TNF-R1 protein expression varied a lot between patients and before and after ILP. ProEMAP and EMAP-II expression were quantified using densitometric analysis and illustrated as percentage of control (recombinant EMAP-II) before and after ILP (Fig. 1*b*, *c*). Because activities are attributed to the active form, as a derivative of these quantitative data the ratio EMAP-II/proEMAP was calculated (Fig. 1*d*). The quantification of TNF-R1 expression is illustrated as total absolute density because no positive control was available (Fig. 1*e*).

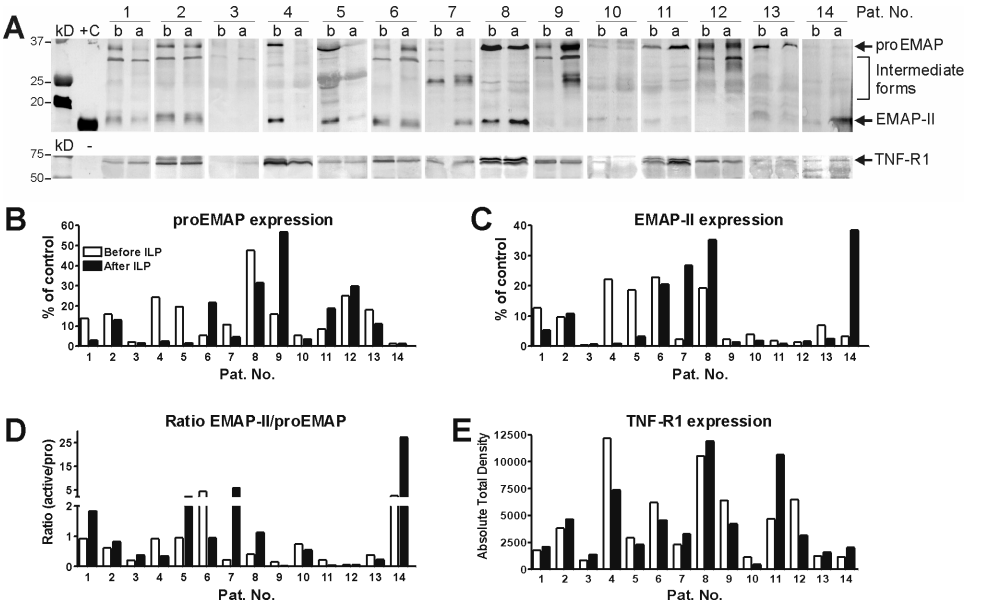

FIGURE 1. Western blot analysis of EMAP-II and TNF-R1 expression in tumour biopsies from sarcoma patients taken right before (b) and after (a) TNF-based ILP.
A. Western blots. +C, 50 ng recombinant EMAP-II protein, for TNF-R1 no positive control was available.
B. Quantification of proEMAP expression before (open bars) and after (closed bars) ILP as compared to the positive control.
C. Quantification of EMAP-II expression before and after ILP as compared to the positive control.
D. Ratio of EMAP-II/proEMAP derived from Fig. *b* and *c* before and after ILP.
E. Quantification of TNF-R1 expression before and after ILP shown as absolute density values.

EMAP-II and TNF-R1 expression before and after ILP in melanoma patients

For 13 melanoma patients (patient 15-27) the same analyses were performed as for the sarcoma patients. Except for patient 24, all melanoma patients show proEMAP expression and EMAP-II was found in all biopsies (Fig. 2*a*). Similar to the sarcoma patients some intermediates forms were observed as well. TNF-R1 expression was found in all melanoma patients although very low in patient 24 and 27. Quantitative analysis of proEMAP and EMAP-II expression was done and expressed as percentage of control (Fig 2*b*, *c*). The derived ratio EMAP-II/proEMAP is shown in Fig. 2*d* and the absolute total density values for TNF-R1 expression in the melanoma patients are depicted in Fig. 2*e*. When comparing Fig. 1*a* and 2*a*, the expression of proEMAP and EMAP-II in melanoma biopsies was more abundant than in sarcoma biopsies.

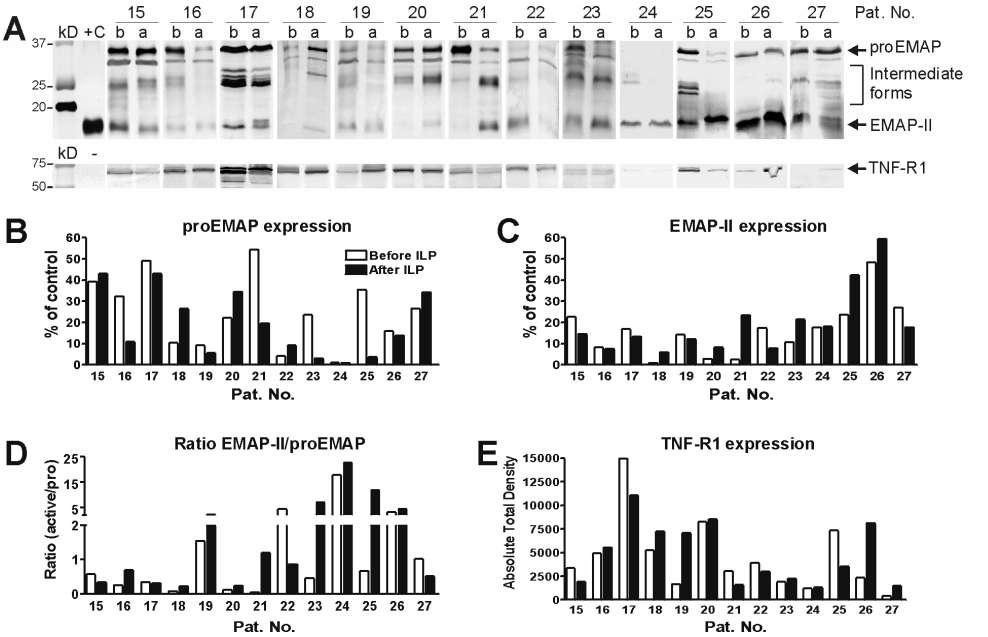

FIGURE 2. Western blot analysis of EMAP-II and TNF-R1 expression in tumour biopsies from melanoma patients taken right before (b) and after (a) TNF-based ILP.
A. Western blots. +C, 50 ng recombinant EMAP-II protein, for TNF-R1 no positive control was available.
B. Quantification of proEMAP expression before (open bars) and after (closed bars) ILP as compared to the positive control.
C. Quantification of EMAP-II expression before and after ILP as compared to the positive control.
D. Ratio of EMAP-II/proEMAP derived from Fig. *b* and *c* before and after ILP.
E. Quantification of TNF-R1 expression before and after ILP shown as absolute density values.

Correlation analysis

To demonstrate statistical correlation between proEMAP, EMAP-II and TNF-R1 expression and response rates we performed Chi-Square analysis. We divided the patients in up- and down-regulation of proEMAP, EMAP-II and TNF-R1 protein expression upon ILP treatment. An upregulation of 1.2 fold and expression of > 5% were set as thresholds. A 1.2 increase was considered relevant in terms of measurements used and to prevent inclusion of observed upregulations that are too small to be biologically relevant. Whether this 1.2 increase is biologically relevant in itself cannot be concluded but local upregulation is known to be of crucial importance for EMAP-II to exert its biological activities (see discussion section). In addition, the patients were divided in complete responders (CR) at one site and partial responders (PR) or stable disease (SD) at the other. The successes (up-regulation and CR) were correlated to the failures (down regulation and PR/SD) for sarcoma and melanoma patients by cross tabulation and Chi-Square analysis. The p-values for significance are shown in Table II.

	MELANOMA	
	TNF-R1↑	CR
proEMAP↑	0.433	0.260
EMAP-II↑	1.000	0.018
Ratio (act/pro)	0.699	0.260
TNF-R1↑	-	1.000

TABLE II. Correlation statistics showing p-values of Chi-Square analysis of melanoma. For sarcomas and melanomas an up-regulation of proEMAP, EMAP-II, ratio or TNF-R1 was compared to an up-regulation of TNF-R1 and number of complete responses (CR). All tests were two sided and the cut-off level for statistical significance was set at $p < 0.05$. Arrow up means > 1.2 times up-regulation after ILP treatment. For sarcomas no correlation was found.

An up-regulation of proEMAP or the ratio did not correlate with an up-regulation of TNF-R1 or a CR for melanoma patients. In contrast, a significant correlation was found between an up-regulation of EMAP-II and a CR for melanomas ($p = 0.018$). Thus, when EMAP-II is upregulated directly after ILP treatment, the patient is expected to have a CR. Up-regulation of EMAP-II therefore could be an independent prognostic marker for a CR of melanoma patients. Between an up-regulation of TNF-R1 and CR no relation was found (Table II). For sarcoma patients no positive correlation was found.

Comparative analysis of proEMAP/EMAP-II expression in sarcoma and melanoma

An upregulation of EMAP-II did correlate with complete response in melanoma patients but not in sarcoma patients. Comparing these two groups for relative proEMAP and EMAP-II expression revealed that for both proEMAP and EMAP-II, both before and after ILP, melanoma tumour biopsies had a higher relative expression (Fig. 3*a*). The differences were most profound for EMAP-II (in melanoma 1.8 times higher before and after ILP), proEMAP was 1.6 and 1.3 times higher in melanoma before and after ILP respectively. For a more detailed analysis we also compared subgroups within sarcoma and melanoma patients. Sarcoma cases were divided according to grade and stage (Fig. 3*b*).

Although some subgroups were very small, some interesting differences were observed. Both before and after ILP proEMAP was the highest in medium-grade sarcomas while for EMAP-II this only was the case after ILP. The abundant upregulation of EMAP-II after ILP in the medium-grade sarcomas (from 8.2 to 25%) resulted from 3 patients (no. 8, 9 and 14) with 1 CR and 2 PR.

A

	BEFORE ILP		AFTER ILP	
	Sarcoma	Melanoma	Sarcoma	Melanoma
ProEMAP (%)	15.2	24.9	14.3	19.0
EMAP-II (%)	9.1	16.4	10.7	19.3

B

	SARCOMA					
	Before ILP			After ILP		
Grade	**Low**	**Med**	**High**	**Low**	**Med**	**High**
ProEMAP (%)	10.6	21.6	14.1	8.3	29.9	10.5
EMAP-II (%)	6.8	8.2	9.9	6.4	25.0	6.9
Stage	**PT**	**LR**	**Met**	**PT**	**LR**	**Met**
ProEMAP (%)	10.6	23.0	12.2	10.7	10.0	37.8
EMAP-II (%)	7.5	14.2	2.0	14.9	8.7	1.1

C

	MELANOMA					
	Before ILP			After ILP		
Stage	**Met,PLN**	**PT,Dmet**	**Met**	**Met,PLN**	**PT,Dmet**	**Met**
ProEMAP (%)	25.0	29.2	19.7	20.2	24.3	8.5
EMAP-II (%)	13.6	15.5	29.6	16.1	12.8	40.4

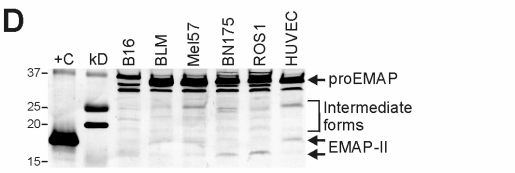

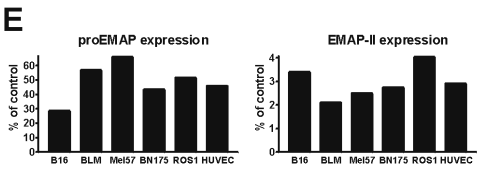

F

Celline	EMAP (ng/ml)
B16	420
BLM	580
Mel57	660
BN175	320
ROS1	26
HUVEC	460

FIGURE 3. Comparative analysis of proEMAP/EMAP-II expression in melanoma and sarcoma tumours.
A. Table showing overall relative proEMAP/EMAP-II expression in the sarcoma and melanoma biopsies before and after ILP. In melanoma all relative values are higher as compared to sarcoma.
B. ProEMAP/EMAP-II expression in sarcoma patients subdivided by grade or stage of the tumour. For abbreviations see legend Table I.
C. ProEMAP/EMAP-II expression in melanoma patients subdivided by stage of the tumour. Note the high EMAP-II expression in 2 patients with metastases after ILP. For abbreviations see legend Table I.
D. Western blot analysis of EMAP expression in tumour cell lines. Three melanomas (B16, BLM, Mel57) were compared with 2 sarcoma lines (BN175, ROS1). HUVEC were used as EC control.
E, Quantification of western blot analysis showing the relative proEMAP/EMAP expression as compared to positive control. Note the very low EMAP-II expression of the cultured (unstimulated) cells. **F** Total EMAP concentration in tumour cell lysates measured by ELISA.

The 2 SD patients (no. 1 and 3) were both high-grade sarcomas and for this group a downregulation for EMAP-II after ILP was found. When comparing the different stages before ILP proEMAP was the highest in the Local Recurrence (LR) patients, while after ILP patients with metastases (Met) had highest proEMAP expression (Fig. 3*b*, lower panel). However, EMAP-II expression in the Met-subgroup was almost absent while the 2 patients (no. 9 and 11) did have a PR. For Primary Tumours (PT) we observe the most abundant upregulation of EMAP-II after ILP (from 7.5 to 14.9%) but although most of the PT sarcoma patients had a PR also two patients of this group had a SD.

Melanoma patients were divided according to stage (Fig. 3*c*). For all subgroups, except for the Met group after ILP, the proEMAP expression was very high. Interestingly, for EMAP-II the opposite was the case: EMAP-II expression was very high after ILP in the Met patient group (40.4%). Patients (no. 23 and 26) within this group did have a CR although also before ILP the EMAP-II expression was

already high in these 2 patients. In conclusion, we observed higher proEMAP/EMAP-II levels in melanoma patients and although these groups were too small to draw any conclusions, some interesting differences were found between the subgroups.

ProEMAP/EMAP-II expression in tumour cell lines

For a further analysis of cellular proEMAP/EMAP-II expression by melanoma and sarcoma cells we evaluated the expression in some melanoma and sarcoma cell lines available in the lab. Using quantitative western blotting the 2 human melanoma cell lines analysed (BLM, Mel57) had the most abundant proEMAP expression although the differences with ROS-1 and HUVEC were small (Fig. 3 *d*, *e*). The relatively high proEMAP levels in the endothelial cell line did correspond with the co-staining experiments (see below). Surprisingly, we observed differences between species of EMAP-II active forms. For the human cells (BLM, Mel57 and HUVEC) the apparent molecular weight was 18-19 kD while for the mouse and rat lines (B16, BN175 and ROS-1) it was around 16-17 kD. For all cell lines the EMAP-II expression was very low (Fig. 3e, right graph). In addition, ELISA was performed for total EMAP within lysates of tumour cells. For Mel57 and BLM melanoma lines EMAP concentration was higher as compared to the other cell lines. The values for the sarcoma lines BN-175 and ROS-1 were lower and very low respectively as determined by the ELISA procedure (Fig. 3*f*).

Immunofluorescent detection of EMAP-II and TNF-R1 in melanoma biopsies

Double fluorescent staining for EMAP-II and TNF-R1 expression before and after ILP treatment are shown in Fig. 4*a*. Before ILP it is obvious that all cells express proEMAP-EMAP-II due to the function of proEMAP in protein translation. In some vessel-like regions throughout the biopsy a higher expression was found (arrow). Before ILP, TNF-R1 expression was found in a fraction of the cells while these high TNF-R1 expressing cells located nearby the vessel-like structures. Evidently, the high expressing EMAP-II cells and the high expressing TNF-R1 cells do not overlap as shown in the merged image (Fig 4*a*, upper panel). After ILP the tumour structure is completely disrupted and no vessel-like structures were observed anymore. EMAP-II expression was still seen in all cells and some clustering of high EMAP-II expressing cells was noted (Fig. 4*a*, lower panel). TNF-R1 expression after ILP was found in a fraction of the cells and its expression seemed reorganized as receptor-clusters (arrowheads).

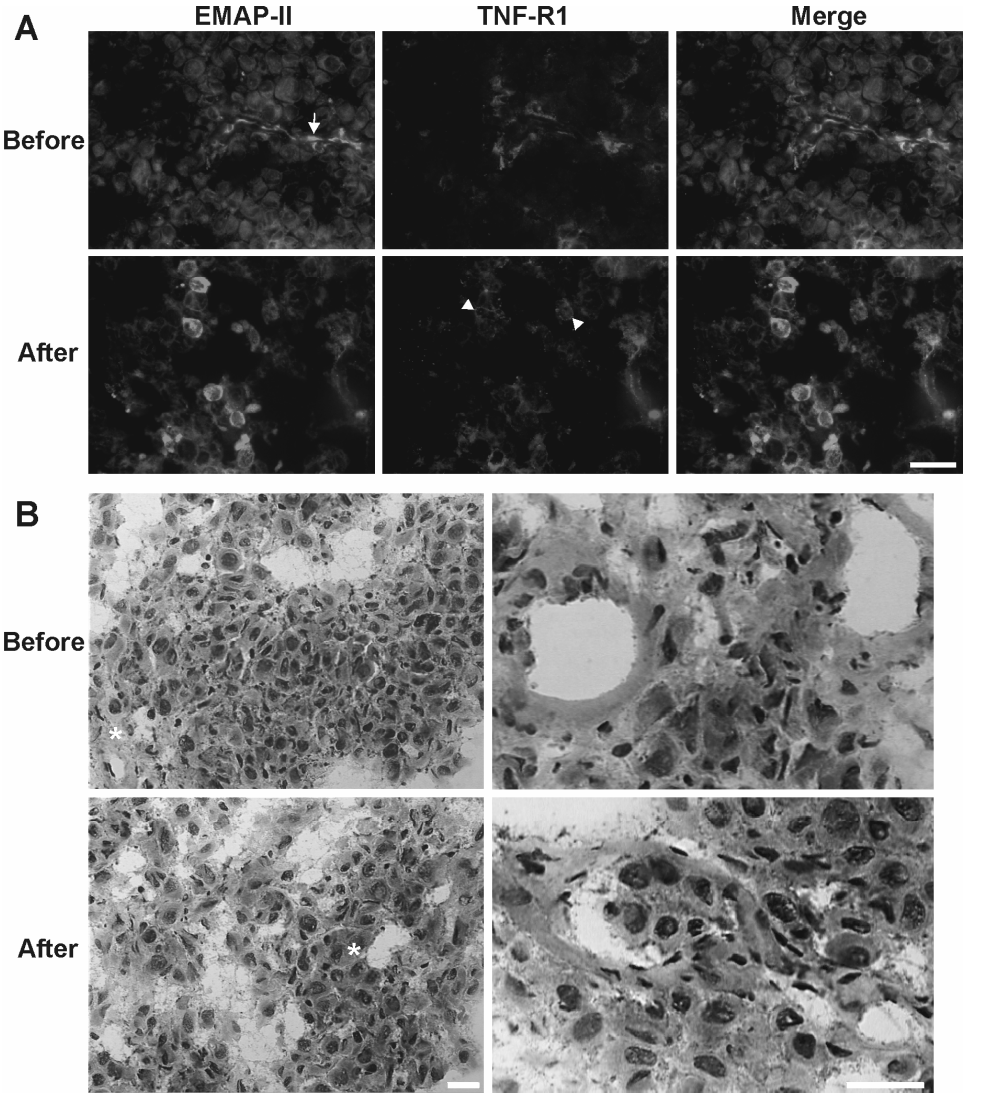

FIGURE 4 (CLR). A. Immunofluorescence stainings for EMAP-II (green) and TNF-R1 (red) of melanoma biopsies taken right before (upper panel) and after (lower panel) TNF-based ILP. Before ILP proEMAP-EMAP-II is present in all cells but some vessel-like regions (arrow) have a higher expression, likely due to local increased expression of mature EMAP-II. TNF-R1 is mainly expressed in the surrounding of these vessel-like regions in a scattered manner. Noteworthy is the observation that high EMAP-II expressing cells and TNF-R1 expressing cells do not overlap. After ILP the tumour structure is extensively damaged. Some high EMAP-II expressing tumour cells clustered to together were observed. TNF-R1 expression was still present in some tumour cells and appeared more organized in clusters (arrowheads) as compared to before ILP. The vessel-like structures are not visible anymore after ILP. Bar, 50 μm.

B. Histological HE staining of melanoma biopsies taken before and after ILP. Before ILP the melanoma showed a heterogeneous structure of tumour cells and infiltrate (left panel). Asterisk indicated a tumour-associated vessel. After ILP the tumour cells are strongly redistributed and the tumour-associated macrophages (also called foamy macrophages) tend to cluster. Tumour vessels before and after ILP are shown at the right panel. Bar, 20 μm.

The high expressing EMAP-II cells after ILP did not correlate with the high expressing TNF-R1 cells. To compare these immunofluorescence data with tumour histology HE stainings were done of the same biopsies (Fig. 4*b*). Before ILP (upper panel) heterogeneous tumour histology is observed with characteristics of malignant melanoma like differences in tumour nuclei dimensions, tumour infiltrate and tumour-associated vessels (asterisk). The right panel show an example of melanoma vessel(s) before ILP. After ILP (lower panel) the tumour histology is reorganised, cells that have a macrophage appearance tend to cluster (asterisk). The vessel in the right panel shows also association with infiltrate-like cells.

Localization of EMAP-II and TNF-R1 in melanoma biopsies before and after ILP

To localize EMAP-II and TNF-R1 expression in the heterogeneous tumour sections we co-stained EMAP-II and TNF-R1 together with endothelial (CD31) and macrophages/monocytes marker (CD68) before and after ILP (Fig. 5).

As shown in Fig. 5*a* the vessel-like structures found with the EMAP-II staining in Fig. 4 indeed (in part) co-stained with CD31. These endothelial cells had a high EMAP-II expression before ILP (Fig. 5*a*, arrow). In contrast, TNF-R1 expressing cells did not co-stain with the endothelium (Fig. 5*a*, upper panel). Before ILP, cells with high TNF-R1 expression located in close proximity to vessels, confirming our results shown in Fig. 4. After ILP, within the disrupted tumour structure high expressing EMAP-II cells were still present clustered together. The CD31 positive cells stained positive for EMAP-II as well. TNF-R1 expression after ILP was again found in receptor-clusters (Fig. 5*a*, arrowheads) and the endothelial cells expressed TNF-R1 at very low levels.

Co-staining with CD68 revealed that high EMAP-II expressing cells or regions were associated with macrophages. Moreover, this co-staining was in close proximity to vessel-like structures (Fig. 5*b*, arrow). The high TNF-R1 expressing cells in the melanoma tissue before ILP were macrophages; a strong co-staining was observed for TNF-R1 and CD68 (Fig. 5*b*, asterisks). After ILP the association of EMAP-II expression and macrophages was still abundant, with similar staining-patterns. For TNF-R1, association with CD68 positive cells was less after ILP as compared to before treatment (Fig. 5*b*, lower panel, arrowheads point receptor-clusters).

Finally, we stained melanoma tumour biopsies for CD31 and CD68 together (Fig. 5*c*). Before ILP, healthy-looking vessels are present and macrophages were distributed quite equally throughout the tumour tissue. After ILP vessels appeared disrupted and macrophages were present in close proximity to these vessel remnants.

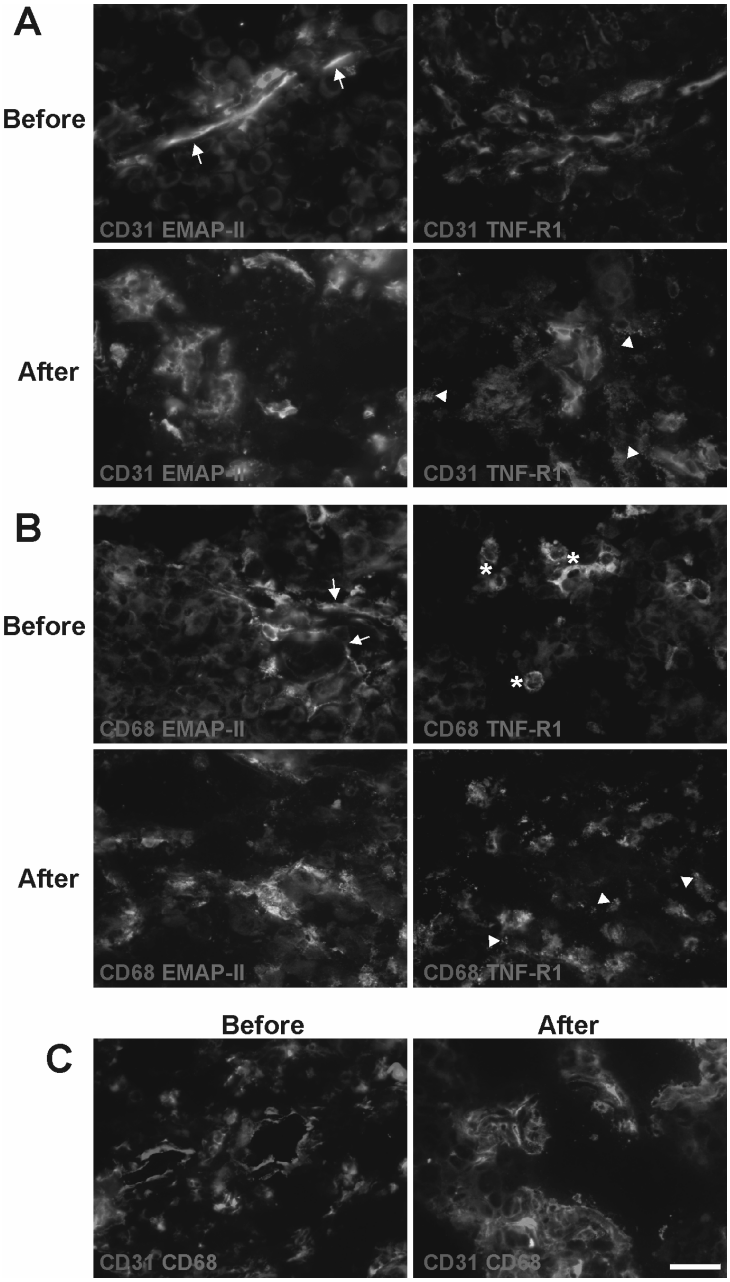

FIGURE 5 (CLR). Immunofluorescence stainings for EMAP-II and TNF-R1 in combination with endothelial marker (CD31, panel *a*) or macrophage/monocyte marker (CD68, panel *b*) and co-staining with both markers (CD31/CD68, panel *c*) of melanoma biopsies taken right before and after TNF-based ILP.

A. Before ILP the high EMAP-II expressing regions in part co-localize with endothelial cells (arrow) while the TNF-R1 expressing cells are surrounding the vessels. No co-localization of TNF-R1 with endothelial cells was observed. After ILP high expressing EMAP-II cells were still present and endothelial cells of the disrupted vessels stained positive as well. TNF-R1 was observed in clusters (arrowheads) and some expression was seen in endothelial cells.

B. Before ILP, high expressing EMAP-II cells/regions co-stained with macrophages in vessel-like regions (arrow). Most tumour-macrophages expressed high levels of TNF-R1 (asterisks). After ILP co-localization of EMAP-II and macrophages is obvious while clustered TNF-R1 expression (arrowheads) was less associated with macrophages.
C. Before ILP, healthy-looking vessels are present and macrophages are equally distributed throughout the tumour. After ILP the tumour vasculature has been disrupted and macrophages were recruited to these endothelial/vessel remnants. Bar: 20 μm

EMAP-II and TNF-R1 expression in normal skin and melanoma

From one melanoma patient (no. 21) besides a melanoma biopsy also a biopsy of normal skin was taken before and after TNF-based ILP. EMAP-II and TNF-R1 expression were determined by quantitative western blotting. Strikingly, in normal skin exactly the opposite occurred compared to the melanoma (Fig. 6*a*). In the normal skin the ILP treatment induced an up-regulation of proEMAP and a down-regulation of EMAP-II, while in the melanoma EMAP-II is upregulated while proEMAP is lower after ILP.

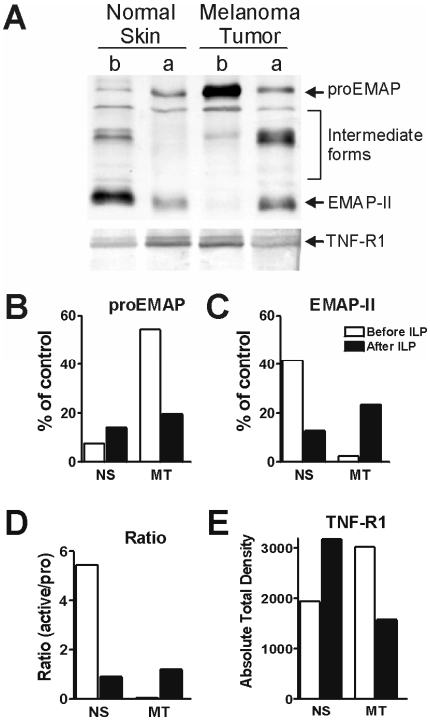

FIGURE 6. Comparison of EMAP-II and TNF-R1 expression in tumour biopsies and normal skin tissue from a melanoma patient before (b) and after (a) TNF-based ILP**.**
A. Western blots.
B. Quantification of proEMAP expression before (open bars) and after (closed bars) ILP as compared to the positive control.
C. Quantification of EMAP-II expression before and after ILP as compared to the positive control.
D. Ratio of EMAP-II/proEMAP derived from Fig. *b* and *c* before and after ILP.
E. Quantification of TNF-R1 expression before and after ILP shown as absolute density values. For EMAP-II and TNF-R1 in the normal skin exactly the opposite is occurring as compared to the melanoma tumour. Abbreviations: NS, normal skin; MT, melanoma tumour.

Quantification is shown in Fig. 6*b* and *c*. The ratio shows the same opposite effects for the normal skin versus the melanoma tumour (Fig. 6*d*). For TNF-R1 also an opposite effect was found; TNF-R1 expression was high after ILP in the normal skin and before ILP in the melanoma tumour (Fig. 6*a*).

DISCUSSION

Here we describe novel data on TNF-R1 and EMAP-II protein expression in cancer patients treated with a TNF-based ILP. For melanoma we report an association between EMAP-II and the response to the TNF-ILP treatment. Our data strongly complement previous knowledge from preclinical and fundamental studies on EMAP-II and might have important implications for patients treated with a TNF-based ILP.

Out of the 350 TNF-based ILPs performed at our institute we selected patients based on the availability of tumour tissue. For this study we needed tumour tissue taken directly before and directly after ILP. Therefore this patient group is unique. The response rates of the sarcoma and melanoma patients in our patient group nicely matches the response rates of larger groups treated by TNF-based ILP [3,22]. For sarcomas our study group had 2 CR (14%), which is somewhat lower as compared to larger cohorts and most likely caused by the relative small group (N=14) used in this mechanistic study. The overall response rate is 86% and comparable with other studies.

We employed both immunologic staining and Western blot analysis, to firstly analyse TNF-R1, proEMAP and EMAP-II expression levels before and after treatment, in a quantitative manner (Figs. 1 and 2), and secondly to provide insight in localization of the proteins within the tumour tissues.

Because of the nature of the biopsies no histological analysis was possible on sarcoma material and only a fraction of the melanoma biopsies can be used. These 3-5 patients were not representing the whole cohort so findings need to be justified as supportive and not conclusive observations. Using these melanoma biopsies we found proEMAP/EMAP-II staining in all cells. In some regions of the tumour we observed higher expression levels, which might be due to an up regulation of protein synthesis but, based on co-staining, we conclude that these regions contained a higher level of the secreted active EMAP-II cytokine. The high expression patterns have a vessel-like structure (Fig. 4), which we could confirm when co-stained with CD31 (Fig. 5*a*) and is in agreement with other reports [23]. For tumour histology analysis we also were restricted to the same melanoma material because we preferred to have biopsies both directly pre- and post-ILP and only frozen material was available, resulting in sections with some gaps. Histological experiments confirmed the reorganisation of tumour

cells. In HE sections after ILP we observed infiltrate-like cells close to the vessels and based on specific staining we concluded that these infiltrate contained macrophages.

Surprisingly, to our knowledge no literature is available on TNF-R1 distribution within tumour tissue before and after ILP treatment. Previously, measurements on TNF-R1 were done in serum of patients to determine the concentration of soluble TNF-R1 in response to TNF-based ILP [24,25]. Here we show for the first time TNF-R1 protein distribution in tumour tissue before and after ILP. We found that TNF-R1 is mainly expressed by cells located closely to vessels but not by endothelial cells themselves. After ILP the vascular structure is disrupted and for TNF-R1 we observed a cluster-like pattern, a feature reported for other members of the death receptor family as well [26]. Expression level of TNF-R1 was however not changed by the perfusion suggesting that rather protein redistribution than up- or down regulation of TNF-R1 is involved in the anti-tumour effects of TNF.

To attribute expression of EMAP-II and TNF-R1 protein to specific cells within the heterogeneous tumour tissue we performed co-staining experiments with endothelial and macrophage/monocyte markers (Fig. 5). Endothelial cells were chosen because of the known anti-vascular activities of TNF in an ILP and the reported anti-angiogenic properties of EMAP-II [1,27] and macrophages/monocytes are very well known for their contribution in tumourgenesis and are one of the major responsive cells to the chemo attractive activities of EMAP-II [28,29]. Co-staining of endothelial cells with EMAP-II implies that high EMAP-II expression may be involved in the anti-vascular effects of TNF. The absence of TNF-R1 on tumour endothelium was unexpected. Only after ILP little positive staining was observed. For endothelial cells *in vitro* it is known that they express TNF-R1 and for EMAP-II an upregulating role has been suggested [16]. It is known that TNF-R1 expression is mainly in the Golgi apparatus and only very small (signalling) fractions are present on the membrane [30]. However, also Golgi-staining was not observed. This might be caused by the tissue staining procedures but this also may reflect a major difference between endothelial cells in culture and those of tumour vessels. The fact that there is no co-staining of endothelial cells and TNF-R1 shows that the underlying mechanism responsible for the TNF response is much more multifaceted than the simple binding of TNF to TNF-R1 on endothelial cells resulting in endothelial cell apoptosis. We speculate that during TNF-based ILP a whole set of cytokines, growth factors and cells are involved, thereby changing the tumour pathophysiology, like cellular organization and vascular flow, which opens windows for TNF and melphalan to exert their anti-tumour activities.

Experiments with co-staining for macrophages confirm this hypothesis and pinpoint macrophages and EMAP-II as important players during TNF-based ILP. The tumour-associated

macrophages are located in regions of high EMAP-II expression and are attracted by the chemo attractive properties of EMAP-II to vascular structures before ILP (Fig. 5*b*). Also after ILP there is still a strong co-localization of EMAP-II and macrophages, which implies that EMAP-II is still after ILP directing macrophages to specific sites. These sites are regions of vascular remnants as revealed by co-staining of endothelial cells and macrophages (Fig. 5*c*). While before ILP the vessels are intact and the macrophages are spread throughout the tumour, after ILP the macrophages are recruited to sites of vascular destruction. Our data show that EMAP-II is an important regulator of this process. For TNF-R1 we observed co-staining with macrophages only before ILP. This might indicate a role for TNF-R1 in activating the tumour-associated macrophages during their suggested role in tumour response.

These observations, the fact that TNF targets endothelial cells within solid tumours and that all these observations were made directly after ILP imply that TNF attributes mainly to these phenomena. Unfortunately, no control tissue was available of (melanoma) patients treated with Melphalan alone for verification, because all patients get the optimal TNF+Melphalan treatment. Additionally, the anti-vascular and cytokine dependent (macrophage) effects will be much lower in the melphalan alone group making adequate evaluation complicated.

The opposing effect of ILP treatment on proEMAP-EMAP-II in the normal skin as compared to the melanoma tumour (Fig. 6) is a remarkable finding but only done in one sample. TNF selectively disrupts tumour vasculature; maybe the effects on EMAP-II and macrophages recruitment may be tumour specific. The high EMAP-II expression in the normal skin can be explained by the high level of cell turnover and replacement, which occurs in healthy skin tissue [31].

Besides the observed EMAP-II effect on macrophages during ILP treatment, an important observation of this study is the relationship between EMAP-II expression and complete response of melanoma patients after TNF-based ILP. Particularly, the correlation was found for the active cytokine EMAP-II, and not for proEMAP, ratio or TNF-R1 (Table II). This correlation between EMAP-II and clinical response strongly suggests an important function of EMAP-II both in mechanism and in clinical outcome. For sarcomas no correlation was found. The relatively small group of patients we studied (N=14) may be responsible for this but moreover, sarcomas are very heterogeneous tumours and our group consists of many different subtypes. In addition, sarcoma tumours had a lower EMAP-II expression as compared to melanomas and depending on tumour type EMAP-II is expressed at different levels and by different mechanisms [12]. A role of EMAP-II in sarcoma regression is not ruled out but for sarcomas additional factors might play crucial roles. We speculate that a certain

threshold of EMAP-II needs to be reached to establish its reported effects and this likely is strongly dependent on tumour type and tumour micro-environmental composition like matrix composition, infiltration and vascular density.

Our results justify further experimental analysis of the function of EMAP-II in anti-tumour activities of TNF. This will lead to more insight in this process and possibilities to intervene and manipulate the EMAP-II expression or activity improving response rates in the clinical setting. In conclusion, we propose that analysis of EMAP-II expression in tumour biopsies of melanoma patients should be implemented in the ILP-procedure so this correlation could be defined in a randomised trial within a larger patient group.

ACKNOWLEDGEMENTS

The presented work was financially supported by grants from Mrace Translational Research Fund from the Erasmus MC, Foundation "Vanderes" and Maxim Pharmaceuticals, Inc., San Diego, CA

REFERENCES

1. Eggermont, A. M., de Wilt, J. H., and ten Hagen, T. L. (2003). Current uses of isolated limb perfusion in the clinic and a model system for new strategies. *Lancet Oncol.* 4, 429-437.
2. Eggermont, A. M., Schraffordt, K. H., Lienard, D., Kroon, B. B., van Geel, A. N., Hoekstra, H. J., and Lejeune, F. J. (1996). Isolated limb perfusion with high-dose tumour necrosis factor-alpha in combination with interferon-gamma and melphalan for nonresectable extremity soft tissue sarcomas: a multicenter trial. *J.Clin.Oncol.* 14, 2653-2665.
3. Eggermont, A. M., Schraffordt, K. H., Klausner, J. M., Kroon, B. B., Schlag, P. M., Lienard, D., van Geel, A. N., Hoekstra, H. J., Meller, I., Nieweg, O. E., Kettelhack, C., Ben Ari, G., Pector, J. C., and Lejeune, F. J. (1996). Isolated limb perfusion with tumour necrosis factor and melphalan for limb salvage in 186 patients with locally advanced soft tissue extremity sarcomas. The cumulative multicenter European experience. *Ann.Surg.* 224, 756-764.
4. Lejeune, F. J., Lienard, D., Eggermont, A. M. M., Schraffordt Koops, H., Rosenkaimer, F., Gerain, J., Klaase, J. M., Kroon, B. B. R., Vanderveken, J., and Schmitz, P. (1994). Rationale for using TNF alpha and chemotherapy in regional therapy of melanoma. *J.Cell Biochem.* 56, 52-61.
5. Fraker, D. L., Alexander, H. R., Andrich, M., and Rosenberg, S. A. (1996). Treatment of patients with melanoma of the extremity using hyperthermic isolated limb perfusion with melphalan, tumour necrosis factor, and interferon gamma: results of a tumour necrosis factor dose-escalation study. *J Clin Oncol* 14, 479-489.
6. Kao, J., Ryan, J., Brett, G., Chen, J., Shen, H., Fan, Y. G., Godman, G., Familletti, P. C., Wang, F., Pan, Y. C., and et al. (1992). Endothelial monocyte-activating polypeptide II. A novel tumour-derived polypeptide that activates host-response mechanisms. *J Biol Chem* 267, 20239-47.
7. Murray, J. C., Clauss, M., Denekamp, J., and Stern, D. (1991). Selective induction of endothelial cell tissue factor in the presence of a tumour-derived mediator: a potential mechanism of flavone acetic acid action in tumour vasculature. *Int.J.Cancer* 49, 254-259.
8. Clauss, M., Murray, J. C., Vianna, M., de Waal, R., Thurston, G., Nawroth, P., Gerlach, H., Bach, R., Familletti, P. C., and Stern, D. (1990). A polypeptide factor produced by fibrosarcoma cells that induces endothelial tissue factor and enhances the procoagulant response to tumour necrosis factor/cachectin. *J Biol Chem* 265, 7078-83.
9. Kao, J., Fan, Y. G., Haehnel, I., Brett, J., Greenberg, S., Clauss, M., Kayton, M., Houck, K., Kisiel, W., Seljelid, R., and et al. (1994). A peptide derived from the amino terminus of endothelial-monocyte-activating polypeptide II modulates mononuclear and polymorphonuclear leukocyte functions, defines an apparently novel cellular interaction site, and induces an acute inflammatory response. *J Biol Chem* 269, 9774-9782.
10. Kao, J., Houck, K., Fan, Y., Haehnel, I., Libutti, S. K., Kayton, M. L., Grikscheit, T., Chabot, J., Nowygrod, R., Greenberg, S., and et al. (1994). Characterization of a novel tumour-derived cytokine. Endothelial-monocyte activating polypeptide II. *J Biol Chem* 269, 25106-19.

11. Schwarz, M. A., Kandel, J., Brett, J., Li, J., Hayward, J., Schwarz, R. E., Chappey, O., Wautier, J. L., Chabot, J., Lo Gerfo, P., and Stern, D. (1999). Endothelial-monocyte activating polypeptide II, a novel antitumour cytokine that suppresses primary and metastatic tumour growth and induces apoptosis in growing endothelial cells. *J Exp Med* 190, 341-54.
12. Murray, J. C., Symonds, P., Ward, W., Huggins, M., Tiga, A., Rice, K., Heng, Y. M., Todd, I., and Robins, R. A. (2004). Colorectal cancer cells induce lymphocyte apoptosis by an endothelial monocyte-activating polypeptide-II-dependent mechanism. *J.Immunol.* 172, 274-281.
13. Shalak, V., Kaminska, M., Mitnacht-Kraus, R., Vandenabeele, P., Clauss, M., and Mirande, M. (2001). The EMAPII cytokine is released from the mammalian multisynthetase complex after cleavage of its p43/proEMAPII component. *J Biol Chem* 276, 23769-23776.
14. Gnant, M. F., Berger, A. C., Huang, J., Puhlmann, M., Wu, P. C., Merino, M. J., Bartlett, D. L., Alexander, H. R., Jr., and Libutti, S. K. (1999). Sensitization of tumour necrosis factor alpha-resistant human melanoma by tumour-specific in vivo transfer of the gene encoding endothelial monocyte-activating polypeptide II using recombinant vaccinia virus. *Cancer Res* 59, 4668-74.
15. Wu, P. C., Alexander, H. R., Huang, J., Hwu, P., Gnant, M., Berger, A. C., Turner, E., Wilson, O., and Libutti, S. K. (1999). In vivo sensitivity of human melanoma to tumour necrosis factor (TNF)-alpha is determined by tumour production of the novel cytokine endothelial-monocyte activating polypeptide II (EMAPII). *Cancer Res* 59, 205-12.
16. Berger, A. C., Alexander, H. R., Wu, P. C., Tang, G., Gnant, M. F., Mixon, A., Turner, E. S., and Libutti, S. K. (2000). Tumour necrosis factor receptor I (p55) is upregulated on endothelial cells by exposure to the tumour-derived cytokine endothelial monocyte- activating polypeptide II (EMAP-II). *Cytokine* 12, 992-1000.
17. Tandle, A. T., Mazzanti, C., Alexander, H. R., Roberts, D. D., and Libutti, S. K. (2005). Endothelial monocyte activating polypeptide-II induced gene expression changes in endothelial cells. *Cytokine* 30, 347-358.
18. Lans, T. E., ten Hagen, T. L., Van Horssen, R., Wu, P. C., van Tiel, S. T., Libutti, S. K., Alexander, H. R., and Eggermont, A. M. (2002). Improved antitumour response to isolated limb perfusion with tumour necrosis factor after upregulation of endothelial monocyte-activating polypeptide II in soft tissue sarcoma. *Ann.Surg.Oncol.* 9, 812-819.
19. WHO (1979). "WHO Handbook for Reporting Results of Cancer Treatment. Geneva: World Health Organisation,".
20. Barnett, G., Jakobsen, A. M., Tas, M., Rice, K., Carmichael, J., and Murray, J. C. (2000). Prostate adenocarcinoma cells release the novel proinflammatory polypeptide EMAP-II in response to stress. *Cancer Res* 60, 2850-7.
21. Murray, J. C., Barnett, G., Tas, M., Jakobsen, A., Brown, J., Powe, D., and Clelland, C. (2000). Immunohistochemical Analysis of Endothelial-Monocyte-Activating Polypeptide-II Expression in Vivo. *Am J Pathol* 157, 2045-2053.
22. Grunhagen, D. J., Brunstein, F., Graveland, W. J., van Geel, A. N., de Wilt, J. H., and Eggermont, A. M. (2004). One hundred consecutive isolated limb perfusions with TNF-alpha and melphalan in melanoma patients with multiple in-transit metastases. *Ann.Surg.* 240, 939-947.
23. Clarijs, R., Schalkwijk, L., Ruiter, D. J., and de Waal, R. M. (2003). EMAP-II expression is associated with macrophage accumulation in primary uveal melanoma. *Invest Ophthalmol.Vis.Sci.* 44, 1801-1806.
24. Aderka, D., Sorkine, P., Abu-Abid, S., Lev, D., Setton, A., Cope, A. P., Wallach, D., and Klausner, J. (1998). Shedding kinetics of soluble tumour necrosis factor (TNF) receptors after systemic TNF leaking during isolated limb perfusion. Relevance to the pathophysiology of septic shock. *J Clin Invest* 101, 650-9.
25. Gerain, J., Lienard, D., Pampallona, S., Baumgartner, M., Ruegg, C., Buurman, W. A., Eggermont, A., and Lejeune, F. (1997). Systemic release of soluble TNF receptors after high-dose TNF in isolated limb perfusion. *Cytokine* 9, 1034-1042.
26. Siegel, R. M., Muppidi, J. R., Sarker, M., Lobito, A., Jen, M., Martin, D., Straus, S. E., and Lenardo, M. J. (2004). SPOTS: signaling protein oligomeric transduction structures are early mediators of death receptor-induced apoptosis at the plasma membrane. *J.Cell Biol.* 167, 735-744.
27. Berger, A. C., Tang, G., Alexander, H. R., and Libutti, S. K. (2000). Endothelial monocyte-activating polypeptide II, a tumour-derived cytokine that plays an important role in inflammation, apoptosis, and angiogenesis [In Process Citation]. *J Immunother* 23, 519-27.
28. Bingle, L., Brown, N. J., and Lewis, C. E. (2002). The role of tumour-associated macrophages in tumour progression: implications for new anticancer therapies. *J.Pathol.* 196, 254-265.
29. Tas, M. P. and Murray, J. C. (1996). Endothelial-monocyte-activating polypeptide II. *Int J Biochem Cell Biol* 28, 837-41.
30. Jones, S. J., Ledgerwood, E. C., Prins, J. B., Galbraith, J., Johnson, D. R., Pober, J. S., and Bradley, J. R. (1999). TNF recruits TRADD to the plasma membrane but not the trans-Golgi network, the principal subcellular location of TNF-R1. *J.Immunol.* 162, 1042-1048.
31. Park, S. G., Shin, H., Shin, Y. K., Lee, Y., Choi, E. C., Park, B. J., and Kim, S. (2005). The novel cytokine p43 stimulates dermal fibroblast proliferation and wound repair. *Am.J.Pathol.* 166, 387-398.

SUMMARY

Tumour motility, motility within tumours. The tumour itself is at least as dynamic as the many fields of research aiming to understand cancer formation and optimize treatments for patients. This thesis describes experiments to study and analyse tumour motility at various levels.

Treatment of cancer in the 21st century can be very successful. However, this success still is limited and almost always temporal. Although there are many treatment modalities nowadays, still it is not completely understood what happens within the tumour upon treatment. Next to the still developing field of 'individual patient diagnostics' based on gene and protein profiling to diagnose cancer earlier, our knowledge of tumour biology still is restricted. Only a few decades ago all treatments were completely focussed on the killing of tumour cells. Mainly initiated by recent advances in microscopic imaging at cellular and molecular level from individual cells in controlled systems to intravital models our knowledge of the tumour microenvironment has greatly increased. Solid tumours are highly dynamic 'organs' and treatment must be multi-targeted to change their microenvironment in such a way that the antitumour effects are optimal and predictive.

Solid tumours are dynamic at multiple levels. During tumour growth they attract endothelial cells to provide themselves with oxygen and nutrients, a process called angiogenesis. Next to endothelial cells and tumour cells there are many other cell types, like macrophages, lymphocytes, pericytes and fibroblast present in solid tumours. All these cells do communicate with each other and move within, through and towards the tumour. Endothelial cell migrate to form new vessels, pericytes are recruited to mature these vessels, immune cells infiltrate the tumour tissue and last but no least tumour cells themselves migrate to blood or lymph vessels to invade and metastasize. On cellular level there is a lot of motility: cell migration, attraction, redistribution within the tumour. But next to cellular level, also within the different cells there is motility. Many proteins are mobilized, transported and redistributed from storage pools to specific compartments of the cell, for example the cell membrane. Further understanding of these different levels of motility in tumours, both fundamentally and induced by treatment was one of the aims of this thesis.

Motility in tumours was studied on several levels: cell migration, both of endothelial and tumour cells, mobilisation of signalling molecules in endothelial cells and redistribution of cells within the tumour. This thesis is divided in two parts. The first part describes results of cell migration studies. The

second part shows results of the role of EMAP-II in the anti-tumour effects of TNF as used in an ILP-setting. Here the results and major conclusions are briefly summarized.

After a short introduction of the process of cell migration (**Chapter 1**) the fist results are described in **Chapter 2** where the set up of a novel cell migration assay is explained. The novel migration approach, called the barrier assay, was tested and compared to the 'scratch' or wound healing assay. We used real-time imaging to obtain a broad set of migration parameters. These real-time data enabled us to correlate migration response and cell morphology. For endothelial cells it was found that bFGF and VEGF both did induce migration but patterns were different. The value of the barrier assay was proven for both endothelial cells and fibroblasts. For endothelial cells a concentration dependent migration-inhibiting effect was found for fibronectin and for fibroblast a concentration independent promoting effect is described, which was enhanced by bFGF. Both effects were absent when 'scratch' assays were used. In addition, this chapter describes the contribution of stabilisation of MT to the observed migration responses. These experiments show that the way of MT stabilisation is treatment and cell specific and a strong, directed migration response is not always accompanied by the same type of MT stabilisation.

The differences between bFGF and VEGF induced endothelial migration are further investigated in **Chapter 3**. Here the exact migration profiles are compared and while bFGF induced a higher migratory response, VEGF induced the highest directionality of the cell movements. These differences were further analysed by studying the cell cytoskeleton. VEGF induced many actin stress fibres, while bFGF treated endothelial cells showed many peripheral bands and actin networks at the cell cortex. This actin positive cell cortex was covered by VASP protein at cell edges. VEGF only showed these staining patterns locally. Next to actin, the MT cytoskeleton was studied and measurements of MT growth rates showed that VEGF did induce much higher growth rates as compared to bFGF and control cells. Because recently a role in directed cell movements was found for CLASP, we investigated CLASP distribution in migrating endothelial cells. In contrast to CLASP2, small amounts of CLASP1 accumulated locally at cell leading edges when treated with VEGF. For bFGF and control cells this was not observed.

Chapter 4 describes another application of the barrier assay. Cell motility of tumour cells was studied using different breast tumour cell lines with different characteristics. In contrast to results obtained with other assays, it is shown that cell lines with mutated E-cadherin have low to absent the capacity to migrate. In addition, treatment with bFGF and fibronectin did not induce migration. For cell

lines with wild-type E-cadherin a moderate migratory response was observed. This response was induced by bFGF. Cell lines with hyper-methylated E-cadherin have high migration capacities and respond to treatment but as migration is already high the induction is mild.

Motility in cells and tumours is studied in the second part of this thesis and the TNF-based ILP treatment of sarcoma and melanoma is used as basis. Experiments from molecule to patients are described to gain insight in the intratumoural expression of proteins and mechanisms of response. EMAP-II plays a central role in this part and its effects on TNF antitumour effects are investigated. **Chapters 5** and **6** broadly introduce and discuss these two cytokines.

Chapter 7 shows data on the production of EMAP-II by tumour cells. ProEMAP, expressed in all cells, is cleaved into active EMAP-II by different mechanisms reported in literature by using different *in vitro* models. This chapter for the first time provides data on tumour cells. MMP-7 was pointed as protease that specifically cleaves proEMAP into mature EMAP-II. Other MMPs (2, 3 and 9) and caspase-3 and 7 were excluded. Specific inhibition of MMP-7 decreased EMAP-II cleavage, activity measurements showed that kinetics of MMP-7 activity overlap EMAP-II release by tumour cells and mass spectrometry confirmed proEMAP cleavage.

Chapter 8 describes the effects of EMAP-II on TNF-R1 signalling in endothelial cells. Endothelial cells are insensitive for TNF treatment but a short pre-treatment of EMAP-II resulted in massive TNF-induced endothelial apoptosis. This striking sensitizing effect was further analysed at TNF-R1 level. EMAP-II did not affect protein expression levels of TNF-R1 but induced a mobilisation of receptors out of Golgi storage pools towards the cell membrane. Also for TRADD an intracellular redistributing effect was induced by EMAP-II resulting in small amounts of membrane-associated TRADD. Strikingly, these mobilising events did occur only in a small fraction of the cells but were always observed in the same cell and in different vesicles.

In **Chapter 9** results with EMAP-II transfected soft tissue sarcoma tumours treated with TNF in a rat ILP model are shown. EMAP-II transfected tumours did respond better to TNF treatment as compared to the wild-type controls. When wild-type tumour bearing rats were pre-treated with intravenous EMAP-II, also a better response to TNF-ILP was observed.

Chapter 10 describes results obtained from patient biopsies analysed for EMAP-II and TNF-R1 expression and distribution in relation the treatment response. Tumour biopsies taken just before and after ILP treatment were analysed and double blind related to clinical outcome. For melanoma patients an upregulation of EMAP-II after perfusion did correlate with a complete response to TNF-

based ILP. For TNF-R1 and proEMAP no relation was found. Sarcoma patients did not show a correlation. Melanoma tumours and cells did show an overall higher protein expression of both proEMAP and EMAP-II when compared to sarcoma tumours and cells. Stainings of melanoma biopsies revealed the intratumoural distribution of EMAP-II and TNF-R1. EMAP-II was found in all cells of the tumour and a marked higher expression was seen in endothelial cells. TNF-R1 expression in contrast was peri-vascular. EMAP-II expression was associated with macrophages both before and after ILP and before ILP the tumour-macrophages showed TNF-R1 expression. Finally, after ILP the tumour-macrophages were recruited to sites of vessel remnants.

CONCLUSIONS

- The 'barrier migration assay' enables real-time analysis of migrating cells along a controlled and manipulative matrix without damaging the cells.
- The 'scratch-induced migration' can strongly interfere with the migration response studied in the 'scratch' or wound-healing assay.
- Fibronectin inhibits migration directionality of endothelial cells and this effect is concentration dependent.
- bFGF treatment together with fibronectin coating induces a strong migration response accompanied by obvious morphological changes in fibroblasts.
- Fibronectin-induced migration in fibroblasts is concentration independent.
- The cellular distribution of stable microtubules in fast moving fibroblasts differs strongly per treatment.
- VEGF and bFGF both induce endothelial migration but VEGF induces a higher directionality of cell movements.
- Migration capacity of breast cancer cell lines is correlated with E-cadherin gene status of these cell lines.

- MMP-7 is involved in the release of EMAP-II by tumour cells via cleavage of proEMAP.
- EMAP-II does not influence TNF-R1 protein expression in endothelial cells.
- EMAP-II facilitates TNF-induced apoptosis in endothelial cells via TNF-R1 and TRADD mobilisation.
- TNF-R1 and TRADD are mobilized in different vesicles in the same endothelial cell.
- Rat soft tissue sarcomas transfected with EMAP-II respond better to TNF administered via ILP as compared to control tumours.
- An upregulation of EMAP-II directly after ILP in melanoma biopsies of patients correlates with and might predict a complete response to TNF-based ILP.
- Within melanoma biopsies, endothelial cells express EMAP-II, while TNF-R1 expression is peri-vascular.

POPUPAIRE SAMENVATTING

Ondanks de vele kennis die er momenteel is op het gebied van kanker(bestrijding) moeten we helaas nog steeds vaststellen dat kanker één van de belangrijkste doodsoorzaken is in Nederland en de rest van de westerse wereld. Gelukkig kunnen we vandaag de dag zeggen dat het krijgen van kanker niet meteen 'het einde' hoeft te betekenen. Kanker kan worden genezen of dragelijker worden. Er zijn goede behandelingen en er is hoogwaardige technische apparatuur om de ziekte snel in beeld te brengen. Deze hoopvolle ontwikkelingen echter, nemen niet weg dat iedereen wel iemand kent die aan kanker lijdt/heeft geleden. Daarom is het goed om te zeggen dat de wetenschap veel weet maar, beter om te zeggen dat de wetenschap veel weet maar veel meer (nog) niet weet. Omdat kanker een zeer complexe ziekte is, moet er ook nog veel onderzocht worden. Veel onderzoek richt zich op het zo vroeg mogelijk ontdekken van kanker om zo de behandeling meer kans van slagen te geven. Het zal in de toekomst waarschijnlijk zelfs mogelijk zijn om het krijgen van kanker te voorspellen op basis van genetische gegevens.

Hoe ontstaat kanker? Cellen zijn de bouwstenen van ons lichaam. Gezonde cellen hebben elk een specifieke functie op een specifieke plaats. Een kankercel heeft twee belangrijke eigenschappen: ongeremde celdeling en de capaciteit om elders in het lichaam te nestelen en uit te groeien (uitzaaiingen of metastasen). Kanker is een ziekte van de genen. Door schade aan het DNA van een cel (mutaties) kan een cel zich zodanig aanpassen dat er geen controle meer is over de celdeling. Mutaties kunnen ontstaan als gevolg van erfelijkheid of door factoren uit de omgeving (leefgewoonten, roken, voeding). Verreweg de meeste mutaties worden gerepareerd door een ingenieus systeem in de cel. Het kan echter zo zijn dat de plaats en hoeveelheid van de mutaties te veel wordt om te repareren. Het ligt voor de hand dat deze genen die, na mutatie eventueel leiden tot ongeremde celgroei, een zeer belangrijke focus zijn van het huidige wetenschappelijk onderzoek.

Naast het ontstaan van kanker zijn er meer belangrijke vragen voor de wetenschap. Vragen als: Hoe 'leeft' een tumor? Hoe is de tumor opgebouwd? Hoe vormt een tumor uitzaaiingen? Wat gebeurt er in een tumor tijdens en na een behandeling? Deze vragen zijn vandaag de dag nog maar zeer beperkt te beantwoorden en in dit proefschrift worden experimenten besproken die hieraan een bescheiden bijdrage kunnen leveren. De titel 'Tumoren in beweging' geeft weer dat de tumor ontzettend dynamisch is. Deze dynamiek op verschillende niveaus is bestudeerd.

Nog niet zo lang geleden bestond het behandelen van tumoren vooral uit het doden van de kankercellen. Het is vooral te danken aan geavanceerde microscopische technieken en andere

beeldanalyse dat de kennis van de tumor en zijn omgeving enorm is toegenomen. Tumoren zijn dynamische 'organen', die met een combinatie van behandelingen moeten worden aangepakt. Op deze manier zou dan de dynamiek van de tumor en zijn omgeving optimaal moeten worden beïnvloed zodat de antitumor effecten van de behandeling zo effectief mogelijk zijn en in de toekomst zelfs voorspelbaar en manipuleerbaar. Om dit te bereiken is uitgebreide kennis nodig van de tumorbiologie, op moleculair, cellulair en fysiologisch niveau.

Een belangrijke ontdekking voor behandeling van kanker is dat vaste tumoren (bv. melanomen) in staat zijn om een eigen vaatbed te ontwikkelen. Dit proces heet angiogenese. Op deze manier kunnen tumoren zichzelf in leven houden. Er is een eigen aan- en afvoer van bloed en voedingsstoffen. Door deze tumorvaten aan te pakken, kan een tumor worden uitgehongerd en afsterven. Het is van groot belang om te weten hoe deze bloedvaten ontstaan en wat het verschil is tussen tumorvaten en gezonde vaten. Deze kennis kan worden toegepast om anti-angiogene therapieën te ontwikkelen en optimaliseren. De cellen die een bloedvat vormen zijn endotheelcellen. Deze cellen vormen de wand van ieder bloedvat. Naast kankercellen, bestaat een tumor dus ook uit endotheelcellen. Daarnaast vinden we in een tumor ook immuuncellen, zoals macrofagen en lymfocyten. Verder zijn er nog fibroblasten, pericyten en het netwerk tussen de cellen, de extra cellulaire matrix. De tumor bestaat dus uit een scala van cellen, die niet zomaar stilzitten. Al deze cellen communiceren met elkaar en migreren (bewegen) door de tumor heen en naar de tumor toe. Endotheelcellen migreren om een nieuw bloedvat te vormen, immuuncellen infiltreren het tumorweefsel en de kankercellen zelf migreren naar de vaten toe om uitzaaiingen te kunnen vormen.

Op cellulair niveau is er dus veel 'in beweging'. Dit geldt ook binnenin iedere cel. Veel eiwitten worden gemobiliseerd en getransporteerd in de cel. Bijvoorbeeld, een receptor eiwit kan worden gemobiliseerd vanuit de opslag (Golgi-apparaat) naar het celmembraan om zo bepaalde signalen op te pikken en door te geven aan de cel. Een signaal kan weer tot gevolg hebben dat de cel gaat migreren, delen of dood gaat. Ook deze moleculaire biologie is dus van essentieel belang om te begrijpen hoe cellen reageren op bepaalde behandelingen. Door de verschillende mechanismen van celsignalering te bestuderen en begrijpen kan het effect van de behandeling worden beïnvloed. Het is dus een beweging op verschillende niveaus: van cellen, naar de tumor toe, in de tumor en binnenin de cel. Het bestuderen van deze dynamiek is het doel van dit proefschrift.

Beweging in tumoren is bestudeerd op verschillende niveaus: celmigratie van endotheel- en tumorcellen, mobilisatie van eiwitten in endotheelcellen en de herverdeling van cellen in een tumor na behandeling. Dit proefschrift is verdeeld in twee delen: het eerste deel gaat over celmigratie en de

ontwikkeling van een nieuwe methode om dit te bestuderen, het tweede deel over de rol van het eiwit EMAP-II op de antitumor effecten van TNF bij de behandeling van sarcomen en melanomen.

In **hoofdstuk 1** wordt een korte introductie gegeven over het proces van celmigratie. De verschillende eiwitten die hierbij een rol spelen worden besproken en in een schema worden de verschillende opeenvolgende stappen van celmigratie weergegeven. De eerste resultaten staan in **hoofdstuk 2** waarin het opzetten en testen van een nieuwe celmigratie methode wordt beschreven. Deze nieuwe methode, de 'barrière-assay', is getest en vergeleken met een bestaande methode, de 'scratch' assay (een methode waarbij cellen worden weg geschraapt om een gebied zonder cellen te creëren waarin de cellen kunnen migreren). Bij de nieuwe methode wordt dit celvrije gebied op een meer gecontroleerde manier gemaakt door het plaatsen (en later verwijderen) van een barrière. Bijkomend voordeel is dat de samenstelling van dit celvrije gebied (de matrix waarover de cellen migreren) in de nieuwe methode gecontroleerd en manipuleerbaar is. De manier waarop cellen dit celvrije gebied in migreren is bekeken onder de microscoop zodat, de migratie 'live' kan worden geanalyseerd. Voor endotheelcellen is gevonden dat de groeifactoren VEGF en bFGF een verschillend migratie patroon induceren. De waarde van de nieuwe assay is bewezen door te kijken naar het effect van bepaalde matrixcomponenten. Voor fibronectine is gevonden dat het de migratie van endotheelcellen remt terwijl het die van fibroblasten juist induceert. Deze twee effecten werden niet gevonden met de 'scratch' methode.

In de volgende twee hoofdstukken worden twee toepassingen van de nieuwe migratie methode beschreven. In **hoofdstuk 3** wordt het verschil tussen VEGF en bFGF geïnduceerde endotheel migratie verder uitgediept. De verschillende migratie profielen worden vergeleken en het blijkt dat bFGF de hoogste migratie afstand induceert, terwijl de VEGF geïnduceerde migratie vooral rechtlijnig en gericht is. Dit betekend dat er bij VEGF minder verandering van migratierichting zijn. Verder zijn een aantal eigenschappen en eiwitten van het cytoskelet van de cellen bestudeerd. Voor VEGF werden hogere groeisnelheden van microtubuli gevonden in vergelijking met bFGF en het microtubuli-bindende eiwit CLASP1 lokaliseert in kleine hoeveelheden aan de randen van migrerende endotheelcellen als deze met VEGF zijn behandeld. Voor bFGF en controle cellen werd dit niet of minder waargenomen.

Hoofdstuk 4 beschrijft migratie experimenten met tumorcellen. In dit hoofdstuk zijn verschillende borstkanker cellijnen met elkaar vergeleken. Van deze cellijnen zijn veel genetische eigenschappen bekend. Cellijnen met een mutatie in het E-cadherine gen bleken niet in staat te

migreren, ook niet als er bFGF en/of fibronectine werd toegevoegd. Cellijnen met het normale gen hadden een lage migratie capaciteit terwijl cellijnen met hypermethylatie van de E-cadherin promoter een erg hoge migratie capaciteit lieten zien. Deze migratie was al zo hoog dat een behandeling geen inducerend effect meer heeft.

In het tweede deel van dit proefschrift worden experimenten beschreven die zijn gedaan om (een deel van) het mechanisme van behandeling van tumoren (sarcomen en melanomen) met TNF te bestuden. Deze tumoren worden in de kliniek behandeld met een geïsoleerde perfusie. Tijdens deze behandeling wordt een arm of been geïsoleerd van de rest van het lichaam zodat, een hoge dosis TNF en chemotherapie kan worden toegediend. Deze behandeling is een mooi voorbeeld van een dubbele targeting: TNF grijpt aan op de tumorvaten en de chemotherapie doodt de kankercellen. Van de patiënten die deze behandeling krijgen, reageert ongeveer 70% goed. Dit betekent dat deze patiënten het arm of been kunnen behouden. Voordat deze behandeling beschikbaar was, was amputatie de enige oplossing. Er is dus een groep van 30% die niet (voldoende) reageert op de behandeling. Om dit proberen te verklaren en mogelijk verbeteren zijn er experimenten opgezet van molecuul tot patiënt rond het eiwit EMAP-II. Er is gekozen voor EMAP-II omdat dit eiwit in muizen in staat blijkt tumoren gevoelig te maken voor TNF. De moleculaire achtergrond van EMAP-II, de verhouding met TNF-effecten op endotheelcellen, effecten in ratten en in tumormateriaal van patiënten zijn onderzocht.

In de **hoofdstukken 5** en **6** wordt de huidige kennis van TNF en EMAP-II samengevat. In **hoofdstuk 7** worden data beschreven die de productie van EMAP-II door tumorcellen verklaart. EMAP-II wordt gevormd uit proEMAP en het exacte mechanisme hiervan is nog onbekend en er zijn verschillende en tegenstrijdige publicaties over in de literatuur. In dit hoofdstuk staan de experimenten waaruit blijkt dat we MMP-7 hebben gevonden als eiwit dat in staat is om proEMAP om te zetten in EMAP-II. Voor andere eiwitten (MMP-2, -3, -9 en caspase-3 , -7) bleek dit niet het geval. Deze bevindingen werden bevestigd toen bleek dat remming van MMP-7 de vorming van EMAP-II remde. Verdere aanwijzingen werden gevonden omdat activiteit van MMP-7 en vorming van EMAP-II op dezelfde tijdsstippen plaatsvindt en door middel van massa spectrometrie, waarmee het knippen van proEMAP werd bevestigd.

Hoofdstuk 8 beschrijft de effecten van EMAP-II op de signalering van TNF-receptor 1 (TNF-R1) in endotheelcellen. Ondanks de effecten van TNF op tumorvaten, blijken endotheelcellen ongevoelig voor TNF. Toen deze endotheelcellen werden voorbehandeld met EMAP-II bleek echter dat TNF is

staat was celdood te induceren. Dit opvallende effect is in meer detail bestudeerd en het bleek dat EMAP-II een mobilisatie van TNF-R1 kon induceren. Na behandeling was er een deel van de TNF-R1 moleculen verplaatst van het Golgi-apparaat naar het celmembraan. Er was geen effect van EMAP-II op de expressie van TNF-R1. Ook voor het adaptor eiwit TRADD werd een mobilisatie gevonden. Deze twee effecten kunnen een mogelijke verklaring zijn voor het effect van EMAP-II in combinatie met TNF op endotheelcellen.

In **hoofdstuk 9** staan de resultaten van experimenten met ratten die tumoren hadden met verschillende expressieniveaus van EMAP-II. Deze ratten werden behandeld met een geïsoleerde pootperfusie en tumoren waarin de EMAP-II was opgereguleerd lieten een betere response zien op behandeling met TNF.

Hoofdstuk 10 beschrijft de resultaten die werden verkregen door biopten van patiënten te analyseren voor de expressie van EMAP-II en TNF-R1 voor en na de behandeling. In een dubbelblinde opzet zijn biopten van patiënten met een sarcoom of melanoom genomen direct voor en direct na de geïsoleerde perfusie, geanalyseerd en gerelateerd aan de response van de patiënten op de behandeling. Voor melanoom patiënten bleek dat een hogere EMAP-II expressie na de behandeling gecorreleerd was aan een goede response. Voor proEMAP en TNF-R1 werd er geen relatie gevonden. Voor de sarcoom patiënten werd geen relatie aangetoond. In verdere analyse bleek dat melanoom tumoren en cellen een hogere EMAP-II expressie hadden in vergelijking met sarcoom tumoren en cellen. Een aantal melanoom biopten is aangekleurd voor EMAP-II en TNF-R1 om de verdeling van deze eiwitten in de tumoren te bestuderen. EMAP-II was aanwezig in alle cellen van de tumor en opvallend hoog in endotheelcellen. Voor TNF-R1 werd een peri-vasculaire aankleuring gevonden: in de cellen rondom de bloedvaten. De expressie van EMAP-II bleek geassocieerd met macrofagen in de tumor en na behandeling waren de macrofagen gehergroepeerd rondom de resten van (kapotte) vaten.

CONCLUSIES

- De 'barrière migratie methode' maakt het mogelijk om migrerende cellen 'live' te volgen terwijl de matrix gecontroleerd en manipuleerbaar is en de cellen intact blijven.
- De migratie die wordt geïnduceerd door het zetten van de 'scratch' kan interfereren met de response die wordt geïnduceerd door de behandeling wanneer celmigratie wordt bestudeerd in de 'scratch migratie assay'.
- Fibronectine remt de gerichtheid van endotheelcelmigratie en dit effect is concentratie afhankelijk.
- bFGF behandeling in combinatie met fibronectine coating induceert een sterke migratie in fibroblasten en de cellen ondergaan hierbij drastische morfologie veranderingen.
- Fibronectine-geïnduceerde migratie van fibroblasten is concentratie onafhankelijk.
- De cellulaire verdeling van stabiele microtubuli in snel migrerende fibroblasten is afhankelijk van de behandeling.
- bFGF en VEGF kunnen beide migratie van endotheelcellen induceren maar, VEGF induceert een hogere gerichtheid van de celbewegingen.
- De migratie capaciteit van borstkanker cellijnen is gecorreleerd aan de status van E-cadherine expressie van deze cellijnen.
- MMP-7 is betrokken bij de vorming van EMAP-II door tumorcellen door middel van het knippen van proEMAP.
- EMAP-II heeft geen effect op de eiwit expressie van TNF-R1 in endotheelcellen.
- EMAP-II beïnvloedt door TNF-geïnduceerde celdood in endotheelcellen via een mobilisatie van TNF-R1 en TRADD.
- TNF-R1 en TRADD worden gemobiliseerd in verschillende blaasjes in dezelfde endotheelcel.
- Een rattensarcoom, getransfecteerd met EMAP-II, reageert beter op een geïsoleerde pootperfusie met TNF dan controle tumoren.
- Een opregulatie van EMAP-II direct na perfusie in biopten van melanoom patiënten is gecorreleerd aan een goede response op een TNF-gebaseerde perfusie en kan deze response mogelijk voorspellen.
- Endotheelcellen in melanoombiopten hebben een hoge EMAP-II eiwitexpressie, terwijl de expressie van TNF-R1 peri-vasculair is.

DANKWOORD

Met veel plezier heb ik dit proefschrift geschreven. Door de hulp en bijdrage van vele mensen is het er gekomen. Het is dan wel mijn proefschrift, promoveren doe je niet alleen. Het maken van een proefschrift geeft een dankbaar en tevreden gevoel. Veel dank ben ik verschuldigd aan een ieder die op welke manier ook betrokken is geweest bij het tot stand komen van dit boek. Op deze plaats wil ik, jullie allemaal enorm bedanken voor alles! Een aantal mensen wil ik hier graag in het bijzonder bedanken.

Om te beginnen mijn promotor Lex Eggermont. Als (moleculair) bioloog promoveren bij een chirurg: het blijft bijzonder. Dit echter, kan alleen als de chirurg er één is als jij: breed georiënteerd en geïnteresseerd in de meest brede zin van het woord. Als de uitspraak van molecuul tot patiënt op iemand van toepassing is, dan wel op jou. Hiermee bespeel je het hele veld en dat is geweldig om mee te maken. Bijzonder vind ik ook dat deze compleetheid zelfs geldt voor je meelevendheid buiten de lab-zaken om. Enorm bedankt voor al je steun en vertrouwen. Ik heb met veel plezier en vrijheid kunnen werken in je lab. De keren dat we elkaar spraken waren altijd gezellig en motiverend tegelijk.

Mijn copromotor, Timo ten Hagen. Al vanaf de eerste keer dat ik het lab 'in de kelder' van de hoogbouw bezocht, was ik onder de indruk van de microscopie opstellingen. Nu een aantal jaren later is dit 'wagenpark' zelfs verdubbeld. Het geeft mooi je passie voor 'imaging' weer en ook je niet aflatende inzet om al die experimenten maar mogelijk te maken. Van het kleinste slangetje tot een rattenbak als waterbad, van een complete microscoop tot up-to-date software, je kon het altijd snel regelen. Ik wil je ontzettend bedanken voor je begeleiding. Je voelde perfect aan wanneer je de touwtjes kon laten vieren en daardoor kon ik groeien naar meer zelfstandigheid. En tot slot natuurlijk de congressen, die elke keer weer leuk een leerzaam waren. Ook je bijzondere skiles zal ik niet snel vergeten. We komen elkaar zeker wel weer eens tegen.

En dan Niels Galjart. Samenwerken met jou heb ik altijd buitengewoon gewaardeerd. Het onderwerp blijft ook ontzettend boeiend en het onderzoek houdt dan ook nog lang niet op (wanneer wel?). Dankjewel voor de discussies en je input en ideeën voor experimenten. Ik heb er veel van geleerd en het was vaak nog gezellig ook. Jouw enthousiasme voor fundamenteel onderzoek werkt aanstekelijk. Ook wil ik je danken voor het plaatsnemen in de promotiecommissie. Zoals we het vaak zeiden tegen elkaar: bedankt, meneer! Zeg ik ook hier: tot ziens, meneer!

Mijn dank gaat ook uit naar de andere leden van de kleine commissie. Riccardo Fodde, bedankt voor je suggesties en frisse kijk op het manuscript. Je kritische houding is precies wat jonge

wetenschappers nodig hebben. Wim Buurman, erg leuk dat u als EMAP-expert in de commissie plaats wilde nemen. Veel dank hiervoor.

Ook de overige leden van de grote commissie wil ik bedanken. Thanks to Ferdy Lejeune. I highly appreciate your presence in Rotterdam again. Also thanks for the cheese-fondue lessons in Lausanne! Rob de Waal, EMAP-expert van den beginne, erg leuk om u in de commissie te hebben, bedankt. Chris Bangma wil ik ook danken voor het plaatsnemen in de commissie.

En dan natuurlijk mijn 'vaste lab-maat' Joost. Een betere running-mate kan een promovendus zich niet wensen. Tsjonge, wat hebben wij een blotjes gedraaid! Met jou samenwerken, zal ik zeker missen. Het ging altijd gemakkelijk en was ook altijd leuk en gezellig. Elke keer weer een gil in de doka als er weer eens een freaking mooie cel voorbij kwam. Ik hoefde je niet te vertellen hoe gaaf of belangrijk de proeven waren, want dat voelde je zelf haarfijn aan. Ik vond het mooi om te zien dat je steeds meer gefascineerd raakte door de moleculaire biologie. Enorm veel dank voor al je hulp! Ook gaaf dat je paranimf wilt zijn. We spreken elkaar zeker nog, zelfs nog over een jaar of 15 bij een concert van de 'PJ2PR-band' waarvan de muzikanten en zanger al hard aan het repeteren zijn.

Verder wil ik ook Debby bedanken. Eerst als stagiaire en later even als collega op het EMAP-project. Dankjewel voor de altijd keurig uitgevoerde experimenten. Het bleek maar weer eens hoe belangrijk dit is toen we al de oude blotjes wilden kleuren. Sorry dat je nu een 'voetbal-maatje' kwijtraakt.

Ook de andere stagiaires die ik mocht begeleiden wil ik bedanken voor hun hulp en inzet. Naast Debby en Joost waren dit Marjon en Veronique. Voor allen geldt: jullie bijdrage was essentieel voor het publiceren van de artikelen. Ik vond het erg leuk om jullie te begeleiden.

Ook de mede promovendi van de grote 'AIO-zaal' wil ik bedanken. De collega's van de 'oude groep': Ann (leuk dat ik je congres- en toeristmaat mocht zijn, volgend jaar weer een sorbet in Dresden?), Lucy (de 'mede-bioloog' op de kamer, ik ben zeer benieuwd wat er uit 'jouw setje melanoompjes' komt), Flavia (it was a great pleasure to work with you, I admired your input as experienced surgeon in the lab, sorry that I did still not bring the CD but at least now you know what your present will be on the 12th of October!). Verder ook de 'nieuwe promovendi': Marna, Sefan en Jill (jullie zorgden voor een verdere verbreding van het lab, zeker qua link met de kliniek). Ik wil jullie allemaal bedanken voor de besprekingen en discussies en veel succes wensen met de experimenten en het maken van jullie proefschrift.

Natuurlijk ook dank aan de andere collega's, Gisela (bedankt voor het carpoolen), Cindy en Sjoerd. Het was altijd leuk om weer eens binnen te wandelen bij jullie. En ook de 'LECO-exen' wil ik

noemen: Saske, Sandra, Titia (jaja, EMAP-II staat in de titel, bedankt voor het 'opstapje' in het project) en Boudewijn (Boudje, bakkie?). Allemaal enorm bedankt voor een goede en gezellige tijd.

Graag wil ik ook mensen van andere afdelingen bedanken voor de goede en vruchtbare samenwerking. Medische Oncologie, Mieke Schutte, hartelijk bedankt voor al je enthousiasme en hulp bij het 'borst-deel'. Ik vond het erg leerzaam om met je samen te werken. Je had altijd veel tijd en je kritische kijk op de resultaten en het hoofdstuk waardeer ik enorm. Ook dit onderzoek is nog niet af en we gaan dit zeker afronden. Proteomics, Theo Luider, het heeft even geduurd maar het is wel mooi gelukt. Er komt een mooie publicatie aan. Bedankt voor je specialistische hulp en kennis. Dit was essentieel voor het resultaat. En ook op de 'wonderschone wereld-blot' kom ik zeker terug. Celbiologie, Xenia en Marja, ik heb met veel plezier gemigreerd met jullie cellen. Pathologie, Nijmegen, William Leenders, hoe het zit met de mutanten kunnen we straks tijdens iedere lunch bespreken, iets wat de snelheid zeker ten goede zal komen. Als laatste natuurlijk Celbiologie, Nijmegen, de eerste mooie resultaten zijn er. Be, bedankt voor je vertrouwen en Wilma, Marieke, Jack en de anderen, het is nu echt begonnen, ik heb er zeer veel zin in!

Tot slot wil ik graag mijn familie en vrienden bedanken. De vrienden uiteraard voor de nodige ontspanning. Niet in de laatste plaats wil ik mijn ouders enorm bedanken voor het stimuleren en mogelijk maken van het benutten van mijn talenten. Tot op de dag van vandaag staan jullie altijd voor ons klaar. Pa en ma, jullie zijn uniek! Ook mijn fantastische zus en broer. Zus, veel succes met je man en gezin in de toekomst, Broer, erg tof dat je paranimf wil zijn en veel succes voor de klas en met je vrouwtje, ik ben ik erg trots op jullie! Ook mijn schoonfamilie wil ik graag bedanken voor al hun steun en interesse. Ook voor deze 'kant' geldt: jullie zijn bijzonder en onmisbaar. Dit geldt natuurlijk niet minder voor Daniëlle. Zonder jouw nuchtere kijk, was het zeker niet gelukt. Met jou heb ik alles al meegemaakt. Enorm veel dank voor je luisterend oor dat er echt elke dag van de afgelopen jaren was! Samen met jou genieten van Silas relativeert alles en maakt me intens dankbaar.

Aan het eind van dit veel gelezen stukje van elk proefschrift, heb ik nog een vraagje aan de niet-ingewijden onder jullie. Waarom ga je niet eens verder met de samenvatting? (een paar pagina's terug). Dit is speciaal voor jullie geschreven en bedoeld om ook de rest van dit boekje een beetje tot de verbeelding te laten spreken. En daar hoef je echt niet alles voor te begrijpen. Ik hoor erg graag wat jullie ervan vinden. Alvast bedankt!

Remco

CURRICULUM VITAE

Naam:	Remco van Horssen
Geboren:	26 oktober 1976

1989-1995	VWO, 'De Lage Waard', Papendrecht
1995-2000	Studie Medische Biologie, Universiteit Utrecht
1998-1999	Wetenschappelijk onderzoek stage, Hubrecht Laboratorium, Nederlands Instituut voor Ontwikkelingsbiologie, Utrecht (Dr. L.H.K. Defize)
19990-2000	Wetenschappelijk onderzoek stage, Vakgroep Medische Oncologie, Universitair Medisch Centrum Utrecht (Dr. M.F.B.G. Gebbink, Prof. dr. E.E. Voest)
2000	Afstudeerscriptie, Hubrecht Laboratorium, Nederlands Instituut voor Ontwikkelingsbiologie, Utrecht (Dr. L.H.K. Defize, Prof. dr. R.H. Plasterk)
2000-2005	Promotieonderzoek, Laboratorium voor Experimentele Chirurgische Oncologie (LECO), Erasmus MC, Rotterdam promotor: Prof. dr. A.M.M. Eggermont co-promotor: Dr. T.L.M. ten Hagen
2005-2006	Post-doc onderzoeker, Laboratorium voor Experimentele Chirurgische Oncologie (LECO), Erasmus MC, Rotterdam
2006-	Post-doc onderzoeker, Afdeling Celbiologie, NCMLS, St. Radboud Universiteit, Nijmegen (Prof. dr. B. Wieringa)

PUBLICATIONS

Lans TE, ten Hagen TLM, van Horssen R, Wu PC, van Tiel ST, Libutti SK, Alexander HR, Eggermont AMM. Improved antitumour response to isolated limb perfusion with tumour necrosis factor after upregulation of endothelial monocyte-activating polypeptide II in soft tissue sarcoma. *Ann Surg Oncol* Oct 9(8): 812-819 (2002).

Lans TE, van Horssen R, de Wilt JHW, Eggermont AMM, ten Hagen TLM. Isolated limb perfusion as a tool to develop gene-therapeutic stratagies: improved anti-tumour response after transfection with EMAP-II. *South West Cancer News* 1 Mar: 29-33 (2002).

Lans TE, van Horssen R, Eggermont AMM, ten Hagen TLM. Involvement of endothelial monocyte activating polypeptide II in tumour necrosis factor-alpha-based anti-cancer therapy. *Anticancer Res* Jul-Aug; 24(4): 2243-2248 (2004).

van Horssen R, Galjart N, Rens JA, Eggermont AM, ten Hagen TL. Novel cell migration assay to study relation of growth factors and extra cellular matrix components during cell motility. *DDH Cancer News* 1 May: 32-34 (2005).

van Horssen R, ten Hagen TLM, Eggermont AMM. TNF in cancer treatment: Molecular insights, anti-tumour effects and clinical utility. *The Oncologist* Apr 11(4): 397-408 (2006).

van Horssen R, Rens JAP, Brunstein F, Van Gils M, Guns V, ten Hagen TLM, Eggermont AMM. Intratumoral expression of TNF-R1 and EMAP-II in relation to response of patients treated with TNF-based isolated limb perfusion. *Int J Canc* 119(6): 1481-1490 (2006).

Drabek K, Van Ham M, Stepanova T, Draegestein K, Keijzer N, Van Horssen R, Van der Reijden M, Akhmanova A, ten Hagen T, Houtsmuller A, Van Capellen G, Smits R, Fodde R, Grosveld F, Galjart N. Murine CLASP-2 regulates persistent motility in mouse embryonic fibroblasts. *Submitted*

van Horssen R, Galjart N, Rens JAP, Eggermont AMM, ten Hagen TLM. Differential Effects of Matrix and Growth Factors on Endothelial and Fibroblast Motility: Application of a Novel Cell Migration Assay. *J Cell Biochem* 30 Jun Epub (2006).

van Horssen R, Rens JAP, Schipper D, Eggermont AMM, ten Hagen TLM. MMP-7 is involved in EMAP-II release of tumour cells by cleavage of ProEMAP/p43. *J Biol Chem* resubmitted

van Horssen R, Rens JAP, Schipper D, Eggermont AMM, ten Hagen TLM. EMAP-II facilitates TNF-R1 apoptotic signaling in endothelial cells via TRADD mobilization. *Submitted*

van Horssen R, Eggermont AMM, ten Hagen TLM. Endothelial Monocyte-activating Polypeptide-II and its functions in (patho)physiological processes. *Cyt Growth Factor Rev* 17(5) in press (2006).

Abstracts (talks)

EMAP-II sensitizes endothelial cells towards TNF-induced apoptosis by facilitating TNF-R1 apoptotic signaling via TRADD-mobilisation. 10th International TNF Superfamily Conference. 29 Sep-2 Oct 2004, Lausanne, Switserland.

Novel cell migration assay to study relation of growth factors and extra cellular matrix components during cell motility. 9th Molecular Medicine Day, 9 Feb 2005, Rotterdam, The Netherlands.

Novel cell migration assay reveals distinct contributions of growth factors and extra cellular matrix components to cell motility. ELSO Meeting, 3-6 Sep 2005, Dresden, Germany.

Other abstracts

Van Horssen R, Rens JAP, Eggermont AMM, ten Hagen TLM. New endothelial cell migration assay discriminates between wound- and tumorangiogenesis and contribution of ECM-components and growth factors. 15th Endothelial Cell Research Symposium, 23 Nov 2004, Maastricht, The Netherlands.

Van Horssen R, Galjart N, Rens JAP, Eggermont AMM, ten Hagen TLM. Novel cell migration assay unveils distinct cell motility responses to growth factors in relation to extracellular matrix components. Cell Migration and Adhesion, Keystone Symposium, 9-14 April 2005, Snowbird, Utah, USA.

Van Horssen R, Rens JAP, Brunstein F, Schipper D, Eggermont AMM, ten Hagen TLM. Role of EMAP-II in TNF antitumor actions during ILP: From molecular signaling to clinical relevance. 10th Molecular Medicine Day, 1 Feb 2006, Rotterdam, The Netherlands.

APPENDIX: COLOUR FIGURES

Chapter 1 (Figure 1, page 18):

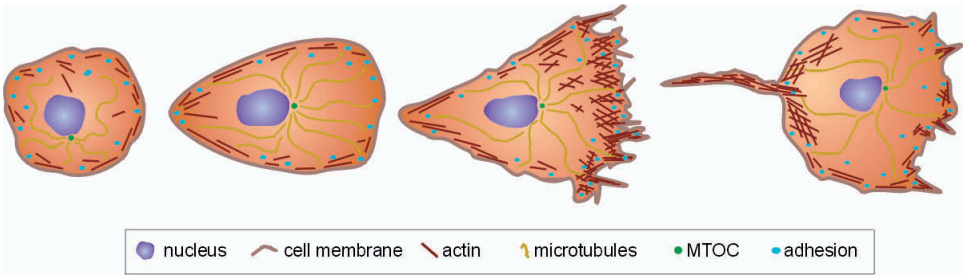

FIGURE 1. Sequential steps during cell migration.
Schematic representation of a cell migrating to the right and of the processes occurring during this movement. Upon a migratory stimulus the cell polarizes and intra cellular structures like MTs and the MTOC are redistributed. Then cellular protrusions are formed by actin polymerisation at the leading edge. New adhesions are formed in the regions of protrusion. MTs target adhesions behind the cell front and at the rear of the cell to support adhesion turnover. Adhesions at the rear of the cell are disassembled and the – often very tiny – tail is retracted by actin-Myosin II interactions. As a result there is a net movement of the cell body.

Chapter 2 (Figure 3, page 33):

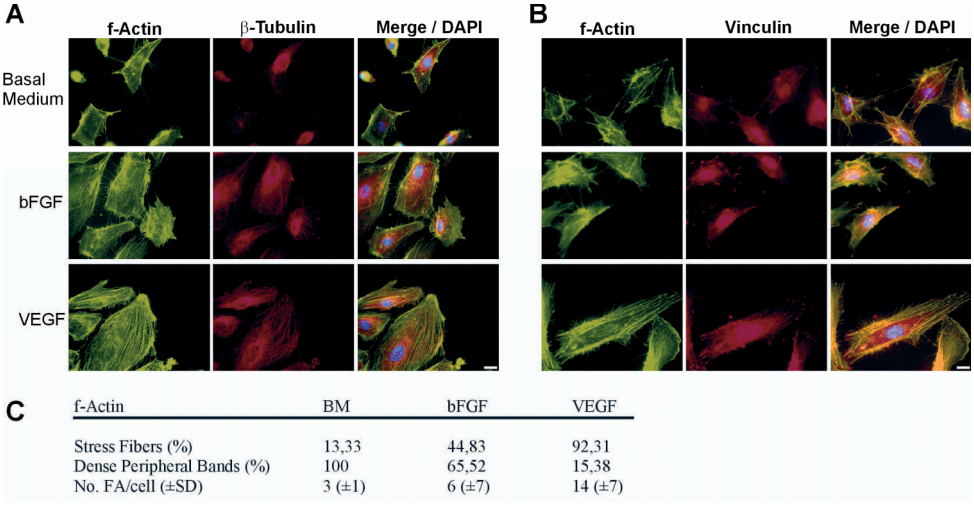

C

f-Actin	BM	bFGF	VEGF
Stress Fibers (%)	13,33	44,83	92,31
Dense Peripheral Bands (%)	100	65,52	15,38
No. FA/cell (±SD)	3 (±1)	6 (±7)	14 (±7)

FIGURE 3. Visualization of cytoskeleton and adhesions of HUVEC in "barrier-based" assay.
HUVEC were induced to migrate for 24 h, fixed and stained for f-actin, β-tubulin and nuclei (A) or f-actin, vinculin and nuclei (B).
A. Cytoskeleton differences in cells at migration front in a negative control with basal medium, treated with bFGF (200 ng/ml) or treated with VEGF (10 ng/ml), Bar, 10 μm.
B. Differences in adhesions number and structure in cells migrating in a negative control with basal medium, treated with bFGF (200 ng/ml) or treated with VEGF (10 ng/ml), bar, 10 μm
C. Quantification of stress fibres, dense peripheral bands and vinculin-positive focal adhesions (FA). For actin some cells contain both types of staining resulting in more than 100 % total.

Chapter 2 (Figure 5, page 39):

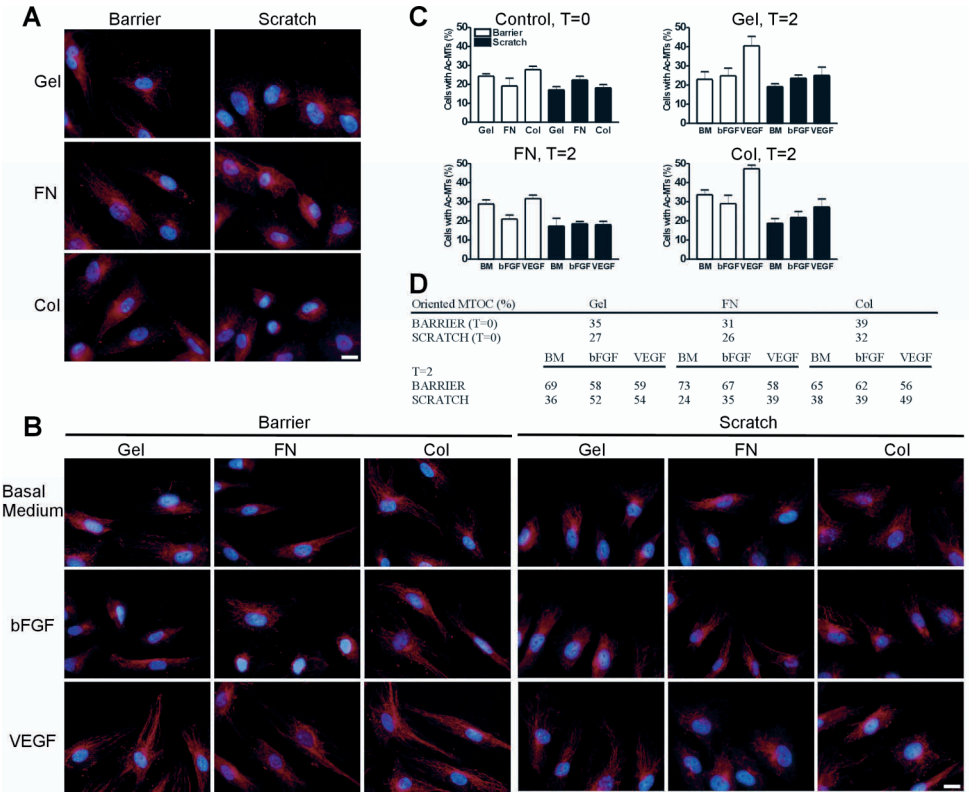

FIGURE 5. MT stabilization and MTOC reorientation during HUVEC migration.
HUVEC were grown on different coatings until confluence and allowed to migrate for 2 h after removal of the barrier, or introduction of a scratch. After 0 h (control) or 2 h the cells were fixed and stained for acetylated MTs (red) and nuclei (blue). Cell-free area is at upper/upper-right for all pictures.

A. Control cells at T=0 h. HUVEC were grown until confluence and immediately after removing the barrier or introducing the scratch, cells were fixed and stained. Bar, 10 μm

B. Migrating HUVEC in both assays, fixed at T=2 h. Except for VEGF-treated cells in the "barrier" assay no differences were seen. The elongated cells bundle their stable MT. Bar, 10 μm

C. Quantification of acetylated MTs. Cells with stable MTs are depicted as percentage of total counted cells. Data represent mean ± SEM of 3 independent experiments.

D. Table represents percentage of cells with MTOC oriented towards the cell-free area after 0 and 2 h for the different treatments in the two assays.

Chapter 2 (Figure 7, page 40):

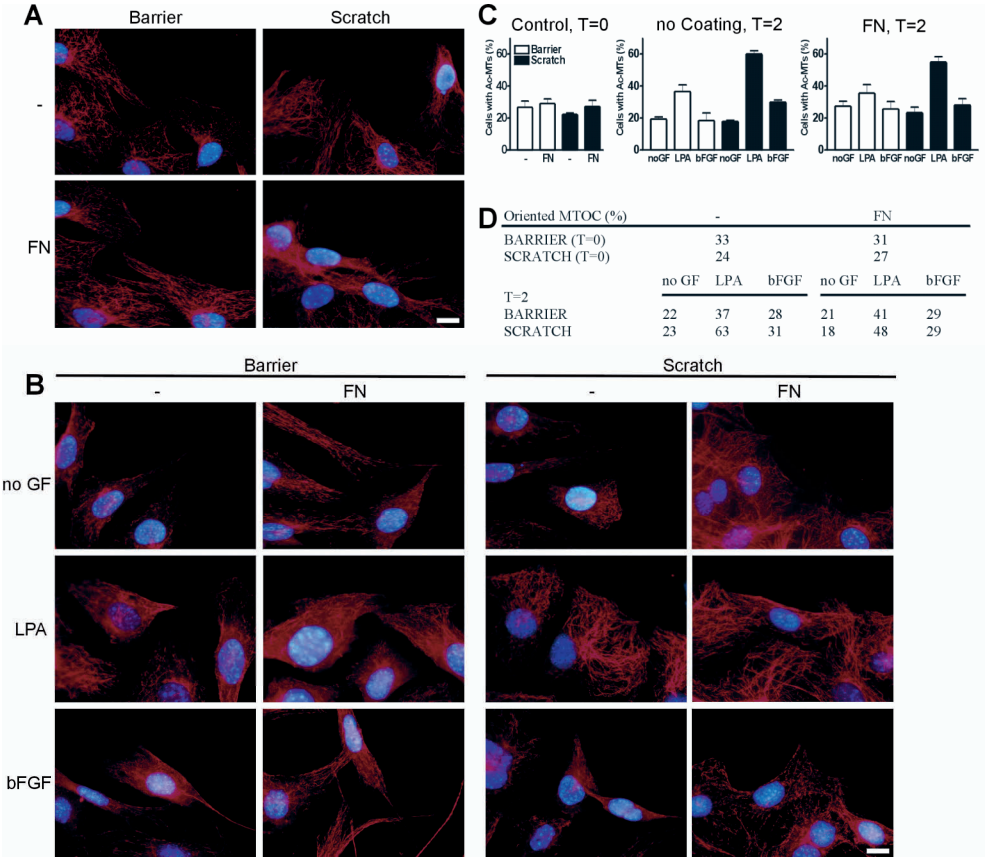

FIGURE 7. MT stabilization and MTOC reorientation during 3T3 migration.
3T3 fibroblasts were grown with and without FN-coating until confluence and allowed to migrate for 2 h after removal of the barrier or introduction of a scratch. After 0 h (control) or 2 h the cells were fixed and stained for acetylated MTs (red) and nuclei (blue). Cell-free area is at upper/upper-right for all pictures.
A. Control cells at T=0 h. 3T3 cells were grown until confluence and immediately after removing the barrier or introducing the scratch, cells were fixed and stained. Bar, 10 μm.
B. Migrating 3T3 cells in both assays, fixed at T=2 h. Especially in the "scratch" assay LPA induced MT stabilization irrespective of coating. Bar, 10 μm.
C. Quantification of acetylated MTs. Cells with stable MTs are depicted as percentage of total counted cells. Data represent mean ± SEM of 3 independent experiments.
D. Table represents percentage of cells with MTOC oriented towards the cell-free area. LPA induces MTOC reorientation in "scratch" assay both with and without FN. In spite of a lack in MTOC reorientation a strong migration profile with accompanied cell morphology was seen when the cells were exposed to bFGF and FN (Fig. 6)

Chapter 3 (Figure 2, page 56):

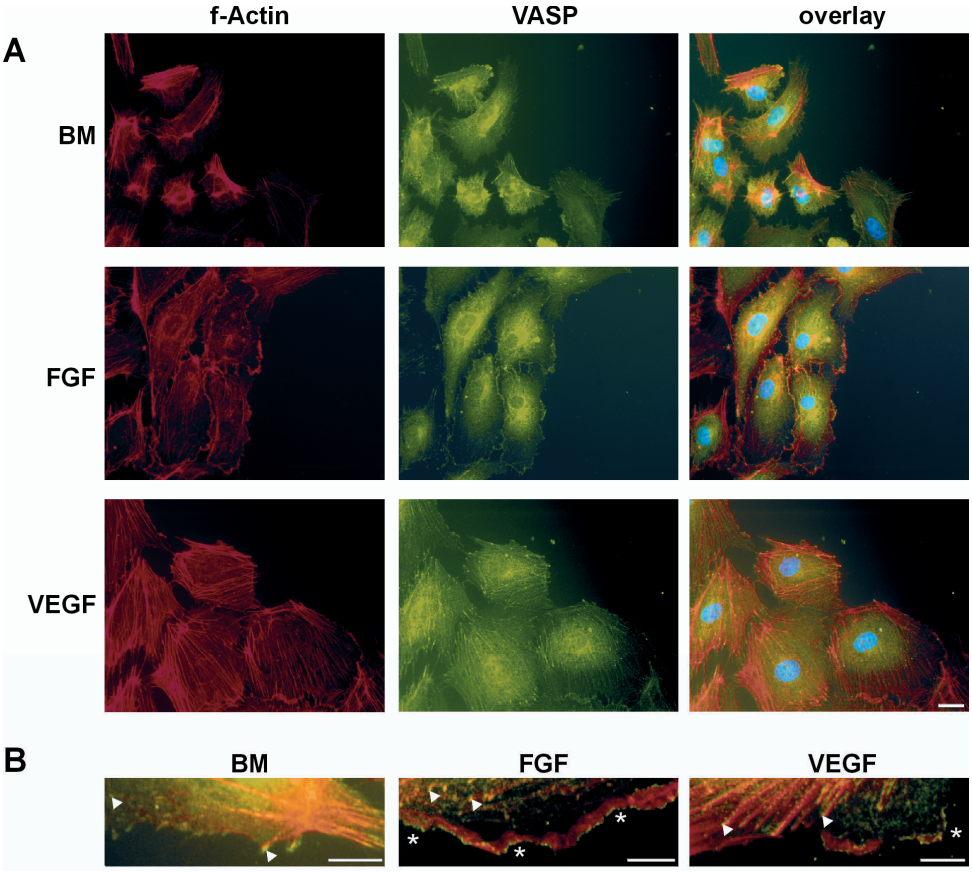

FIGURE 2. Actin and VASP distribution in migrating HUVEC.
A. HUVEC were induced to migrate for 24 h, fixed and stained for f-Actin (red), Ena/VASP (green) and nuclei (blue). In basal medium controls the actin is mainly visible as dens peripheral bands and VASP is mainly cytoplasmic. Upon bFGF treatment, actin staining is observed at the edges of the cells and a positive VASP signal was found at the most distal site of this rim at the leading edge and cell rims. VEGF induced many stress fibers and VASP was mainly located in focal adhesions. Bar: 10 μm.
B. Enlargement of cell rims of HUVEC at migration fronts. Arrowheads point VASP located at ends of actin fibers as focal adhesions, Asterisks point membrane-expressed VASP. In bFGF treated we observed VASP along whole membranes while in VEGF treated cells this expression was locally. Bar: 5 μm.

Chapter 3 (Figure 4, page 58):

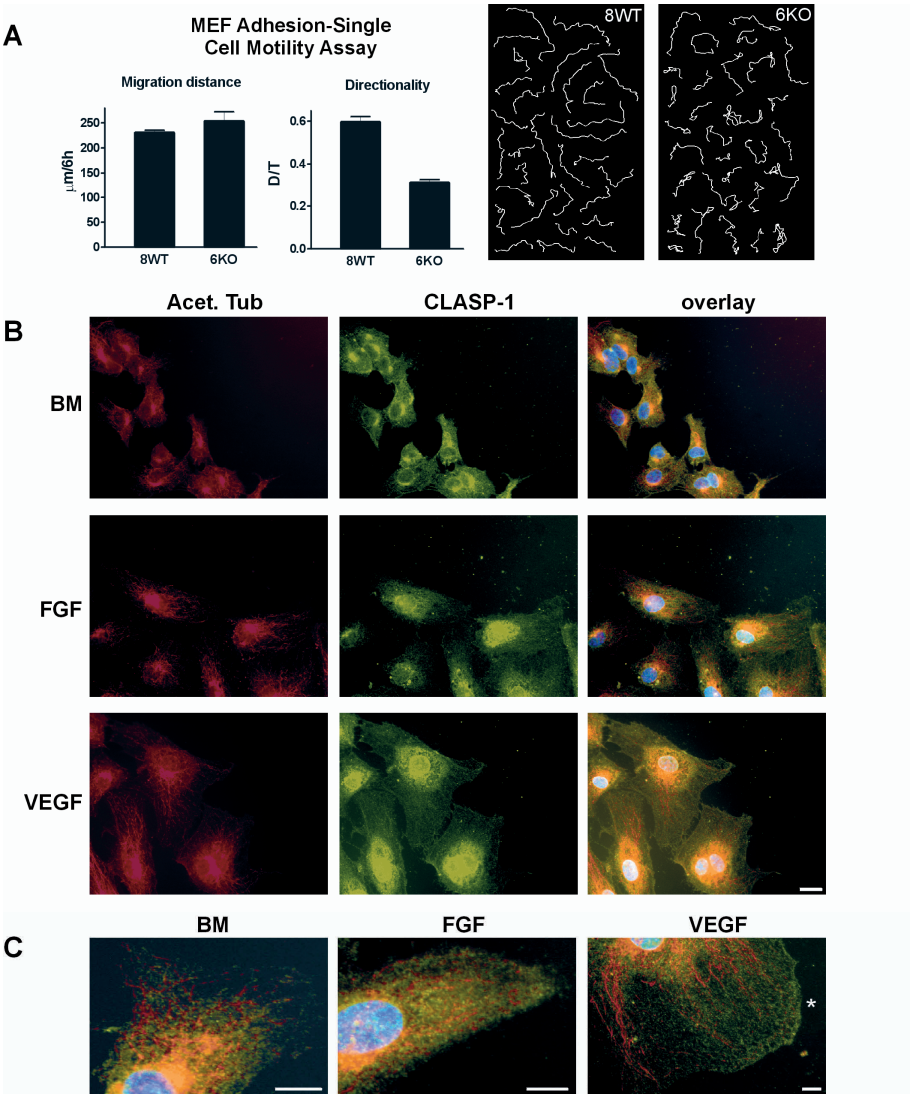

FIGURE 4. Role of CLASPs in directionality of cell movements.
A. Mouse Embryonic Fibroblasts isolated from wild-type (8WT) and CLASP-2 knouckout mice (6KO) were allowed to adhere and single cell motility was measured under the microscope for 6h. No difference on migration distance was found while directionality was decreased in 6KO cells. Right part shows the migration tracks of 30 cells derived from 3 independent experiments.
B. HUVEC were induced to migrate for 24 h, fixed and stained for stable MTs (red), CLASP1 (green) and nuclei (blue). In BM cells we observed low amounts of stable MTs and CLASP1 was location was Golgi-associated and distributed throughout the cytoplasm. bFGF treatment did induce some nuclear CLASP1 and a mild increase in stable MTs. VEGF cells have slightly more stable MTs and s small accumulation of CLASP1 at local sites in the leading edge. Bar: 10 μm.
C. Enlargement of cell leading edges of BM, bFGF and VEGF treated HUVEC. Asterisk shows local CLASP1 accumulation. Bar: 5 μm.

Chapter 3 (Figure 5, page 60):

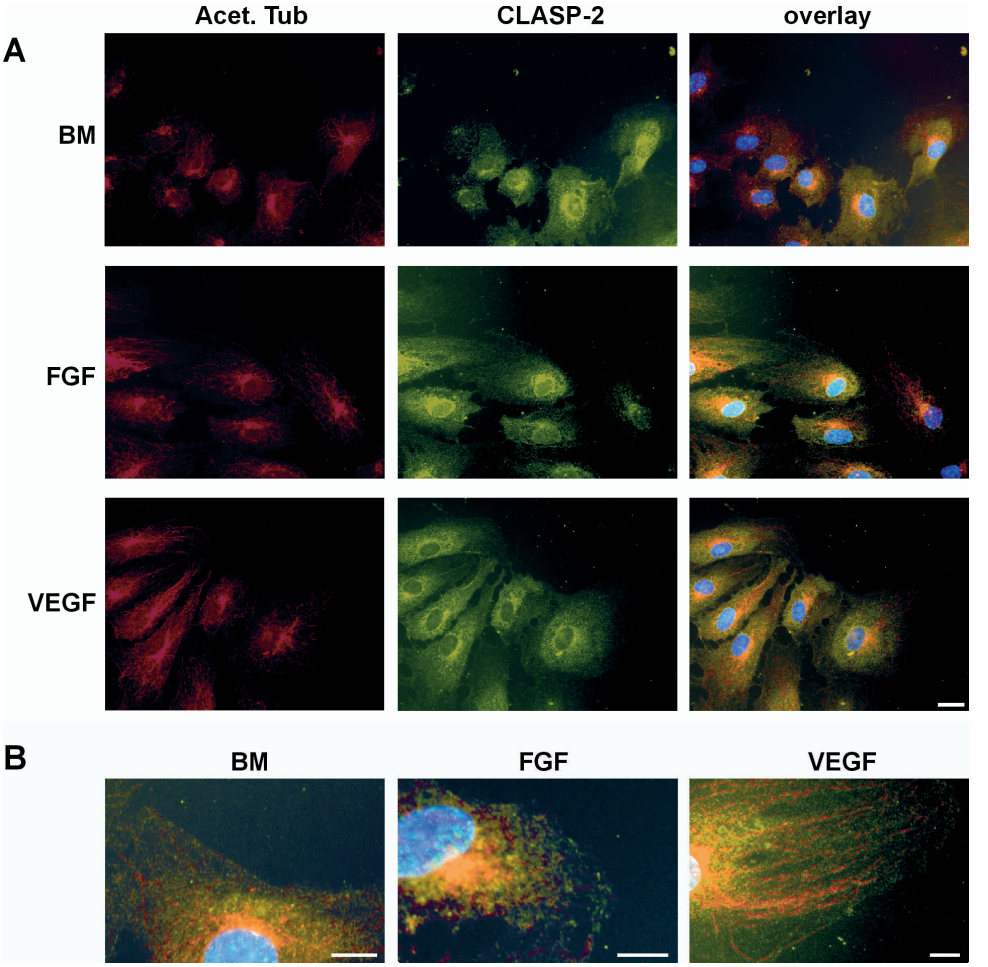

FIGURE 5. CLASP2 distribution in migrating HUVEC.
A. HUVEC were induced to migrate for 24 h, fixed and stained for stable MTs (red), CLASP2 (green) and nuclei (blue). For the stable MTs staining again a small increase was observed for the VEGF treated cells. For CLASP2 no clear differences were observed between the different treatments. CLASP2 was found rather diffuse throughout the cytoplasm and no nuclear signal was seen. Bar: 10 μm.
B. Enlargement of cells at migration fronts. Bar: 5 μm.

Chapter 5 (Figure 1, page 84):

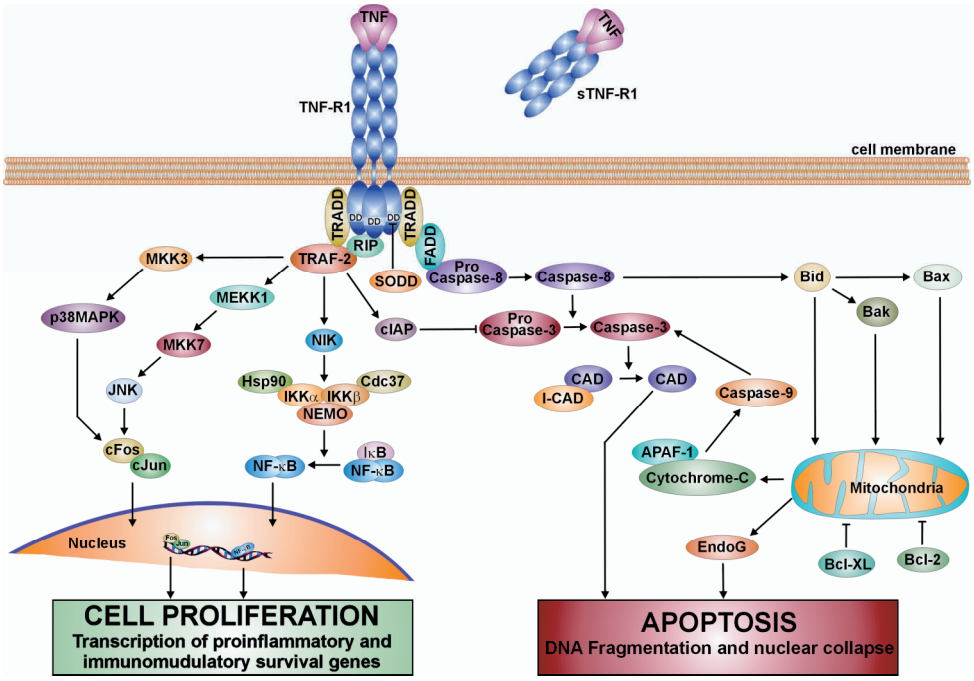

FIGURE 1. TNF-R1 signaling pathway.
TNF activates both survival and proliferation pathways along with apoptotic pathways via TNF-R1. The separate pathways are well defined while the survival-death balance regulation remains unclear. Abbreviations: APAF-1: apoptosis protein activating factor-1, Bcl-2: B-cell lymphoma-2, Bid, Bak, Bax and Bcl-XL: mitochondrial proteins of the Bcl-2 family, CAD: caspase-activated DNAse, Caspase-3/8/9: cysteine aspartase (apoptotic protease) 3/8/9, Cdc37: co-chaperon of HSP90, cIAP: cytoplasmic inhibitor of apoptosis, cFos/cJun: transcription factors, DD: death domain, EndoG: mitochondrial DNAse, FADD: fas-associated DD, HSP90: heat shock protein-90, I-CAD: inhibitor of CAD, I-kB: inhibitor of NF- kB, IKKalpha/beta: I-kB kinase, JNK: cJun n-terminal kinase, MEKK1: MAPK/ERK kinase-1, MKK3/7: MAPK kinase 3/7, NEMO: NF-kB essential modulator, NF-kB: nuclear factor kappa B transcription factor, NIK: NF-kB inducing kinase, p38MAPK: p38 mitogen activated protein kinase, RIP: receptor interacting protein, SODD: silencer of DD, sTNF-R1: soluble TNF-R1, TNF: tumour necrosis factor alpha, TNF-R1: TNF receptor 1, TRADD: TNF receptor-associated DD, TRAF-2: TNF receptor-associated factor-2.

Chapter 5 (Figure 2, page 86):

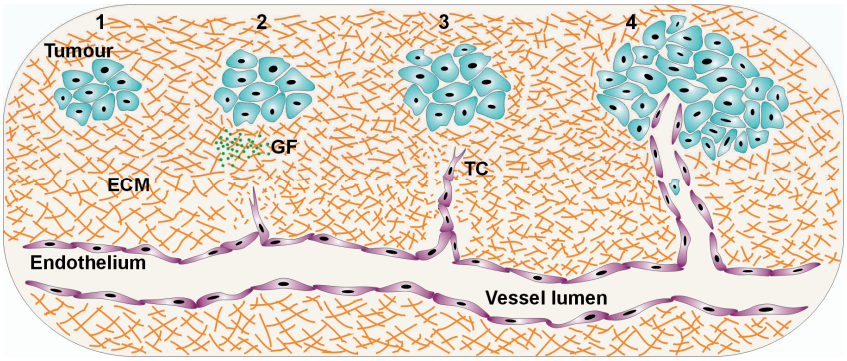

FIGURE 2. The sequential steps during tumourangiogenesis.
The dormant tumour in stage 1 starts to secrete angiogenic growth factors (GF) after its 'angiogenic switch', which is accomplished by an imbalance in pro- and anti-angiogenic factors. These GF activate endothelial cells of surrounding vessels and these cells start to migrate (stage 2) and proliferate towards the tumour. An endothelial tip cell (TC) is guiding this sprouting process (stage 3). In stage 4 the novel sprout has formed a lumen and the tumour is connected to the vasculature thereby ensuring its growth and enabling itself to metastasize hematogenically.

Chapter 5 (Figure 3, page 87):

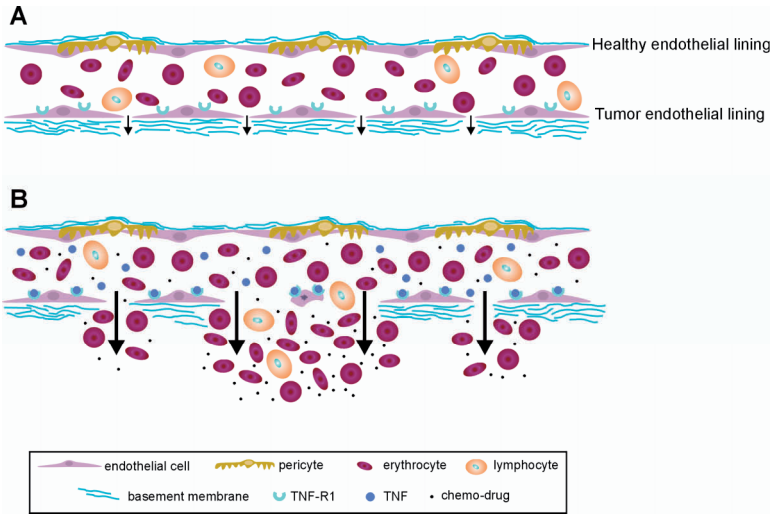

FIGURE 3. Differences between healthy and tumour endothelium and a proposed mechanism of the TNF effect.
A. Schematic representation of a vessel with healthy endothelial lining (upper) and tumour endothelial lining (lower). Healthy endothelium is a continuous lining of endothelial cells, covered with pericytes and with a thin basement membrane. The permeability is low and extravasation is tightly organized. In contrast, tumour endothelium does not consist of a continuous lining of endothelial cells, it lacks pericyte coverage and the basement membrane is thickened. This phenotype results in an increased permeability of tumour vessel (small arrows). We hypothesize that the tumour endothelium exhibits a higher TNF-R1 expression due to TNF-R1 upregulating factors produced by vessel-surrounding cells.
B. Upon TNF treatment in an ILP the healthy endothelium stays intact because it is TNF-insensitive by lacking TNF-R1 expression on the membrane. Tumour endothelium binds TNF, which affects endothelial phenotype and induces apoptosis in some endothelial cells. These two processes result in an enormous induction of vessel permeability (big arrows). As a result the chemo-drug is well distributed throughout the tumour and a strong extravasation of erythrocytes results in a massive hemorrhagic tumour necrosis. The selectively targeted tumour vessels are non-functional anymore and regress.

Chapter 5 (Figure 4, page 92):

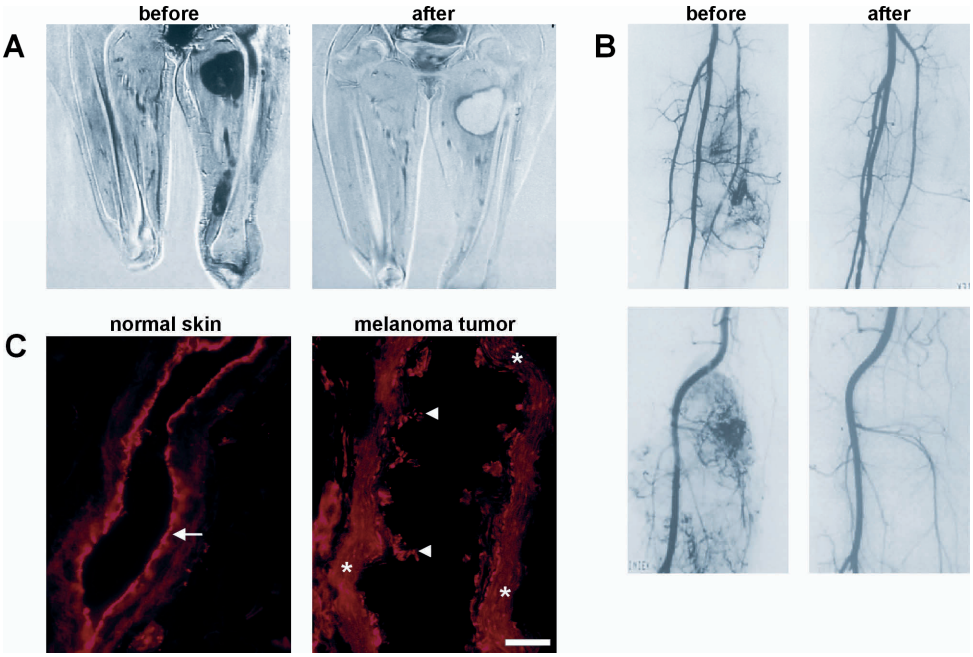

FIGURE 4. Anti-tumour and anti-vascular effects of TNF upon ILP treatment of sarcoma and melanoma patients.
A. MRI of a patient with a high-grade leiomyosarcoma in the upper leg showing tumour mass before treatment (left) while 5 weeks after ILP with TNF and melphalan there is no gadolinium uptake in the tumour remnants (right). Tumour remnants were resected and all necrotic.
B. Angiographies of 2 patients with rapidly growing sarcomas in the leg before (left) and after (right) ILP with TNF and melphalan. Angiographies clearly show the well-developed tumour vasculature before ILP, which is selectively destructed after treatment while the normal vessel are still present and intact. Both patients were classified as complete responders.
C. Endothelial lining of tumour vessels is destructed. Endothelial staining (CD-31) of vessels in normal skin (left) and melanoma (right) in biopsies of a melanoma patient taken after ILP. Vessels in the normal skin show a continuous endothelial lining (arrow) while in the melanoma-associated vessel this lining is disrupted and the endothelial cells detach from the basement membrane (arrowheads). The elastic fibers (asterisks, stained aspecific) in the thickened basement membrane are also visible in the melanoma vessel. Scale bar: 50 μm.

Chapter 8 (Figure 1, page 148):

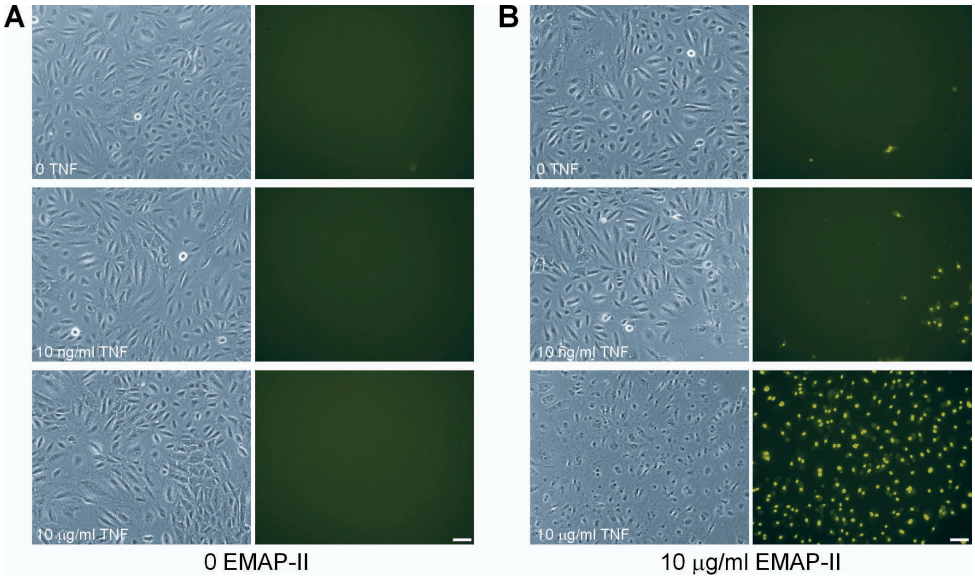

FIGURE 1. EMAP-II sensitises HUVEC towards TNF-induced apoptosis.
A. HUVEC were treated with 0, 10 ng/ml or 10 µg/ml TNF for 1 h after 1 h pre-treatment with standard culture medium (control). Pictures were taken to show monolayer morphology (left) and apoptotic cells (right). No TNF effect was observed. Bar, 100 µm.
B. HUVEC were treated with 0, 10 ng/ml or 10 µg/ml TNF for 1 h after a 1 h pre-treatment with 10 µg/ml EMAP-II. High dose TNF induced massive apoptotic cell death after EMAP-II pre-treatment. At low dose some EC undergo apoptosis. Bar, 100 µm.

Chapter 8 (Figure 2, page 149):

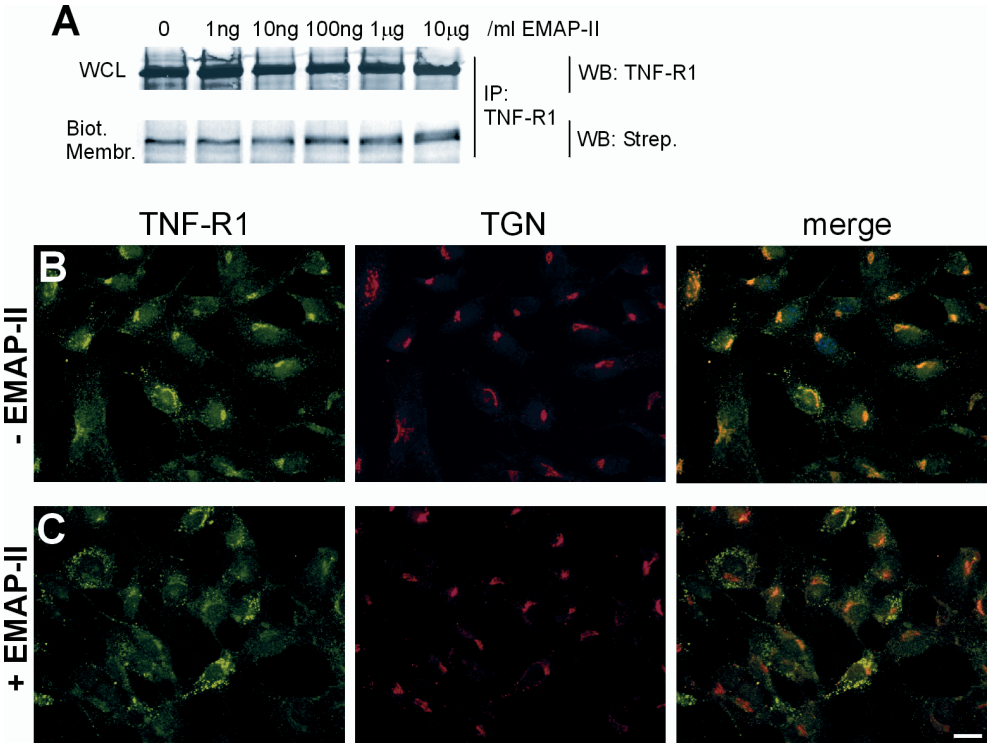

FIGURE 2. EMAP-II induces TNF-R1 redistribution in HUVEC.
A. Immunoprecipitation and western blot analysis of TNF-R1 in whole cell lysate (WCL) and cell membranes upon 1 h EMAP-II treatment. Total TNF-R1 expression was not altered, while the membrane-bound TNF-R1 fraction was increased at increasing EMAP-II concentrations.
B. Immunofluorescent staining for TNF-R1 and TGN (trans-Golgi network) of non-treated HUVEC. TNF-R1 expression is mainly Golgi-associated (merged image).
C. Immunofluorescent staining for TNF-R1 and TGN after 1 h EMAP-II (10 μg/ml) treatment. The Golgi-associated TNF-R1 expression was clearly decreased. The overlapping yellow staining is almost completely absent indicating TNF-R1 redistribution out of Golgi storage pools. Bar, 20 μm.

Chapter 8 (Figure 3, page 150):

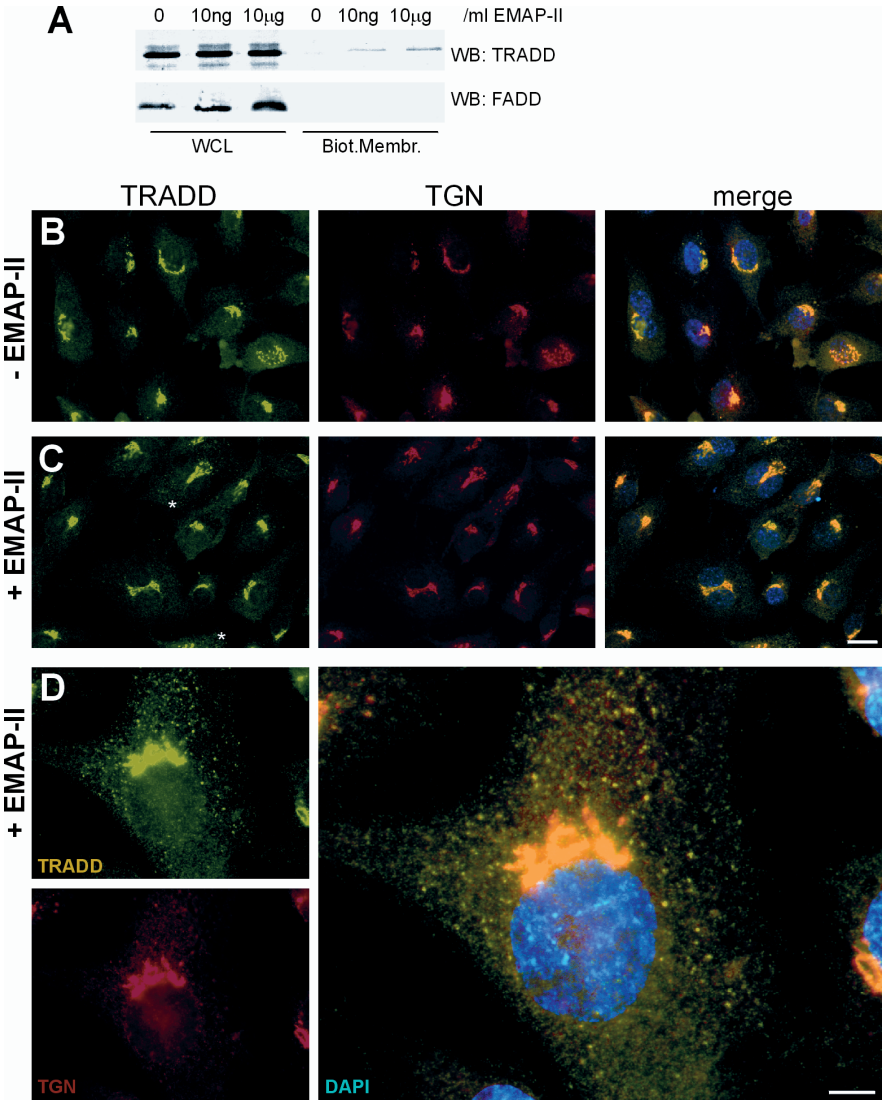

FIGURE 3. EMAP-II induces mobilization and membrane-expression of TRADD in HUVEC.
A. Western blot analysis of TRADD and FADD in whole cell lysate (WCL) and cell membranes in HUVEC treated with 0, 10 ng/ml, 10 µg/ml EMAP-II for 1 h. EMAP-II induced small amounts of TRADD membrane-expression. FADD expression was upregulated in the cell lysate.
B. Immunofluorescent staining for TRADD and TGN (trans-Golgi network) of non-treated HUVEC. TRADD expression is almost exclusively within the Golgi apparatus.
C. Immunofluorescent staining for TRADD and TGN after 1 h EMAP-II (10 µg/ml) treatment. TRADD expression appeared mainly Golgi-associated as shown by the yellow overlap in the merged image. In addition some TRADD-containing vesicles were observed (asterisks). Bar, 20 µm.
D. High magnification image of a treated EC showing TRADD mobilization in small vesicles, staining positive for TRADD (green) and negative for TGN (red). Bar, 5 µm.

Chapter 8 (Figure 4, page 152)

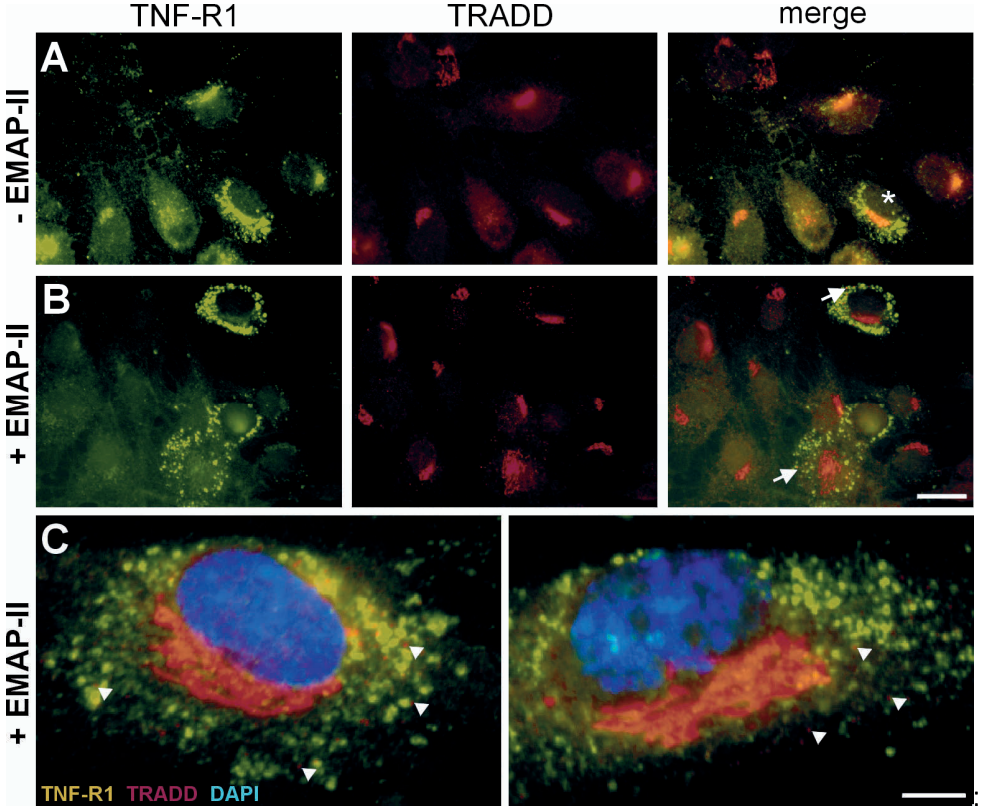

FIGURE 4. TNF-R1 and TRADD are transported in different vesicles within the same cell.
A. Immunofluorescent staining for TNF-R1 and TRADD of non-treated HUVEC. Both proteins were mainly expressed in the Golgi. Also in sporadically observed EC with TNF-R1 redistribution, the Golgi showed co-staining and no TRADD-positive vesicles were seen (asterisk).
B. Immunofluorescent staining for TRADD and TGN after 1 h EMAP-II (10 μg/ml) treatment. TNF-R1 expression in the Golgi is decreased while TRADD expression was still Golgi-associated. Merged images did not show co-localization (yellow) in Golgi anymore. Cells with TNF-R1 redistribution stained positive for TRADD-containing vesicles as well (arrows), Bar, 20 μm.
C. High magnification images of two EMAP-II treated EC showing TNF-R1 redistribution and TRADD mobilization. The small amounts of mobilized TRADD (red, arrow-heads) located in different vesicles as compared to the abundantly present TNF-R1 (green). Bar, 5 μm.

Chapter 9 (Figure 2, page 165):

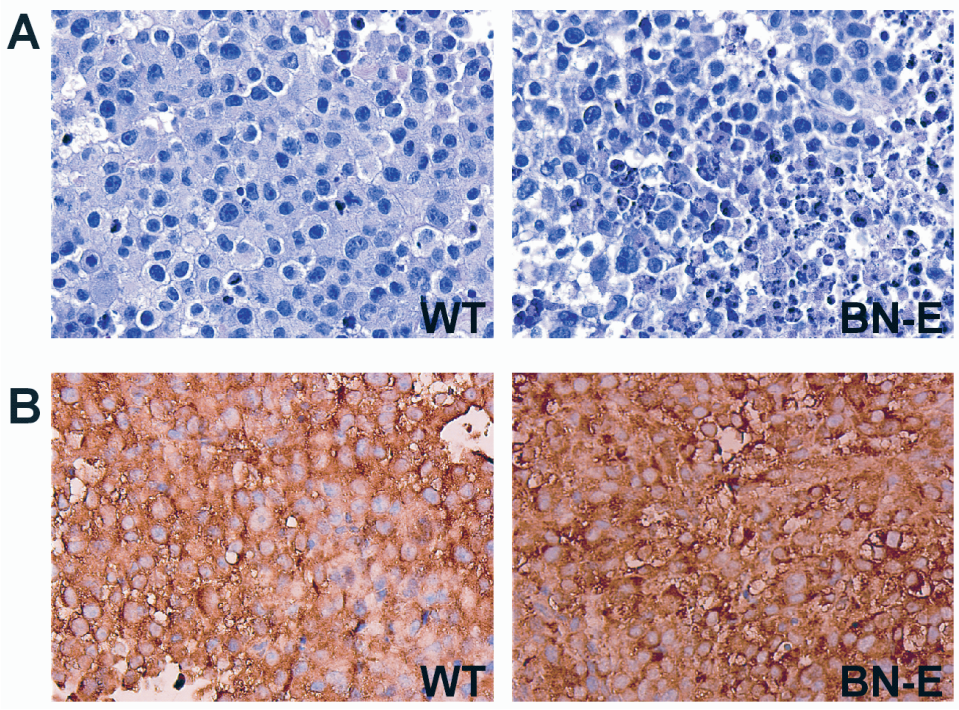

FIGURE 2. Histological and immunohistochemical analysis of wild-type and BN-E tumours.
A. H&E staining.
B. Immunohistichemical staining for EMAP-II. Transfected tumour cells look somewhat smaller. EMAP-II is expressed by all cells and staining patterns are comparable.

Chapter 10 (Figure 4, page 183):

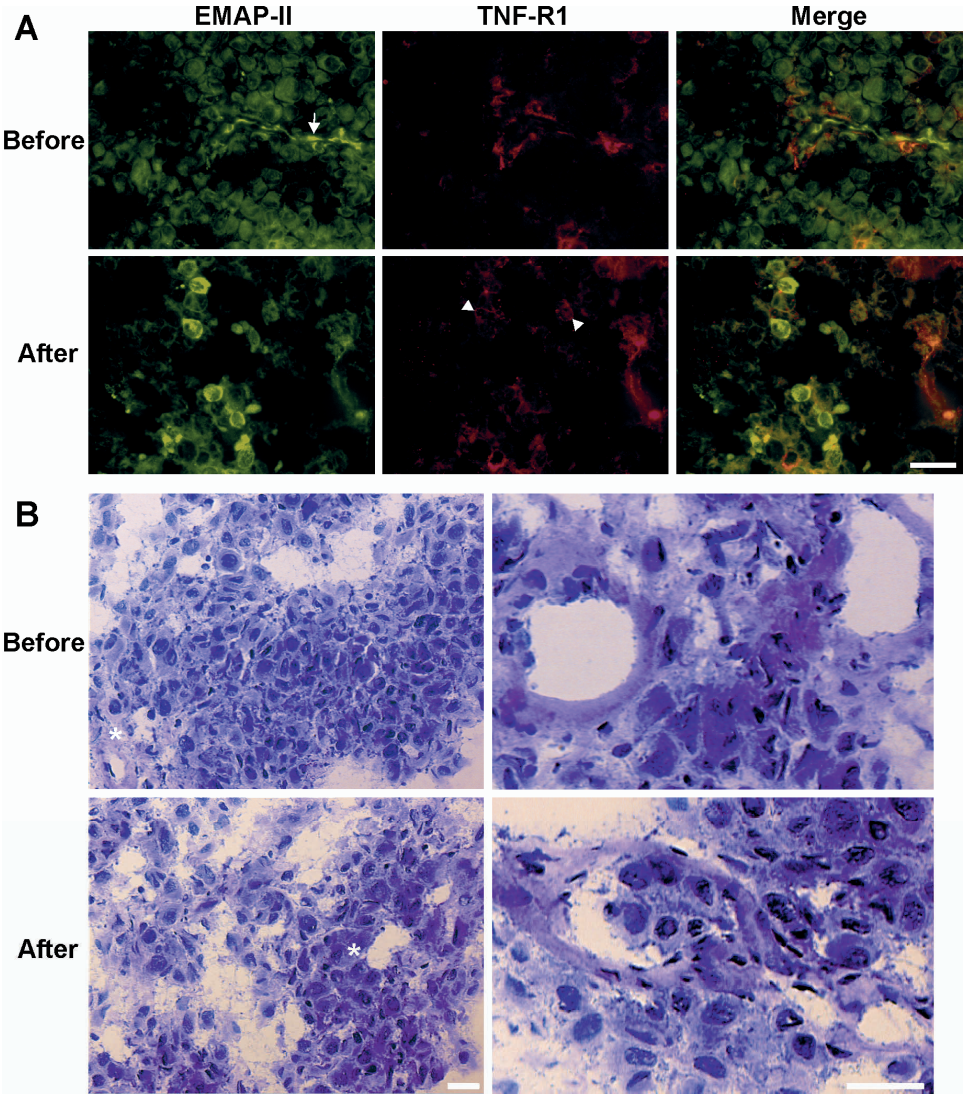

FIGURE 4. A. Immunofluorescence stainings for EMAP-II (green) and TNF-R1 (red) of melanoma biopsies taken right before (upper panel) and after (lower panel) TNF-based ILP. Before ILP proEMAP-EMAP-II is present in all cells but some vessel-like regions (arrow) have a higher expression, likely due to local increased expression of mature EMAP-II. TNF-R1 is mainly expressed in the surrounding of these vessel-like regions in a scattered manner. Noteworthy is the observation that high EMAP-II expressing cells and TNF-R1 expressing cells do not overlap. After ILP the tumour structure is extensively damaged. Some high EMAP-II expressing tumour cells clustered to together were observed. TNF-R1 expression was still present in some tumour cells and appeared more organized in clusters (arrowheads) as compared to before ILP. The vessel-like structures are not visible anymore after ILP. Bar, 50 μm.
B. Histological HE staining of melanoma biopsies taken before and after ILP. Before ILP the melanoma showed a heterogeneous structure of tumour cells and infiltrate (left panel). Asterisk indicates a tumour-associated vessel. After ILP the tumour cells are strongly redistributed and the tumour-associated macrophages (also called foamy macrophages) tend to cluster. Tumour vessels before and after ILP are shown at the right panel. Bar, 20 μm.

Chapter 10 (Figure 5, page 185):

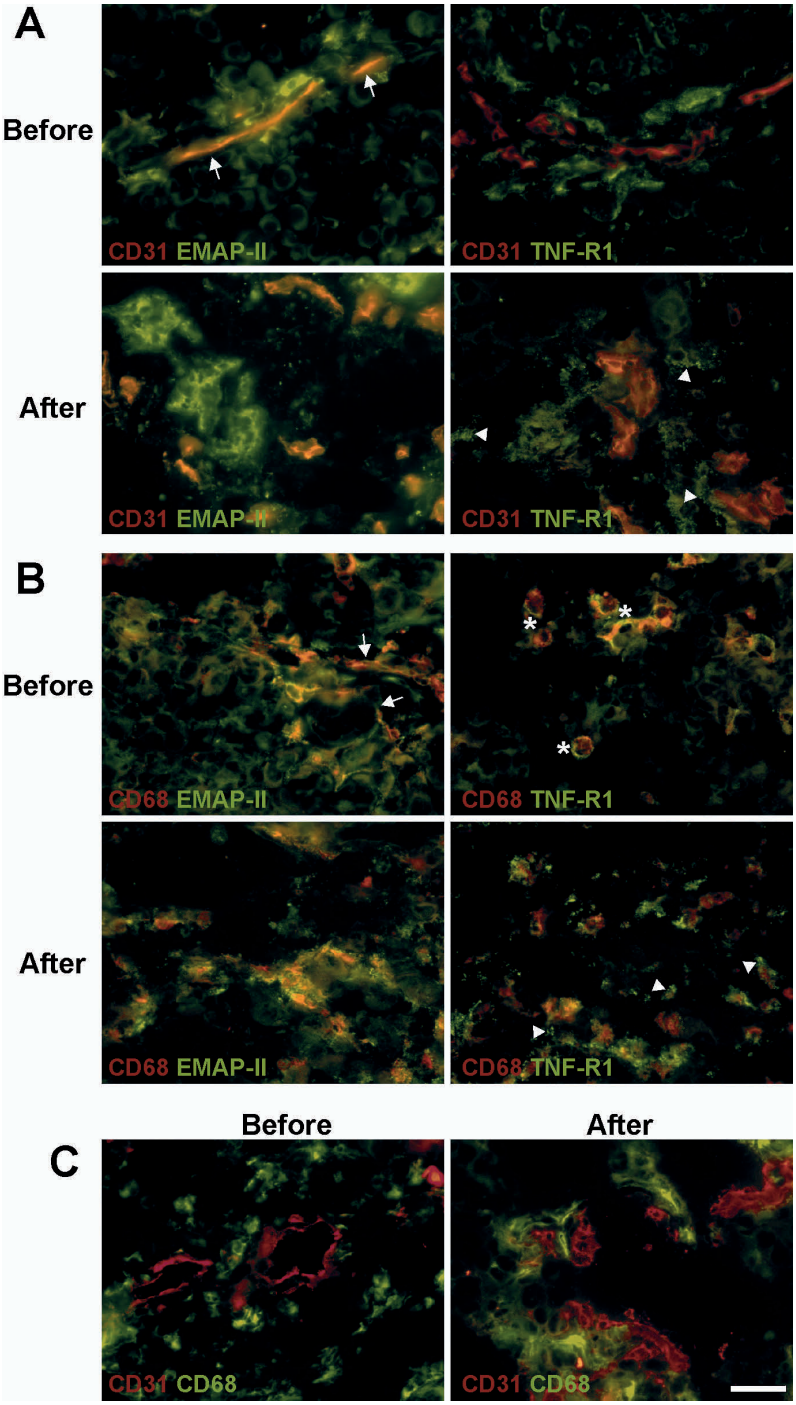

FIGURE 5. Immunofluorescence stainings for EMAP-II and TNF-R1 in combination with endothelial marker (CD31, panel *a*) or macrophage/monocyte marker (CD68, panel *b*) and co-staining with both markers (CD31/CD68, panel *c*) of melanoma biopsies taken right before and after TNF-based ILP.

A. Before ILP the high EMAP-II expressing regions in part co-localize with endothelial cells (arrow) while the TNF-R1 expressing cells are surrounding the vessels. No co-localization of TNF-R1 with endothelial cells was observed. After ILP high expressing EMAP-II cells were still present and endothelial cells of the disrupted vessels stained positive as well. TNF-R1 was observed in clusters (arrowheads) and some expression was seen in endothelial cells.

B. Before ILP, high expressing EMAP-II cells/regions co-stained with macrophages in vessel-like regions (arrow). Most tumor-macrophages expressed high levels of TNF-R1 (asterisks). After ILP co-localization of EMAP-II and macrophages is obvious while clustered TNF-R1 expression (arrowheads) was less associated with macrophages.

C. Before ILP, healthy-looking vessels are present and macrophages are equally distributed throughout the tumor. After ILP the tumor vasculature has been disrupted and macrophages were recruited to these endothelial/vessel remnants. Bar: 20 μm